PERFORMANCE ANALYSIS AND ECONOMETRIC ASSESSMENT OF A COMMUNITY WASTE POWER PLANT BIOGAS SYSTEM

OLUWASEUN OLANREWAJU AKINTE

A DISSERTATION SUBMITTED IN PARTIAL FULFILLMENT OF THE REQUIREMENTS FOR THE DEGREE OF DOCTOR OF ENGINEERING

PROGRAM IN ENERGY AND MATERIALS ENGINEERING

FACULTY OF ENGINEERING

RAJAMANGALA UNIVERSITY OF TECHNOLOGY THANYABURI

ACADEMIC YEAR 2024

PERFORMANCE ANALYSIS AND ECONOMETRIC ASSESSMENT OF A COMMUNITY WASTE POWER PLANT BIOGAS SYSTEM

OLUWASEUN OLANREWAJU AKINTE

A DISSERTATION SUBMITTED IN PARTIAL FULFILLMENT OF THE REQUIREMENTS FOR THE DEGREE OF DOCTOR OF ENGINEERING

PROGRAM IN ENERGY AND MATERIALS ENGINEERING

FACULTY OF ENGINEERING

RAJAMANGALA UNIVERSITY OF TECHNOLOGY THANYABURI

ACADEMIC YEAR 2024

Dissertation Title	Performance Analysis and Econometric Assessment of a Community Waste Power Plant Biogas System
Name-Surname	Mr. Oluwaseun Olanrewaju Akinte
Program	Energy and Materials Engineering
Dissertation Advisor	Associate Professor Boonyang Plangklang, Dr.-Ing.
Academic Year	2024

DISSERTATION COMMITTEE

..... Chairman
(Professor Piya Kovintavewat, Ph.D.)

..... Committee
(Associate Professor Wirachai Roynarin, Ph.D.)

..... Committee
(Professor Krischonme Bhumkittipich, D.Eng.)

..... Committee
(Associate Professor Sirichai Dangeam, D.Eng.)

..... Committee
(Associate Professor Boonyang Plangklang, Dr.-Ing.)

Approved by the Faculty of Engineering, Rajamangala University of Technology Thanyaburi in Partial Fulfillment of the Requirements for the Degree of Doctor of Engineering

..... Dean of Faculty of Engineering
(Associate Professor Sorapong Pavasupree, Ph.D.)
4 December 2024

Dissertation Title	Performance Analysis and Econometric Assessment of a Community Waste Power Plant Biogas System
Name – Surname	Mr. Oluwaseun Olanrewaju Akinte
Program	Energy and Materials Engineering
Dissertation Advisor	Associate Professor Boonyang Plangklang, Dr.-Ing.
Academic Year	2024

ABSTRACT

The global composition of energy consumption is experiencing a massive transformation as a result of nonrenewable energy resources, and the consumption of conventional energy causes greenhouse gas emissions. The clean and sustainable energy development system known as renewable energy system serves as the main focus in replacing conventional energy sources. The enhancement of energy network stability and smoothing operation of intermittent energy generation from renewable energy power sources, therefore, is being processed by the energy storage system during the power flow. The technologies associated with energy storage systems are updated and improved continuously to meet up with energy demand to reduce the rate of fuel consumption for greater reliability and minimizing energy cost when connected to the grid system or disconnected from the grid network.

This dissertation focused on a flexible and steady clean energy source from municipal wastes that was integrated successfully with the utility grid operation in On-Nut community in Bangkok, Thailand. The configuration of biomass gasifier system from municipal wastes with storage system following dispatched algorithms was designed with the grid system as a unified microgrid network. The proposed generating system was modeled experimentally, mathematically, and schematically to determine the most efficient power generation management, energy cost productivity, and sectional energy contribution between the biogas generators and grid system. An optimized controlling algorithm with feedback control systems was designed by an industrial HOMER analysis application to perform technical supervision and econometrics of the energy flow management by switching operation to the most productive electric energy cost service and efficient operational network system from the integrated power system architectures operating energetically in different modes.

The research results showed that the proposed configuration of biogas-grid connected lithium-ion storage network recorded the highest level of technical efficiency in terms of energy purchase of 239,764 kWh and energy sales to the grid of 1,959,426 kWh. The lowest net energy purchase was 1,719,661 kWh while the configuration of biogas-grid connected zinc bromide storage network attained the most economical energy system in terms of overall cost of $ 8,647,863.00 and the operating cost of $ 143,974.00. The investment return rate was 17.00 % and the internal return rate was 20.30 %. The payback period was 4.83 years.

Keywords: integrated hybrid power network, energy storage technique, econometric estimation-hybrid energy configuration assessment, feedback control systems

Acknowledgement

I am expressing a heartfelt gratitude to my potential advisor Associate Professor (Dr) Boonyang Plangklang for his quality experience, in-depth guidance, intellectual knowledge, and exposing me to the experimental resources of an industrial power sector at On-nut community which hasenabled and encouraged me to carry out my research work and prepare my thesis successfully. Furthermore, I am very grateful for the scholarship opportunity and available resources provided by the E-CUBE-I scholarship program of Rajamangala University of Technology Thanyaburi (RMUTT) which has facilitated and fascinated the successful outcome and immense contribution of my research program in the field of Energy and Materials Engineering in attaining mydegree. Extensively, I appreciate the committees of Energy and Materials Engineering program namely, Associate Professor (Dr) Wirachai Roynarin, Professor (Dr) Piya Kovintavewat, Associate Professor (Dr) Krischonme Bhumkittipich, Associate Professor (Dr) Sirichai Dangeam, and Associate Professor (Dr) Boonrit Prasartkaew for their quality suggestions and comments which has strengthened me to work harder in achieving this goal.

Lastly, I appreciate my lovely wife (Mrs Hellen Idowu Adeboye Akinte), family and beloved well-wishers who have also supported me in prayers, encouraged me, and assisted me financially in aiding my succesful journey to Thailand in order to accomplish my apex degree.

Oluwaseun Olanrewaju Akinte

Table of Contents

Page

Table of Contents (Continued)

Page

Table of Contents (Continued)

Page

Table of Contents (Continued)

Page

List of Tables

Page

List of Figure

Page

List of Figure (Continued)

Page

List of Figure (Continued)

Page

List of Figures (Continued)

Page

List of Abbreviation

AC	Flowing Alternating Current	(A)
A_{Eghg}	Annual Energy Generated from Microgrid Network	(kWh)
BMA	Bangkok Metropolitan Area	
Calvbio	Calorific Value of Biogas Generator	(Calorie/kg)
CAT-NG	Caterpillar Natural gas Generator	(kW)
CG 170-12	12 Cylinders Caterpillar (Natural gas) Generator	(kW)
CHG (t)	Charging States of Batteries	(%)
CHP	Combined Heat and Power Flow	(MJ and kW)
DC	Flowing Direct Current	(A)
DC_{rg}	Discharging Depth of Batteries	(%)
E_{co}	Electricity Cost of Utility Grid	($USD/hr)
$Elec_{biog}$ (t)	Output Electricity of Biogas Generator	(kWh/yr)
$Elec_{grid}$ (t)	Output Electricity of Utility Grid	(kWh/yr)
Engen	Excitation Voltage of Synchronous Generator	(V)
ERS	Energy Reserve System	(kWh/Ah)
GDP	Gross Domestic Product	($USD)
GHe	Greenhouse Gases Emission	(kg)
HOMER	Hybrid Optimization Multiple Energy Resources	
IHOGA	Integrated Hybridized Optimization by Genetic Algorithm	
IRRA	Internal Return's Rate	(%)
LECE	Levelized Electricity Cost	($USD/kWh)
MJ/kg	Mega Joule per Kilogram	
MSW	Municipal Solidified Wastes	(tonnes)
MYT	Maximum Yielding Technology	
NPCO	Total Net Present Cost	($USD/yr)
Paccel	Acceleration Power of Utility Synchronized Generator	(kW)
Pgen	Output Real Power per Phase of Synchronized Generator	(kW)

List of Abbreviation (Continued)

Poelect	Output Electrical Power of Synchronized Generator	(kW)
Pomech	Input Mechanical Power of Synchronized Generator	(kW)
Pu-network	Output Power of Microgrid Network	(kW)
PW_{biog} (t)	Output Power of Biogas Generator	(kW)
PW_{gn} (t)	Output Power of Storage System	(kW)
PW_{i} (t)	Input Power of Electronic Conversion System	(kW)
PW_{op} (t)	Output Power of Electronic Conversion System	(kW)
PW_{ug} (t)	Output Power of Utility Grid	(kW)
Qgen	Reactive Power per Phase of Synchronized Generator	(kVAR)
RDF	Fuel Derived from Refuse	(tonnes/day)
ROIV	Investment Return	(%)
Solar PVs	Solar Photovoltaic Plant	(kW)
T	Period of Energy Generation and Emission from Microgrid	(hr)
T.so	Total Solid	(tonnes)
U_{ec}	Greenhouse Emission Cost	($USD)
USD	United State Dollar Currency	($USD)
Vobus	Terminal Voltage of Synchronized Generator	(V)
Xoreact12	Impedance of Synchronized Generator	(Ω)

Acronyms

C	Carbon	(kg)
$C_d H_e$	Unburnt Hydrocarbon	(kg)
CH_4	Natural gas emission	(kg)
$C_{-6}H_{-12}O_{-6}$	Carbohydrates	(kg)
$C_{-12}H_{-24}O_{-6}$	Fats and Oil	(kg)
$C_{-13}H_{-25}O_{-7}N_{-3}S_{-1}$	Protein	(kg)
CO	Carbon (I) Oxide emission	(kg)

List of Abbreviation (Continued)

CO_2	Carbon (IV) Oxide gas emission	(kg)
Cu	Copper	(kg)
FB	Flow batteries	(V)
H_2	Hydrogen gas emission	(kg)
H_2O	Water gas or steam emission	(kg)
K	Potassium	(kg)
Li^+	Lithium-ion battery	(V)
N_2	Nitrogen gas emission	(kg)
NH_3	Ammonia gas emission	(kg)
NO_x	Nitrogen Oxide gas emission	(kg)
N_2O	Nitrogen (I) Oxide gas emission	(kg)
O_2	Oxygen gas emission	(kg)
O_3	Ozone layer	(kg)
PM_X	Particulate Matter	(kg)
P	Phosphorus	(kg)
SO_2	Sulphur (IV) Oxide gas emission	(kg)
Zn	Zinc	(kg)
Zn-Brm	Zinc Bromide flow batteries	(kWh)

CHAPTER 1
INTRODUCTION

1.1 Overview

The electric energy supply to remote environment and areas in isolation is very important in obtaining livelihood improvement and economic growth in other to attain development in these areas [1]. The application of fossil fuel power plants and extension of grid system are informal (traditional) methods of electric power generation and supply to the areas (remote and isolated) which is becoming less attractive as an alternative due to depletion in the resources of fossil fuel, globally, and its inconveniency in transportation towards the isolated/remote areas causing environmental pollution. The extension services of grid system to the remote environment and communities in isolation can be uneconomically viable as a result of high capital investment [2]. The utilized renewable energy sources have led to extensive attraction with reduction of emission (pollution) as an advantage, globally. The unstable and uncertainty in the nature of renewable generators (solar photovoltaic system and wind generator) and their respective resources (solar irradiation/wind speed) have attracted issues on over sizing the components so as to secure energy system's reliability, thereby causing increment in the power system's cost. To overcome these constraints, integrated renewable energy sources combining various alternative resources with energy storage or a backup fossil power plant can produce effectiveness in cost estimation and reliability of the generation sources for remote/isolated villages having limitation or no connection to the grid system [3].

Integrated renewable energy sources in island (off-grid) and grid integration were studied and reviewed with respect to their different architectures, optimization and planning techniques [4]. The integrated island/off-grid mode alternative energy sources for isolated/remote areas electrification have been developed globally in developing countries on a wide variation [5]. An integrated off-grid mode biogas generator/solar PVs plant system was designed to produce reliable electricity for a residential area and farming agriculture in Pakistan within a small village [6]. An independent integration of hydropower-solar PVs plant-wind turbine plant-storage (batteries) system was analyzed and used in the electrification of a rural village (located in the southern part of India) [7].

Hence, the previous research possesses a limited concentration on a specified energy system at a particular location having lesser discussion and analysis on potential capacity and flexible hybrid alternative energy system as proposed under different scenario in terms of external infrastructural condition subjected to changes when connected to the grid system. The grid mode connection of hydropower plant was designed to serve the energy demand (load) from Pakistan with remote villages [8]. A grid integration of biogas generator-solar PVs plant-fossil power plant (diesel) system of a village in Iran was achieved by adopting technical analysis and optimization design [9]. In [10], a technological-economic performance study was carried out on the feasibility of island fossil power plant (diesel)-solar power plant system connection to the national generating grid in Tanzania. Previous research has not focused much on the interaction impact between the grid energy system and the renewable generating sources.

The optimal system architectures and their respective sizing was used to analyze the technical-economic value of the integrated renewable production sources in terms of energy system's cost analysis [11]. Furthermore, the production of electric power and energy from individual energy resources was analyzed annually in [12]. The fuel prices, solar insolation and wind speed as the available energy resources was used as a variable study to calculate the response analysis (sensitiveness) of the energy system [13]. The investigation from the variation effect of the optimal energy system architectural components' cost was carried out [14]. The authors in [9] considered variations in sensitivity imbalanced economical modes (conditions) including main economical indications (inflation and discount rates) of the optimized energy systems' architecture. The future growth of villages/communities in isolated/remote areas and transition of events are not fully sufficient in relation to energy demand growth and incentives of government policy as considerations from the various research works done by different scientists/authors.

1.2 Review on Wastes to Energy Management

The generated municipal solidified wastes (non-liquid wastes from households, individual person, hospitals, schools, etc.) and non-municipal solidified wastes (large wastes categories from industrial, mining, and agricultural wastes) are increasing due to global population growth. The accumulation of garbage wastes (food wastes) is caused by denser areas that are populated and tourist attracted environments [15]. Enormous volumes of biodegradable substances and agricultural wastes pose some challenges to the agricultural sector making consumption for humans and wastes from livestock unsuitable. The yearly global waste production value in estimation ranges from 7.0×10^9 to 9.0×10^9 tonnes/year, beyond 2.0×10^9 tonnes/year of municipal solidified wastes [16-17] whose production projection's value by 2050 is expected to attain a value of 3.40×10^9 tonnes/year. Close to 33.3 % of food production for consumption by human was discarded with an estimated value of 1.30×10^9 tonnes, yearly [18]. In modern societies, the issue associated with wastes and management of wastes has attracted devoted efforts in reducing accumulated wastes in landfill areas, separation of wastes as a developing process in countries that are developed, making disposal recycling of wastes cheaper and easier. Most biological wastes are compostable and can undergo natural decomposition and burning process.

The by-product of treating industrial wastewater and municipal wastes is waste sludge generation which requires disposal. Irrespective of reducing wastes effectively, ending up as landfills, conventional processing can pose several adverse effects to the human environment comprising of greenhouse effect emissions with soil, groundwater, and air contamination. The wastes-energy conversion (formation of gases) technique is one of the environmentalisms in friendly management process of wastes by which wastes from biodegradable substances are processed into gasification (biogas) by anaerobic breakdown (digestion) reaction. The biogas power plants utilize biomass resources efficiently, reduce CO_2 emissions, friendly energy to the environment and possess impact economically in a favorable way. In general, accepting biogas power plants from residential areas is welcoming, however, the harmful effect due to generally accepting the

biogas system arises from odors which is not pleasant within the biogas power plant's vicinity, hazardous nature, noise pollution, food productivity competition and traffic [19].

Generally, raw biomass materials for biomass gasifier plants can be categorized into 6 components namely.

1.2.1 Animal Wastes

Animal wastes comprises of urine, manures from animal, washing stables' wastewater which are ideal for anaerobic breakdown (digestion) as raw materials. The animal wastes' estimation is a function of the animal category, weight of animal, method of feeding and ingredients of feed [20]. Animal manures are in substantial quantities having low content of drying matter, resulting in low yield of biogas per unit of the constituent (raw material) processing and elevated transport digestate or constituent costs as disadvantages. In addition, animal wastes may consist of antibiotics and heavy metal compounds possessing effects during the anaerobic breakdown process or in reusing digestates which is unfavorable [20-21]. The final product's quality is affected by the organic matter content of the material in a significant way and the content of moisture and stimulating micro-organisms growth [21]. Recently, implementing the concentration of freeze technique is another method of recovering agro-industrial waste digestate's nutrients, making easy transportation of animal wastes when its volume is reduced [22]. The old (traditional) methods of dehydrating high moisture materials are expensive with negative effects on the environment. The most suitable method for municipal solidified wastes, paper industry, pulp wastes, green wastes and residual from sewage treatment is bio-drying. The wastes are dried (auto-thermal processing) when there is a release of thermal energy during non-combustible breakdown of biodegradable wastes' fraction (anaerobic breakdown) by the influence of micro-organisms (bacteria and fungi) while the concentration of air circulation (aeration) removes the moisture [23].

1.2.2 Field/Garden Wastes

This is another raw material (field/garden wastes) that can be used to produce biogas, high biogas yield per fresh weight unit, low cost of transportation, boosting high fraction of dry matter and low liquid digestion production. The high cellulose, lignin and hemi-cellulose levels require lengthy time of retention for digestion. The ratio of carbon-nitrogen is beyond 50 which is not favorable for micro-organisms normal growth, alongside increasing delay in starting up the anaerobic breakdown or delay in starting up the biomass gasifier generator [20]. The increment of bio-stabilization effectiveness, low consumption of energy and shorter periods resulting from mixing wastes with additives to achieve uniform results, more than 7.50 % of digestate added, reduced the carbon-nitrogen ratio and accelerates the processing, consequently [24]. Removing residues from the digesters poses difficulty during field and garden wastes' processing [25-26]. The maize possesses the highest yield of biogas with wheat and rice as follows [20, 27].

1.2.3 Organic Industrial Wastes

Organic industrial wastes comprise majorly of processing fruits, sugar, food, starch, and beverage wastes production in large proportions. The most suitable wastes for bio-digestion possess high fats, hydrocarbon contents and proteins [28-31].

1.2.4 Municipal Solidified Wastes

These are solid wastes generated or produced from people on daily basis including wastes from households, cleaning, and commercial activities. The compositions of organic wastes are fractions of garden wastes, households' wastes, and similar wastes from organic matters. Plastics, metallic, glasses and sand impurities can negatively affect the biomass generator's operation; hence, the impurities must be removed before operational performance [20, 27, 32-34]. The process involved in bio-drying reduces some pathogens' number or eliminates them completely. The abundance of Escherichia coli's effect on municipal solidified wastes cannot be satisfied completely. A major challenge with Escherichia coli's resistance as a drug is its outspread over the coverage area of landfill and its adverse effect on personnel treating wastes' processing and storage operation [35].

1.2.5 Food Wastes

Food wastes composition are restaurants' food waste, hotel wastes, kitchen wastes, canteen wastes, fruit processing's' waste, flour wastes, fat and vegetable's wastes, etc. when compared with other wastes' type, high contents of impurities, salt and fat are present in food wastes which include utensils, bones, and other parts of kitchen wares that can cause damages to pipes, equipment and pumps which must be taken away during the stage of pretreatment [36-38]. Hot trub productions from breweries in large quantities where beers are manufactured occupy landfills. The wastes source from hot trub is valuable for energy conversion process (wastes to energy) containing Escherichia coli. Hot trub from recent research is applicable as cosmetology or sedatives in medicine which can reduce landfill deposit quantities [39]. Disposing breweries' sediment by directing them to municipal sewage system will increase wastewater treatment's cost which is not rational from economic and ecological viewing point [40].

1.2.6 Sludge

Sludge from municipal solidified wastes consists of other forms of sludge and wastes production from treatment of municipal wastewater plant with high content of water, enormous volume and instability. During the processing of primary and secondary sedimentations, sludge is produced with high concentration of organic matter having a simple digestion and anaerobic treatment suitability with possession of manure from animal producing biogas as a similar capacity. The central focus is to diminish the growth and wastes' numeral from food and global municipal solidified wastes rapidly; current technologies in managing wastes serve as a burden to the human atmosphere, the adoption of anaerobic breakdown processing makes biogas production the most alternative solution in an attractive way, contributing to de-carbonizing the society at the same time. The wastes are processed, leading to higher proportion of gases from renewable energy system of the energy sources. The purification and upgrading of the biogas production to bio methane involves investment on energy technologies in existence that can enable injecting bio methane into national networks of methane gas and promoting the application of bio methane fuel for fuel cell vehicles, thereby, reducing emissions from greenhouse gases.

1.3 Challenges of Waste Management

Managing wastes of different categories poses constraint due to heterogeneous nature they exhibit. The challenges of waste management are not limited to developed countries, globally, having high populated density producing enormous waste quantities. It (constraints of waste management) is not only associated with tourist countries that are highly developed with excess food. Managing wastes in rural areas and countries undergoing development is also an important challenge due to improper awareness, low social-economical position of the major population, technologies/improper management and treatment of the wastes.

1.4 Constraints in The Environment

Improper management of wastes can cause hazard to the environment thereby leaving negative impact to the atmosphere, leading to air contamination from generation of gases through combustion process, incineration of wastes and landfill release. Air contamination in the environment can cause health challenges when bacteria spread to the atmosphere, penetration of rodents and flies from landfill, resulting in the release of greenhouse gas (CO_2, CH_4) footprint. The ground water can be contaminated through landfills of municipal solidified wastes leading to leachates that are uncontrollable [41-45]. Composts and landfills comprise of accumulated food wastes' growth in quantity causing increased emission of greenhouse gases, increased rate of consumed water in agriculture and the application of plastics in packaging food unnecessarily [46]. The generation of wastes from agriculture through livestock farming, intensively, causes pollution on the soil despite the consideration of manures from animal as an additional benefit to the soil by enriching its (soil) organic matter and nutrients in maintaining the soil properties, physically in terms of retaining moisture and structure of the soil.

The excess application and recurrent use of manure to the soil has led to accumulation of heavy metals (copper (Cu) and zinc (Zn)) and macronutrients (potassium (K), nitrogen (N), and phosphorus (P)) thereby causing harm to animal's health when they feed on pastures predominantly. Farming through livestock causes water pollution which is related with removing soil's minerals while beyond hundreds of gaseous compounds

causes air pollution through releasing gases to the atmosphere (environment) by the system of ventilation, forming fresh deposit or excrete storage with microbe reactions from urine, raising ammonia gas (NH_3) and smelling gases from fowl [47]. Processing wastewater and treating sewage sludge produces the same soil pollution's effect as intensive farming from livestock which (negative impact) can be delayed or instantly, depending on the method of waste disposal or managing wastes [48].

1.5 Related Challenges on Methods of Waste Management

Human activities involving electrical and heat energy production produces 25 % of greenhouse emission (gases), 24 % of emission from forestry, agriculture and land application varieties, 21 % of emission from industries, 14 % of emission from transport sector, 6 % of emission from buildings and 10 % of emission from other energy sources such as natural gas (CH_4), carbon di oxide (CO_2), nitrogen mono oxide (N_2O) and gases from fluorine [49]. The easiest way of managing wastes with lowest cost generation is through public landfills, requiring no personnel with a highly qualified position. They (low position personnel) are the most adopted solution for waste management irrespective of their harmful effects (wastes) to the human health. Gases from landfill produced by organic matter decomposition in the process of anaerobic breakdown has a major effect (pollution) on the environment and represents the lowest favorable alternative in the rank of managing wastes. The gases comprise of natural gas (CH_4), carbon di oxide (CO_2) and beyond 200 organic compounds that are volatile (non-natural gas) [50]. Emissions from landfill possess effect on the depletion of ozone (O_3) layer and change in climate causing eco-toxicity, acidification and eutrophication. There is possible spontaneous explosion, ignition and draining surface contamination at the precipitation stage with pollution occurrence from ground water and soil during wastes management. Pollution from ground water will be intensively reduced if there is a system for appropriate treatment of leachate on landfill [51-53].

Combustion reaction can occur spontaneously and faster when polymeric materials (decomposition of wastes organic matter) are stored as a result of anaerobic breakdown of some parts of organic matters, which can be avoided by the addition of calcium oxide doses in small quantity thereby causing deactivation and elimination of micro-organisms

effectively from recent research view [54]. Managing organic wastes to attain sustainable soil and environment serve as a practice in composting with minimum emission effect to the environment. The pit of composting assists in controlling the carbon coverage area and limiting its harmful effects to the atmosphere against poor methods of disposing wastes [55]. The incineration of wastes is not appropriate for high moisture content of wastes, wastes having low values of calorie and wastes with chlorine. The management of such wastes releases materials that are toxic to the environment which is a major concern with harmful effect on the human health leading to more emission of greenhouse gases. In addition, incineration plants with low rating (power) possess efficiencies that are low. Personnel with higher qualification are assigned for this operational task requiring high capital/operational and maintenance cost [51, 53].

1.6 Problem Statement

The addressed challenges facing the existing energy system technology and the proposed energy network design are stated below.

Microgrid network flexible operation with unstable load (energy demand), biomass gasifier generating fraction and energy penetration on utility grid network, econometrics and technical reliability of the utility grid-biomass gasifier generator-batteries generation network, and biomass feedstock (fuel energy) conversion to electricity and applications.

1.7 Purpose of the Generating System's Design

The purpose of the proposed generating system technology (biogas generators, grid system, Li^+, FB and Zn-Brm batteries) design is:

- To perform feasibility study and reliability measure on the technical operation of the hybrid generators' network architectures (grid system-biogas generators, grid system-biogas generators-Li^+ battery, grid system-biogas generators-FB battery and grid system-biogas generators-Zn-Brm battery).
- To perform the econometric analysis for each energy system's configuration setting which comprises of capital cost, operation/maintenance cost, overall net present cost value, energy consumption cost and inflation on electric energy tariff in relation to sensitivity analysis, respectively.

- To determine the energy production fraction from each component of the architectural system design (biogas generators-grid system-Li^+ battery, biogas generators-grid system, biogas generators-grid system-FB battery, and biogas generators-grid system-Zn-Brm batteries), respectively.

1.8 Scope of Research (Proposal)

The integrated power system (biogas generators, grid network and batteries) will involve an experimental design from the On-nut power plant management industry and a multi-control algorithm application on the microgrid system to build feasible architectures of the integrated energy system which will be optimized with simulation by a complex operation of HOMER PRO grid analysis network to produce the respective energy waveform sensitivity. The aims and objectives of the hybrid energy network are:

- To investigate different power generation management strategies for the integrated renewable generators (biogas power plant and grid system) by using hybrid lithium (Li-ion)-flow battery (FB)-zinc bromide (Zn-Brm) battery technologies to improve the energy system's flexible operation.
- To explore the available renewable energy (biogas generator) system in determining the optimization of the biogas generators-grid network configuration with reference to the most economically viable and cost-efficient operation between the biogas generator and grid energy system during power flow and energy production services within the community (On-nut).
- To investigate the performance impact of the batteries (lithium-ion, flow battery, and zinc bromide) on the various possible designed energy system architectures (biogas generators-grid-Li^+ battery, biogas generators-grid-FB battery, and biogas generators-grid- zinc bromide battery), respectively.

1.9 Outline of Thesis

Chapter 1: INTRODUCTION

Background study, overview, aims and objectives were described in Chapter 1.

Chapter 2: LITERATURE REVIEW

Review on technological approach to renewable energy sources, grid-alternative energy network connection, econometrics of previous hybrid energy system architectures was highlighted in Chapter 2.

Chapter 3: METHODOLOGY

Analysis and modelling of biomass resources (feedstock materials from On-nut community) for conversion to energy production, biogas generator-grid network-batteries, and biogas generator-grid system configurations, mathematical modeling of the energy sources-energy storage systems-energy conversion unit with their parameters for design, hybrid energy sources-microgrid system simulation analysis, technological-economic analysis of the grid-alternative power system configuration was adopted for this project.

Chapter 4: DISCUSSION ON EXPERIMENTAL AND SIMULATION MODEL

Results from the experimental model of On-nut biogas power plant generation station and simulation model of the biogas generators/grid network, biogas generators/grid network/Li^+ battery, biogas generators/grid network/flow battery, and biogas generators/grid network/Zn-Brm battery architectures were analyzed duly.

Chapter 5: CONCLUSION

Conclusion presents the final chapter of this thesis with critical appraisal and the most effective operational performance from the architectures of biogas generators in grid connected mode, biogas generator in island mode connection with storage systems, and biogas generators in grid connected mode with batteries in terms of their econometric values and efficiency. The need for recommendation of solid-state batteries and solar photovoltaic system to be integrated with the existing technology of the biogas generators-grid system network to boost the technical and econometric performance of the integrated power system network is essential, respectively.

CHAPTER 2
LITERATURE REVIEW

2.1 Renewable Share in Southeast Asia

The energy transition from Southeast Asia is a primary function of alternative energies rollout, efficiency improvement and end users' electrification. There is 50 % gap of emission between the policies in scenario stated and the scenario in sustainable development by 2050. Fuels with low emission such as hydrogen, bio-energy, capturing carbon/utilization/storage and hydrogen fuels possess important role in addition with methane gas replacing fossil fuels (oil and coal) with an approximation of 30 % gap of emission closure between the scenario in sustainable development and policies in scenario stated in 2050. The bio-energy's modern form can replace non-renewable fuels (fossil fuels) in transportation, production of power, industries and purified cooking. Southeast Asia has enormous mandate to hybridize bio-fuels in transportation and policies for co-firing support, present day cooking stoves, bio-methane and biogas. Bio-energy can be beneficial to the environment if feedstocks are sustainable and there is no competition with production of food and biodiversity's negative impacts [56].

Hydrogen fuel and hydrogen with low carbon (NH_3: ammonia, C_aH_b: synthetic hydrocarbon) can assist in the reduction of emission from industry and transportation with long distance. During the production of thermal power, co-firing ammonia with the thermal generation can assist in providing fuel with low carbon which is dispatch able. The exportation of hydrogen in small quantities to Japan started from Brunei Darussalam while Thailand; Malaysia, Philippine and Indonesia have engaged in pilot program of fuel cell and green hydrogen systems for power generation. Feasibility studies were conducted from Indonesia and Malaysia in co-firing ammonia gas in coal generators with plans to perform the same operation in Vietnam, Singapore, and Thailand. Capturing carbon/utilization/storage can reduce emissions of carbon di oxide (CO_2) from the generation of fuel and hydrogen having low carbon. Plans of executing 7 capturing carbon/utilization/storage projects on a large scale in Southeast Asia with multiple links to boost the processing of natural gas, storing gases at offshore and recovering oil. The scenario in sustainable development reported 50 % of liquid share between fuels that are

abated and low emissions. The annual average investment on these fuels amount to $10 billion USD till 2050 which is 50 % of today's investment level in non-renewable fuels (fossil fuels). Hurdles on several regulations and risk in marketing must be properly addressed in scaling up fuels (with low carbon) deployment in Southeast Asia. Fossil fuel with higher prices poses affordability and emission issues as a challenge despite technologies to reduce emissions. They (fossil fuel) are costly and immature. Malaysia and Indonesia have cooperation with Japan for the supply chain development on NH_3, H_2 and capturing carbon/utilization/storage with similar processing of initiative in Singapore and Thailand [56].

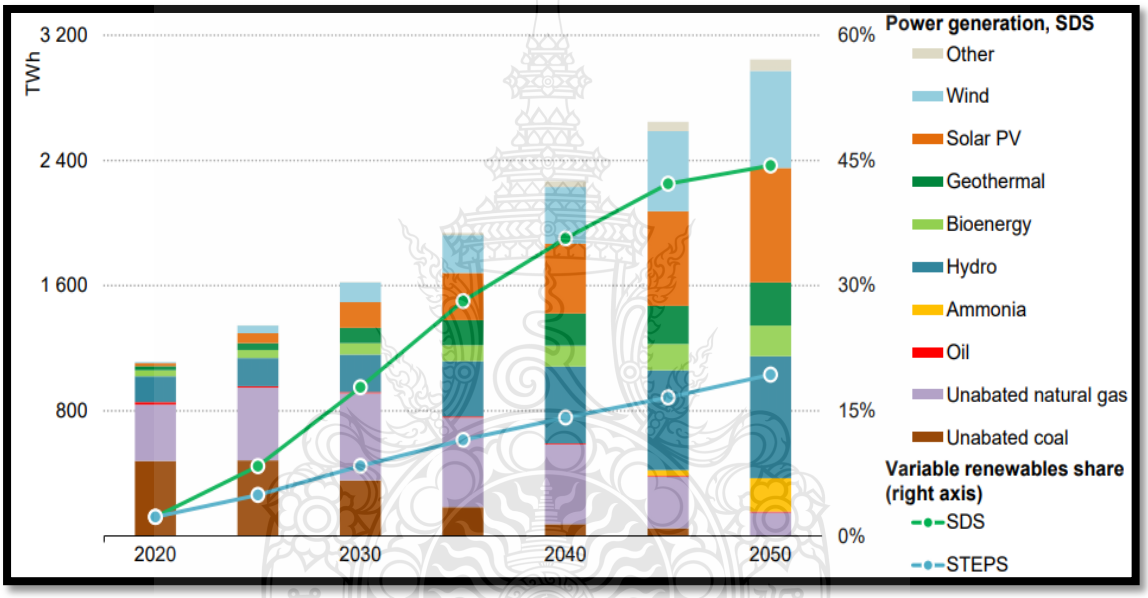

Figure 2.1 Renewable Share and Power Production in Southeast Asia; others (coal/capturing carbon/utilization/storage medium); SDS (scenarios with sustainable development); STEPS (scenarios with stated policies): 2020 - 2050 [56].

2.2 Energy Demand and Economic Growth in Southeast Asia

The economy and population growth in Southeast Asia has enabled the outlook projection of its energy sector, globally. Over the last decade, its (Southeast Asia) population growth has increased to 10 % with an estimation of 660,000,000 inhabitants

in the region. The average economic growth in Southeast Asia was 4.2 % between the year ranges, 2010-2019. The territories comprising of the interrelation of Southeast Asia countries are distinct in their developmental stage, geographical map, historical views, governmental practices/activities and industrial process. The per capita's energy demand in Cambodia or Myanmar is about 25 % of the global average while Singapore possesses more than 3 times of the global average. The economic growth in Malaysia and Thailand is due to their manufacturing increment while industrial services are a driving force for Philippine's economic growth. The priorities on energy policies for each country differs with their methods of approach in fixing new supply of energy to meeting energy demand expansion, climate goals achievement, accessibility to a reliable, affordable and contemporary (modern) energy system. The pandemic situation has affected Southeast Asia leading to a drop in gross domestic product (GDP) by 4 % and a fall in energy demand by 3 % in the year 2020. During the year's (2021) second half, there was a tremendous increment in the valuation of oil and gas due to intensification of Russia invading Ukraine at the early period of 2022, thereby, striping the energy security's risk, affordability and the increasing region's reliability on oil importation. Southeast Asian countries are most vulnerable to changes in climate, posing a serious threat to the region with frequent and violent increase in floods and typhoons. The region's resultant main (primary) energy demand has experienced a rapid increment over 20 years ago with increment in oil, methane (CH_4) gas and coal application with alternative energy usage. The steel, iron and cement industrial sectors form the largest growth level in a region. From the year 2000, the power production has risen to almost triple its value with coal fired energy generators producing the largest increment. The displacement of traditional biomass application in buildings by electricity is due to development in economy and population growth of the urban areas [56].

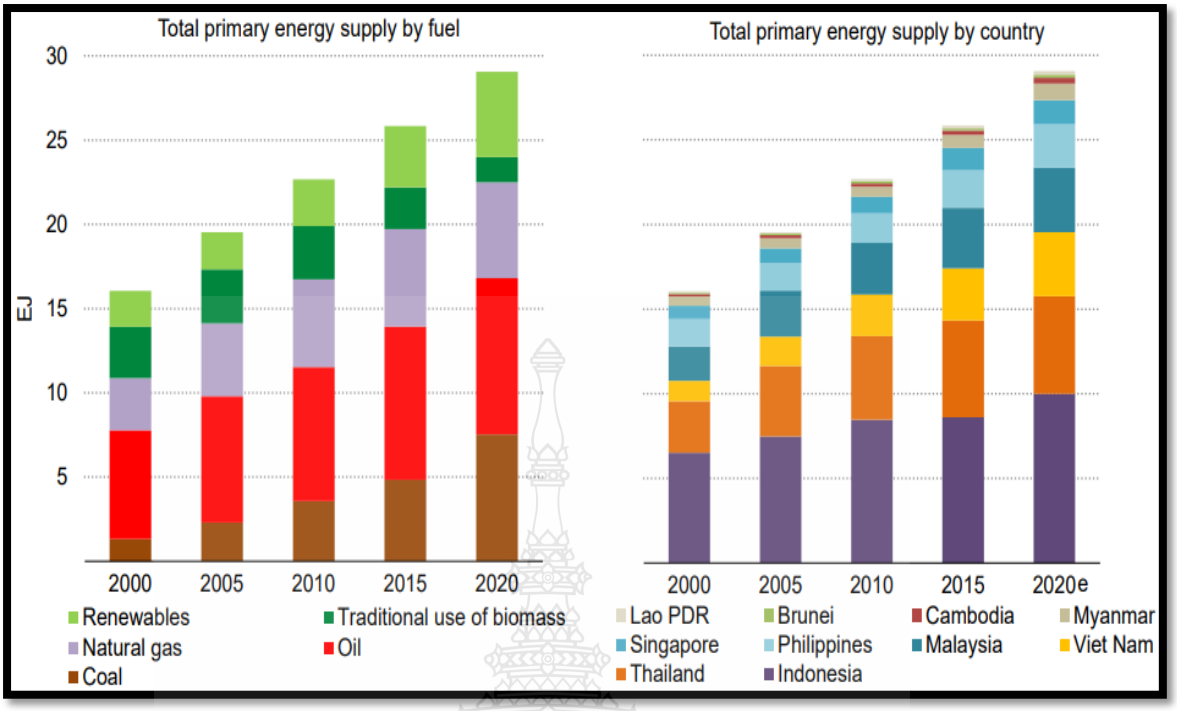

Figure 2.11 Overall Main Energy Supplied by Fuel in Southeast Asia: 2000-2020 [56].

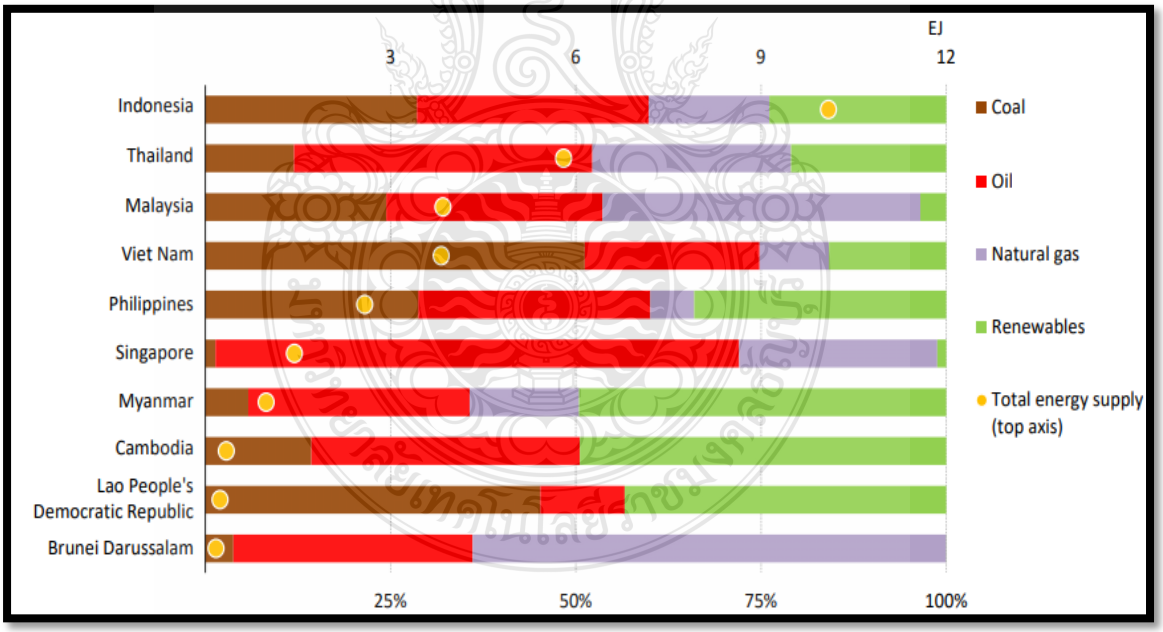

Figure 2.12 Overall Energy Supplied by Fuel in Southeast Asia: 2019 [56].

2.3 Fossil Fuel and Modern Renewable Energy

The population and economic growth in Southeast Asia have led to 80 % expansion of the total energy supply within the year range (2000-2020) despite a temporal drop in energy demand in the year 2020. Over 90 % of the energy demand's growth is made up of fossil fuels. The expansion factor from coal demand is 6 and its percentage ration in the gross supply of power rose from 8-26 % within the year range (2000-2020), respectively. From the year 2000, the demand increase in oil is beyond 40 % while its percentage drop in the total supply of energy share ranges within 40-32 %. Majority of the oil increment application arises from automobile system ownership growth: 27 vehicles/1000 citizens from 2000 to 59 vehicles/1000 citizens in 2020 with activities from truck freight and slight off-set from a drop in power production of oil-fired energy system. In 2000, the oil demand form 12 % of power production and dropped below 3% in the year 2020, an indication that oil form below 2 % of the overall power production in the present Southeast Asia below 20 % in 2000. The consumption of natural gas increased beyond 80 % within the year range (2000-2020) with 20 % maintenance of the overall energy mixture. The percentage application of natural gas at the industrial and electrical sectors today is 70 %. The energy production from the modern alternative energy systems is beyond twice the energy production in 2000-2020, respectively. The solar and wind energy power plants have experienced rapid increment in previous years. The present hydropower, geothermal, and bio-energy systems comprise of more than 98 % share in the overall present alternative energy in Southeast Asia. The main location of geothermal resources is in Philippines and Indonesia. Myanmar, Cambodia and Laos are involved in the development of hydropower's domestic resources over their high precipitation and hill terrains.

The biomass' traditional application (fuel for cooking) has reduced repeatedly over 2 decades, and its overall application split equally during the period (2 decades ago) due to action from firm policy to increase electricity access and shifting to renewable (clean energy as a fuel for cooking) energy. Accessing electricity share increased beyond 35% for the past 20 years to attain a higher percentage (95 %) in 2020. In totality, the trending region has concealed some situations at different level within nations individually. The

coal reliability, fossil fuel share, varies broadly across the sector/area/region. Malaysia and Thailand with manufacturing economies possess higher fossil fuel shares while Laos and Myanmar with lower economies rely heavily on agricultural activities [56].

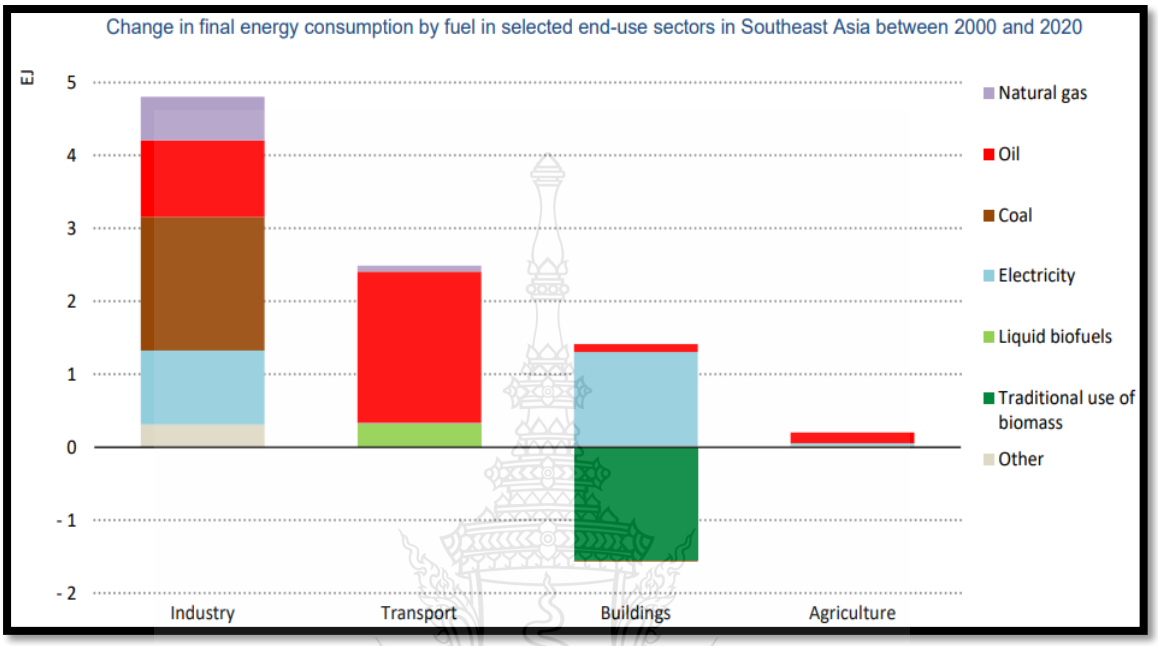

Figure 2.13 Transportation and Industrial Sectors Leading Energy Consumption Growth [56].

2.4 Previous Research on Econometric Value of Energy Systems' Configuration

The hybrid energy network from recent studies when considering off-grid (island) energy production in rural regions/areas has become a preferred option. The application of hybridized generation network in electrifying areas (rural) in Sri-Lanka was conducted by Kolhe et al. [57] and in conclusion was economically viable for the grid/island architectural condition with a diesel generator/solar/batteries/wind hybrid system. The energy source to load distance have an econometric feasible effect on a modelled diesel plant/batteries/solar generator system which was able to produce power reliability and more econometric feasibility than the fossil fuel (diesel) generator as demonstrated by Odou et al. [3]. The utilization of hydropower plant as an alternative energy-based system research project from a remote (Palari village) area in India provided an improved cost-effectiveness with analysis based on measurement from specific government in place in reducing cost will make the alternative energy-based system to be cost effective

otherwise, it may not be cost effective all the time as illustrated by Sen and Bhattacharyya [12].

A rural electricity study in India was presented by Rajbongshi et al. [1] which was observed to reduce energy cost when connected to the grid system. When there is capacity shortage from the hybridized energy network or peak energy hourly demand, the grid system can supply the deficit power through grid purchase. The electric energy's cost reduced to $0.0640/kWh from $0.1450/kWh according to their report study. Analyzing different architectures of hybrid energy network from China in Harbin's housing estate located in a cold weather, the world solar insolation affected the electric energy's valuation and the present valuation fraction values of the fossil generator (diesel) in the solar generator/diesel plant energy system. The utilization of the hybrid energy configuration in lower solar insolation areas experienced more feasibility than the fossil (diesel) plant as concluded by Li et al. [14]. Li et al. [58] carried out a solar PVs system's effectiveness in China with 5 climate (different) zones. The investigation showed that solar plant generators were essential component in the reduction of carbon (IV) oxide emission. The introduction of batteries (battery bank) when the generating grid was in connection with the solar plant system was not cost-effective. Hence, the solar plant/grid network system without connection to the batteries will be the most convenient architectural system under their investigation. A diesel/solar plant/battery/wind energy standalone system at a sea in south China's location in Malaysia for a huge center of resort was proposed by Hossain et al. [59]. The simulation analysis optimized the most suitable energy system from HOMER microgrid application software comprising of 240 batteries/3 diesel plants/5 wind plants/7MW solar generator/600kW bi-directional power converter. The wind speed range for the wind plant operation is 2.0-3.0 ms^{-1} ideal for Malaysia with low wind speed in consideration to their study. The energy system architecture reduced CO_2/greenhouse emission and was cost effective in terms of electricity/net present cost values from HOMER software application. The diesel price ($0.2/litre) of a power diesel plant (standalone energy system) at a time under a case study in one of the Saudi Arabia's (Rawdat Ben Habbas) village will be the most feasible option economically [60]. The hybrid configuration of the energy system illustrated a battery/diesel plant/21 % solar energy penetration/power electronic converter system's

feasibility at increased or decreased diesel price ($6/litre). Therefore, the feasible operation of the energy system's configuration was affected significantly by the diesel price. The application of IHOGA power software to manage energy system was conducted by Tawfik et al. [61] in optimizing energy sources' architectures that should accompany the pattern of energy demand on daily basis as a means of increasing the utilization of power directly instead of energizing (charging) the batteries.

The size of the battery bank was reduced effectively by the developed approach. The energy demand management pattern reduced the fraction of the present cost value by 0.154 and the charging energy of the battery by 0.513 leading to a factor value of 0.5 cost reduction of the battery, in addition, reducing the excess energy value to 0.557. An alternative energy generator was designed as a standalone energy source in Iran (Khash site) by Haratian et al. [62] consisted of wind turbine/solar generator/battery system. The solar generator/battery energy system was discovered to be the most valuable-productive energy source providing a present cost fraction of $8,173 and energy cost of $0.546/kWh. The cost might increase from the increasing discount rate as illustrated from the sensitivity analysis while the present cost fraction reduces. The wind speed differences (3-6 m/s) also had an effective considerable degree on the net present/energy cost values. The simulation design of diesel/wind/solar/batteries energy system for electric generation and reverse osmosis desalination in a remote region was carried out by Mehrjerdi et al. [63] with discoveries from the high concentration of alternative energy penetration on osmosis desalination system at the lowest energy cost level. A grid disintegrated solar/diesel/battery/wind energy generation system was designed and simulated by Elkadeem et al. [64] for an irrigation/agricultural application showing the fractional present cost (NPC) of the hybridized energy network to be $24.16 million with its energy cost level of $0.387/kWh having a 39.94 % positive investment return. The energy source network design could attain emission reduction of 95 % with much dependence on wind speed and solar insolation from the energy system cost based on sensitivity analysis. Gabra et al. [65] realized the effective performance of solar plant/diesel generator with wind turbines in small scale as a case study in Africa's remote areas with a conclusion on the feasibility of small, scaled wind turbine plants (depending) on higher average wind speed beyond 6.0 ms^{-1} in remote areas. Therefore, the application of wind turbine systems

was only on the Africa's horn while the diesel generator and solar plant were more feasible in other African countries, economically.

Further statement from the researchers on capital cost stability was caused by the lead acid battery/wind turbine plant maturity. In Ontario, Canada (sandy lake), the effectiveness of a 7-scenario hybrid generator system was developed by Rahman et al. [66] to determine the most appropriate efficient energy system comprising of different architectures of alternative based energy sources (100 %/80 %/65 %/50 %/35 %/21 %). The conventional energy system amongst the 7-scenario hybrid network produced the least energy cost ($0.34/kWh) with the highest level of emission (1,232 tonnes of CO_2/year). While 80 % of the alternative energy sources (renewable) provided higher energy cost of 72 % with lower emission (CO_2) level of 83 % based on the sensitivity analysis performance and discovering that lower rate in discount, higher speed of the wind and lower price of the diesel makes the hybrid energy system more economically viable when considering its energy cost. The above reports from several researchers have indicated the island hybrid generator (energy) system's implementation can be more preferable than the fossil plant system. Regarding effective cost, the cost of installing hybrid alternative generating sources is greater than the fossil fuel plants. The unstable fossil fuel prices weaken the fossil generators with little effect on the hybrid renewable generators. Hence, a reduced operating cost can be secured.

2.5 Unification of Renewable Energy System, Utility Grid Network, and Energy Reserve Systems

Challenges relating to frequency stability, energy/power feedback, intermittency of power generated from unstable renewable generating sources (solar photovoltaic plant and wind turbine plant), voltage sagging, voltage flickering, energy system efficiency, flexible energy system improvement, harmonics from reactive AC loads, and voltage fluctuation from the utility grid network are resolved by the services rendered from the renewable generators(power sources) integrated with energy reservation system. The energy reserve system smoothens and mitigates the generated intermittent power from unstable renewable energy sources (solar PV and generating wind plant) because of the varying resources (insolation from solar and wind speed) from the environment [67-72]. Frequency stability is very important for the island power grid system or microgrid

network to overcome power mismatch and energy demand by regulating the energy system frequency and maintaining power stability [67, 72]. The voltage of the distributed network undergoes regulation through the utilization of multiple energy storage systems being distributed which divides the grid system strategically into many regions where each region is implemented by voltage compensation through the energy storage distribution. Feedback power flow to the power generated sources that are not intentional can cause serious damage to the power system equipment and services rendered by the personnel. Increments in risk of feedback power flow have occurred due to an increment in the renewable generators integrated into the grid distribution network. When there is surplus electricity after meeting the energy demand, feedback power flow will occur, to avoid this hazard, it is necessary to utilize energy reserve systems in consuming the power from the renewable generating sources with minimization in the surplus power-energy production from the alternative energy systems than resizing the power distribution of the alternative sources lower than the energy network through energy demand where excessive power production from the renewable energy sources will be curtailed thereby limiting the development of renewable generating system and causing ineffectiveness in the utilization of energy [73-75]. Jia et al. [76] utilized energy reservation systems for the increment of renewable generation consumption by adopting a threshold method of variable charging/discharging for the management of the storage systems thereby improving their energy efficiencies to avoid curtailed energy from the renewable power sources.

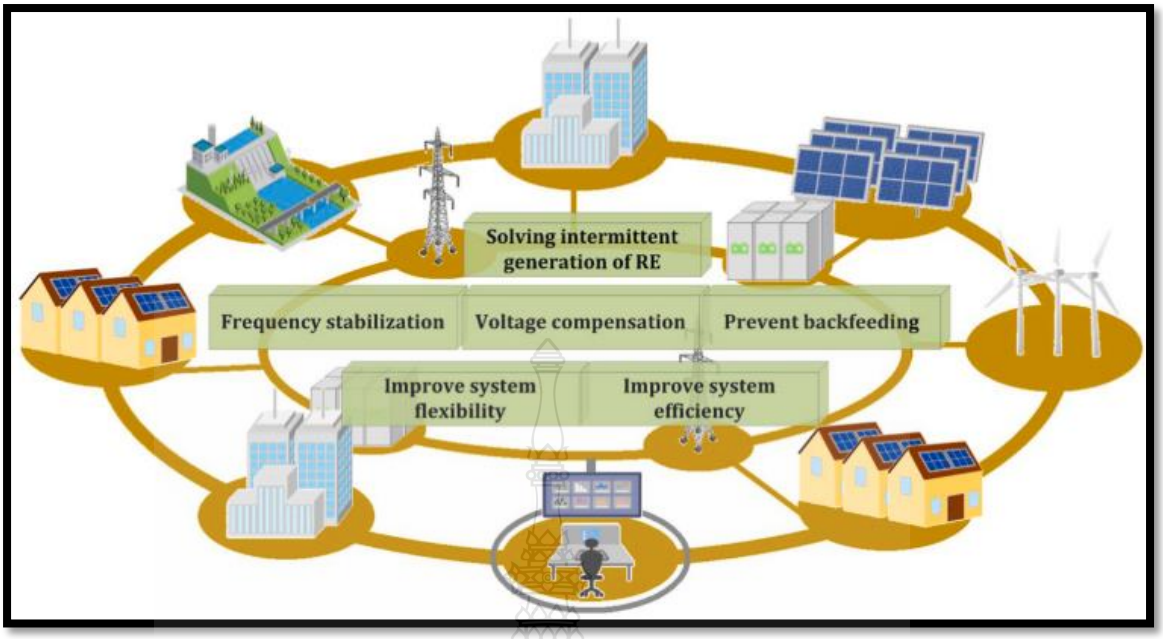

Figure 2.14 Energy Storage Services on Renewable Energy System/Utility Grid Network [67-76].

2.5.1 Integration of Renewable Energy System/Energy Storage Unit Configuration

The storage units support the renewable energy sources in different regions of the utility power grid (electric power generation, electric power distribution grid, microgrid conversion (AC-DC), off-grid (stand-alone) energy network, and smart buildings). Various configurations of the integrated renewable energy sources-energy storage applications are depicted below with their functions.

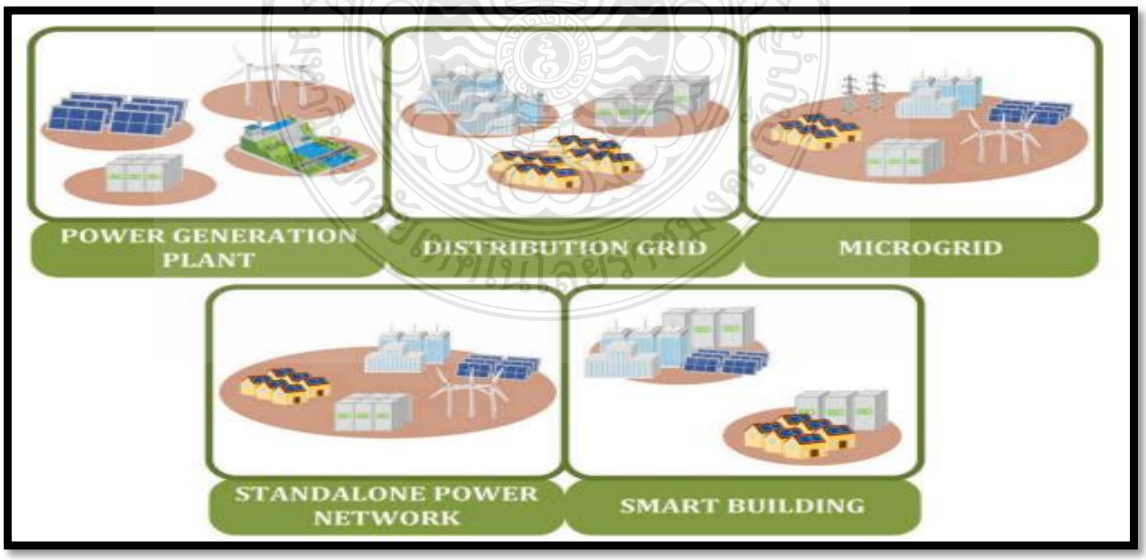

Figure 2.15 Application of Storage System in Utility Grid.

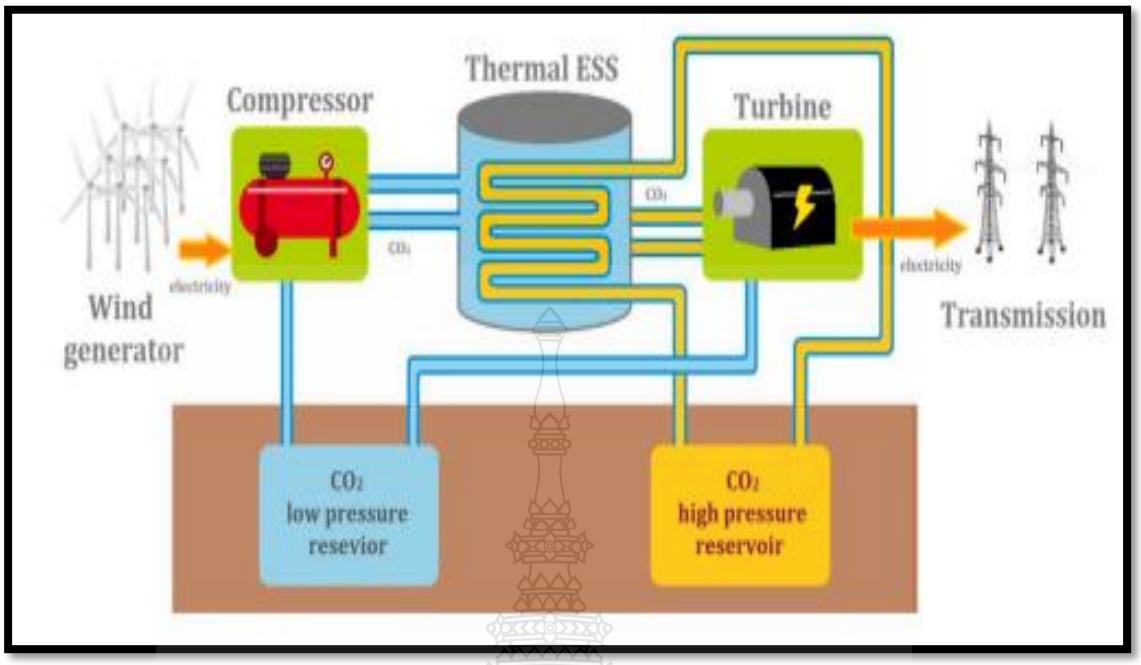

Figure 2.16 Configuration of CO_2 (Thermal compressed) Energy Storage: Wind Power System [77].

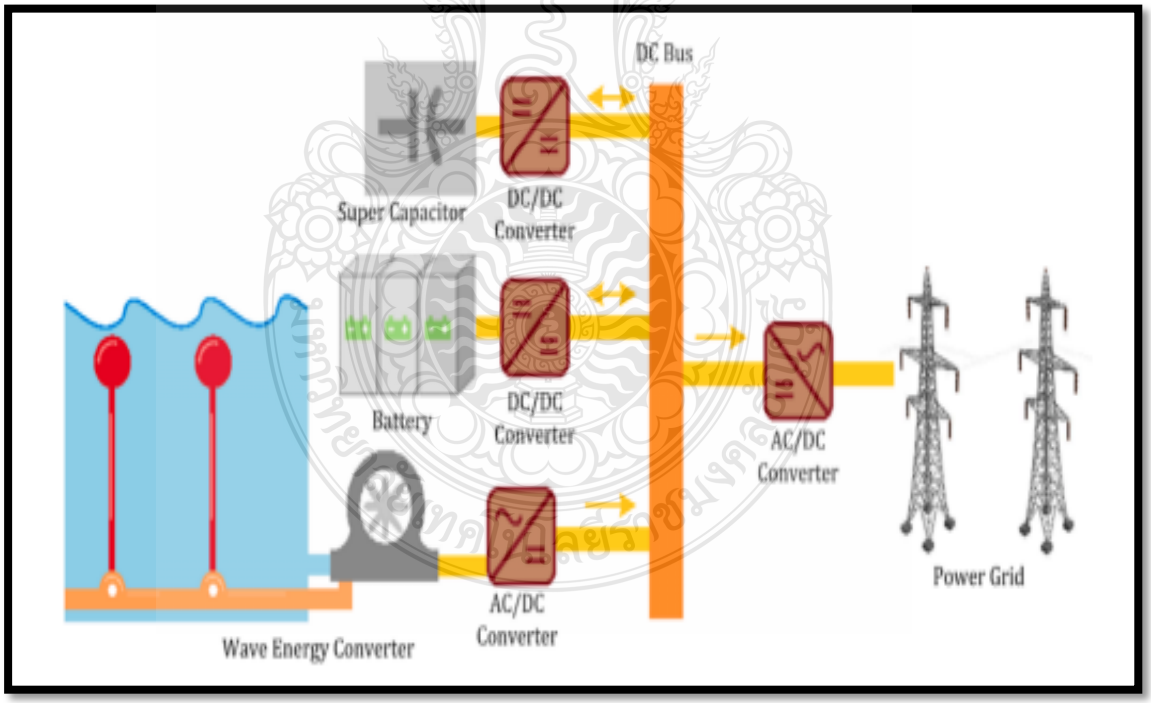

Figure 2.17 Hybridized Energy Reservations: Wave Energy Generation Architecture [70].

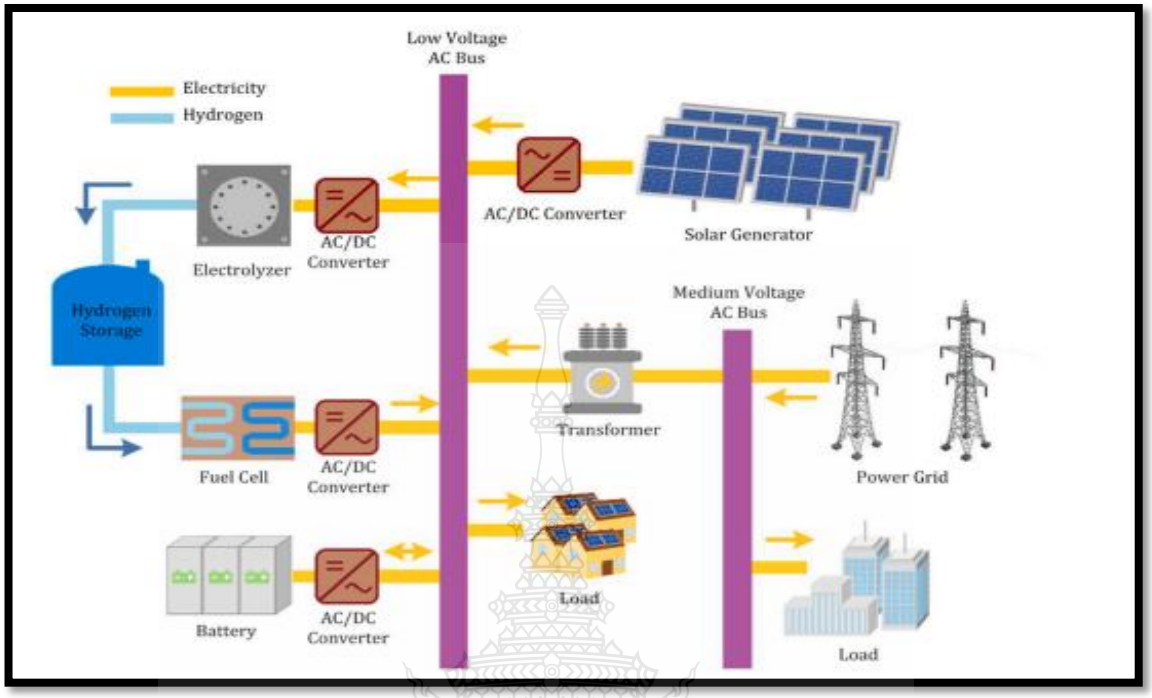

Figure 2.18 Hybridized Energy Reservations: Solar Power Distribution Architecture [78].

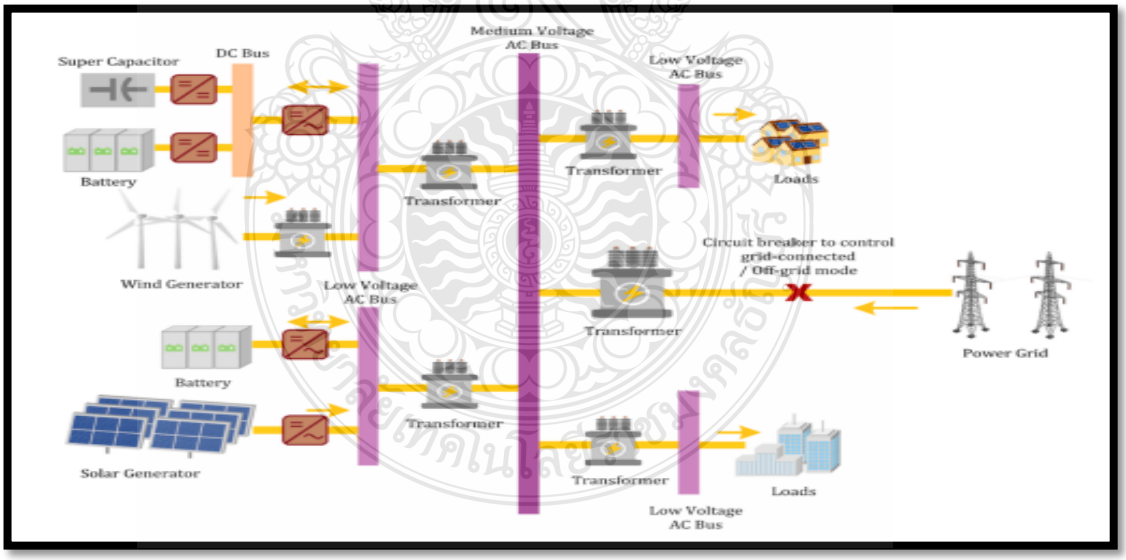

Figure 2.19 Energy Reservation: Alternating Current Microgrid Architecture [68, 73].

Inconsistency in the production of electric power and fluctuation in its amplitude is the major reason for restriction in the dispatching of renewable energy resources' properties which restricts the penetration of renewable generators' capabilities on the utility power grid network. The storage system balances the inconsistent power production and variation in energy demand. In Fig.2.16, CO_2 (thermal) energy is stored from the wind power energizing the thermal compressor which has high and low pressures of CO_2 energy storage from two caverns, electric energy produced due to excess power generated finds its usage from the compressor (compresses released CO_2) of low pressure to high-pressure caverns. The generated heat from compression is stored in thermal energy storage, when there is an increase in energy demand, high-pressure CO_2 will be released from the cavern and subjected to heat in the power turbine plant to produce electric power. Transfer of electric energy is stored in batteries, mechanical (kinetic) energy is accumulated in a flywheel system and heat (thermal) energy is accumulated in a compressed air system (storage). In Fig.2.17, [70] utilized hybridized generators for the regulation of wave energy harvest, AC energy is produced from the wave energy which undergoes conversion to DC energy by a rectifier, and the DC energy is stored in the batteries which can transform the dispatch able power sources before energy is transmitted to the AC loads. [78] increased the flexible renewable energy power distribution by proposing a hybrid energy storage tracking system to feed solar power distribution schedules from Fig.2.18, the batteries and hydrogen form the hybrid energy storage unit with regulation from short term conduction of the batteries providing fast response for the hybrid power system while large scaled-long term energy storage systems are done by applying hydrogen storage system possessing low losses and larger potential capacity. In Fig.2.19, Xu and Shen [68] and Li et al. [73] introduced a microgrid network operating on modal AC energy, the energy production from the hybridized generating plants (solar plant-wind turbine) was converted to AC energy and undergoes distribution through the AC bus to the AC loads.

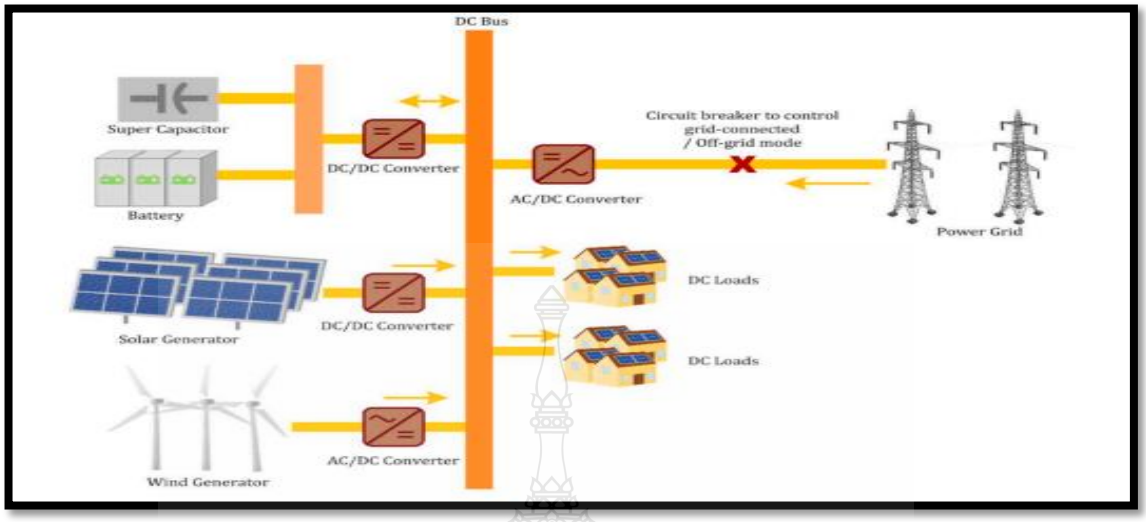

Figure 2.20 Configuration of Dual Energy Storage: Direct Current Microgrid System [79].

Ghosh et al. [79] proposed an ultra-capacitor (super capacitor) and battery bank as a dual-energy storage unit for a direct current (DC) microgrid network. The solar and wind generators supply power to the utility generator (grid) with support from the dual energy storage system and also energize the DC loads as shown in Fig.2.20. The wind generator and solar generator supply their power (DC energy) to charge the super capacitor and batteries by storing energy on them, the microgrid network utilizes the solar and wind generators effectively with few energy converters, a simple structure used and high energy-power efficiency.

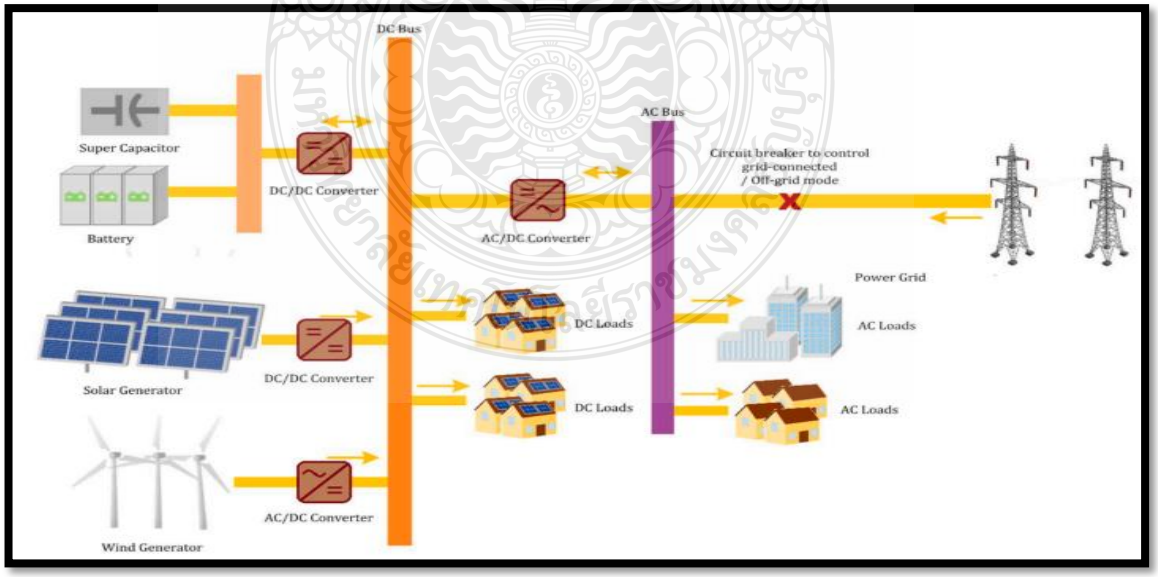

Figure 2.21 Configuration of Hybrid Energy Storage: Alternating Current Microgrid [71, 80].

In [71] and [80], there is a modification in the direct current (DC) microgrid network to back up the DC/AC loads by using a DC-AC converter which converts the DC energy to AC energy (inverter) from Fig.2.21.

2.5.2 Off-grid Network/Smart Building

Jing et al. [81] introduced an off-grid system (standalone energy network) to produce electrification and energization for the DC and AC appliances (loads) in a rural household as depicted from Fig.2.22 because transmission of electric power to low energy demand rural areas is not practically providing solutions. The off-grid network has a hybridized reservation system (super capacitor and batteries), solar photovoltaic generator, and AC-DC converter (inverter) in construction where there is an unavailable electric power network. The network architecture increases the energy system's efficiency and the hybrid storage flexibility. The hybrid storage system and solar PV plant are connected to the shared direct current bus passively with their sufficient capacities for power supply sustenance when one of the energy resources is intermittent (solar radiation). There are 2 configurations of hybrid energy set up which have an energy storage (batteries) system and a solar photovoltaic plant with a shared DC or AC bus on a smart building. An illustration from Fig.2.23 depicts both configurations on the building possessing effective utilization of connecting the shared direct current bus with more energy cost efficiency as the solar PV generator supplies power to the building and charges the batteries when the grid system is on or out of operation.

When the power grid is on and the solar photovoltaic plant operates below the required capacity, the power grid backs up the solar generator, energizes the building, and charges the batteries with a shared AC bus between the grid and the building. When both energy sources (solar plant and power grid) are at their fullest capacity, they both provide power supply for the building and as well charge the batteries [67, 82].

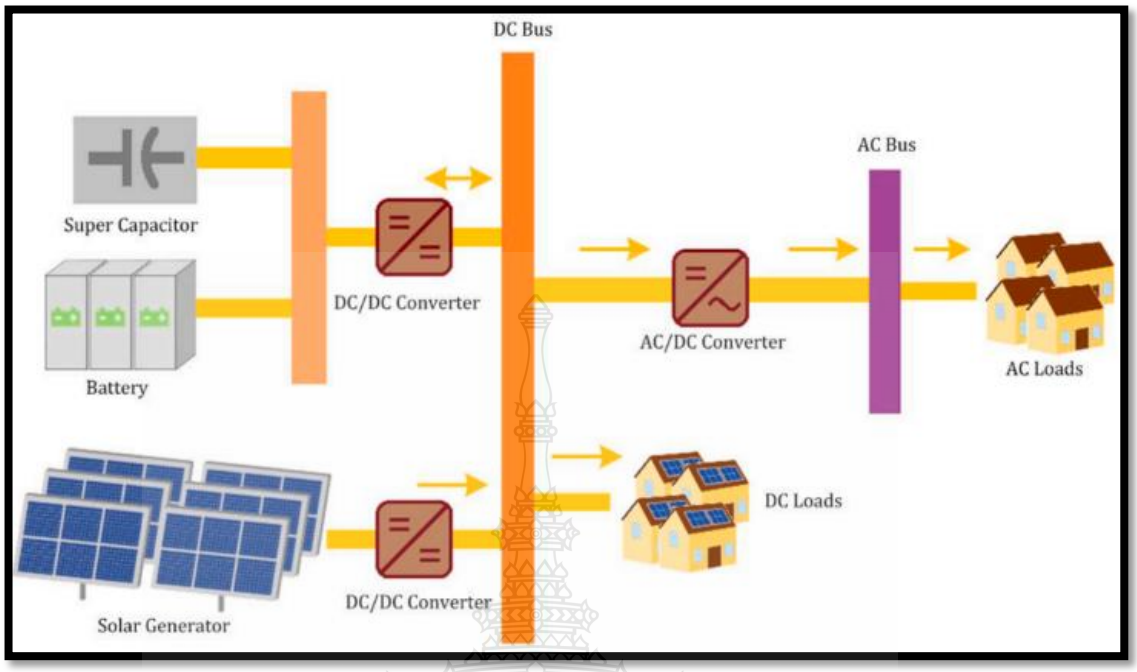

Figure 2.22 Hybridized Energy Reservations: Direct Current Microgrid Architecture [81].

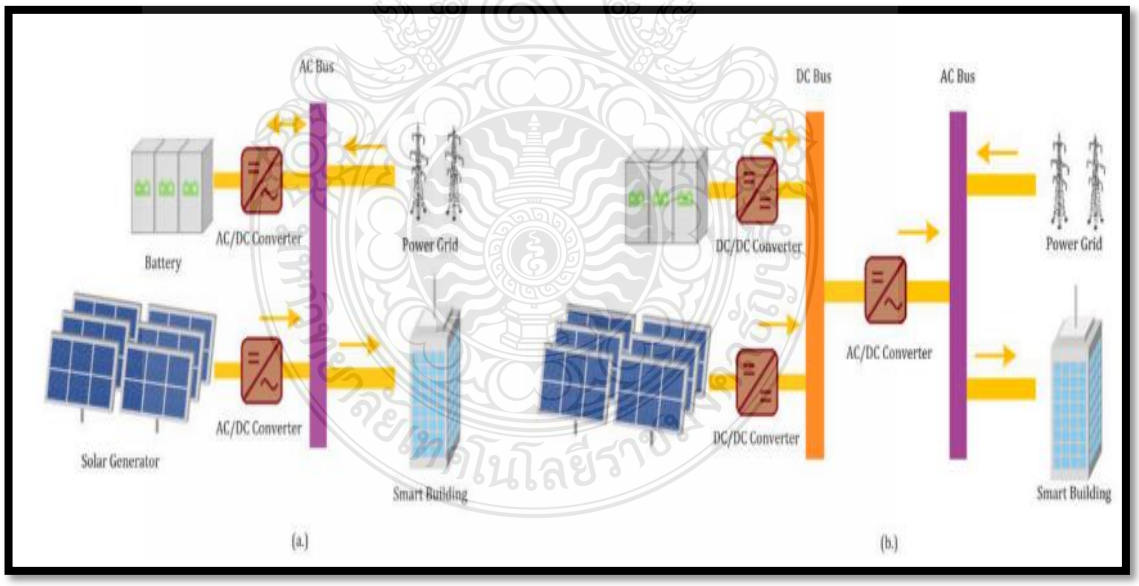

Figure 2.23 Configuration of Energy Storage: Smart Building System on Shared AC and DC Bus [67, 82].

Electric automobiles (vehicles) have been utilized to function and act as a replacement for energy storage units by adopting vehicle-power grid technology as a concept which was used by Aznavi et al. [72]. The successful utilization of electric automobiles to effectively manage energy flow and mitigates intermittent energy in smart homes from Fig.2.24 [72] was proven practically.

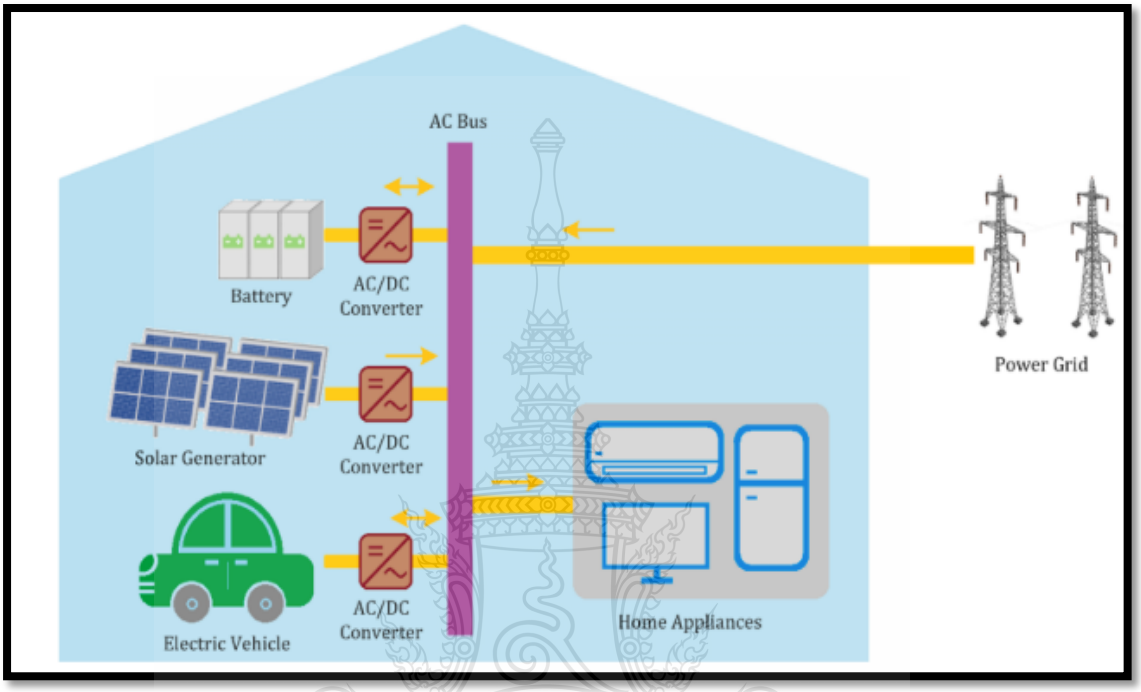

Figure 2.24 Configuration of Electric Automobile: Smart Environment System [72].

The current project proposal consists of a grid network, biomass generator, lithium ion, flow battery, and zinc bromide flow batteries power system with a multi-control functional system (cycle charger, generator order, and load follower) and bidirectional energy converter-charging controller that will operate as a communication interaction (interface) for the biomass generator, grid network and the storage systems (Li^+, FB, and Zn-Brm batteries). Where the biomass gasifier and the batteries will operate as a backup energy supply against outage, irregularity or schedule energy flow rate from the grid system within the community of On-nut Bangkok metropolitan area. The load following control system will allow the grid generator network to provide electric energy in feeding the loads (AC, DC, and deferrable) while the biomass gasifier will be responsible for charging the batteries and energizing the storage load (deferrable load), respectively. If the load following control unit with the generators (hybrid energy sources) are economically beneficial, the excess electric energy from the grid's ramp up will be sold

to the generating grid network. The cycle charging control unit allows the grid generator to operate at a full output power flow thereby isolating the biomass generator from supplying electricity. The excess electricity will flow to the dump load and charge the batteries, respectively. The generator order controller will provide a schedule operation for the biogas generators to support the batteries and grid network in order to reduce the operating cost of the microgrid network. An investigation on the technical-econometric performance analysis of the first biogas power plant at On-nut community in Thailand which consists of 4 architectures namely: biogas/grid energy system, biogas/grid/Li-ion battery system, biogas/grid/zinc bromide battery system, and biogas/grid/flow battery system in feeding the load will be experimented to determine the best cost-effective generating system, maximum energy distribution measure system and power efficient system from the listed architectural system design.

2.6 Energy Conversion in Biomass

The biological/physical/chemical/thermal processing of recovering or disposing wastes operation in conformity with regulations governing wastes, sorting of wastes, changing the wastes' properties by reducing its size (volume), biodegradable substances' content in facilitating waste approach or increasing wastes' recovery possibilities is known as waste treatment [83]. Wastes producing fuel can occur by a gasification/hydrolysis/pyrolysis processes known as heat (thermal) decomposition or through fermentation/anaerobic breakdown reaction known as biological process. The previous/current research has discovered that the incineration of wastes mixture, fuel gasification parts from organic wastes' application in raw materials and wastes for anaerobic breakdown (digestion) is economical [84]. The conversion of wastes to energy in a plant system is to reduce the size (volume), produce hygiene, avoid environmental pollution, adding nutrient to the soil, conservation of resources, general acceptability, hazard substance immobilization and cost affordability are the ultimate goals of biomass energy plants. Hence, the management of wastes remains a paramount issue. The percentage contribution of municipal solidified wastes in developed countries for energy production is 5 % of the gross demand in power-energy. The efficient application of biomass energy can lessen conventional fuel demand [85]. In Asian countries, about 73.0-

821.0 kg of municipal solidified wastes was generated yearly per capita while in European countries, the quantity generated was 560 kg yearly per capita. The yearly production quantity of wastes per capita is increasing steadily in all cases. The percentage composition of biodegradable wastes ranges from 25.0-80.0 % of all the available wastes, making biotechnology important at the engineering sector through managing bio-wastes in developing/developed countries. There are diversifications from organic wastes' origin. The wastes from agriculture, municipal solidified wastes and industrial wastes comprises of the overall wastes' quantity. Converting organic matters through micro-organisms by chemical reaction form the process in treating bio-wastes which digest and convert the organic matter to function in the ecosystem's nutrient cycle. The groups of microbiological process in organic wastes are broad and bound closely towards one another dynamically and metabolically. Adapting to factors of the environment can lead to instant undesired microorganisms in groups; therefore, knowing the interactive communities of microbes is very important in order to treat the wastes' organic fraction successfully [86].

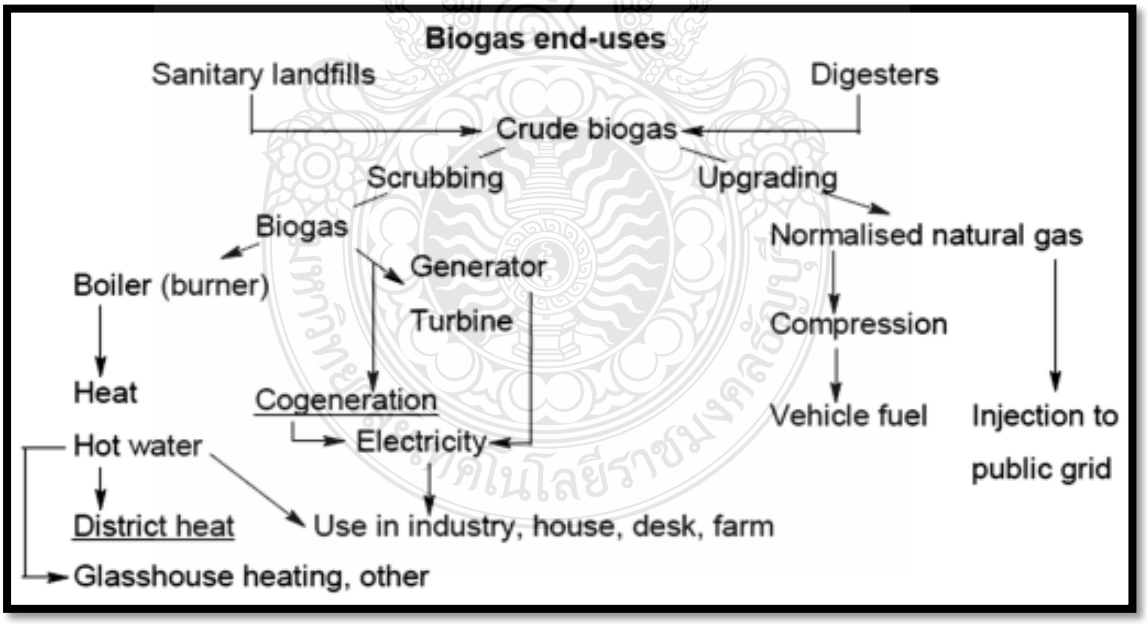

Figure 2.25 Energy Utilization of Biogas Production [103].

2.6.1 Fuel Production from Biomass

Bio-fuels from plants (biomass) are prospective replacement for conventional fuels and a better option of cultivating technologies to enable the sustainability of bio-fuels production [87]. The bio-fuels are renewable energy sources developed for emission reduction of greenhouse gases and global warming prevention. The classifications of bio-fuels are into 4 generations having a common goal of reducing emission from the environment and satisfying the world's demand of energy. The highest production of bio-fuels and efficiency from energy generation with lesser efficiency in emission reduction (greenhouse gases) comes from the first generational bio-fuels [88]. Hence, it cannot substitute conventional fuels (fossil) because of demand for food, involving suitable biomass application such as maize, wheat, and sugar beets, etc. [89]. The unsuitable biomass application such as grasses, woods, wastes and straws (producing bio-fuels) with effective cost limitations in its production increment to a feasible commercial level occurs at the second generational bio-fuels [90]. The least emission of net gases (greenhouse) requiring higher energy processing which is less friendly to the environment occurs at the third generational biofuels. The sustained capacity source for the production of biofuels in the future is represented by the raw materials of the third/fourth generational biofuels [91] which is non-competitive between fuels and food, serving as alternatives that is more favorable [92]. The application of macro/micro algae (microorganisms) as a raw material to produce fuel occurs at the third generational biofuels while modifying the genetics of the microorganisms through engineering algae's gasification and pyrolysis occurs at the fourth generational biofuels [89]. There are many challenges arising from plants' cultivation to producing biofuels ethically such as the intention of food growth for biofuel production purpose is suitable when considering crises of hunger from parts of the global environment. Microalgae producing biofuels has gone through extensive research in decades, recently. The capacity potential of 58,700 litres/hectare of oil production from microalgae which produces 121,104 litres/hectare of biodiesel in return seems optimistic as a substitute for fossil fuels [87]. The cheap and abundant non-suitable raw materials for biofuel generation are at the second generational biofuels. Much focus from researchers is on by-product of woods and forest trees (garden wastes/leaves/saw dust/grasses/chips from hard wood/bark of trees/branches). Raw material application can

also be found in distilleries' grain, breweries and cereal consumption [90]. The raw material application for producing second generational biofuels are wastes from forest, wastes from agriculture, energy yielding crops, wastes from industries and municipal solidified wastes. Energy production from biomass in liquid state can be processed from raw material of ligno-cellulosic through bio-chemical/thermo-chemical process of conversion. The raw material (feedstock) as a fuel source is heated with oxygen to form thermo-chemical process of conversion which completely converts the organic compounds. The evolution of CO and H_2 gases (synthetic gases) by gasification and pyrolysis process regenerates biofuel carbon of long chain based on the technology of fischer/tropsch Integrated with technology advancement (looping of calcium to capture carbon [89] in providing superficial/simplified ways of generating clean energy than conventional fuels (e-methane). The reliance on enzymes and microorganisms for converting cellulose/hemi-cellulose and sugar reduction generates the bio-chemical process of conversion which involves pre-treating the raw material of ligno-cellulosic, hydrolysis (biological/enzymes), sugar reduction fermentation and bioethanol advanced processing [90].

2.6.2 Anaerobic Breakdown Reaction

The biodegradable substance (material) undergoes chemical conversion to produce biogas during anaerobic breakdown (digestion), releasing natural gas (CH_4), carbon (IV) oxide (CO_2) and H_2O (water) through fermentation of microbes without oxygen, depositing behind an organic mixture in wet form which is partially stable. Anaerobic breakdown can be an applied wet process for moisture content materials above 85.0 % or an applied dry process for moisture content materials below 80.0 %. Less energy is required in anaerobic breakdown processing when compared to aerobic breakdown processing (requiring more energy), thereby, generating (anaerobic breakdown) smaller biological heat quantity [86]. The anaerobic breakdown process having different application potential of biogas production and digestate can be schematically depicted from Fig.2.26.

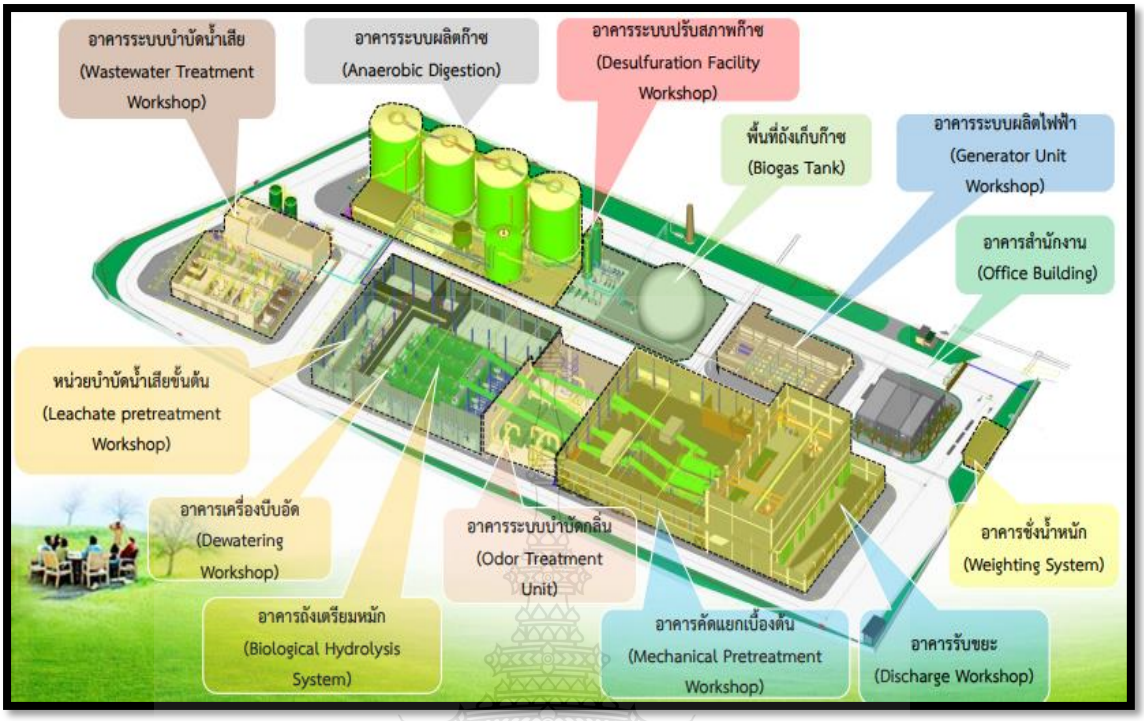

Figure 2.26 Wastes Management Process from Anaerobic Breakdown Reaction [93-95].

The conversion of biodegradable material to combustion of gases (biogas) occurs during anaerobic breakdown reaction process comprising of carbon (IV) oxide and natural gas. The onsite burning of biogas produces electric energy and heat which can undergo purification and application as a source of fuel. Furthermore, the biogas can serve as an external fuel supply to the national power grid plant using gases as a fuel source through national power grid gas injection provided the standard of purification after proper upgrade has been met. The leftover liquid or wet solid material is a suspension of the materials that are non-degradable (residues from microbes, digestate by-products, microbes and organic matters that are non-degradable). The digestate is known as the partial stabilization of the wet mixtures which can undergo advanced separation into fractions of solid and liquid substances [93-95].

In theory, organic substances (fats and oil, proteins, and carbohydrates) as components of all substrates are applicable for anaerobic breakdown. The equation of organic matter conversion to combustible gases (biogas) is written below:

$$C_aH_bO_cN_dS_e + zH_{-2}O \rightarrow yCH_{-4} + qNH_{-3} + nH_{-2}S + (a\text{-}y)\ CO_{-2} \quad (1)$$

Where $y = 0.1250\ [(4.0a + 1.0b - 2.0c - 3.0(d + 2.0e))]$ and $y = 0.2500\ [(4.0a - 1.0b - 2.0c + 3.0(d + e)]$ (2)

The equations relating the chemical reaction of carbohydrates conversion, protein conversion and fats/oil conversion into combustible gases can be expressed below.

$$C_{-6}H_{-12}O_{-6} \rightarrow 3[CH_{-4} + CO_{-2}]\text{: Carbohydrates} \quad (3)$$

$$C_{-13}H_{-25}O_{-7}N_{-3}S_{-1} + 6H_{-2}O \rightarrow 6.5(CH_{-4} + CO_{-2}) + 3NH_{-3} + H_{-2}S\text{: Protein} \quad (4)$$

$$C_{-12}H_{-24}O_{-6} + 3H_{-2}O \rightarrow 1.5(5CH_{-4} + 3CO_{-2})\text{: Fats/oil} \quad (5)$$

The production portion between the natural gas (methane) and carbon (IV) oxide is a function of the material's input composition and digestion's degree. This method aids waste management improvement in meeting the management of sustained energy production. The application of biomass wastes to generate biogas produces a neutral cycle of carbon. The anaerobic breakdown process occurs in ruminants' stomach and swamps comprising of natural environments. The duration process of anaerobic breakdown takes 3.0-6.0 weeks which depends on the material input's ease of conversion rate to combustible gases and the application of technological classification. The biogas energy yield can be increased through mechanical pretreatment, joint digestion of two or more organic materials, bio-reactor addition to the environment (bio-augmentation), gaseous biofuel's mixture (hy-thane), load rate of organic matter, designed pattern of the reactor and temperature [96]. The method of mechanical pretreatment involves preparing substrate and low temperature soluble mechanical substance heat treatment. It has impact on the energy yield of the biogas production during anaerobic breakdown process with sludge of wastewater because of the anaerobic breakdown acceleration consequence and higher capacity of dissolving sludge [97]. Wastes with high percentage of lignin concentration in wood matter require longer time to produce the desired yield of biogas energy. Recovering wastes from anaerobic breakdown process has its advantages and disadvantages as tabulated in table 1.

Table 1 Advantage(s)/Disadvantage (s) of Anaerobic Breakdown [93, 95].

Advantages	Disadvantages
Energy production by producing high quality soil fertilizer	Less heat released, resulting in lower and less efficient destruction of pathogens in aerobic composting
No need for additional power to turn the pile of waste for the purpose of obtaining oxygen	Unsuitable for waste containing less organic matter
Closed system allows the use of all produced gases	Requirement for waste separation to improve decommissioning efficiency
Monitoring greenhouse gases' emission	Pretreatment is essential
No unwanted odor, rodents, and flies	Temperature sensitivity
The modular construction of the plant and closed process require smaller land (footprint) areas	Post-processing is required
Net positive environmental gain	Two to four months of startup time.
Possible implementation on a small scale	
Low power consumption	
Almost complete retention of nutrients in the fertilizer	
Possibility to store sludge for a longer period	
Construction costs are relatively low	
Low sludge production	
Low nutrient demand	
High organic removal	

Anaerobic breakdown process occurs in four stages (biological-chemical) of reaction which are: hydrolysis, acido-genesis, aceto-genesis and methano-genesis, respectively. The breakdown's (digestion) first stage is hydrolysis. Organic matters in complex form (fats/oil, proteins and carbohydrates) are digested into molecules of organic substance solubilization comprising of fatty acids/amino acids/sugar and varieties of components. The volatility in the by-product of other toxic substances and fatty acids makes hydrolysis the slowest processing stage. Pretreatment of substrate can accelerate hydrolysis. Acido-genesis in the second stage (fermentation) involves digestion of hydrolysis' organic component into hydrogen, fatty acids in short chain, by-products' varieties and carbon (IV) oxide. The aceto-genesis process (in the third phase) of anaerobic breakdown involves transformation of organic acids from the second stage to acetic acid, carbon (IV) oxide and hydrogen. Methano-genesis (in the fourth phase) involves the production of methane by methano-gens in two groups where acetic acid is broken down to natural gas and carbon (IV) oxide by one group and the application of carbon (IV) oxide and hydrogen gas to produce methane gas by the second group [20, 98-102]. Raw materials' pretreatment can improve biogas energy yield through chemo-lysis reaction, pyrolysis reaction and enzyme-o-lysis reaction processing [95, 103-104].

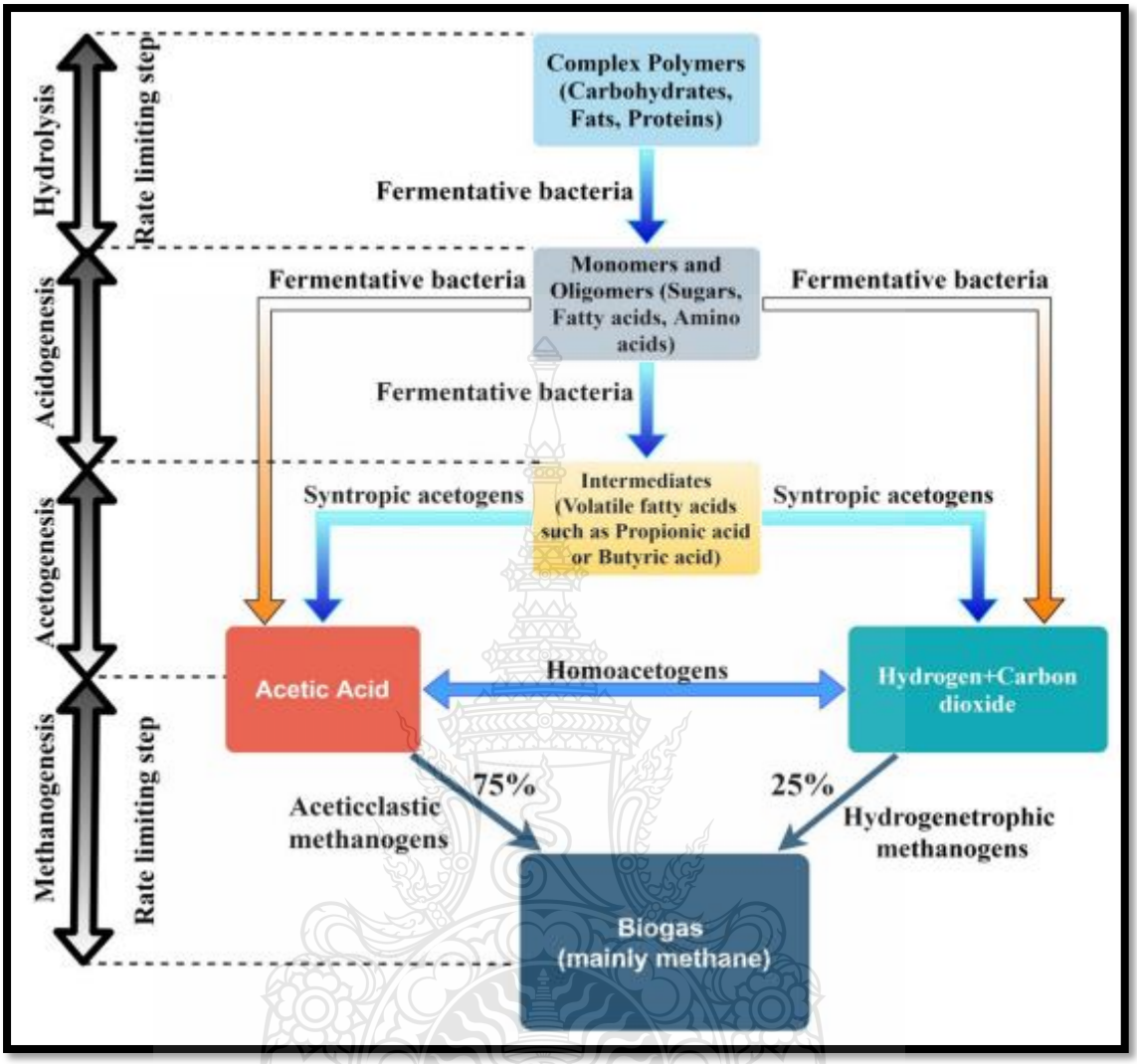

Figure 2.27 Production of Biogas from Anaerobic Breakdown Process [103].

Renewable energy production and wastes reduction emanates from the positive effects of anaerobic breakdown through aquatic plants application on it. Weed of alligator, growth of macro-algae/water plants in ponds, macro-algae and hyacinth form the aquatic plants which are built in eutropic water/wetlands artificially can undergo rapid reproduction containing organic matter in high concentration, thereby, enabling them as raw materials in an ideal way for anaerobic breakdown [20]. The application of water hyacinth as a raw material potential (feedstock) to produce fuel source (biogas) is rich in nutrients and nitrogen, possessing materials of fermentation in high contents. They (water hyacinth) are known as aquatic weeds growing fast [105-106]. The high rate of growth/biological production, survival at different zones of climate in the world, small water quality

requirement within the environment and low life process of duckweed (lemina minor) makes it a promising material for energy application [107]. There is ongoing research on bio-plastic anaerobic degradation showing poly-3-hydroxy-butyrate-co-3-hydroxy-valerate as the relevant bio-plastic polymers which can undergo degradation by releasing energy through anaerobic breakdown [108]. Globally, China possesses the largest biogas power plant (in quantity) from wastes [96]. The proportional value of digester system from agriculture in Germany amount to 1900 plants from a total digester plant value of 2,429 compositions in Europe [96]. The mobilized percentage value for the technical biomass energy capacity of animal wastes (manure) which was utilized for generation of energy in Germany was estimated to be 50 % [109]. In totality, from anaerobic breakdown, the biogas (bio-methane) technical capacity from the European Union by estimation range from 151×10^9-246×10^9 $N.m^3$ [96].

2.6.3 Combustible Gas (Biogas) Purification from Anaerobic breakdown Process

The anaerobic breakdown yielding biogas energy finds its application in combustion engines, space heating /cooling system for residential/commercial areas, competitive fuel price for transportation and generators/power gas turbines. Provided there are appropriate upgrades regarding the technologies of anaerobic breakdown process [96]. The major components of biogas energy are carbon (IV) oxide and natural gas (CH_4), respectively with oxygen, ammonia, nitrogen, hydrogen sulphide and hydrogen as accompanying impurities. The compositional volume of biogas energy ranges from 50 % to 75 % of natural gas, 25 % to 45 % of carbon (IV) oxide, 2 % to 7 % of vaporized water, below 1 % of hydrogen sulphide gas, and below 2 % of ammonia gas [108]. The composition volume is appropriate, generally, for applications with less requirement (from electric energy and heat production of power generator's residence) requiring minimum upgrade. The purification of biogas energy is needed by removing carbon (IV) oxide gases with other impurities that are not needed like compounds of sulphur for other varieties of application. The effect of impurities in the biogas system utilization causes explosion when there is high concentration of oxygen gases, corrosion from hydrogen sulphide gases, toxicity from chlorine gases forming poly-halogen-di-oxins [110], production of micro-crystalline silica deposit from siloxanes that create clogs as a blockage to free

movement of gases to the channeled vessel or pipe. The treatment of 60 % content level of bio-methane to methane will reduce the capital investment cost and cost of processing. Beyond 85.0 % of the natural gas (methane) content in bio-methane attains the minimal standard requirement from European nations which can be publicly utilized as a fuel source for automobiles [111]. Nevertheless, the high cost of processing the treatment with capital investment (treatment of bio-methane to methane) poses a setback [112].

2.6.4 Injecting Bio-methane Gases

The injection of bio methane to the grid system (using gas as a fuel source) producing electric energy is not difficult as bio methane and natural gas possess chemical composition similarities. The enablement of bio methane injection to the transmission power grid network requires more equipment in addition (injecting technology and upgrading the biogas). Investing on bio methane injection is economically viable when the local production quantity of bio methane or biogas is more than the energy demand of the distribution power grid network and its grid sales to the transmission power grid network. Connecting the power grid network directly to the biogas generator system is another alternative option of bio methane injection to the transmission power grid system which includes essential facilities for injection and upgrading the quality of biogas system. European countries like Spain/Sweden/Denmark/France/Germany/Netherlands/Italy perform bio methane injection into the gas transmission grid system. The anticipation for further investment and project increment of bio methane's injection to the transmission power grid network by Slovenia/Sweden/Belgium/Netherlands/Italy/France/Denmark is to enable the adaptation of their development program, nationally. This will increase the countries' percentage involved in the project of injecting bio methane to the grid system by 70 % in years to come [113].

2.6.5 Analyzing Wastes Producing Biogas Fuel from Global Environment

Globally, the sufficient number of micro-digesters needed for family amounted to 50 $\times 10^6$ plants [114]. There are 132,000 global biogas engineering projects with 10.5×10^9 Watts (installed potential) having a total number of 17,783 biogas project location in Europe. The available global number of plants for upgrading from biogas to bio methane fuel is 700 plants, comprising of 540 plants from Europe [114, 115]. Presently, majority of the wastes power plant are to process wastes management into compost for biodegradable wastes suitability which is accompanied by general landfill and incineration of wastes. In totality, the generation volume of wastewater from the global atmosphere within a year amounted to 380×10^9 m^3. The summary of global plants for treating wastewater with anaerobic breakdown technology can be seen from table2 with recorded data of the plant's location, commissioning period, categories of applied input material for the production of biogas fuel and generated amount of fuel (biogas) from the plant [116-118]. Analyzing the existing global wastes management plants and European wastes management plants, the processed quantity/type of wastes from the annual individual plant, upgrading capability of biogas plant and the production quantity of methane was the principal focus. The most produced biogas fuel by several wastes management plant from nations around the globe and Europe is depicted from Fig.2.28 and Fig.2.29. Where Fig.2.28a and Fig.2.29a indicates the number of wastes management plants for anaerobic breakdown reaction across the globe and Europe while Fig.2.28b and Fig.2.29b depicts the graphical relationship over the number of wastes management plant, biogas power plants during their upgrade and sludge from wastewater to biogas power plants with a potential magnitude below the population equivalence of 8000 across the globe and Europe, respectively [114, 115, 117, 119-120].

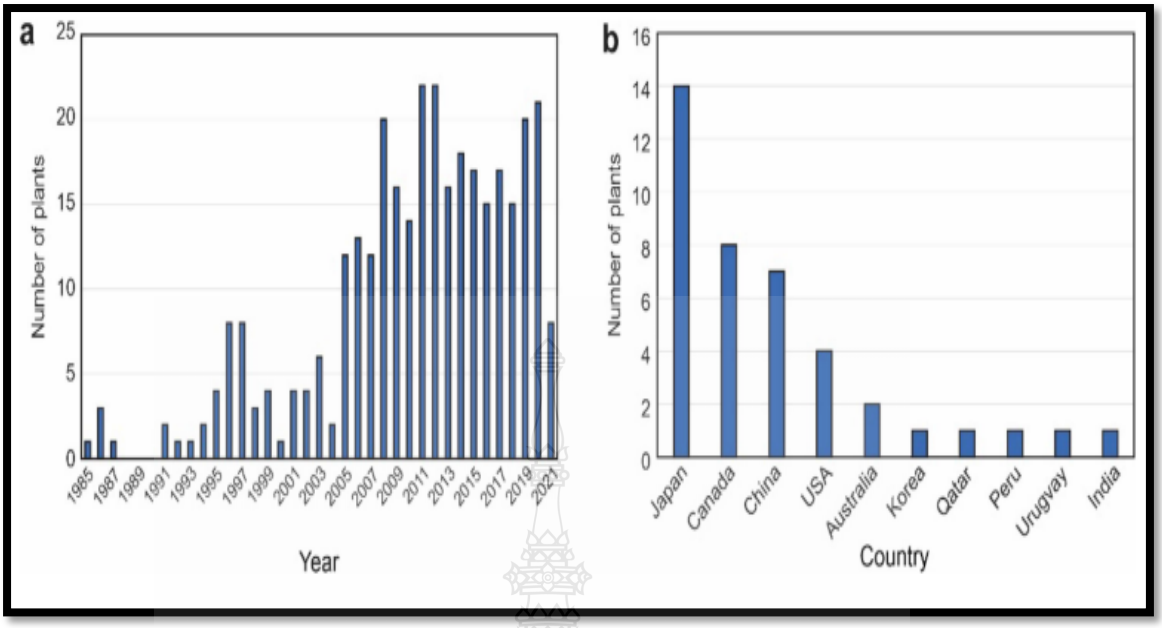

Figure 2.28 (a) Number of biomass generators processing anaerobic breakdown for chosen nations in the globe;

(b) Upgrading the biogas generator and sludge from wastewater to biogas power plant for chosen nations across the globe (2019) [117].

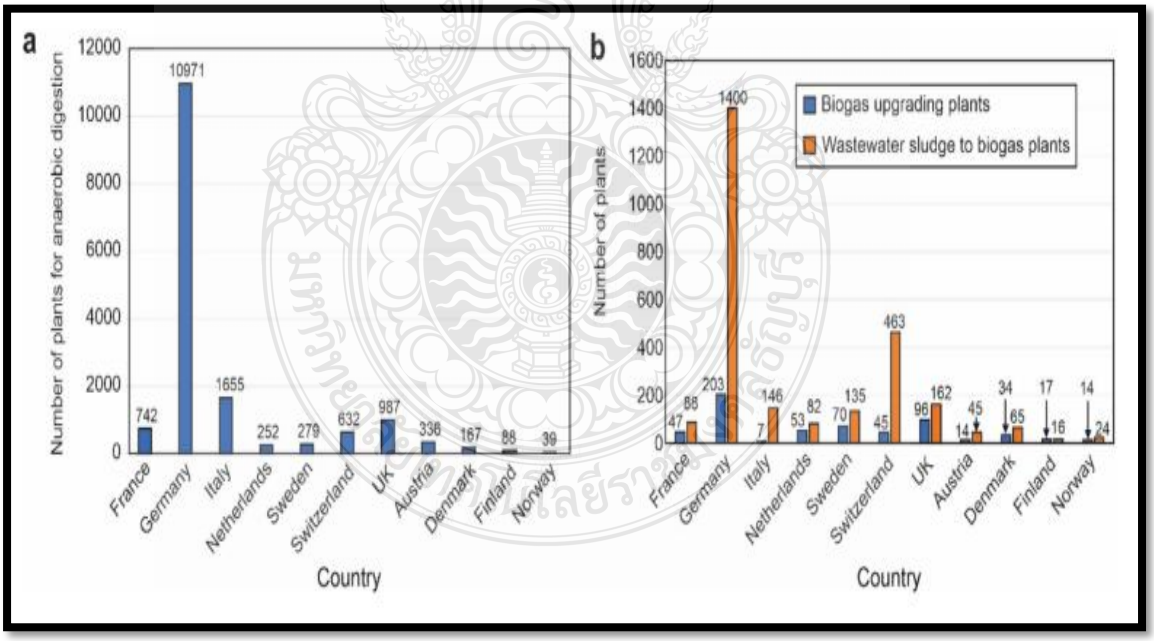

Figure 2.29 (a) Number of biomass generators processing anaerobic breakdown in Europe;

(b) Upgrading the biogas generator and sludge from wastewater to biogas power plant in Europe (2019) [121].

The significant increment in the number of advanced biomass generators beyond the year 2005 was observed globally from Fig.2.30 and in Europe from the provided data analysis depicted from Fig.2.31 with a conclusion that the biomass generator is increasing in number at a faster rate in Europe in comparison with the global environment as depicted from Fig.2.30and represented in Fig.2.32b [122]. Germany, France, Switzerland, and Holland (in order) are the leading European countries in the production of biomass gasifier plants from Fig.2.31.

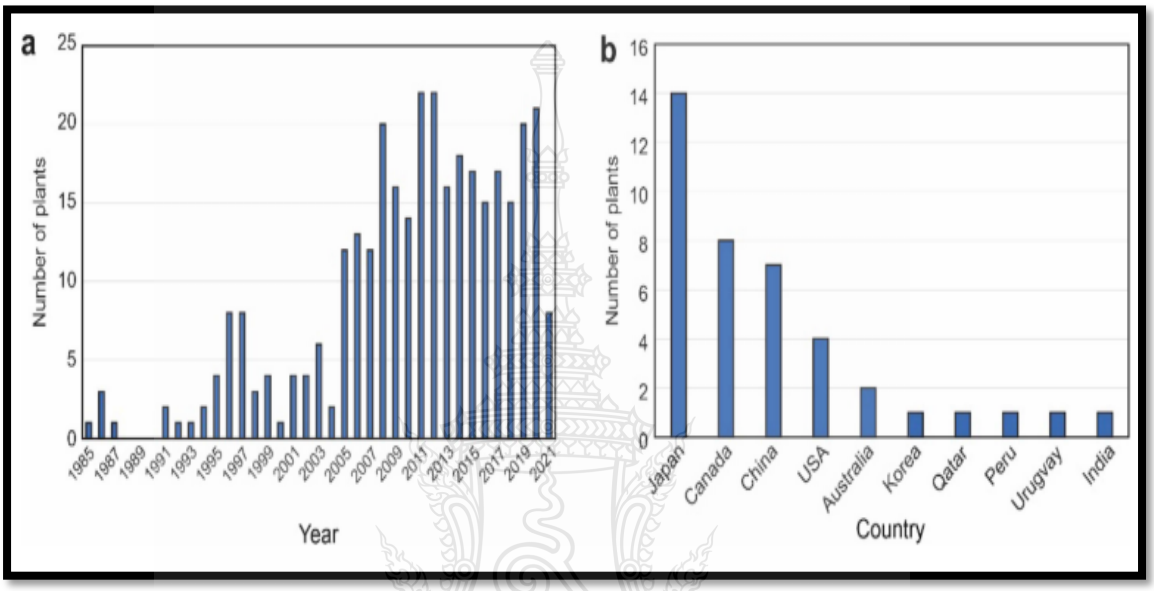

Figure 2.30 (a) Advanced quantity of biomass gasifier plants from the periodic duration (1998-2022) of chosen nations across the globe;

(b) Quantity of biomass gasifier generator for chosen nations across the globe [122].

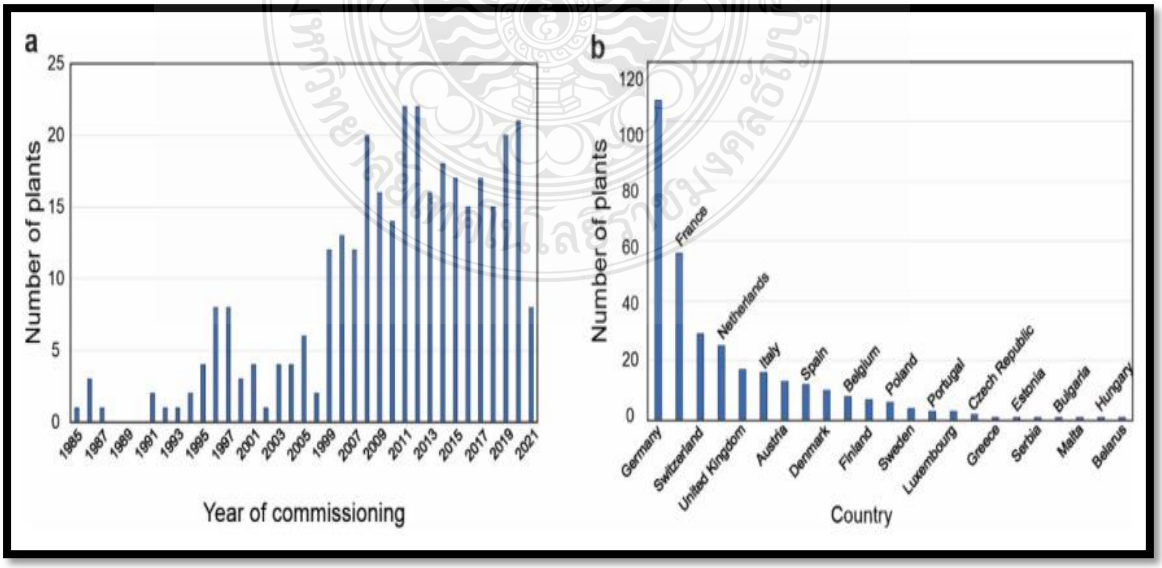

Figure 2.31 (a) Quantity of biomass generators processing anaerobic breakdown of

wastes from the periodic duration (1985-2021) of chosen nations across Europe;

(b) The quantity of biomass gasifier generator processing anaerobic breakdown of wastes for chosen nations in Europe [122].

Majority of the biomass gasifier systems process wastes from agriculture, food, varieties of organic wastes, biological wastes and green wastes as depicted from Fig.2.32a. The analysis categorized European gasifier generators into 13 classes in accordance with the annual processed wastes' quantity. The gasifier generators from discovery processed a range of wastes (10,000-20,000 tonnes/year of wastes) as evidence from Fig.2.32b [121, 122].

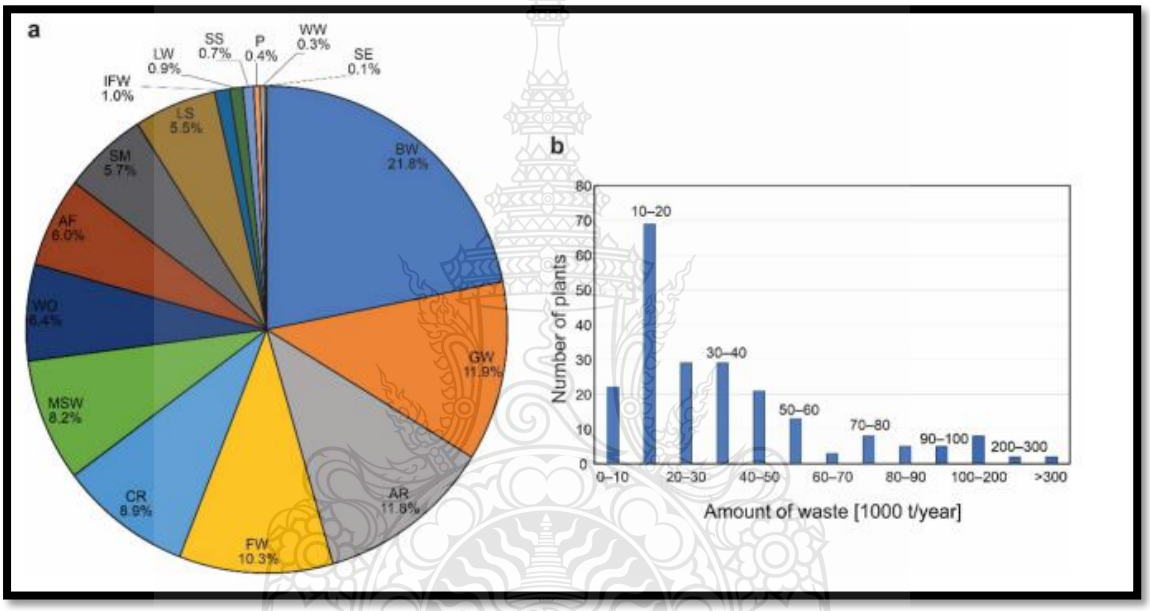

Figure 2.32 (a) Proportional relationship for categories of input wastes for anaerobic breakdown reaction in chosen biomass plants in Europe;

(b) The potential of wastes to biogas generator for chosen biogas generators in Europe (2019) [121, 122].

The utmost installed wastes to biogas conversion plant capacities does not permit the enhancement or modernization from biogas to bio-methane fuel to be fed directly into the grid system that makes use of gas as a fuel source. 134 biogas plants possess the feasibility enhancement from biogas to bio-methane fuel out of 383 biogas plants in totality as analyzed, while the enhancement of biogas technology was not feasible for 86 biogas plants. The rest of the biogas plants are yet to be identified [117].

2.7 Types of Biomass Gasifier Generators

The gasification process (thermo-chemical) converts carbon materials into combustion through a restricted supply quantity of oxygen gas. The gases obtained from biomass feedstock are known as synthetic and wood gases comprising of hydrogen and carbon (1) oxide fuels with natural gas (in small quantity). Other compounds like nitrogen oxide gases (NO_x) and Sulphur gases based on chemical components of the fuel are also included. The synthetic and producer gases consist of gas mixtures such as 18.0-22.0 % of carbon (1) oxide (CO), 8.0-12.0 % of hydrogen gas (H_2), 8.0-12.0 % of carbon (IV) oxide (CO_2), 2.0-4.0 % of natural gas (methane:CH_4), and 45.0-50.0 % of nitrogen gas (N_2).

- The typical condition for gasification restricts a value below 30.0 % of oxygen gas level for combustion process to be completed as a requirement.
- Further processing of raw production leads to end products.
- Low or negative feedstock values are improved through gasification when they (feedstock) are converted to end products and fuel for marketing.
- The specifications for gases are different for varieties of usage when utilizing gases from the gasification of biomass feedstock.
- The categories for gasification processing, agent of gasification and temperature of gasification is dependent on the gas composition during gasification.
- The applications and general composition of biomass gasifier forms synthetic and producer gases as the primary types of gases from the gasification process.

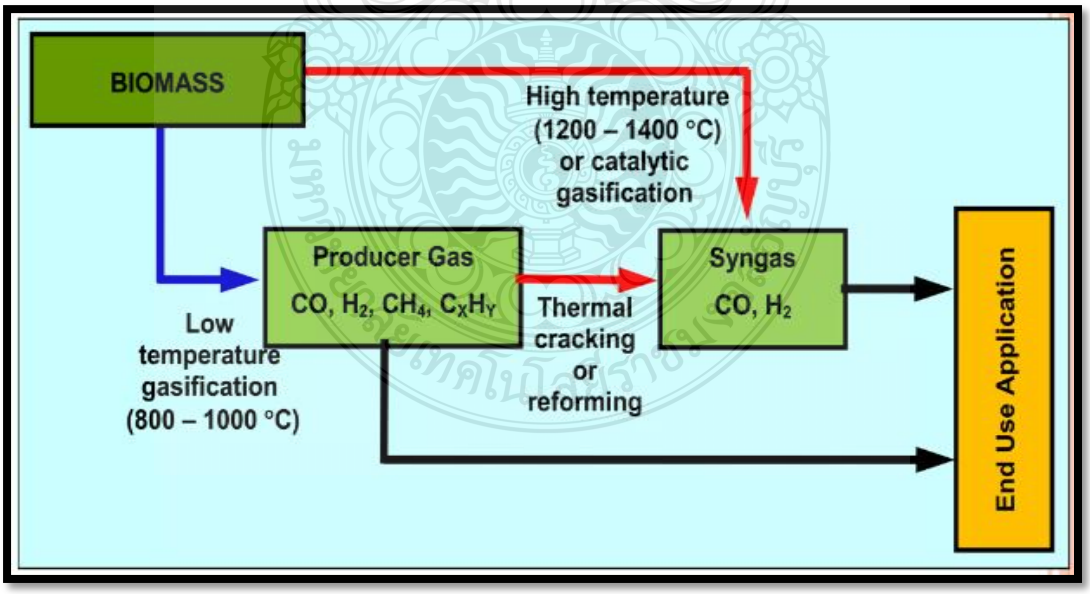

Figure 2.33 Synthetic and Producer Gases [123].

2.7.1 Properties of Synthetic and Producer Gases

- Producer gases are produced at low temperatures range (800-1000 ^{0}C) during gasification and comprises of CH_4, H_2, CO, aromatic hydrocarbons (benzene and its derivatives), tars (asides carbon (IV) oxide: CO_2, water: H_2O, nitrogen gas: N_2 air gasification) and aliphatic hydrocarbons (alkanes, alkenes and alkynes).
- The synthetic gases (H_2 and CO) contain 50.0 % gas energy while the remaining gas energy compositions are from aromatic hydrocarbon and natural gas (CH_4).
- Synthetic gases are generated at higher temperature (1200-1400 ^{0}C) or by a catalyst gasifier which converts the biomass completely to hydrogen gas (H_2) and carbon (1) oxide (CO).
- Synthetic gases can be generated from producer gases through a reforming or thermal cracking process.
- Synthetic gases are similar to gases derived (chemically) from conventional sources (fossil).

The agent of gasification is pure oxygen or atmospheric air as oxidants. Low heating value (calorific)gas is produced from air biomass gasifier containing 50.0 % of nitrogen gas which can be used as a fuel source for furnaces and engines. Pure oxygen biomass gasification produces medium heating value of gas which contains no nitrogen gas. The pure oxygen biomass gasifier system reacts at a faster rate than the atmospheric air biomass gasifier system with additional investment cost in association with the system (oxygen plant) [123].

2.7.2 Reactions from Gasification Process

Production of fuel gas from biomass feedstock comprises of primary reactions that occur in the biomass gasifier system.

- **Drying reaction zone:** Fuel from biomass feedstock contain 10.0-35.0 % water content. When the feedstock is heated to a high temperature of 100 ^{0}C. The water content in them (feedstock) transform to steam.
- **Pyrolysis reaction zone:** After the drying zone reaction, continuous heating makes the biomass feedstock undergo pyrolysis reaction which involves complete burning of the biomass feedstock without oxygen supply. The biomass feedstock is decomposed or undergoes separation into 3 different matters (solid, liquid and gaseous states). The solid matter produces charcoal, the liquid matter produces tar, and the gaseous matter produces flue gases.
- **Oxidation reaction zone:** Atmospheric air is channelled inside the gasifier system after decomposition of the feedstock to form oxidation reaction at a specified

temperature range (700 ^{0}C - 1400 ^{0}C). The carbon solid matter (charcoal) of the fuel reacts with the atmospheric air (oxygen gas) to produce carbon (IV) and heat energy.

$$C_{(S)} + O_{2\,(g)} \rightarrow CO_{2\,(g)} + \text{heat energy} \quad (6)$$

- **Reduction reaction zone:** Under the reduction reaction at higher temperature when there is insufficient oxygen gas supply, carbon (IV) oxide, hydrogen gas and natural gas are produced [123].

$$C_{(So)} + CO_{2\,(gs)} \rightarrow 2CO_{(gs)} \quad (7)$$

$$C_{(So)} + H_2O_{(gs)} \rightarrow CO_{(gs)} + H_{2\,(gs)} \quad (8)$$

$$CO_{(gs)} + H_2O_{(gs)} \rightarrow CO_{2\,(gs)} + H_{2\,(gs)} \quad (9)$$

$$C_{(so)} + 2H_{2\,(gs)} \rightarrow CH_{4\,(gs)} \quad (10)$$

Designing a bio-gasifier system is dependent on the available feedstock (fuel source), size and shape of the feedstock, water content of the feedstock, content of ashes and usage at the end. There are different categories of bio-gasifier systems with reference to their sizes and design based on their specifications. They are categorized as fixed bed bio-gasifier and fluidized bed bio-gasifier systems. The inter-activity of atmospheric air, oxygen gas, biomass feedstock, and steam in the fixed bed bio-gasifier system form the gasification system which can be broadly divided into up-draft bio-gasifier, down-draft bio-gasifier and cross-draft bio-gasifier systems, shown from Fig.2.34.

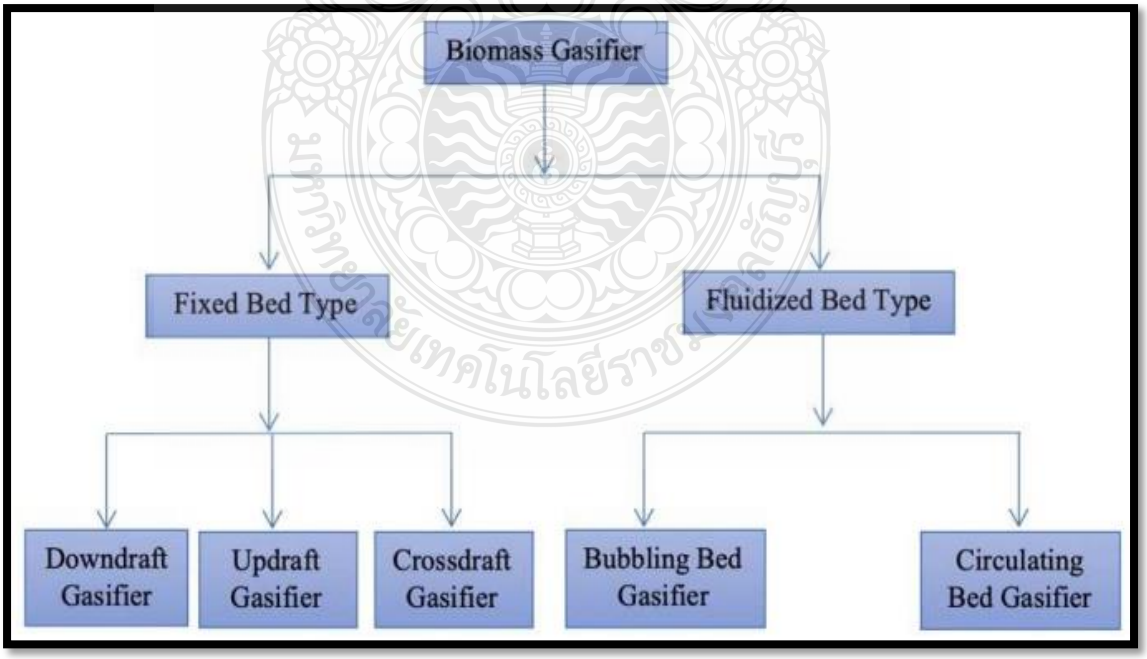

Figure 2.34 Classes of Bio-gasifier Systems [124].

2.7.3 Fixed Bed Bio-gasifier System

The oldest form of bio-gasifier system is the fixed bed or moving bed bio-gasifier. The fixed bed bio-gasifier is categorized further into up-draft, down-draft, and cross-draft bio-gasifier systems from Fig.2.34. The categories of the fixed bed bio-gasifier system operations are based on their fuel flow directions and the bio-gasifiers' oxidant. The fixed bed bio-gasifier classifications are appropriate for small-scaled usage rating of 10 megawatts (decentralized power production system using biomass feedstock as a fuel source). This system is less expensive, simple in design with lower heating (calorific) value of producer gas [123].

2.7.3.1 Down-draft Bio-gasifier System

The down-draft bio-gasifier system enables air inter-activity with the biomass feedstock in downward movement resulting in wastes and gases moving together (co-currently) known as co-current bio-gasifiers. The decomposed products from the drying reaction zone and pyrolysis reaction are enforced to move into the oxidation reaction zone for thermal cracking or reforming materials that are volatile and producing low concentration of tar to yield good fuel gas quality. The air interaction with the pyrolysis zone will contact the char by accelerating the flame, thereby, maintaining the pyrolysis reaction process. The gases produced from the pyrolysis reaction zone end without oxygen are carbon (IV) oxide: CO_2, carbon (I) oxide: CO, hydrogen gas: H_2 and water: H_2O known as flaming reaction pyrolysis. At the flaming reaction pyrolysis, the produced gases from the down-draft bio-gasifier system was due to high concentration of tar (99.0 %) consumed during the process forming low concentration of particulate matter and content of tar from the gas making it appropriate for decentralized small-scaled power production usage [124].

2.7.3.2 Up-draft Bio-gasifier System

This type of bio-gasifier system enables the introduction of atmospheric air, oxygen gas and steam (bio-gasifier agents) inter-activity with biomass feedstock and combustion gases at the bottom in opposite current movement (counter current bio-gasifier) with the products from pyrolysis and steam from drying reaction zone. The gas production from the reduction reaction with high heating value flows out of the reactor. Evaporation of steam into the combustion reaction zone occurs in some updraft bio-gasifier systems to produce fuel gas of good quality and prevent over heating of the bio-gasifier system. The up-draft bio-gasifier possesses the highest thermal output (efficiency) as the hot gas production is channeled within the fuel-bed system leaving the unit of gasification at low temperature. Some portion of heat sensitivity of the producer gas is applied within the bio-gasifier system to dry the biomass feedstock and generate steam [125]. Up-draft bio-gasifier systems possess good thermal output (efficiency), drop in small pressure and formation of slag at a slight tendency as advantages. This bio-gasifier system is appropriate for the requirement of high temperature flame with an acceptable moderate quantity of dust from the fuel (gas). The fuel's water content, low productivity of synthetic

gas, delay startup period of the system, poor reaction potential and substantial sensitiveness to tar form the bottlenecks of the system [123].

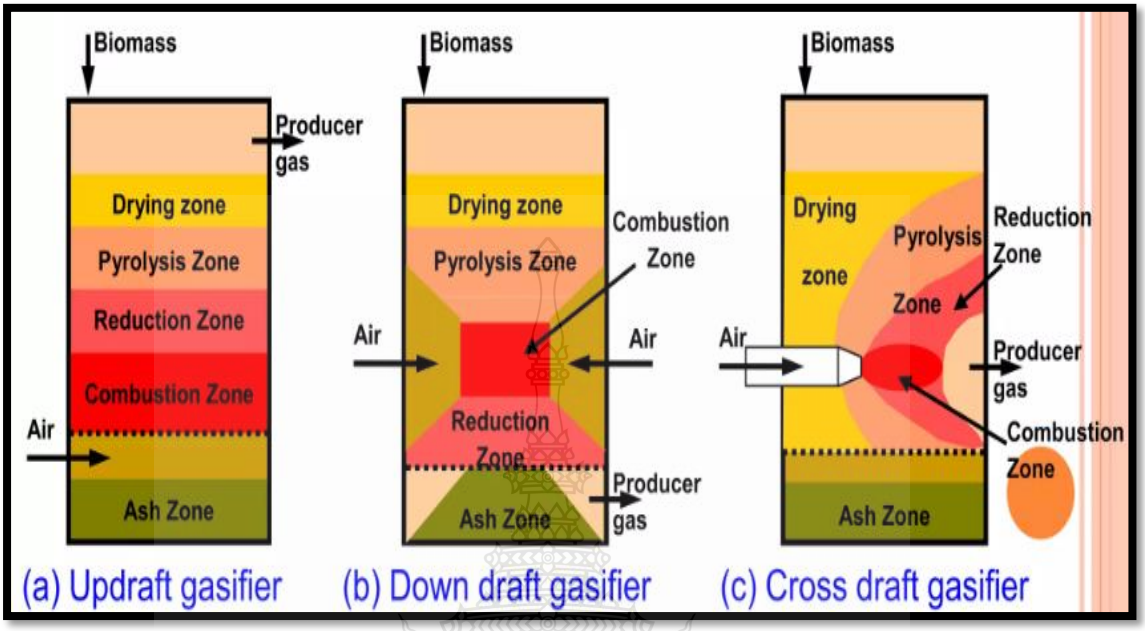

Figure 2.35 Categories of Fixed Bed Bio-gasifier System and Mode of Operation [123].

2.7.3.3 Cross-draft Bio-gasifier System

In this system, the feedstock introduction occurs at the top of the bio-gasifier system. The bio-gasifier agent introduction occurs at one of the bio-gasifier system sides. The production gas is channeled out from the other side of the bio-gasifier system. The production gas exit and bio-gasifier agent entry are maintained nearly at equal level. The downward movement of the fuel in the bio-gasifier system is dried, volatile free, undergoes pyrolysis reaction and gasification before flowing out of the bio-gasifier system. The location of the oxidation reaction zone is close to the bio-gasifying agent entry and the location of the gasification reaction zone is close to the exit. The location of the pyrolysis reaction zone is beyond the oxidation reaction zone and reduction reaction zone. The location of the drying reaction zone is beyond the pyrolysis reaction zone. There is separation between the oxidation reaction and reduction reaction zones at the cross-draft bio-gasifier ash zone which imposes restriction on varieties of fuel usage. The high temperature of gas exit from the cross-draft bio-gasifier system affects the composition of gases by producing higher concentration of carbon (1) oxide gas and low concentration of CH_4 and H_2, respectively [126].

2.7.4 Fluidized Bed Bio-gasifier System

- Fluidized bed bio-gasification is different from down-draft and up-draft bio-gasification methods; the bio-gasifier agent (air) is channelled through the processing fuel (coal and biomass feedstocks). The water content is of more importance as a factor during this process.
- The presence of sand (reactive material) is inside the reactor which (sand particles) will aid the product gases from the bio-gasifier to react further. The passing of air (bio-gasifying agent) across the fuel will maintain the fuel suspension in mid-air. The fuel suspension is known as the fluidized bed bio-gasification.
- Another stream of the bio-gasifying agent that will not maintain the fuel suspension is needed during this process for optimal efficiency. The attachment of a cyclone can be applied for the separation of synthetic gas from the char or reactive particles which can increase the processing efficiency.
- Fluidized bed bio-gasifier system is more complicated and expensive with higher calorific (heating) value of synthetic gas production.

The biomass feedstock is introduced into the char and sand (inert fluidized bed material) of the fluidized bed bio-gasifier. The biomass feedstock (fuel source) is supplied above or directly to the fluidized bed bio-gasifier system based on the fuel's size/density and the effect of bed velocities on the fuel. The maintenance temperature of the bed media during normal operation ranges from 550 ^{0}C to 1000 ^{0}C. The fuel introduction within the temperature range condition precedes its drying reaction and pyrolysis reaction rapidly by evaporating all fractions of gases from the fuel at a relative low temperature. The char as remnant undergoes oxidation within the fluidized bed to produce heat for the continuation of drying reaction and volatile removal reaction zones. The fluidized bed bio-gasifier produce large quantity of heat within a short period due to abrasive occurrence between the biomass feedstock and inert fluidized bed material providing a steady bed temperature range (800 ^{0}C to 1000 ^{0}C). Fluidized bed bio-gasifier operates as hot bed-based sand particles with uniform agitation by the air. The location of air distribution through the nozzles is at the bed's bottom [123].

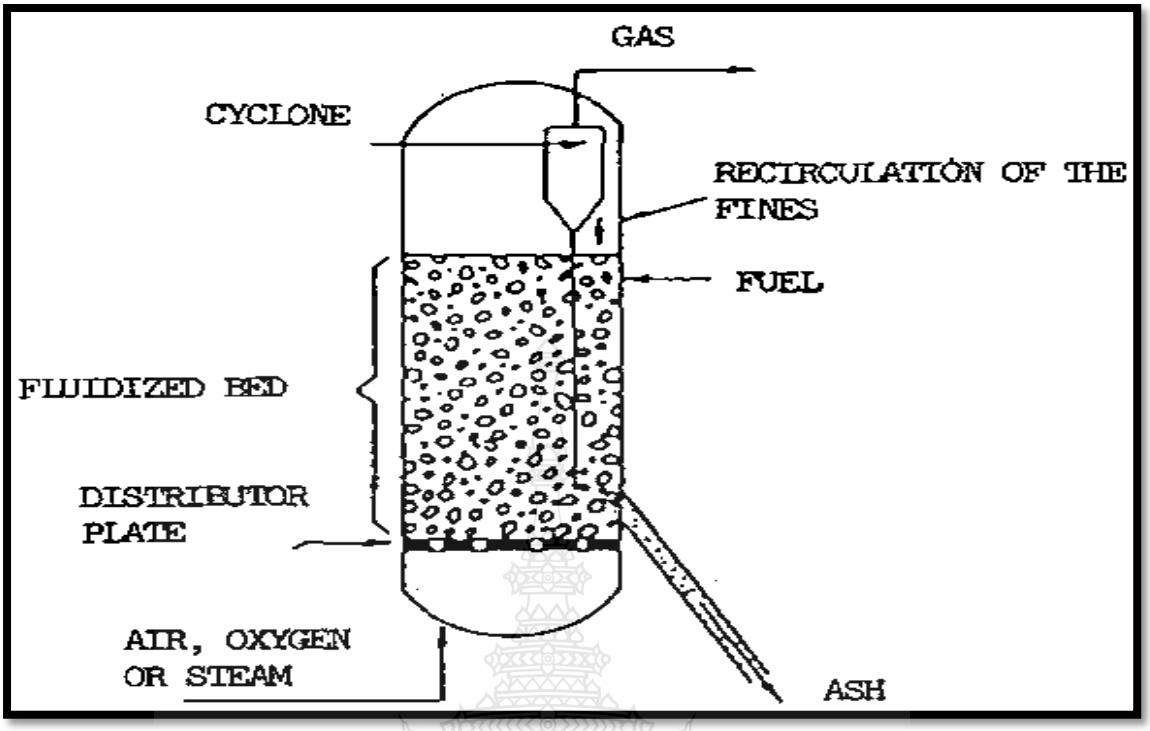

Figure 2.36 Fluidized Bed Bio-gasifier System [123].

The categories of fluidized bed bio-gasifier system are bubbling bed bio-gasifier and circulating bed bio-gasifier systems.

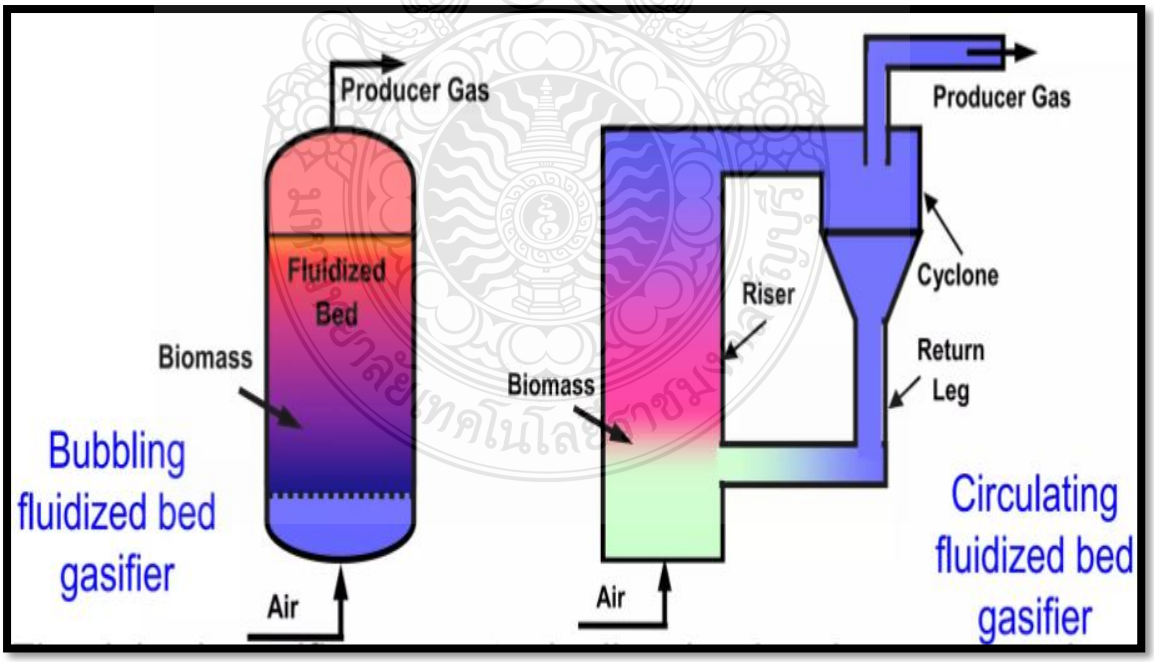

Figure 2.37 Categories of Fluidized Bed Bio-gasifier System and Mode of Operation [123].

2.7.4.1 Bubbling-Fluidized Bio-gasifier Bed System

Increasing the fluid gas velocity of a reactor based solid particles will suspend the solid particles by an upward gas flow. During this process, the drag force inter-activity of the fluid and particles counterbalances the particles weight and drop in pressure at any given 2 points (in-between) through the bed's height equals fluid weight and particles weight within that particular section. The bed attains a minimum fluid condition at this point with velocity in correspondence known as minimum velocity fluidization. As the minimum velocity fluidization increases beyond its level, formation of bubbles commences. The small bubbles formation increases in sizes while flowing across the bed. Across the bed's path upward, there is withdrawal of particles by the bubbles from their surroundings causing the particles to move. Approaching the surface of the bed will burst the bubbles and splash the particles into region with free board [124].

2.7.4.2 Circulating Fluidized Bio-gasifier Bed System

This system comprises of a down comer, riser of high velocity, loop seal, cyclone separator, and L (vertical and horizontal standing) valve. If the bio-gasifying agent velocity increases above the bubbling fluidized bio-gasifier bed, the distribution of solid particles along the height of the entire riser will occur and the majority of the particles will undergo gas entrainment. The cyclone separator separates the gas from the particles with downward movement from the loop seal by the down comer and moving to the riser's bottom causes a solid circular loop formation (circulating fluidized bio-gasifier bed system). The cyclone separator arrest particles and feed them (the particles) to the riser by the vertical and horizontal standing valve (L valve) or loop seal application. The circular solid flux is monitored by the loop seal and riser's velocity. The difference in pressure from the circulating fluidized bio-gasifier bed system with different parts form the driving force of the solid circulation. Gases with higher velocity in this system produce more bed particles and gas mixture intensively with excellent solid-gas connection [124].

2.7.4.3 Entrained Flow Bio-gasifier Bed System

The entrained flow bio-gasifier bed system utilizes the co-current flow of the solid biomass feedstock (fuel) and bio-gasifying agent (air or pure oxygen gas) as feeders on top of the reactor system to be channeled to the gasifier. The bio-gasifying agent carries the fuel in the reactor with an operational temperature range (1200 ^{0}C to 1600 ^{0}C) and pressure range (20.0 bars to 80.0 bars). This bio-gasifier system uses any fuel category with low water content (moisture) and low content of ash for reduction in consumption rate of the oxygen gas. The short resident period (0.50 s to 4.00 s) of the fuel particles requires high temperatures (1200 ^{0}C to 1500 ^{0}C) for gasification. The fuel is converted rapidly by the high temperature and extreme turbulent movement inside the bio-gasifier system, allowing high throughput energy flow. The product gas in entrained flow bio-gasifier system contains low condensed gases and low tar concentration because of the operating temperature. The operational temperature of the bio-gasifier system is higher

than the fusion temperature of the ash, thereby, causing a major fraction removal from the ash as slag. This type of bio-gasifier system has gone through suitable commercialization for large scaled applications (integration of bio-gasification combined cycle coal generator) above 100 Mega Watts rating with advanced gasification technology for refinery wastes and coal (fossil fuels). Globally, most integration of bio-gasification combined cycle generators installed uses entrained flow bio-gasifier bed system technology which is still going through development process [124].

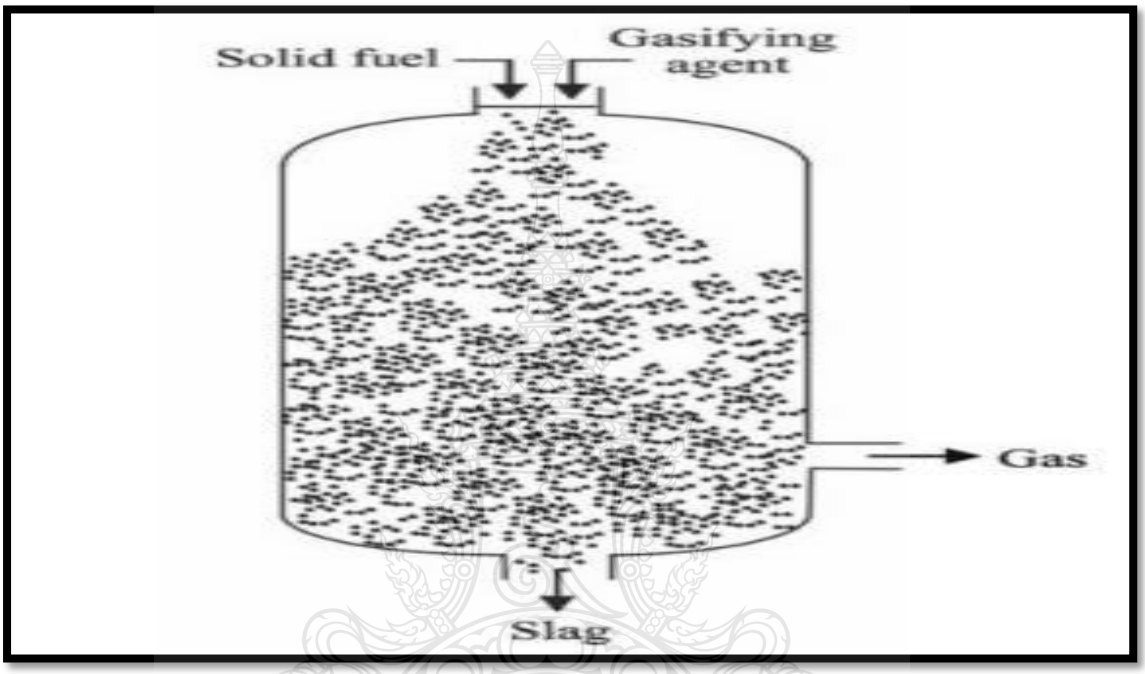

Figure 2.38 Entrained Flow Bio-gasifier Bed System [124].

2.8 Current Energy System Technology of On-Nut Waste Power Plant

The current generating system design for municipal solidified wastes project management on energy production from On-nut solidified wastes disposal axis uses 3 units of an electric power CG170-12 cylinders natural gas (each with a power rating of 1000 kWelc, 400 V_L, 50 Hz) generator connected to the utility grid to support the grid, serve the manufacturing plants, promote grid sales, and meet maximum electric demand continuously.

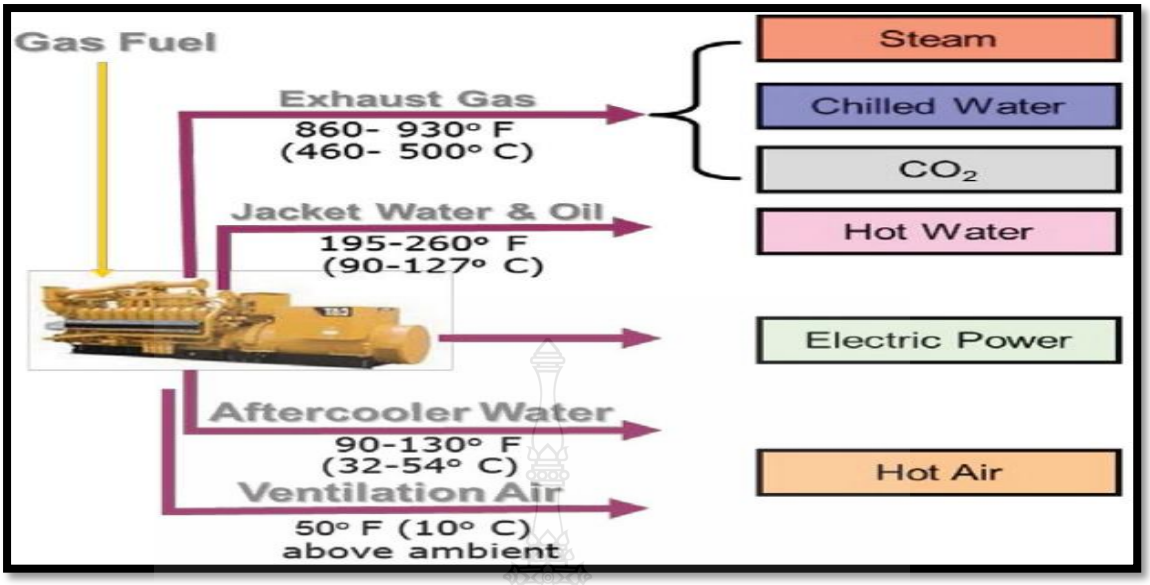

Figure 2.39 Natural Gas Generator Engine Circuit and Heat Recovery [127].

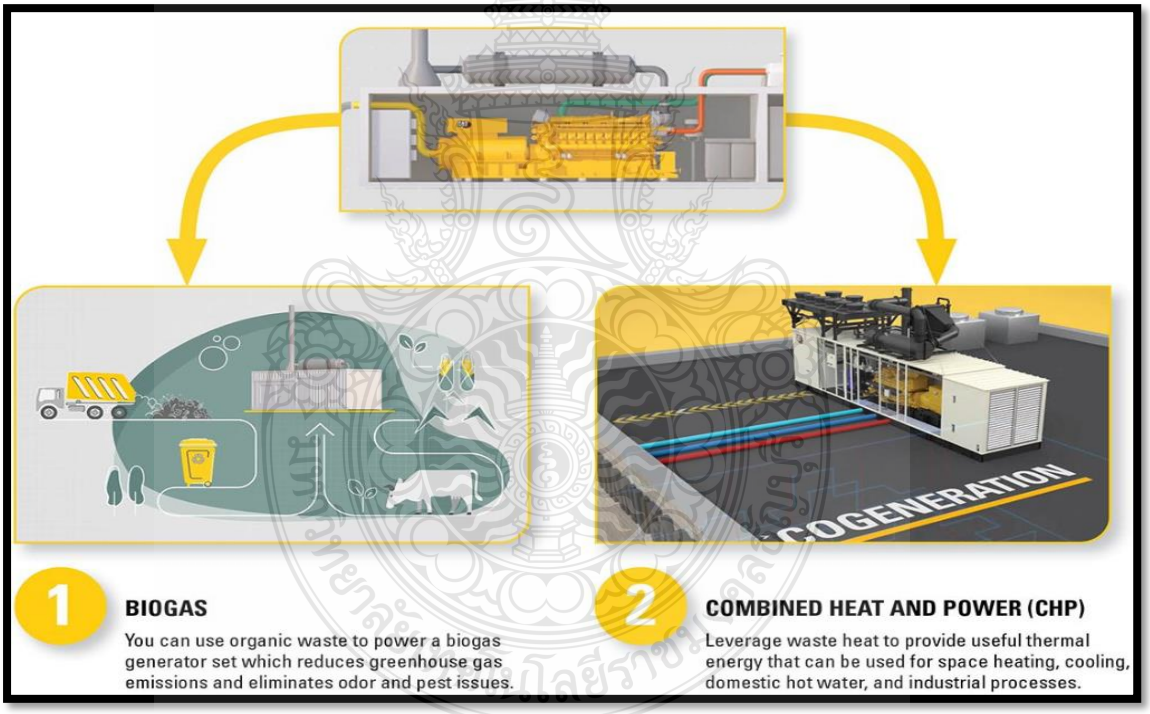

Figure 2.40 Natural Gas Generator Energy Conversions [128].

Another unit of an off-grid electric power CG170-12 cylinders natural gas (power rating of 1200 kWelc, 400 V_L, 50 Hz) generator serves the health centers, shopping axes, residential apartments, data axis, and resorts to reduce carbon coverage and operating costs simultaneously. The byproducts (biogas) as a useful fuel from anaerobic breakdown of organic wastes is formed from farms, manufacturing biodiesel, ethanol, and food processors as renewable resources producing fuel for the natural gas generator to generate electric energy, produce organic fertilizer from carbon (IV) oxide to increase the production of crops, and hot water production for heating facilities. The component of the biogas generator includes control panel, alternator, air filter, turbo charger and throttle performing high efficiency, low cost of operation, sustainable energy flow and fast response to high transient demand when the grid system is disconnected from the biogas plant. The turbo charger will enhance the power production of the biogas generator to keep running in overcoming transient load when the system is in off-grid mode.

CHAPTER 3
MATERIALS AND METHODOLOGY

3.1 On-Nut Community Wastes Composition

The data composition from On-nut community wastes that was channeled to the wastes' disposal central (On-nut) environment office in Bangkok can be illustrated from Fig.3.1. The food scraps had the largest (46.97 %, water content: 72.0 %) average municipal solidified wastes composition followed by the plastics/foam having the second largest average composition (25.28 %, water content: 37.0 %) with paper as the third largest fraction (13.70 %, water content: 47.0 %), respectively. The remaining heterogeneous wastes composition are woods and leaves (6.21 %, water content: 45.0 %), glass (2.46 %, water content: 10.0 %), textiles (1.86 %, water content: 55.0 %), metals (1.75 %, water content: 5.0 %), bones and shell (1.11 %, water content: 10.0 %) with lower values. The sequential and water content from the heterogeneous wastes of the community possesses a value of 54.0 % as a humidity for the design with its respective mean water content of 44.54 %.

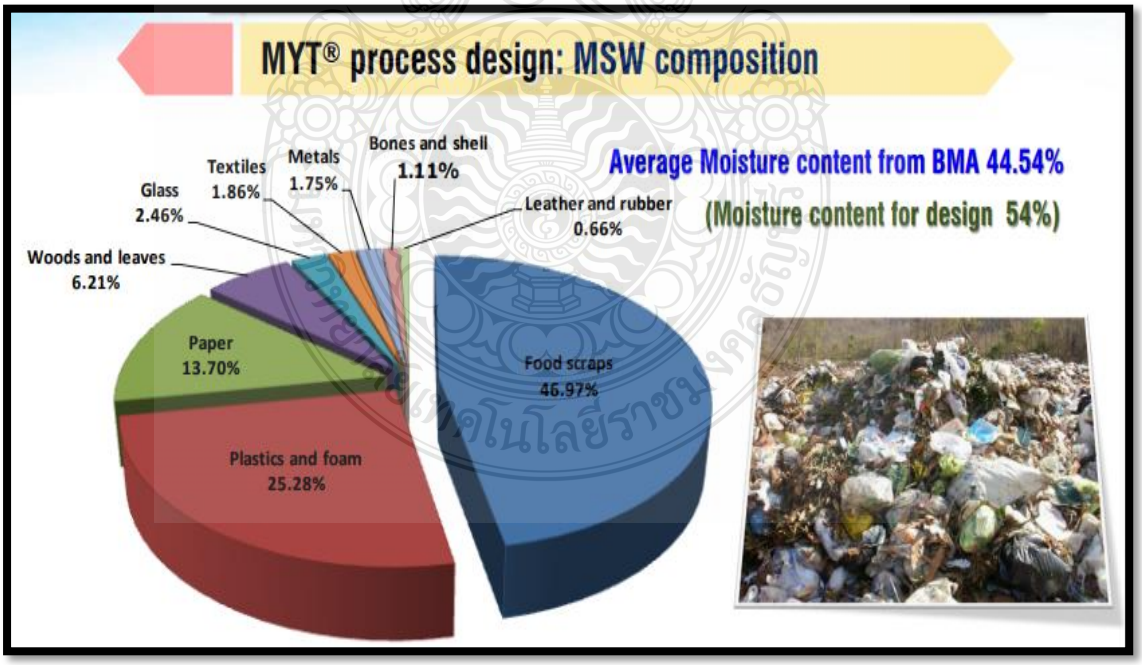

Figure 3.1 Solidified-Hazardous Wastes and Division of Managing Night soil in On-Nut.

3.2 Current Wastes to Power Conversion Technology of On-Nut Community

The waste management system was designed to produce 800 tonnes of biomass energy every day at the central disposal unit of On-nut wastes community management with a therapy system and maximum yielding technology (MYT) of treating wastewater system. The maximum yielding technology is a management innovation waste that was produced in Germany and appropriate for mixed wastes and Bangkok wastes application of managing community wastes system and their properties at the disposable centre as a proposal. Focusing on the community wastes at night to produce fuel from garbage responds to utilizing wastes as a renewable energy source. Fuel can be derived from refuse (plastics, papers, etc.) and energy production from biogas having organic wastes through anaerobic breakdown process. The generating capacity of the biogas plant in On-nut community is 4.064 MW with a sale capacity of 3.045 MW to the utility grid.

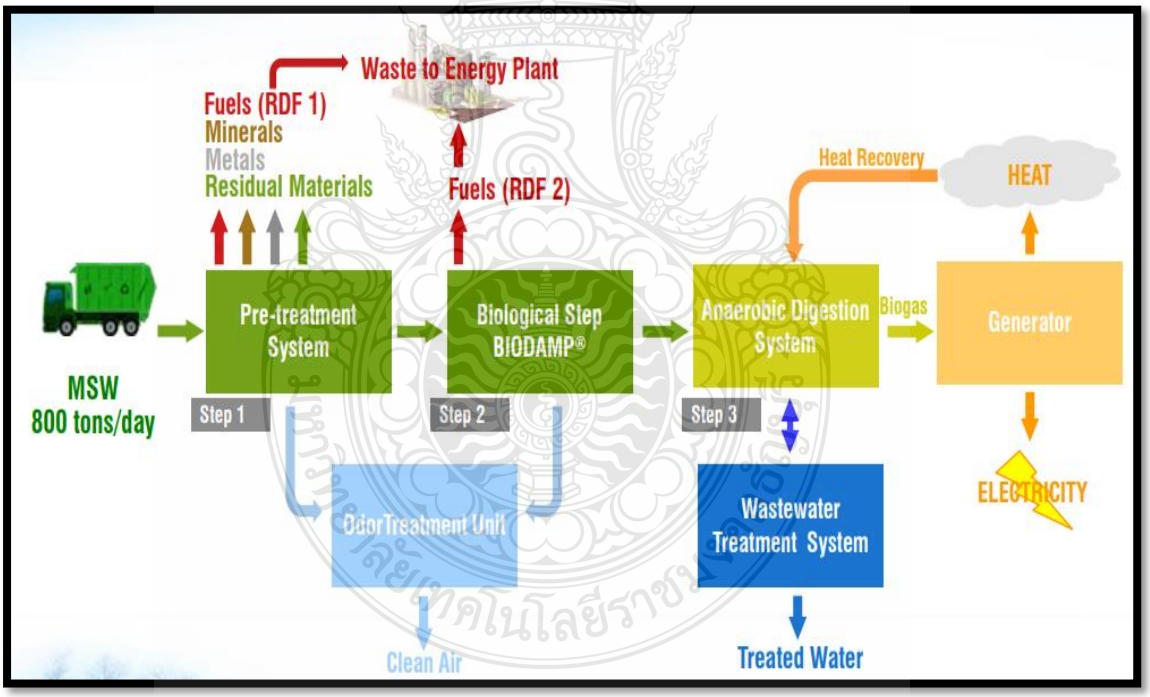

Figure 3.11 Wastes to Power Conversion Technology from On-Nut Community;
Generating Capacity: 4.046 MW, Capacity Sales to Grid: =<3.045 MW
Biomass Resources: 800 tonnes/day.

The maximum yielding technology and wastes management system of On-nut community was designed by adopting four main systems classified into three steps of managing wastes system and the pollution control system namely.

- The pre-treatment system (sorting system at the preliminary stage) comprises of wastes reception and mechanical pre-treatment. This entails wastes collection and separation of wastes in large quantities (120 mm) known as fuel derived from refuse. The fuel derived from refuse (R.D.F 1) and metal wastes in small quantities (less than 120 mm) will undergo therapy importation.
- Biological step-hydrolysis system comprises of the bio-damp and compression tank for screw pressing. The solid wastes (fuel derived from refuse: R.D.F 2) and water are concentrated.
- Anaerobic breakdown system will produce biogas fuel (no air degradation/wastewater treatment) from the concentrated solid wastes (R.D.F 2) and water that will be channelled towards it (anaerobic breakdown system). The wastewater produced from the process of air fermentation comprises of the first wastewater sent back to fill up the bio-damp (fermentation tank) while the second part of the wastewater will be sent to the wastewater treatment system's therapy.
- Odour treatment unit (removal of odour) comprises of a collection system that will send the odour to the bio-filter therapy to remove and prevent air pollution from circulating to the environment.

3.3 Proposed Wastes to Power Conversion Technology

The systematic design of a newly proposed hybridized energy system will involve.

- The integration of a hybridized storage system (lithium-ion, flow, and zinc bromide batteries) to the utility grid and biomass generator network.
- Adopting a multi-purpose control system (cycle charging monitoring and load following controllers) that are operational interface over the biogas generators, utility grid system, and batteries to serve the energy demand effectively.

- The grid-forming, grid following, utility scaled-battery dedicated power and energy converter model with industrial HOMER PRO energy analysis will investigate the performance analysis, reliability measures and econometric assessment of the first community (On-nut) waste biogas power plant system in Thailand with respect to the system configurations (utility grid-biogas generators and utility grid-biogas generators-batteries).

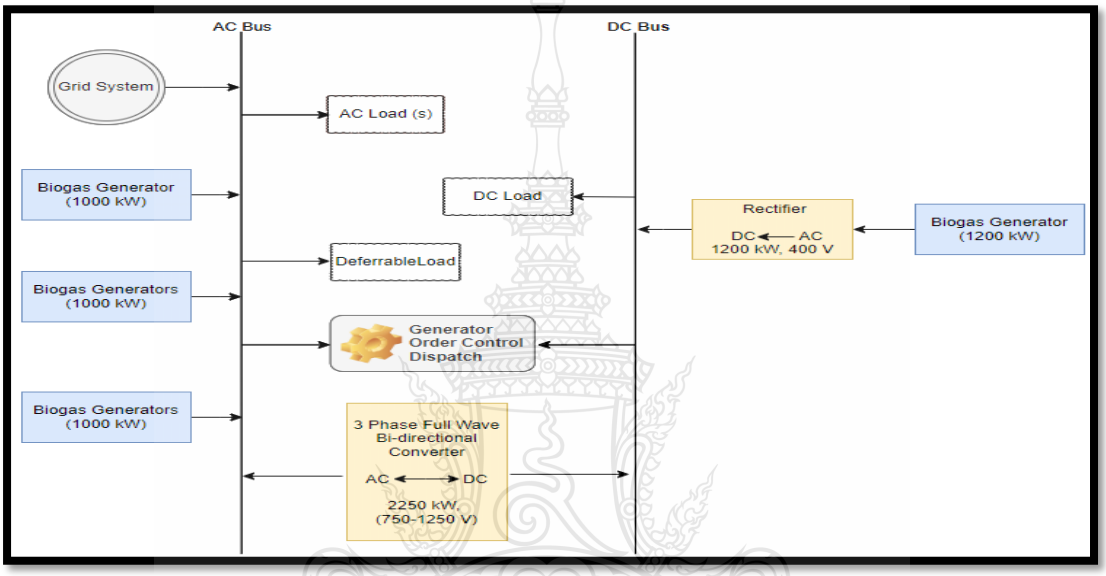

Figure 3.12 Current Schematic Operation**:** Grid System/Biogas Generators.

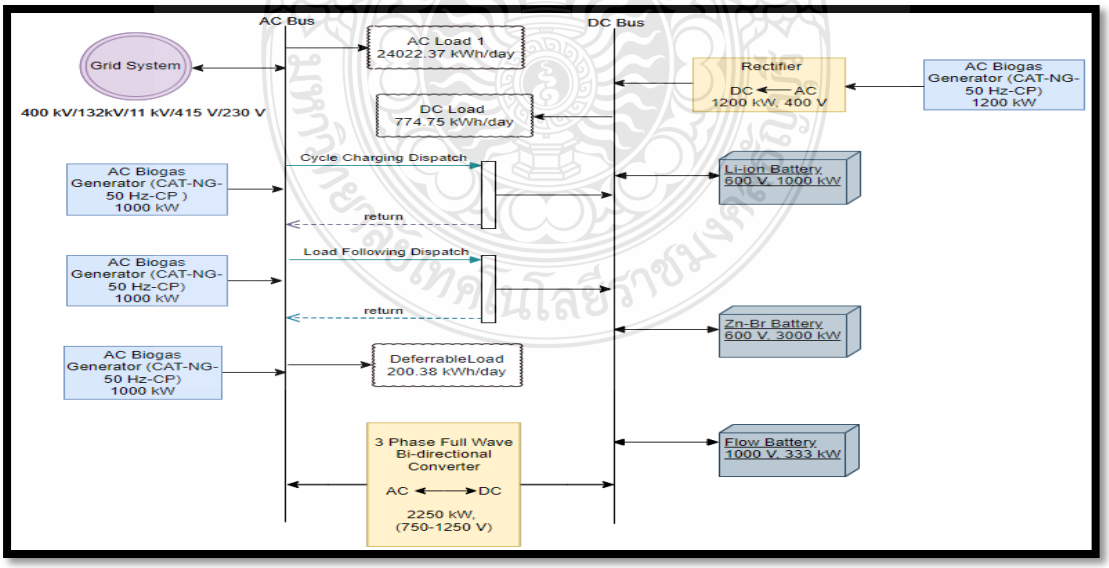

Figure 3.13 Proposed Schematic Operations: Grid System/Biogas Generators /Batteries.

3.4 Proposed Energy Management Algorithm

The flow chat of the hybridized energy network from Fig.3.14 consists of biomass fuel resources, biogas generator, utility grid, batteries' potential, technological-econometric, and load estimate potential values of the microgrid operation as the input data to be measured. The power system architectures are grid-biogas generator-batteries and off-grid-biogas generator-batteries.

The energy balance equation is expressed below.

$$E_{getr}(t) + E_{bgs}(t) = E_{bys}(t) + E_{losses}(t) + E_{cve}(t) + E_{dmd}(t) \quad (11)$$

Where $E_{getr}(t)$ = Energy generated from the utility grid (kWh)

$E_{bgs}(t)$ = Energy generated from the biogas generator (kWh)

$E_{bys}(t)$ = Energy generated from the batteries' potential (kWh)

$E_{losses}(t)$ = Energy loss from the entire network (kWh)

$E_{cve}(t)$ = Energy production from power converter (kWh)

$E_{dmd}(t)$ = Energy demand (kWh).

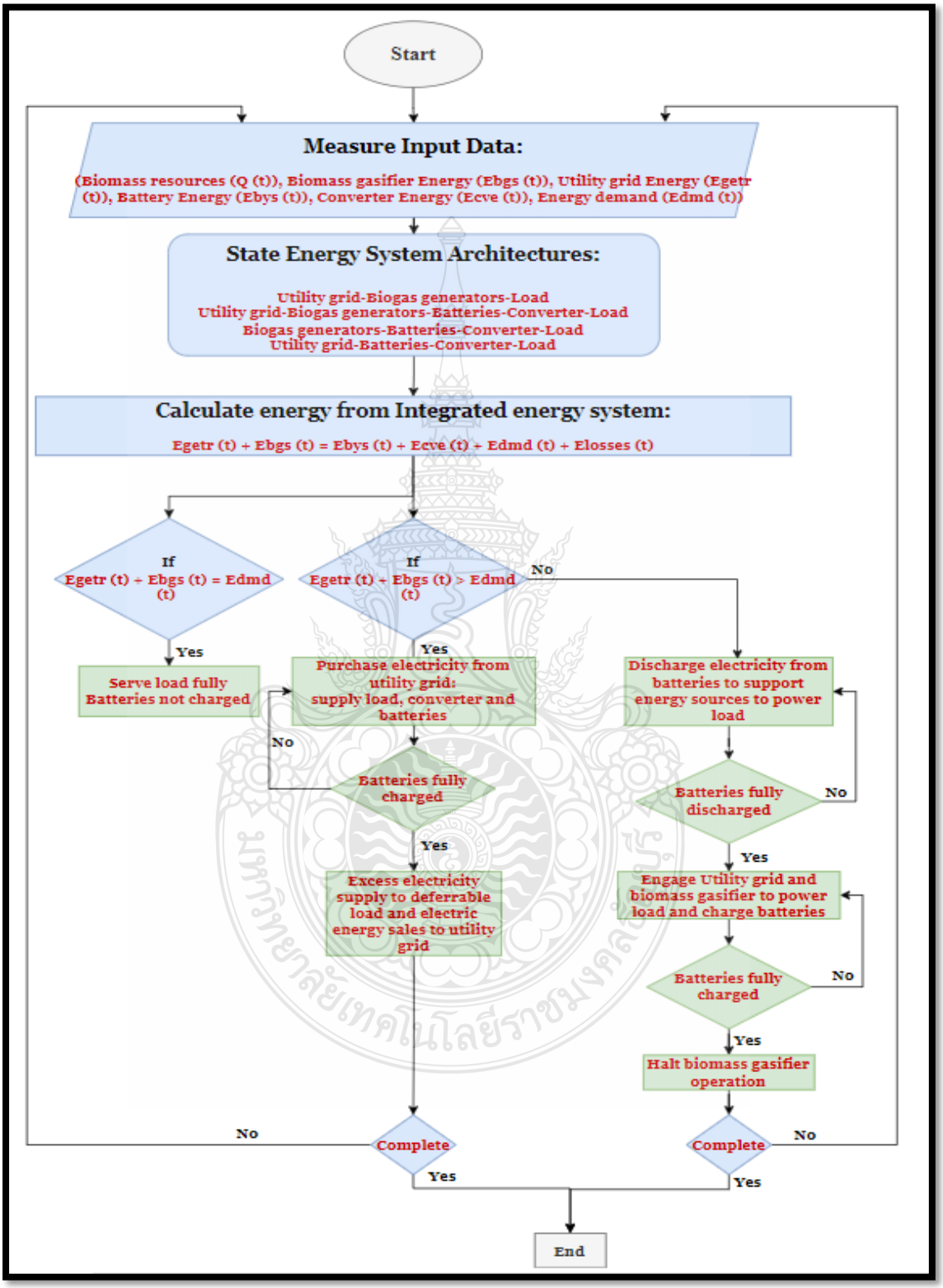

Figure 3.14 Proposed Energy Control and Power Stability Strategy.

3.5 Hybrid Network Components

The hybridized energy system comprises of a network that will operate with AC energy generators (utility grid and biogas plant), power conversion system and DC hybrid storage system (Lithium-ion, flow battery, and zinc bromide batteries), respectively. The power network optimization in terms of sizing and architectures depend upon the modelled hybridized power generators.

3.5.1 Grid network modelling

The grid energy network from the schematic design in Figure 3.12 and Figure 3.13 provides electric power from its energy generation sources (natural gas, coal, hydropower, sunlight, and wind converts energy from the mechanical turbine into electric power) to the consumer unit with sections mainly on electric power generation, power transmission, and power distribution. When the AC loads and storage unit are fully met from the potential capacity of the hybrid power sources, the surfeit electricity flows back (grid sales) to the grid system with a grid power price: of $ 0.150/kWh and net excess price from the grid: of $ 0.100/kWh involving a calculated annual net purchase from net metering in this simulation process.

When the energy from the grid system is more than the demand (load), a power swing occurs with its equation expressed mathematically as:

$$I\,(d^2\,\delta^0/\,d^2\,t^2) = P_{omech} - P_{oelect} = P_{omech} - [(E_{ngen} \times V_{obus})/(X_{oreact12}) \quad (12)$$

$$\text{Where } P_{oelect} = [(E_{ngen} \times V_{obus} \times \sin\delta^0)/(X_{oreact12})] \quad (13)$$

At maximum power angle, $\delta^0 = 90^0$ or $\delta = \frac{\pi}{2}\ radian$ and $\sin\delta^0 = \sin(90^0) = 1$

$$P_{oelect} = [(E_{ngen} \times V_{obus} \times 1)/(X_{oreact12})]$$

$$P_{oelect} = [(E_{ngen} \times V_{obus})/(X_{oreact12})] \quad (14)$$

The synchronous excited voltage utility generator leads its terminal voltage by a power angle (δ^0).

$$V_{obus} = V_{obus} < 0^0,\ E_{ngen} = E_{ngen} < \delta^0$$

$$\text{Hence, } I\,(d^2\,\delta^0/\,d^2\,t^2) = P_{omech} - P_{oelect} = P_{accel} \quad (15)$$

I = inertia constant (kgm^2), δ^0 = utility generator power angle (^{0}), P_{accel} = acceleration power of the utility synchronous generator (kW), $P_{o\text{-}mech}$ = input mechanical power to the synchronized generator (kW), P_{oelect} = output power (electrical) of the synchronized generator (kW), E_{ngen} = excitation voltage of the synchronized generator at no load (V),

V_{obus} = terminal voltage of the synchronized generator (V), $X_{oreact12}$ = impedance of the synchronized generator (Ω).

Where $I = 2H_f/\omega$

$$(2H_f/\omega)\, d^2\delta^0/dt^2 = P_{omech} - P_{oelect} = P_{accel} \quad (16)$$

At stability, when power supply = power demand, $P_{omech} - P_{oelect} = 0$ (17)

$$\text{Hence, } P_{accel} = 0,\ P_{o\text{-}mech} = P_{oelect} \quad (18)$$

ω = angular velocity of the synchronous generator (rad/sec)

H = electric field density of the synchronized generator (N/C)

The complex equation for the output power flow per phase of the synchronous generator is given as:

$$S_{gen} = P_{gen} + jQ_{gen} \quad (19)$$

$$= \frac{Vobus * Engen}{Zgen} \cos(\Theta_{im} - \delta^0) + j\frac{Vobus * Engen}{Zgen} \sin(\Theta_{im} - \delta^0) - V_{obus}^2/z_{gen}(\cos\Theta_{im} + j\sin\Theta_{im}) \quad (19)$$

The impedance of the synchronous utility generator can be stated in equation 16

$$Zgen = R_{arm} + j\,X_{oreact12} = Zgen \angle \text{im} \quad (20)$$

The synchronous generator output power real (P_{gen}) and reactive (Q_{gen}) per phase are mathematically expressed as:

$$P_{gen} = \frac{Vobus \times Engen}{Zgen}\sin(\delta^0 + \alpha_{im}) - (V_{obus}^2/z_{gen}^2) \times Rarm \quad (21)$$

$$Q_{gen} = \frac{Vobus \times Engen}{Zgen}\, cos(\delta^0 + \alpha_{im}) - (V_{obus}^2/z_{gen}^2) \times Xoreact_{12} \quad (22)$$

$Zgen$ = impedance of the synchronous generator in ohms

R_{arm} = armature resistance of the synchronous generator in ohms

Θ_{im} = angle of impedance for the synchronous generator in degree [129,130].

3.5.2 Greenhouse effect modelling

The emission of green house gases from the hybrid energy network operation involving the grid integration is of much concern to the human environment. The investigation of emission and absorption of radiation within the range of heat infra-red energy is a priority when analyzing the hybrid energy network due to increment in the capacity of the global warming rate. The production of clean energy is the appropriate choice for a sustainable techology in power system by integration of renewable energy system support to minimize or reduce emission from the world's sector relating to

energy production. The ozone (O_3), natural gas (CH_4), nitogen (I) oxide (N_2O), carbon (IV) oxide (CO_2), and water (H_2O) vapour form the main (primary) greenhouse gases on the atmospheric environment of the earth's surface. The batteriesand biogas generator from the hybrid energy generation network produces the low radiant energy (harmless emission) while the fossil fuel energy from the grid system form the green house gases thereby causing greenhouse effect on the atmosphere, which is very harmful to the human health and mathematically expressed below.

$$A_{Eghg} = \text{Minimum}\left(\sum_{T=1\ hour}^{T=8760\ hours} (T \times [\pi\ (CO_2 + SO_2 + NO_X) \times P_{u\text{-}network}]) \right) \quad (23)$$

A_{Eghg} = Annual energy generated from the renewable energy-grid network connection producing emission of greenhouse gases (kWh)

$\pi\ (CO_2 + SO_2 + NO_X)$ = Factor of emission from carbon (IV) oxide, Sulphur (IV) oxide, and nitrogen oxide.

$P_{u\text{-}network}$ = Output power generation from the hybrid energy network (kW)

T = Period of energy generation and emission from the hybrid energy sources (hours)

Inhabitants of Onnut community purchase electric energy from the utility grid and biogas generator to maintain daily living.The emission factors from carbon compound is needed in calculating the benefits from Onnut environment when the microgrid network utilizes biogas sustainable generator to produce electric energy, thereby, reducing emission from carbon compound produced by the utility grid towards the environment. The emission factor of the microgrid netwoirk can be estimated below [129].

$$GHe = \frac{El \times Gf}{1000} \quad (24)$$

GH_e = emission from greenhouse gases (kg), El = electric energy consumed (kWh), Gf = emission factor from greenhouse gases at Onnut community ($gkWh^{-1}$) [131, 132].

3.5.3 Biogas power generator

The feedstock resources comprises of woods/leaves, glass, textiles, metals, bones/shell, leather/rubber, paper, plastics/foam and food scraps that will be used as a fuel supply source from the community to power the biogas generatorin producing electricity.The generated output electricity from the biomass plant can be represented by equation 25.

$$Elec_{biog} = \frac{\text{Available biogas fuel } (A_{bgl}) \times Calvbio \times \eta bgs \times \Delta top \times 0.277778}{36500 \times hbgs} \quad (25)$$

$Elec_{biog}$ = Output electricity flow from the biogas generator (kWh/yr)

A_{bgl} = Annual available biogas fuel in $kg.yr^{-1}$

Cal_{vbio} = Heating value of the biogas fuel = 20.0 MJ per kg

Δtop = Annual operation period of biogas generator in hrs/yr

ηbgs = Efficiency of the biogas generator during energy conversion in %

$hbgs$ = Period of operating the biogas generator annually (hours) [129-130].

3.5.4 Hybrid batteries

The generated electricity and consumption of energy from the power system operation depends on the hybrid storage quantities and their present charging state at a given period. The storage system charges when the excess electricity generated from the microgrid network is beyond the demand requirement. The available energy stored in the batteries at a specific period is given by equation 26. The microgrid's reliability can be improved through a backup energy source (batteries and dispatch able biogas plant) in supporting the utility grid source against congestion and outage (shortage in capacity) from the power sources. The application of hybrid (lithium ion, flow, and zinc bromide batteries) reserve system and biogas plant will maintain a steady power flow operation.

$$E_{gn}(t_r) = E_{gn}(t_r - 1) + (1 - ṡ) + [(E_{ne}(t) - (E_{qe}(t) \div \eta_{cve})] \times \eta_{gn} \quad (26)$$

$$E_{gn}(t_r) = E_{gn}(t_r - 1) + (1 - ṡ) - [(E_{qe}(t) \div \eta_{cve}) - E_{ne}(t)] \quad (27)$$

$E_{gn}(t_r)$ = Quantity of current energy in the batteries measured in kWh

$E_{gn}(t_r - 1)$ = Quantity of preceding energy in the batteries measured in kWh

$ṡ$ = Rate of auto emission from the batteries

η_{cve} = regulating efficiency of the power converter (%)

η_{gn} = regulating efficiency of the batteries during charging and discharging modes (%)

$E_{qe}(t)$ = Energy demand (kWh)

$E_{ne}(t)$ = Overall electricity production from the microgrid system (kWh)

$$\text{Where } E_{ne}(t) = Elec_{biog}(t) + Elec_{grid}(t) \quad (28)$$

$Elec_{grid}(t)$ = output electricity from the utility grid (kWh)

The boundaries relating the minimum and maximum charging states of the batteries is given by equation 29.

$$CHG_{min} \leq CHG(t) \leq CHG_{max} \quad (29)$$

Where CHG_{min} and CHG_{max} represent the minimum charging state (%) and maximum charging state (100 %) estimations. The minimum charging state of the batteries can be stated from the equation below.

$$CHG_{min} = 1 - Dcrg \quad (30)$$

Where Dcrg represents the discharging depth of the batteries (%).

The operational cost and capital investment of the batteries are increased by the batteries' settings. Hence, the life span of the batteries can be estimated from equation 31.

$$S_{byt} = MINIM\left(\frac{M_{byt} \times R_{sng}}{R_{yr,bytP}}, Q_{MAXIM,lyf}\right) \quad (31)$$

Where S_{byt} =Lifespan of the batteries (years), M_{byt} = Battery pack with a definite quantity of batteries, R_{sng} = Throughput lifespan of each battery in the pack (years), $R_{yr,bytP}$ = yearly throughput of the battery pack (total cyclic energy of the battery pack annually) in years, $Q_{MAXIM,lyf}$ = maximum lifespan of the batteries irrespective of their cyclic throughput (years)[129, 130].

3.5.5 Electronic energy conversion system

The electricity flowing from the output electronic conversion system is given by the equation below.

$$PW_c = V_{mg} \times (I_{biog} + I_{ug} + I_{gn}) \quad (32)$$

V_{mg} = Microgrid's nominal voltage multiplier on the storage system (batteries) in Volt.

The I_{ug}, I_{biog} and I_{gn} are the resultant rectified currents from the biogas generator, utility grid and batteries, respectively. The regulating efficiency of the electronic conversion system relates the output to the input power ratios generated. When energy is converted between the DC and AC buses by the full wave power electronics converter, losses occur which affects the microgrid system, resulting in efficiency loss.

$$PW_i(t) \times \eta_{cve} = PW_{op}(t) \quad (33)$$

$PW_i(t)$ = Input Power flowinginto the electronic conversion system (kW)

η_{cve} = Conversion efficiency of the electronic system (%)

$PW_{op}(t)$ = Output power flowing from the electronic conversion system (kW)

The production of efficiency when energy is converted between the DC and AC buses by the electronic (3 phase) power conversion system is estimated below.

$$\eta cve = \frac{PWop(t)}{PWug(t) + PWbiog(t) + PWgn(t)} \quad (34)$$

Where $PW_{ug}(t)$, $PW_{biog}(t)$ and $PW_{gn}(t)$ represents the output power flowing from the utility grid, biogas generator and the storage system (batteries), respectively [129-130].

3.6 Econometrics index

Calculating the econometric indexes of the microgrid system comprises of the overall (total net) present cost (NPCO), balanced (levelized) electricity cost (LECE), initial base (capital) cost, cost of operating the microgrid network and emission of gases to the atmospheric environment that will be evaluated from the generation of electricity by the integrated microgrid network. The internal return's rate (IRRA) and investment return (ROIV) will be calculatedfrom the microgrid operation by adopting industrial HOMER PRO energy analysiswith the grid forming/grid following model. The NPCO is the stability between the current estimated cash invested originally and the flow of net cash generated by the microgrid system at a discount rate of the base (capital) cost. The invested cost comprises of the initial capital (money) invested on the microgrid's components, in operating-maintaining-replacing the microgrid components, and buying electric power from the utility grid to avert capacity shortage. The application of NPCO calculates the scheme of the microgrid system's economics. If NPCO>0, the microgrid system will experience life span losses, otherwise, profits will be made from the microgrid system. The NPCO is estimated in equation 35.

$$NPCO = \frac{C_{yr,TC}}{CRE_{m,Lsyt}} \tag{35}$$

$C_{yr,TC}$ = yearly overall cost of the microgrid system ($ USD/yr), $CRE_{m,Lsyt}$ = factor of recovery from capital, m = interest's rate (%), Lsyt = lifespan of the microgrid network (years).

The generated cost estimated after balancing (leveling) the generated power in operational cycle and operational cycle cost gives the LECE estimated from equation 36.

$$LECE = \frac{\sum_{v=0}^{V} C_v \left(1+ m\right)^{-v}}{\sum_{v=0}^{V} E_v \left(1+ m\right)^{-v}} \tag{36}$$

C_v = overall annual cost ($USD/yr), E_v = overall electric energy consumed annually (kWh/yr), m= interest's rate (%) on discount rate basis.

The IRRA gives the rate of discount during the life span of the energy system at which the value of the net present flow equals 0 estimated in equation 37.

$$IRRA = \sum_{tm=0}^{V} NPF_{tm} \left(\frac{Pi}{D, IRRA, tm}\right) = 0 \tag{37}$$

NPF_{tm} = overall flow of cash annually ($USD/yr), Pi = principal value ($ USD), D = value of end cash ($USD).

Investment's return (RI) is the returned value after investing on the project which means the financial return on investing on the microgrid network. The estimated equation is given below.

$$RIV = \frac{IN_V - EX_P}{EX_P} \tag{38}$$

RIV = Investment's return ($USD), IN_V = overall investment's income ($USD), EX_P = overall investment's expenses ($USD) [131].

CHAPTER 4
EXPERIMENTAL ANALYSIS AND SIMULATION

4.1 Mechanical Processing System for On-Nut Biomass Wastes

The disintegration of bags and raw wastes (overall wastes: 800.00 tonnes/day) separation is known as the pre-treatment (mechanical) processing system. Wastes are channeled through the hopper's feeder plate with some water freely filtered out and channeled to the filtrate pre-treatment processor. The filtered solidified wastes are channeled through the conveyor's belt to a manually sorted place and enormous substances as interference (in garbage) undergo separation with disposition and the manually sorted garbage enters a drum screen with disintegrated bag. Following the drum screen, the sieved material above 120.0 mm (322.890 tonnes/day) will be conveyed and disposed (inclined) with enormous substances as interference. The sieved material lesser than 120.0 mm (444.580 tonnes/day) are extracted and conveyed to the biological-hydrolysis processing system. Metals that are magnetically selected undergo recycling as depicted from the modelled graphical display of the mechanical-biological wastes treatment process below.

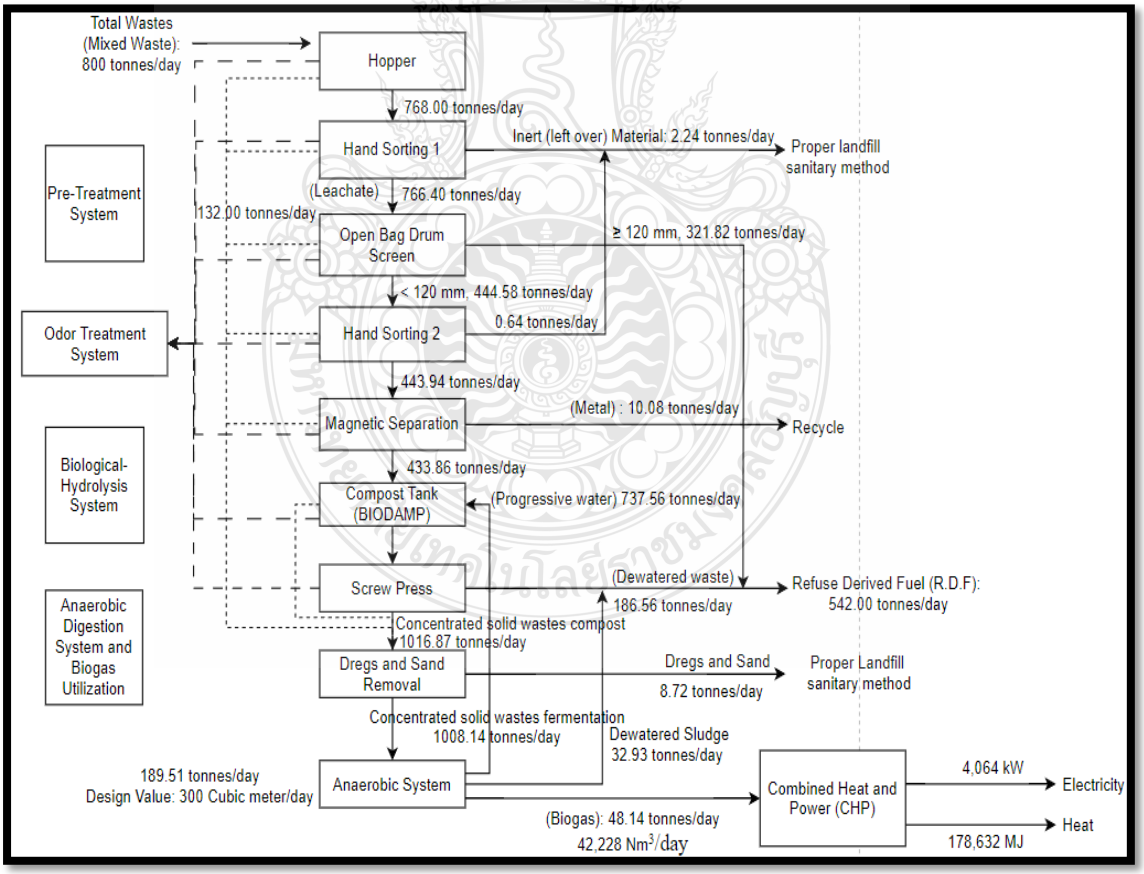

Figure 4.1 Modelled Mechanical/Biological Wastes Treatment Unit Estimation.

The biological-hydrolysis processing system comprises of a preparation tank for fermentation and a machine for compression (screw press: 1016.870 tonnes/day) to obtain the solidified wastes (known as fuel derived from refuse: R.D.F 2) and concentrated solidified wastes leachate high bowl for transportation to the anaerobic breakdown tank. Thereby producing biogas fuel supply (48.14 tonnes/day; 42,228.000 m^3/day) to the biomass plant to produce electric energy-heat (178,632.000 MJ) and power (4,064.000 kW) for distributed extension of electricity from Fig.4.1.

Input wastes quantity before treatment = 800 tonnes/day

Output wastes quantity after treatment = 189.51 tonnes/day

Percentage utilization of waste (%) = [Output wastes quantity after treatment/ Input wastes quantity before treatment] × 100 %

Percentage utilization of waste (%) = 189.51/800.00 = 0.2369 × 100 % = 23.69 %.

From Fig.4.1, the concentrated wastes left after proper treatment before anaerobic digestion to produce biogas fuel was 189.51 tonnes/day as compared against the total wastes supply (800.00 tonnes/day) before treatment. The percentage utilization of wastes left before conversion to biogas fuel is 23.69 %.

Percentage wastes loss = (100 %) – (percentage utilization of wastes left before conversion to biogas fuel)

Percentage wastes loss = 100 % - 23.69 % = 76.31 %.

76.31 % of biomass wastes was lost during the treatment process from Fig.4.1

The concentrated biomass wastes left (189.51 tonnes/day) after treatment underwent anaerobic breakdown system to generate biogas fuel quantity of 42,228 m^3/day; 48.14 tonnes/day from Fig.4.1

Quantity of biogas fuel production from anaerobic breakdown = 48.14 tonnes/day

Percentage composition of biogas fuel production = [Quantity of biogas fuel production from anaerobic breakdown/ Output wastes quantity after treatment] × 100 %

Percentage composition of biogas fuel production = [48.14/189.51] × 100 % = 0.2540 × 100 % = 25.40 %

Therefore, the percentage composition of biogas fuel production from the concentrated biomass wastes after treatment was 25.40 %.

4.1.1 Wastes Treatment Result

The capacity potential of the single line pre-treatment processing system theoretically is 50.00 tonnes per hour. The product productions after the treatment process are

undersized materials, oversized materials, leachate, metal, wastes, large interference substances, etc. The composition and properties of each product (material) are tabulated from the table below and their specific composition may change with respect to wastes composition.

Table 2 Treatment Output

Material component (s)	Quantity
Wastes	800 tonnes/day
Enormous interference substance	≤ 1.0 %
Metal	(1.0 - 2.0) %
Leachate	(3.0 - 5.0) %
Undersized material	(50.0 – 60.0) %
Oversized material	(30.0 - 45.0) %

4.1.2 Balancing the masses of wastes to power conversion system

The mean value (average) of the solidified wastes composition can be utilized for the calculation of the mass balance of the stages involved in the conversion process of the wastes to electricity system when managing the solidified wastes (800 tonnes/day) as tabulated in table 3. The equations relating the total solid (T.so), percentage composition of the total solid (% T.so) and percentage content of water (% W.co) from the wastes are stated below.

$$\text{Total solid (T.so)} = W_{eg} - W_{tr} \tag{39}$$

$$\text{Percentage total solid (\% T.so)} = \frac{W_{eg} - W_{tr}}{W_{eg}} \times 100\% \tag{40}$$

$$\text{Percentage water content (\% } W_{ct}\text{)} = \frac{W_{tr}}{W_{eg}} \times 100\% \tag{41}$$

Where W_{eg} = Weight of input plant (materials) for processing in tonnes

W_{tr} = Weight of water content (tonnes).

Table 3 Wastes to Mass Balance System

Conversion system	**Processing**	**Materials W_{eg} (tonnes)**	**Solid T.so W_{eg} - W_{tr} (tonnes)**	**Water content W_{tr} (tonnes)**	**Solid volatility (tonnes)**	**(%)T.so** $\frac{W_{eg} - W_{tr}}{W_{eg}} \times 100\%$	**(%) W_{ct}** $\frac{W_{tr}}{W_{eg}} \times 100\%$
Wastes reception	Input garbage	800.000	367.690	432.310	105.210	45.961	54.040
	Leachate	32.000	0.640	31.360	0.000	2.000	98.000
	Solid wastes density	1.600	1.120	0.480	0.000	70.000	30.000
	Solid wastes discharge (output)	766.400	365.930	400.470	0.000	47.750	52.250
Sorting section (pre-treatment)	Oversized garbage	321.820	185.780	136.040	0.000	57.730	42.270
	Inert (left over) material	0.640	0.510	0.130	0.000	80.000	20.000
	Metal	10.080	9.580	0.500	0.000	95.040	5.000
	Solid wastes conveyed to compost tank	433.860	170.060	263.800	0.000	39.200	60.800
Fermentation process: Biological-hydrolysis preparation	Water recirculation	737.560	1.480	736.090	0.590	0.200	99.800
	Material mixture	1171.430	171.540	999.890	100.540	14.640	85.360
	Wastes compression for dewatering	186.560	111.940	74.620	0.000	60.000	40.000
	Fermentation of concentrated solidified wastes (liquid leachate)	1016.870	60.240	956.620	0.000	5.920	94.080

Table 3 Wastes to Mass Balance System (Continued)

	Inert (leftover) material	8. 720	3.660	5.060	0.000	42.000	58.000
	Fermentation of concentrated solidified wastes (leachate pre-treated)	1008.140	56.580	951.560	50.270	5.610	94.390
Anaerobic breakdown system (Biogas generation)	Concentrated solidified wastes fermentation water flows to the system (input)	1008.140	56.580	982.920	50.270	5.610	94.390
	Biogas fuel	48.140	48.140	0.000	0.000	100.000	0.000
	Residue	960.000	8.440	982.920	0.000	0.880	99.120
	Water removal sludge	32.930	6.590	26.340	0.000	20.000	80.000
	Sludge in biogas generation system: biogas slurry	927.070	1.850	925.220	0.000	0.200	99.800
Treatment of wastewater	Input: Wastewater channeling the system	189.510	0.380	189.130	0.000	0.200	99.800
	Water removal sludge	1.190	0.240	0.960	0.000	20.000	80.000
	Water treated	188.320	0.140	188.180	0.000	0.070	99.930

4.1.3 Electric Energy Generation from Biogas Fuel

The biogas fuel production from the anaerobic breakdown system produced 42,228.000 m^3 of biogas fuel and 92,902.640 kWh electric energy per day which in

equivalence amounted to power generation of 4,064.000 kW capacity (operated for 22.86 hours) from table 4 and table 5.

Table 4 Wastes to Energy (Electricity) Conversion

Processing	Value	Unit
Input wastes	800.000	tonnes/day
Food wastes fraction	46.970	%
Water content of food wastes	72.000	%
Input of volatile solids in wastes	105.210	tonnes/day
Undersized food wastes fraction	95.000	%
Undersized volatile solids in food wastes	99.950	tonnes/day
Water recirculation	737.560	tonnes/day
Fraction of volatile solids in water recirculation	0.080	%
Volatile solids in water recirculation (volume)	0.590	tonnes/day
Input volume of volatile solids channel to compost tank (bio-damp)	100.540	tonnes/day
Rate of volatile solids degradation in compost tank (bio-damp)	45.000	%
Rate of volatile solid degradation in anaerobic breakdown	80.000	%
Rate of biogas production from volatile solids	1200.000	m^3/tonne of volatile solids
Biogas fuel generation	42,228.000	m^3/day
Energy production capacity per unit	2.200	kWh/m^3
Energy yield	92,902.640	kWh/day
Generated power capacity	4,064.450	kW
Lower heating gas value	20.000	MJ/m^3

Table 5 Quantity of Solidified Wastes and Residual Material Yield in Wastes Treatment

Treatment process	Machineries	Product (s)	Quantity	
			Unit (s)	Percentage (%)
On-nut solidified wastes channel to the processor system	Wastes storage location (project office)	Wastes	800.000 tonnes/day	100.000
Pre-treatment (separation) system	Rotational garbage trapping (drum) plate (screen)	Solidified wastes fuel (R.D.F 1)	321.820 tonnes/day	40.230
	Magnetic separator (metallic separator)	Solidified metallic wastes	10.080 tonnes/day	1.260

Table 5 Quantity of Solidified Wastes and Residual Material Yield in Wastes Treatment (Continued)

		Inert solidified material (leftover)	2.240 tonnes/day	0.280
Fermentation processing (biological hydrolysis) system	Fermentation processing compost (bio-damp) tank	Concentrated solidified wastes Liquid (water)	1016.870 tonnes/day	0.000
	Screwing press	Solidified wastes fuel (R.D.F 2)	186.560 tonnes/day	23.320
Biogas and energy generation (Anaerobic breakdown and biogas fuel application) system	Removal of sand and dregs Gravel and sand separator	Solidified inert material	8.720 tonnes/day	1.090
	Fermentation of biogas (tank) Anaerobic breakdown tank	Biogas fuel	48.140 tonnes/day 42,228 Nm^3/day	0.000
	Centrifuge of sludge	Solidified wastes fuel (R.D.F 2)	32.930 tonnes/day	4.120
	Generation of power and heat	Electric power	4,064.000 kW	0.000
		Energy	215,952.000 MJ	0.000

The fraction of metallic solidified wastes, inert solidified material, fuel derived refuse (wastes fuel, R.D.F) and biogas fuel from the wastes to energy conversion (mass) balance system from table 4 has been determined with power capacity generation as summarized from table 6 below.

Table 6 Power and Mass Stability of Wastes to Power Conversion Technology

Product/Material	**Output yield**
Fuel derived refuse (R.D.F 1)	322.000 tonnes/day
Fuel derived refuse (R.D.F 2)	220.000 tonnes/day
Power generation from biogas fuel	4,064.000 kW
Power usage in project	1,019.000 kW
Electric power sales	3,045.000 kW

The generation of biogas fuel from the biomass wastes treatment system at On-nut community comprises of a buffer tank (tank for wastewater) and four anaerobic breakdown tanks (reactor) with their respective dimension calculation from table 7 and table 8, respectively.

Table 7 Buffer Tank (Wastewater Container) Dimension

Dimension (s)	Quantity	Unit (s)	Equation
Input water channel to the buffer tank	1008.140	tonnes/day	None
Required period of water retention	1.000	day	None
Required volume	1007.940	m^3	Area × height = A.H
Diameter (designed)	12.000	m	None
Height (designed)	12.000	m	None
Height to diameter ratio (designed)	1.000	unit less	$\frac{H}{D}$
Effectiveness of height	11.000	m	H - 1
Effectiveness of volume	1243.440	m^3	$\frac{3.140 \times D^2 \times G}{4}$

Table 8 Anaerobic Breakdown (Reactor) Estimation

Dimension (s)	Quantity	Unit (s)	Equation
Input system	1008.140	tonnes/day	none
Input concentration of biomass	74,798.850	mgL^{-1}	none
Rate of volume loading	5.000	kgm^{-3} (input concentration of biomass)	none
Required volume	15,081.600	m^3	$\frac{A \times H}{1000 \times C}$
Reactor's number	4.000	unitless	none
Reactor's volume (per system)	3770.400	unitless	$\frac{D}{H}$
Diameter design	15.000	m	none
Height design	22.500	m	none
Height to diameter ratio design	1.500	unitless	$\frac{G}{P}$
Effectiveness of height	21.500	m	G - 1
Effectiveness of volume	3797.440	m^3	$\frac{3.140 \times D^2 \times J}{4}$
Period of quarantine	15.070	day	$\frac{2.000 \times k}{A}$

4.2 Anaerobic Breakdown Model

The biomass' mass (solidified form) can be estimated below under the fixed (invariable) biomass volume.

$$M_{biom}(t) = [1 - \vartheta(t)] \times \rho_{bio-eff} \times V_{cell-bio} \tag{42}$$

$\rho_{bio-eff}$ = biomass density's effectiveness (kgm^{-3})

$\vartheta(t)$ = current biomass' porosity (constant)

$V_{cell-bio}$ = Volume of biomass cell (m^3).

$$\text{The current biomass' porosity, } \vartheta(t) = 1 - \frac{\sum_p C_p(t)}{\rho_{bio-eff}} \tag{43}$$

$\sum_p C_p(t)$ = summation of solidified concentrations under steady and active variables (p) of levo-glucosan, hydrochloric, and chlorine gases [133].

4.3 Biomass Wastes Model

Considering the mass-balance of the wastes treatment system, a dynamic model with differential equations involves state vector variables, (components' concentration and anaerobic biomass in activity), E: rate of dilution (ratio of inflow volume (m^3/d) to the breakdown volume of the breakdown liquid in m^3), rated matrix equation or stoichiometry (C), r (z): the matrix's rate of reaction), and m (z): the mass movement dynamics (involving liquid-gas interactions, mostly) [134].

$$\frac{dZ}{dt} = (Z_{in} - Z) \times E + C \times r(Z) - m(Z) \tag{44}$$

4.4 Characteristics of Biomass Elements

The calorific (heat) estimation, proximate-ultimate analysis forms the properties of biomass energy conversion. The energy contents (measured in Mega Joule per kilo gram) during the process of biomass conversion must be known and compared with coal (as a traditional resource). Biomass resources can be further described on proximate analysis basis with reports of its water content (moisture) accompanied by contents of combustible matter that is volatile, ash and fixed (constant) carbon. The importance of ultimate analysis illustrates the composition of biomass relating to 5 different top elements such as Sulphur-S, Carbon-C, Nitrogen-N, Oxygen-O and Hydrogen-H contents. The description of hemi cellulose, lignin, cellulose, fat and carbohydrates form the compositional contents as other characteristics of the biomass energy conversion. The thermal conversion of biomass during excess air availability (combustion reaction) releases heat (as total energy) which is known as its calorific or heating value. The biomass' calorific value is measured in $kJ.kg^{-1}$. The internal combustion system uses gasoline as a running fuel during its operation, thereby, generating a calorific value of 47.0 Mega Joule per kilogram while diesel fuel generates46.0 Mega Joule per kilogram ($MJ.kg^{-1}$). The calorific value for biomass ranges from 15.0-25.0 $MJ.kg^{-1}$.

4.5 Analysing Ultimate Biomass Resources and Calorific Value

The application of bomb calorimeter was used to measure the biomass' calorific value. The biomass feedstock properties are classified into calorific value (energy contents of biomass materials), ultimate analysis (composition of biomass materials: stoichiometry ratio of Carbon, Oxygen, Hydrogen, Sulphur, and Nitrogen elements) and proximate analysis (water content, constant carbon/ash, and matters with volatile combustion). Table 9 provided the calorific value and ultimate analysis of the biomass resources from On-nut community. When the bomb calorimeter (equipment) for the biomass calorific value measurement was not available, the application of Boie-Dulong equations was adopted as illustrated from equations 45 and 46, respectively.

Table 9 Calorific Value and Ultimate Analysis of On-Nut Biomass Resources

Material	Elements (% Dry Weight)						Calorific values
	Carbon C (%)	Hydrogen H (%)	Nitrogen N (%)	Sulphur S (%)	Oxygen O (%)	Ash (%)	MJ/kg
Food scraps	48.0	6.4	2.6	0.4	32.6	10.0	4.0
Woods and Leaves	49.5	6.0	0.2	0.1	42.7	1.5	18.0
Paper	43.5	6.0	0.3	0.2	44.0	6.0	16.0
Textile	55.0	6.6	4.6	0.1	31.2	2.5	19.0
Leather and Rubber	60.0	8.0	10.0	0.4	11.6	10.0	17.0
Plastics and foam	60.0	7.2	0.0	0.0	22.8	10.0	35.0
Metals	4.8	0.6	0.1	0.0	4.5	90.0	0.6
Bones and shell	0.0	0.0	0.0	0.0	0.0	0.0	0.0
Glass	0.5	0.1	0.1	0	0.4	98.9	0.1

Table 10 Mass Fraction of Solid Biomass Resources from On-Nut Community

Material	Elements (% mass fraction)					
	Carbon (C) % Mass	Hydrogen (H) % Mass	Nitrogen (N) % Mass	Sulphur (S) % Mass	Oxygen (O) % Mass	Ash % Mass
Food scraps	9.60	1.28	0.52	0.08	6.52	2.00
Woods and Leaves	0.24	0.03	0.02	0.00	0.19	0.02
Paper	1.96	0.27	0.01	0.01	1.98	0.27
Textile	2.20	0.26	0.18	0.00	1.25	0.10
Leather and Rubber	-	-	-	-	-	-
Plastics and foam	7.50	0.90	0.00	0.00	2.85	1.25
Metals	0.07	0.01	0.00	0.00	0.07	1.35
Bones and shell	-	-	-	-	-	-
Glass	0.03	0.01	0.01	0.00	0.02	5.44

The mathematical expression of Dulong's equation is stated below.

Calorific value ($kJ.kg^{-1}$) = [3.3823 × 10^4 × C] + [1.44250 × 10^5 × ($H - \frac{O}{8}$)] + [9.419 × 10^3× S] (45)

The mass fraction of the elements in the biomass material are Sulphur (S), oxygen (O), hydrogen (H), nitrogen (N) and carbon (C), respectively, [135]. From Table 10, the calorific value ($MJ.kg^{-1}$) of the individual biomass material can be estimated from the experimental data of the ultimate analysis above.

By substituting the mass fraction of the elements in each of the biomass material (S, O, H, N, and C) into equation 45.

Food scraps: [3.3823 × 10^4 × 0.48] + [1.44250 × 10^5 × (0.064 – 0.04075)] + [9.419 × 10^3× 0.004] = 16235.04 + 3353.8125 + 37.676 = 19626.5285$kJ.kg^{-1}$ = 19.6 $MJ.kg^{-1}$.

Woods and Leaves: [3.3823 × 10^4 × 0.495] + [1.44250 × 10^5 × (0.06 – 0.053375)] + [9.419 × 10^3× 0.001] = 16742.385 + 955.65625 + 9.419 = 17707.46025 $kJ.kg^{-1}$ = 17.7 $MJ.kg^{-1}$.

Paper: [3.3823 × 10^4 × 0.435] + [1.44250 × 10^5 × (0.06 – 0.055)] + [9.419 × 10^3× 0.002] = 14713.005 + 721.25 + 18.838 = 15453.093 $kJ.kg^{-1}$ = 15.5 $MJ.kg^{-1}$.

Textile: [3.3823 × 10^4 × 0.55] + [1.44250 × 10^5 × ($0.066 - \frac{0.312}{8}$)] + [9.419 × 10^3× 0.001] = 18602.65 + 3894.75 + 9.419 = 22506.819$kJ.kg^{-1}$ = 22.5 $MJ.kg^{-1}$.

Leather and rubber: [3.3823 × 10^4 × 0.60] + [1.44250 × 10^5 × (0.08 - 0.0145)] + [9.419 × 10^3× 0.004] = 20293.80 + 9448.375 + 37.676 = 29779.851$kJ.kg^{-1}$ = 29.8 $MJ.kg^{-1}$.

Plastics and foam: [3.3823 × 10^4 × 0.60] + [1.44250 × 10^5 × (0.072 – 0.0285)] + [9.419 × 10^3× 0] = 20293.80 + 6274.875 + 0 = 26568.675 $kJ.kg^{-1}$ = 26.6 $MJ.kg^{-1}$.

Metals: [3.3823 × 10^4 × 0.048] + [1.44250 × 10^5 × (0.006-0.005625)] + [9.419 × 10^3×0] = 1623.504 + 54.09375 + 0 = 1677.59775 $kJ.kg^{-1}$ = 1.7 $MJ.kg^{-1}$.

Bones and shell: [3.3823 × 10^4 × 0] + [1.44250 × 10^5 × (0)] + [9.419 × 10^3× 0] = 0.0.

Glass: $[3.3823 \times 10^4 \times 0.005] + [1.44250 \times 10^5 \times (0.001\text{-}0.0005)] + [9.419 \times 10^3 \times 0] = 169.115 + 72.125 + 0 = 241.24\ kJ.kg^{-1} = 0.2\ MJ.kg^{-1}$.

It could be noted that the estimated calorific value of the individual biomass material using the Dulong's equation is totally different from the experimental calorific value of the biomass materials from Table 10. The validity of Dulong's equation holds when the content of oxygen from the biomass materials is below 10 %. From the table above, the content of oxygen from food scraps (32.6 %), woods and leaves (42.7 %), paper (44.0 %), textile (31.2 %), leather and rubber (11.6 %), plastics and foam (22.8 %) are beyond 10 % resulting in their respective huge differences between the experimental and estimated calorific values. Hence, the Dulong's equation validity is feasible for the biomass materials such as metals (4.5 %), glass (0.4 %) and bones and shells (0.0 %) with slight differences between their estimated calorific values (1.7 $MJ.kg^{-1}$, 0.2 $MJ.kg^{-1}$, and 0.0 $MJ.kg^{-1}$) and experimental calorific values (0.6 $MJ.kg^{-1}$, 0.1 $MJ.kg^{-1}$, and 0.0 $MJ.kg^{-1}$), respectively.

The Boie's expression from equation 46can be written below.

$$\textbf{Calorific value} = (3.5160 \times 10^4 \times C) + (1.16225 \times 10^5 \times H) - (1.1090 \times 10^4 \times O) + (6.280 \times 10^3 \times N) + (1.0465 \times 10^4 \times S) \quad (46)$$

Where the mass fraction of the elements in the biomass materials are sulphur (S), oxygen (O), hydrogen (H), nitrogen (N) and carbon (C), respectively with reference to their experimental values. Considering the conversion of the biomass material to ashes during thermal processing, it was observed experimentally that the woods and leaves had the lowest percentage of ashes (0.02 %) followed by the textile (0.10 %) and paper (0.27 %) as having the second and third lowest percentage of mass ashes. The glass recorded the highest percentage of ashes (5.44 %) during the thermal conversion process from Table 10. Furthermore, Dulong's and Boie's equations are valid because the content of oxygen from the biomass materials in Table 10 is below 10 %.

4.6 Three Phase Biogas Energy Generators

The solid wastes management from On-nut community project intersecting Bangkok comprises of 4 units of biogas generators for electric energy generation. The input capacity of biomass resources (feedstock) fed as a fuel source into each unit of the biogas generator is 200 tons/day. Hence, the total feedstock for the 4 units of biogas generators amount to 800 tonnes/day. Three units of the biogas generators (each with a capacity production of 1000 kW, frequency of operation: 50 Hz, line voltage: 400 ± 10.0 % V and angular frequency: 1500 revolution/minute) are connected in parallel with the grid system for the purpose of electric sales (3000 kW) and electric purchases (1000 kW : 1200 kW) from the grid system while the remaining single unit of the off-grid biogas generator (capacity production of 1200 kW, frequency of operation: 50 Hz, line voltage: 400 ± 10.0 % V and angular frequency: 1500 revolution/minute) was designed to primarily assist in feeding the load of the community (self-consumption), respectively, as depicted from Fig.4.11 below.

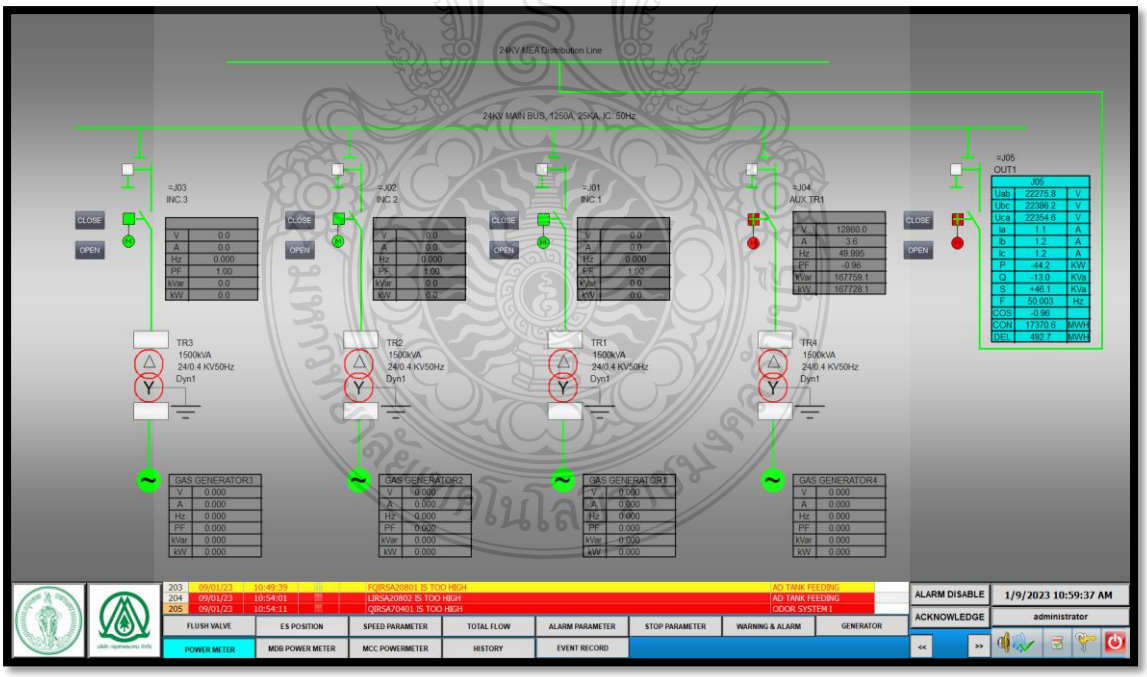

Figure 4.11 Modelled Grid/Biogas Generators' System from On-Nut Community.

The distribution line voltage rating from the metropolitan electric power in authority which flows through the main electrical bus is 24 kV, 1250 A, 25 kA, 50 Hz frequency

and processed by the operation of a control circuit through a cross link polyethylene material cable of 24 kV in connection with a cable box. A star-delta transformer steps down the line voltage (24 kV) to 400 V. The single phase and three phase standard voltages are 230 V and 400 V, respectively. Low voltages cable of 600 V/1000 V connects the step-down voltage from the star-delta transformer to each of the biogas generator. The figure above only depicts the control line system for the microgrid network before starting operation.

4.7 Experimental and Energy Flow Analysis of Grid/Biogas Network from On- Nut

The project (solid wastes management) producing electricity for On-nut community was schematically designed with the biogas generators, grid system, batteries and loads having their specified capacity in order below.

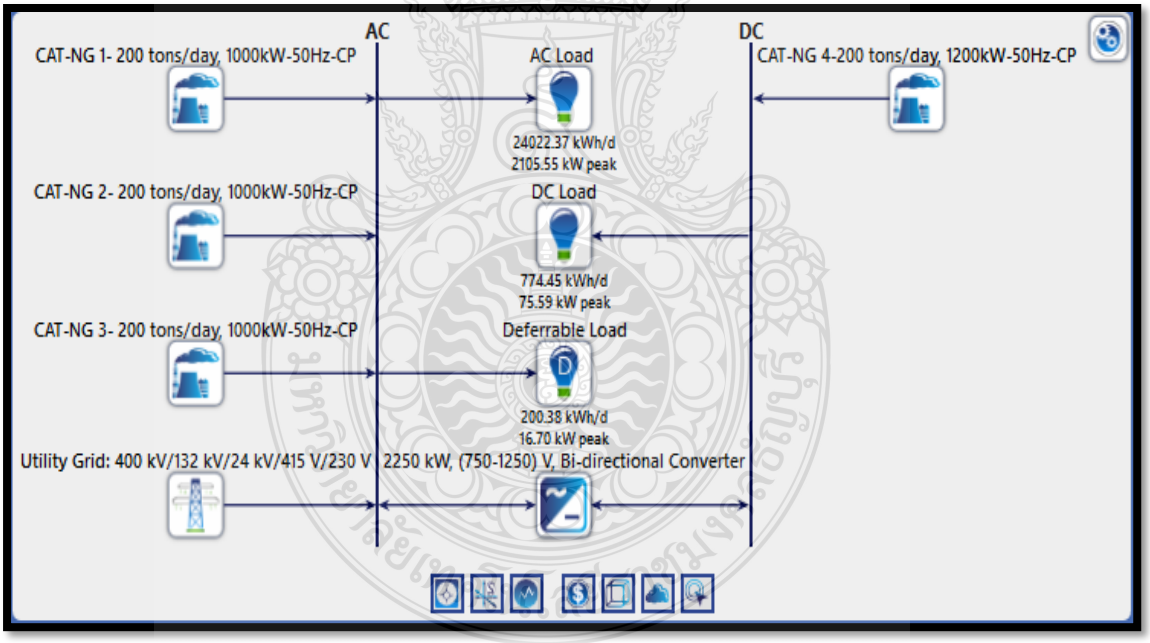

Figure 4.12 Simulation of Current Microgrid Model for On-Nut Community.

Three units of biogas generators (each biogas generator with a capacity of 1000 kW, 400 V) are in connection and operation with the grid system (400 kV/132 kV/24 kV/415 V/230 V) at On-nut community without any external backup plan (storage systems like batteries as energy supporting system). A generator order control system was adopted by

the community to trigger the biogas plants (CAT-NG 1, CAT-NG 2, and CAT-NG 3) in their respective order of operational schedule to primarily reduce the purchasing electric cost from the grid system, increase electric production sales to the grid system and satisfy the energy demand as the load increases tremendously. While the ultimate objective of the fourth biogas generator (CAT-NG 4) is to assist the grid connected biogas generators in energizing the load and improving grid sales, respectively. CAT-NG 1 biogas plant generated a low percentage (4.87 %; 551,000 kWh/yr) of annual energy production above the grid annual generation fractional contribution (2.16 %; 244,775 kWh/yr) in feeding the annual energy demanded (11,103,188 kWh/yr) with 97.87 % of energy contribution from the biogas generators (CAT-NG 1: 4.87 %; 551,000 kWh/yr and CAT-NG 4: 93.0 %; 10,512,000 kWh/yr), respectively. The biogas generators generated more grid sales (17.8 %; 1,979,046 kWh/yr) than the grid purchases (2.16 %; 244,775 kWh/yr) from the biogas-grid network with complete isolation of the second and third biogas plants (to reduce operational cost and cost of biogas fuel usage). The biogas generators (CAT-NG 1 and CAT-NG 4) have demonstrated their reliability performance in energy delivery above the grid network with no shortage potential, fully met electric load, and renewable fraction of 92.8 % from Fig.4.13

Figure 4.13 Modelled Energy Flow Analysis of Grid Connected/1000 kW: 1200 kW Biogas Generators.

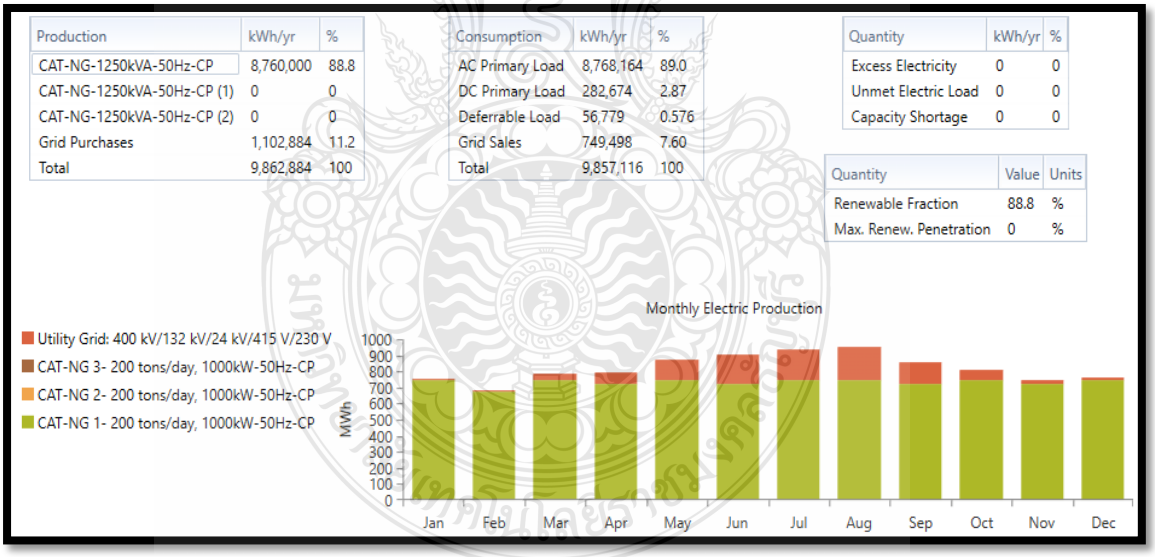

Figure 4.14 Modelled Energy Flow Analysis of Grid Connected 1000 kW Biogas Generators.

When the 3 units of biogas generators (1000 kW each) was in operation with the grid system without involving the operation of 1200 kW biogas generator from Fig.4.14, a single unit of the 1000 kW biogas generator produced a larger proportion of energy (88.8

%; 8,760,000 kWh/yr) than the grid energy share (11.2 %; 1,102,884 kWh/yr). Both energy system (biogas generator and grid system) produced a total annual energy of 9,862,884 kWh/yr beyond the demand requirement (9,857,116 kWh/yr) with a renewable fraction of 88.8 % in overcoming capacity shortage and unmet load potential. The second and third biogas generators (1000 kW each) were isolated from operating with the grid system in other to minimize cost of operation and biogas fuel usage since a single unit of the biogas plant can operate effectively with the grid system to produce sufficient energy in overcoming the load capacity. Furthermore, the energy system design from Fig.4.14 bought more energy (11.2 %; 1,102,884 kWh/yr) from the grid system than the electricity (7.60 %; 749,498 kWh/yr) sold to the grid system. Hence, the integration of three units of 1000 kW generators-grid system operation was not economical.

4.7.1 Ratio of performance on current biogas generators

The ratio of performance from the biogas generators relates their actual output thermal energy flow to their peak input thermal energy flow production under optimization condition when considering their excess energy losses under thermal and conduction losses. It is also called the efficiency of the biogas generators expressed metrically in percentage. The higher the ratio of performance of the biogas plants, the better their performances. From Table 4, the lower heating gas value of methane from the biogas production is 20.0 MJ/m^3.

Lower heating gas value = 20.0 MJ/m^3, 1.0 m^3 = 1.0 kg.

Hence, lower heating gas value of methane in mega joules per kilogram = 20.0 MJ/kg

Biogas fuel production per day = 48.14 tonnes/day, 1.0 tonne = 1000 kg

Hence, biogas fuel production in kg per day = 48.14 × 1000 kg = 48,140 kg/day.

Total lower heating gas value of methane in MJ = 20.0 MJ/kg × 48,140 kg/day = 962,800 MJ.

The peak input thermal energy flow = 962,800 MJ

Actual output thermal energy flow from experimental model (Fig.4.1) = 178,632 MJ

$$\text{Ratio of performance} = \frac{Actual\ Output\ Thermal\ Energy\ Flow\ (MJ)}{Peak\ Input\ Thermal\ Energy\ Flow\ (MJ)} \quad (47)$$

Therefore, ratio of performance (efficiency) of the biogas generators = $\frac{178{,}632\ \text{MJ}}{962{,}800\ \text{MJ}}$ = 0.1855

Hence, the ratio of performance for the current biogas generators in On-Nut community = 18.55 %.

The output operation of the 1200 kW biogas generator supporting the grid-biogas network produced an annual electric energy magnitude of 10,512,000 kWh/yr within 365 days (8760 hrs), thereby, consuming 3,819 tons of biogas fuel annually with an annual fuel energy input of 4,084,030 kWh/yr under an average excess electrical efficiency production of 257 %. The average, minimum, and maximum output power of the biogas generator remains at a capacity of 1200 kW from Fig.4.15, respectively.

Figure 4.15 Output Operation of 1200 kW Biogas Generator.

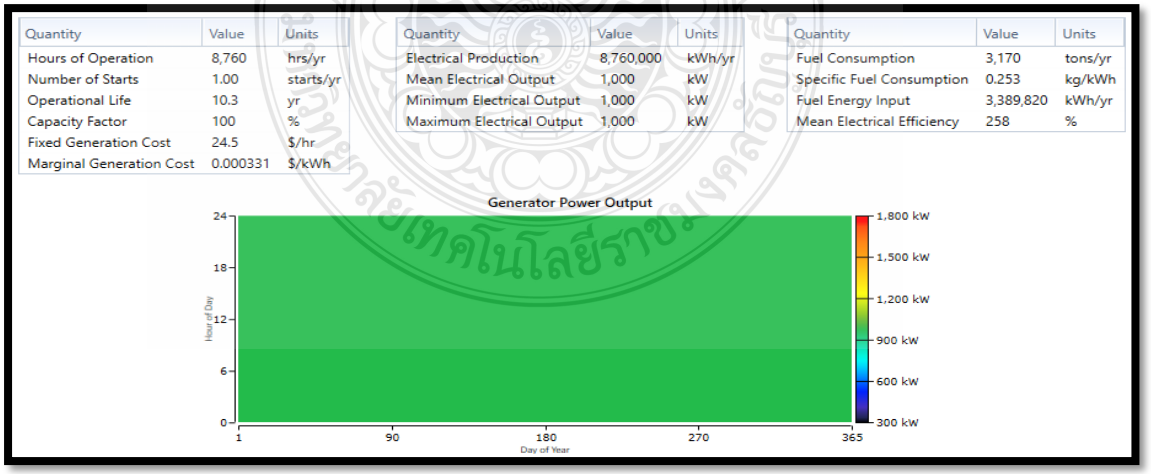

Figure 4.16 Output Operation of 1000 kW Biogas Generator.

The 1000 kW biogas generator in connection with the grid network tend to produce lower energy (8,760,000 kWh/yr) and lesser fuel consumption (3,170 tons/yr) than the 1200 kW biogas plant energy (10,512,000 kWh) and fuel consumption (3,819 tons/yr) from Fig.4.15 and Fig.4.16, respectively. Likewise, the annual fuel energy input (3,389,820 kWh/yr) of the 1000 kW biogas plant was lower than the fuel energy input (4,084,030 kWh/yr) of the 1200 kW biogas plant as a result of differences in their power capacities. The average excess electrical efficiency (258 %) of the 1000 kW biogas generator is slightly higher than the 1200 kW biogas generator (257 %) irrespective of the same hours of operation they possess. However, the constant generation cost ($29.4/hr) and marginal generation cost ($ 0.000334/kWh) of the 1200 kW generator was higher than the 1000 kW capacity generator ($ 24.5/hr, $ 0.000331/kWh).

4.7.2 Fuel curve properties of 1000 kW and 1200 kW biogas generators

The biogas fuel characteristics of the 1000 kW and 1200 kW biogas generators can be represented in Fig.4.17 with respect to their intercept coefficients, slopes (ratio of fuel consumption variation to output power variation), operating capacities and bio-fuel flow consumption rate. The flow rate of the biogas fuel consumed by the generators varies directly with the output power production of the biogas generators, respectively. This means that as the output power of the generators increase gradually (linearly), their fuel consumption also increases linearly with reference to their power capacities variation as plotted from the graphs below. The tabulated fuel curve for 1000 kW biogas generator provided the minimum output power (503 kW), average output power (750 kW) and maximum output power (1000 kW) in order of their consumption flow rate (139 m^3/hr, 194 m^3/hr, and 254 m^3/hr). The consumption rate from the 1000 kW biogas generator is very low in comparison with the high consumption rate (97.633 m^3/hr, 162.186 m^3/hr, 232.019 m^3/hr, and 308.083 m^3/hr) from 1200 kW biogas generator (as the output power varies from 300 kW-1200 kW). The modelled equation relating the referenced generating capacity, intercept coefficient, and slope (ratio of fuel consumption variation to output power variation) is expressed in equation 48.

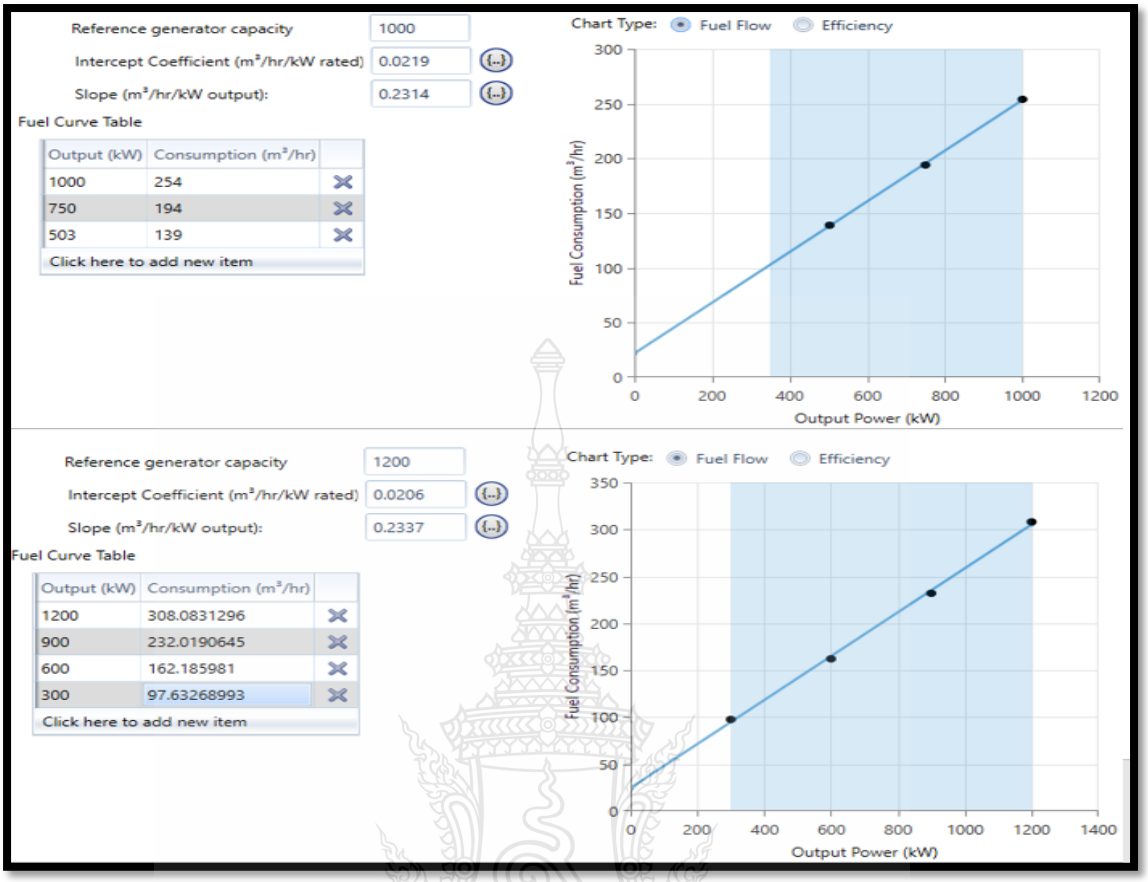

Figure 4.17 Bio-fuel Table and Fuel Flow of 1000 kW and 1200 kW Biogas Generators.

$$P(t) = (d \times A_{BIOG}) + (n \times Q_{rav}) \quad (48)$$

P (t) = Biogas consumption (m^3/hr)

d = Rated biogas fuel curve interception coefficient of the generators (m^3/hr/kW)

A_{BIOG} = Biogas generator producing power (kW)

n = Biogas fuel curve slope of the generators (m^3/hr/kW)

Q_{rav} = Average output power of the biogas generators (kW) [136].

Where d = 0.0219 m^3/hr/kW and n = 0.2314 m^3/hr/kW for 1000 kW biogas generator, d = 0.0206 m^3/hr/kW and n = 0.2337 m^3/hr/kW for 1200 kW biogas generator.

$$\text{Therefore, } P(t) = (0.0219 \times 1000) + (0.2314 \times Q_{rav}) = 21.9 + 0.2314Q_{rav} \quad (49)$$

$$P(t) = (0.0206 \times 1200) + (0.2337 \times Q_{rav}) = 24.72 + 0.2337Q_{rav} \quad (50)$$

The above expression indicates the reliance of biogas fuel consumption on the generators' output power production, respectively.

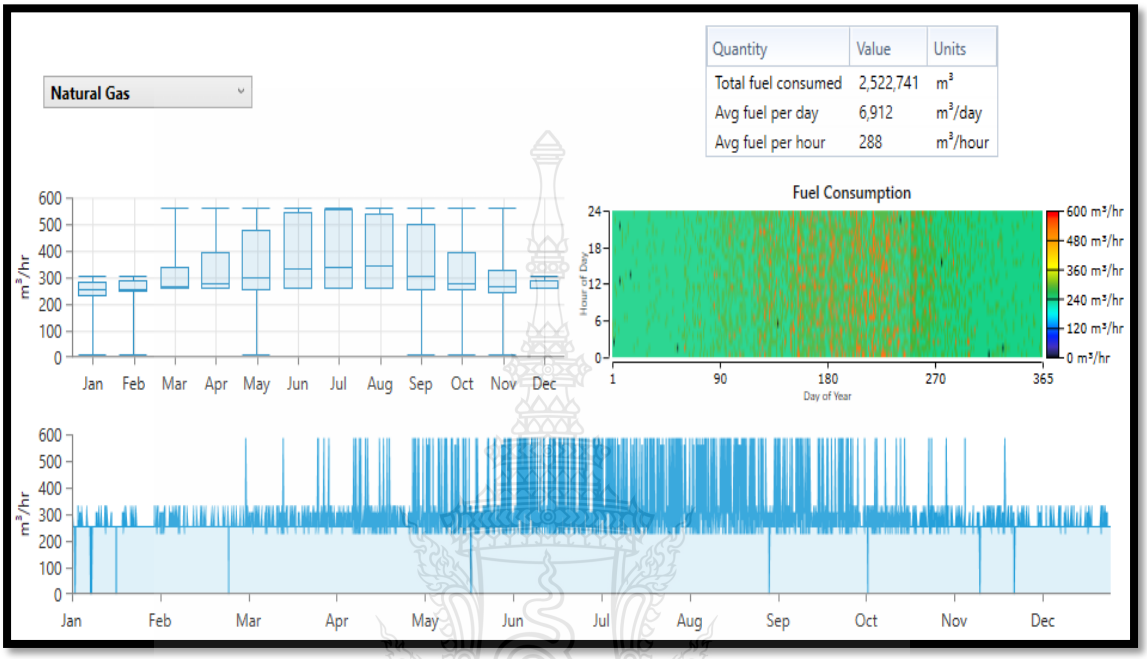

Figure 4.18 Fuel Summary of Biogas Generators/Grid System Operation.

During the grid-biogas generators operation, it was observed that the total annual volume of biogas fuel consumed by the generators was 2,522,741 m^3 with an average consumption value of 6,912 m^3 per day and 288 m^3/hour. Explaining from the table and waveform plots on how the concentration of biogas fuel consumption rate was distributed from January to December in Fig.4.18. In the month of January, February, and December, the utilization of biogas fuel for electric production was very low which amounted to 300 m^3/hr. The maximum consumption rate of biogas fuel by the generators between March and November was 585 m^3/hour because of high level of energy demanded and grid sales activities from the biogas plant to the grid system during this periodical range. The month of August possessed the highest average value of biogas fuel consumption rate (360 m^3/hr) by the generators to feed a peak demand of 2105.5 kW from Fig.4.12, respectively. Hence, the biogas fuel was greatly utilized in August when compared to other months.

4.7.3 Econometric assessment and emission from grid-biogas network

When the highest energy level of demand from the biogas-grid network happens at a specific time, the architecture of biogas generator and batteries will supply electricity to the needed energy privately under grid connection. In the absence of utmost energy demand period and there is excess electric energy production from the biogas generator company, the excess energy undergoes transmission to the grid system for energy sales according to the estimated cost of the utility grid. There is a contract agreement between the biogas generator company at On-nut community and the utility grid management to allow the utility grid management to perform excess energy purchase from the biogas company. The generated unit cost of electricity will experience reduction in price and greenhouse's cost of emission. The contract between the two organizations (biogas company and grid management) will also allow the grid management to sell electricity to the biogas company in covering the energy demanded and improving the power production reliability if there is low generation from the biogas energy company. The modelled equation relating the electricity's cost from the utility grid based on price indication or communication signal is given below.

$$E_{co} = \sum_{t=1.00}^{T} \lambda co(t) \times B_{gps}(t) - \lambda co(t) \times B_{gso}(t) \tag{51}$$

Where $B_{gps}(t)$ = Biogas network purchasing power production from the grid network during a specified time, t_{me} (kW)

$B_{gso}(t)$ = Biogas network selling excess power production to the grid network during a specified time, t_{me} (kW).

$\lambda co(t)$ = Application period of utility grid pricing communication ($USD/kWh).

The greenhouse emissions' cost, U_{ec} ($USD), from the utility grid generators producing thermal energy is given by the expression below.

$$U_{ec} = \sum_{t=1.00}^{T} [\gamma_{eka} + (\beta_{ekb} \times B_{gps}(t)) + (\alpha_{ekc} \times (B_{gps}(t))^2)] \tag{52}$$

γ_{eka} , β_{ekb} , and α_{ekc} represents the radiation co-efficient (emission constant) of the grid power alternators [137].

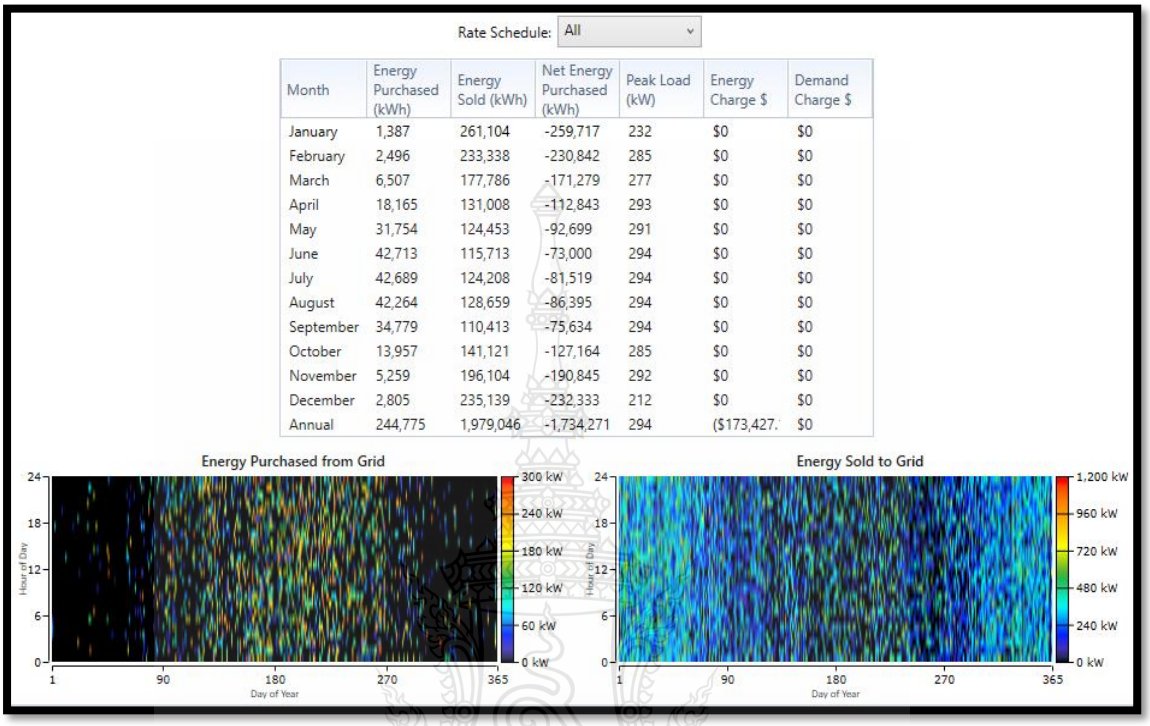

Month	Energy Purchased (kWh)	Energy Sold (kWh)	Net Energy Purchased (kWh)	Peak Load (kW)	Energy Charge $	Demand Charge $
January	1,387	261,104	-259,717	232	$0	$0
February	2,496	233,338	-230,842	285	$0	$0
March	6,507	177,786	-171,279	277	$0	$0
April	18,165	131,008	-112,843	293	$0	$0
May	31,754	124,453	-92,699	291	$0	$0
June	42,713	115,713	-73,000	294	$0	$0
July	42,689	124,208	-81,519	294	$0	$0
August	42,264	128,659	-86,395	294	$0	$0
September	34,779	110,413	-75,634	294	$0	$0
October	13,957	141,121	-127,164	285	$0	$0
November	5,259	196,104	-190,845	292	$0	$0
December	2,805	235,139	-232,333	212	$0	$0
Annual	244,775	1,979,046	-1,734,271	294	($173,427.	$0

Figure 4.19 Energy Trade of 1000 kW/1200 kW Biogas Generators/Utility Grid Network.

The energy exchange between the utility grid network and the biogas generators can be depicted from Fig.4.19 The difference between energy purchased from the grid system and energy sold to the grid system gives the net energy purchased (energy purchased in kWh – energy sold in kWh). The biogas generators-grid network system was efficient enough to produce more energy sales (1,979,046 kWh) than the energy purchased from the grid system (244,775 kWh) which is economically advantageous. The negative value of net energy purchased (-1,734,271 kWh) between the grid system and biogas generators indicate the effective performance and high reliability of the biogas generators in producing more energy than the grid system, reducing grid tariff, and fulfilling the load capacity without unmet load and capacity shortage potential. The highest peak demand occurred constantly in the month of June, July, August, and September during the year with a high energy charge of $173,427. The energy trade analysis of the hybrid network

from Fig.4.19 shows the potential capacity of the biogas generators over the grid supply. The month of January, December, and February recorded high energy sales in descending order (261,104 kWh, 235,139 kWh, and 233,338 kWh) from the biogas plants to the grid system above other months, reflecting the econometric/technical viability and efficiency of the renewable energy system over the grid system capable of operating independently without relying absolutely on the grid system.

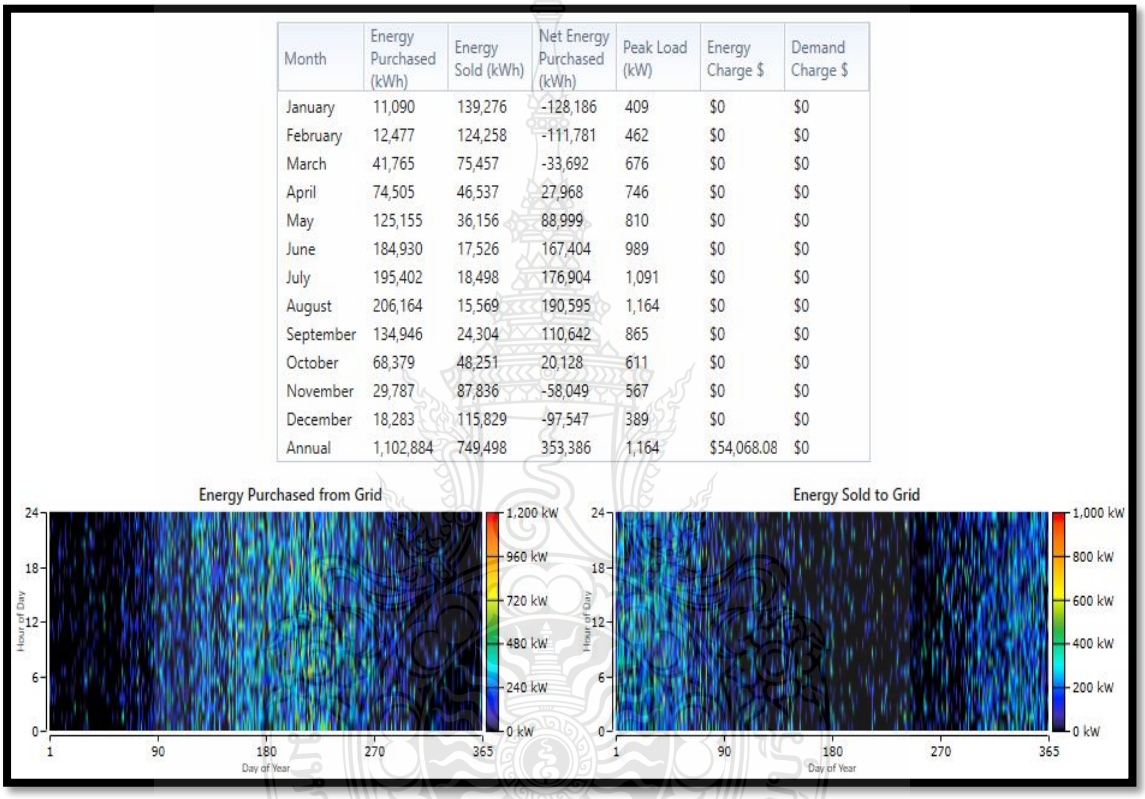

Month	Energy Purchased (kWh)	Energy Sold (kWh)	Net Energy Purchased (kWh)	Peak Load (kW)	Energy Charge $	Demand Charge $
January	11,090	139,276	-128,186	409	$0	$0
February	12,477	124,258	-111,781	462	$0	$0
March	41,765	75,457	-33,692	676	$0	$0
April	74,505	46,537	27,968	746	$0	$0
May	125,155	36,156	88,999	810	$0	$0
June	184,930	17,526	167,404	989	$0	$0
July	195,402	18,498	176,904	1,091	$0	$0
August	206,164	15,569	190,595	1,164	$0	$0
September	134,946	24,304	110,642	865	$0	$0
October	68,379	48,251	20,128	611	$0	$0
November	29,787	87,836	-58,049	567	$0	$0
December	18,283	115,829	-97,547	389	$0	$0
Annual	1,102,884	749,498	353,386	1,164	$54,068.08	$0

Figure 4.20 Energy Trade of 1000 kW Biogas Generators/Utility Grid Network.

From Fig.4.20, the net energy purchased value of 1000 kW biogas generators-utility grid configuration system was positive because the annual energy (1,102,884 kWh/yr) purchased from the grid system was greater than the annual energy (749,498 kWh/yr) sold to the grid system with a lower annual energy charge of $54,068.08 as compared against the 1000 kW/1200 kW biogas generators/utility grid architecture system having higher energy charge ($173,427) from Fig.4.19, also, the configuration system from Fig.4.20 recorded higher peak values of demand than the configuration system from Fig.4.19 The highest energy demand from system configuration of Fig.4.20 occur in the

month of August with a peak value of 1,164 kW followed by the month of July having the second highest energy demand (1,091 kW), respectively. Hence, the 1000 kW/1200 kW biogas generators/utility grid configuration was more productive economically and technically than the 1000 kW biogas generators/utility grid configuration.

Quantity	Value	Units
Carbon Dioxide	1,277	kg/yr
Carbon Monoxide	2.44	kg/yr
Unburned Hydrocarbons	1.57	kg/yr
Particulate Matter	0.764	kg/yr
Sulfur Dioxide	0	kg/yr
Nitrogen Oxides	73.0	kg/yr

Figure 4.21 Emission Properties of Utility Grid/Biogas Generators Network.

The effect of biogas generators-grid system integration within On-nut environment reduced greenhouse emission and energy production from the grid generators (fossil generators). Fig.4.21 illustrated the mass emission properties of gases between the four units of biogas generators and the grid system operation. The annual mass emission of gases produced from the biogas generators/grid unified operation network reduced the annual mass emission of the greenhouse gases tremendously (CO_2: 1,277 kg/yr, CO: 2.44 kg/yr, unburnt $C_d H_e$: 1.57 kg/yr, PM_x: 0.764 kg/yr, SO_2: 0 kg/yr and NO_x: 73.0 kg/yr gases). A prove of positive impacts from the unification (4 biogas generators) of renewable generators with the grid system of On-nut community's environment by reducing emission level of unwanted gases.

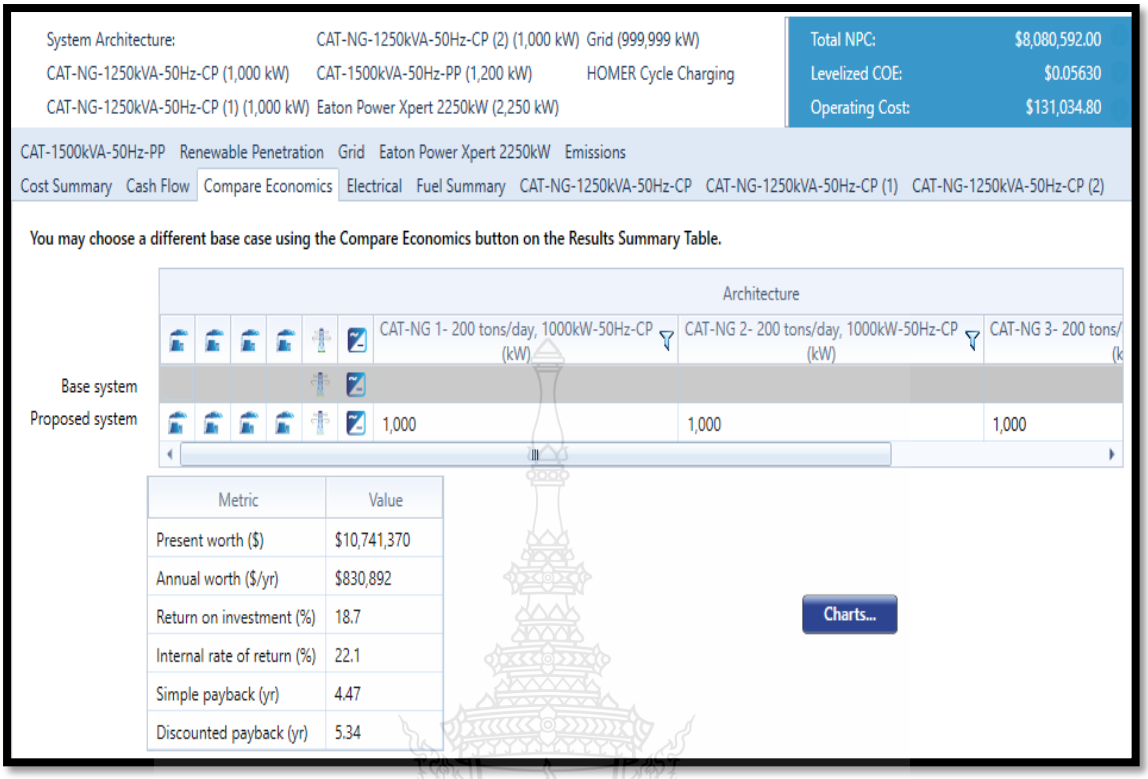

Figure 4.22 Econometric Efficiency of 1000 kW/1200 kW Biogas Generators/Grid Network.

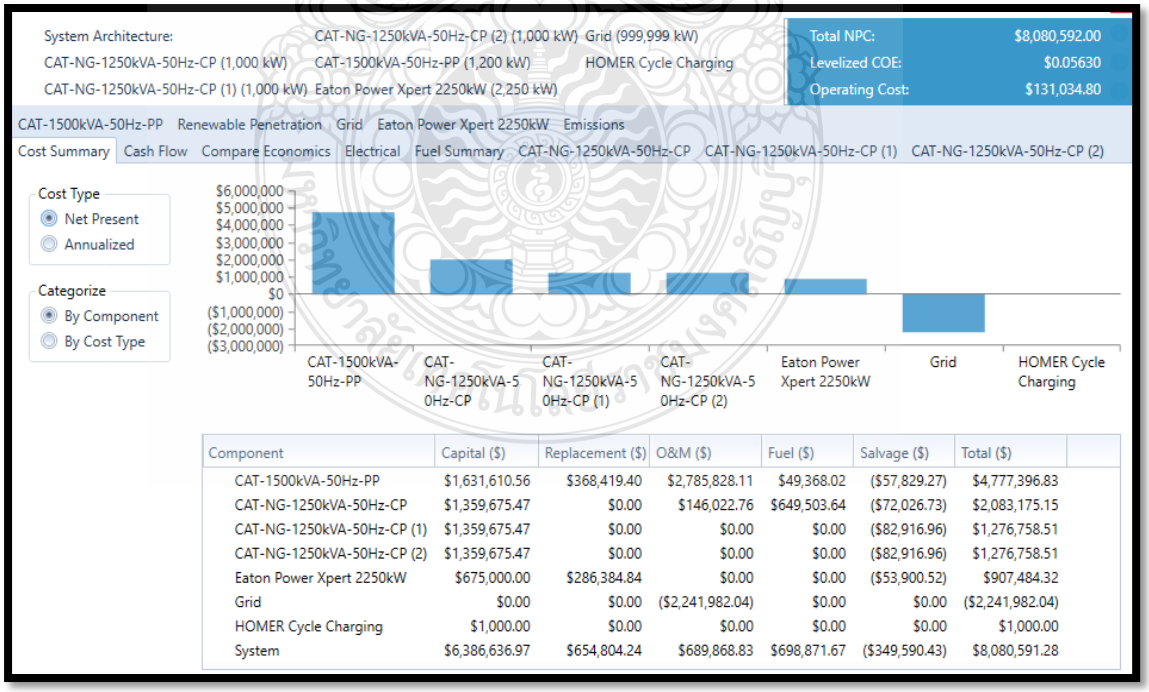

Figure 4.23 Cost Summary of 1000 kW/1200 kW Biogas Generators/Grid Network.

Considering the lowest cost and base case systems; the investment return (18.7 %), internal return rates (22.1 %: net current value at which cash flow balance equals 0), payback time (4.47 years), discount tolerance on payback time (5.34 years) of the biogas generators operating with the grid system from Fig.4.22 It was experimentally discovered from Fig.4.24 that the single unit of 1200 kW biogas generator/grid operation tends to be more economically efficient [investment return (73.0 %), internal return rates (79.0 %: net current value at which cash flow balance equals 0), payback time (1.3 years), discount tolerance on payback time (1.37 years)] than the unified biogas generators/grid service. In addition, the current ($10,741,370) and annual ($830,892) worth of the unified biogas generators/grid operation was lower in value compared to the worth price operation of 1200 kW biogas generator/grid service [current ($14,665,760) and annual ($1,134,461 USD) worth]. It takes shorter period (1.3 years) for the1200 kW biogas generator-grid operation to recover the capital invested with interest rates than the 4 units of biogas generators-grid operation (4.47 years) period over the lifespan (25 years) community project.

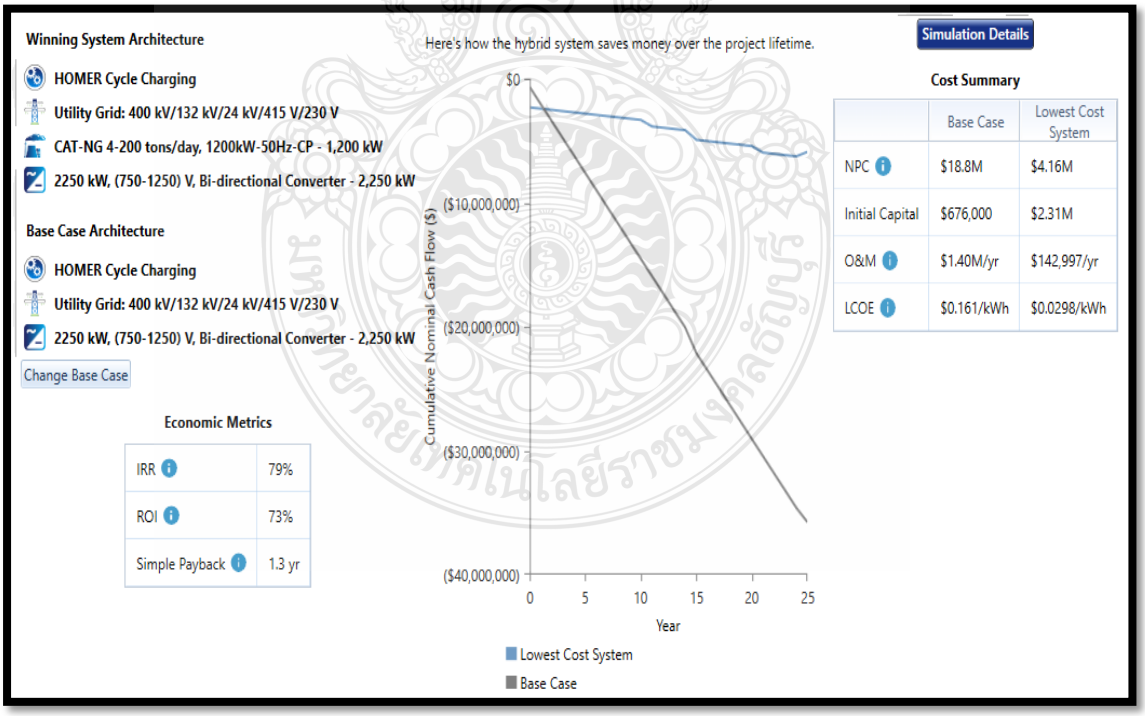

Figure 4.24 Cost Summary and Economics of 1200 kW Biogas Generator/Grid Service.

The levelized electric energy cost is the average value of overall annual cost ($/yr) of implementing the project to the overall electric energy consumed by the project annually. Levelized electric energy cost measures assessment and compares different configuration of energy system production in order to determine the econometric feasibility of the project. The net annual current valuation, levelized electric energy valuation, and operating valuation of the unified biogas generators/grid architecture from Fig.4.23 are $8,080,592.00, $0.05630/kWh, and $131,034.80/yr, respectively, which was higher in economic value than the 1200 kW biogas generator/grid architecture with net annual current valuation, levelized electricity valuation, and operating valuation of $4,156,205.00, $0.02980/kWh, $142,996.90 from Fig.4.24. It should be noted (from Fig.4.23 and Fig.4.24) that the capital investment of the1000 kW/1200 kW biogas generators/grid architecture ($6,386,636.97) was greater in value than the 1200 kW biogas plant/grid architecture ($2,307,610.56). Generally, the overall cost of setting up the 1200 kW biogas plant/grid network ($4,156,205.28) was found to be cheaper in value as compared against the 1000 kW/1200 kW biogas plants/grid network cost ($8,080,951.28) by taking the salvage, fuel, replacement and maintenance costs into consideration from the community project. It takes longer period (4.47 years) for the operation of 1000 kW/1200 kW biogas generators/grid system architecture to payback the amount invested on the project with investment return (18.7 %), levelized electric energy cost ($0.05630/kWh), internal return rate (22.1 %), and operating cost ($131,034.80) from Fig.4.23.As compared against the 1200 kW biogas generator/grid architecture from Fig.4.24 with levelized electric energy cost of $0.02980/kWh, payback period (1.3 years), investment return (73 %), internal return rate (79 %), and operating cost ($142,996.90) when considering the relationship between the lowest cost and base case systems graphically. Economically and technically, the energy system configuration of 1200 kW biogas generator/grid network is viable than the configuration of 1000 kW/1200 kW biogas generators/grid network. However, if the configuration of 1200 kW biogas generator/grid network is operating alone without any support from the other biogas generators (3 units of 1000 kW biogas power plants) with

an increment in load capacity higher than the 1200 kW biogas generator, the grid system will operate to support the 1200 kW biogas generator, thereby, preventing the entire microgrid network from shutting down and maintaining continuous power flow operation for the community.

4.8 Energy Flow Analysis of Proposed Grid-Biogas-Batteries Energy System

ERS (energy reserve system) occupies a crucial role in the activities of power generation technologies for smoothing the variable (intermittent) electric generation from clean sustainable systems (renewable energy systems) and system stability enhancement.The storage system that was adopted for the biogas generators-grid project in the community was an electrochemical (Li-ion: Li^+, flow battery: FB, and zinc bromide: Zn-Brm batteries) storage technology with their properties summarized below. Consideration of the hybrid ERS is based on the complexity of market demand. Also, applications of different ERS technologies (short/medium/long terms) for the current power system operation was investigated with power generation coverage, transmission/distribution network, and energy demand. The requirements for the distinct technical performance of ERS are a function of its application. Their specific uses were subdivided into short, medium and long-term applications based on their lengthy discharge duration shown from the figure below.

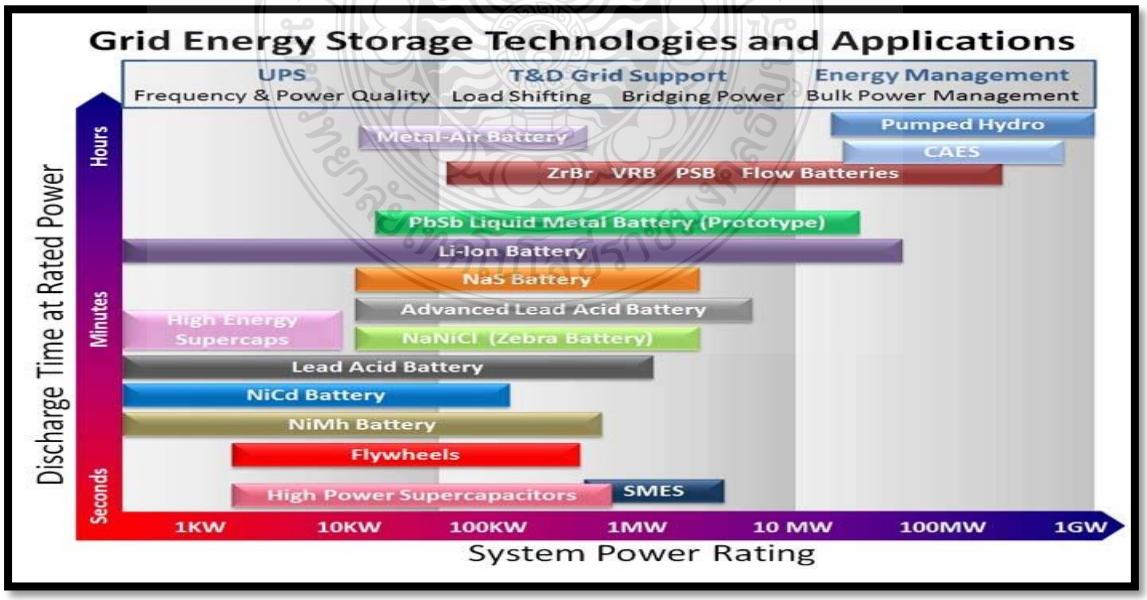

Figure 4.25 Output Power Discharge Ratings of Scalable ERS Application [138].

The energy storage system has a prominent aspect in fixing and smoothing sustainable energy systems which is an important phase for the future power grid. Most of the energy reserve technologies are not adequate for maturity to attain commercial-scale usage. Electrochemical reserve systems (Li-ion, Zn-Brm, and Pb acid batteries) have experienced a spontaneous increment in capacity installation. The high energy density of lithium-ion batteries coupled with its top efficiency cycle occupies most project works in ERS. Biomass storage and gas reserve systems with other storage technologies are ongoing in the stage of research that achieves no future carbon emission as one of their efficient ways. Energy storage systems possess a broad usage in association with power generation, transmission grid, power transformation, power distribution, and energy consumers (five key components in power system). The technical performance of Li-ion, flow, and Zinc bromide (Zn-Brm) batteries with the 4 units of biogas generators-utility grid generation network was analyzed below with reference to their emission, econometric and electrical properties, respectively.

The wastes treatment process can cause delay in the production of biogas fuel to be fed to the biogas generators for electric production due to advanced technology involved in sorting, filtering, separating and removing impurities from the biomass wastes. The proposed batteries will support critical energy demand during slow response from the operational startup of the biogas generators, grid outage or temporal drop in electric generation from the utility grid or biogas generators. The batteries will provide fast response in bridging power gaps between the generators and load effectively. In addition, they can minimize charges leveled up by the grid system when maximum load arises against the microgrid network.

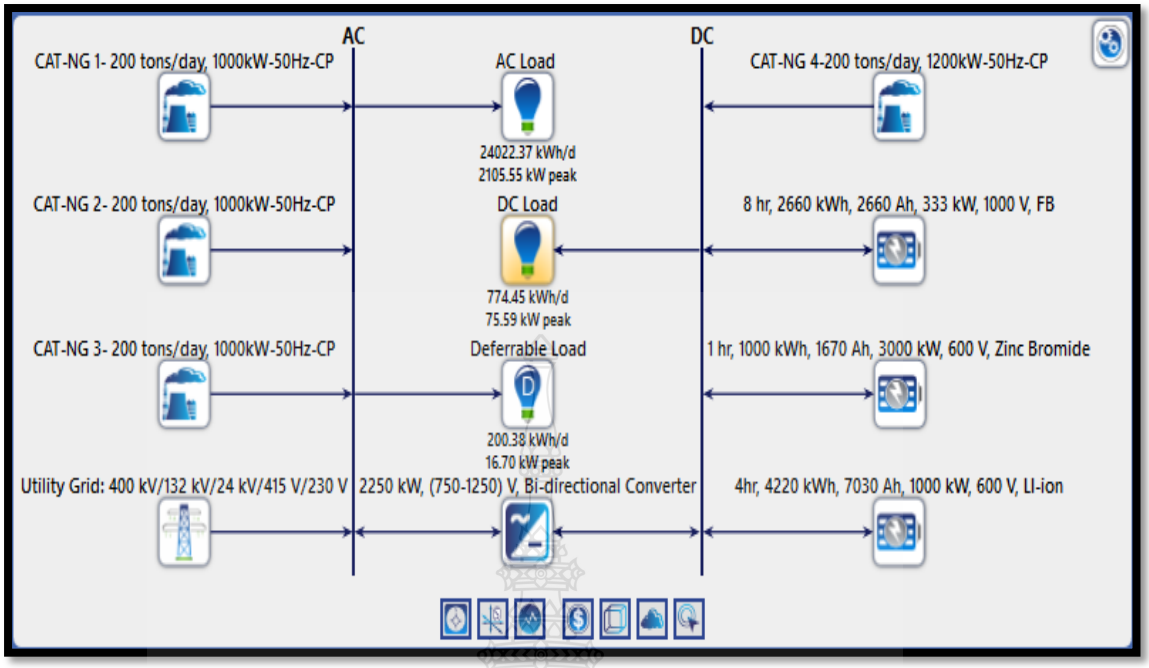

Figure 4.26 Schematics of Proposed Microgrid Model for On-Nut Community.

The figure above (Fig.4.26) depicts the proposed technological design of the microgrid network for the community. This network integrates the storage systems (Li-ion, FB, and Zn-Brm batteries) into the utility grid-biogas generating architecture to determine the effective performance of the entire network system. The lithium-ion storage operation had a peak charging level of 80 % in January while the months of March, May, August, and September recorded 44.0 % charging level uniformly. The months of February, April, June, July, October, November, and December recorded 20.0 % minimum charging level. The percentage frequency distribution of energy from Li-ion battery annually was 97.44 % with a lower output energy (83,519 kWh/yr) than the input energy (89,243 kWh/yr), and energy losses of 9,097 kWh/yr, respectively, from the biogas generators-grid-Li-ion configuration. The lithium-ion battery operated autonomously for a period of 3.24 hours with annual cyclic energy flow of 88,037 kWh/yr, no mean energy cost ($0/kWh), and columbic's efficiency of 93.59 %from Fig.4.27. The Zn-Brm battery produced a steady minimum and maximum charging level (20.0 % and 100.0 %) in January, February, March, September, October, and November. It experienced an annual frequency distribution drop of 63.95 % and columbic efficiency of 90.08 %. Between April-August and December, there was a change in the charging level from 90.0 %-82.0 %. In contrary,

Zn-Brm battery had lower autonomous operational period (0.768 hr) than Li-ion battery (3.24 hr) because the high energy consumed and released by the Zn-Brm was more than the Li-ion system. The mean energy cost of Zn-Brm battery from Fig.4.28 was found to be the same with Li-ion and flow batteries' average cost of $0/kWh from Fig.4.29. While the annual output energy, input energy, energy losses and cyclic flow energy production (904,014 kWh/yr, 1,003,616 kWh/yr, 100,403 kWh/yr, and 952,914 kWh/yr) of Zn-Brm battery was discovered to be higher than Li-ion's energy flow properties.

The operations from the batteries in Fig.4.27, Fig.4.28, and Fig.4.29 assisted the microgrid network in optimizing electricity cost, decarbonization, voltage support provision, and regulating frequency of the microgrid network as the voltage of the batteries change.

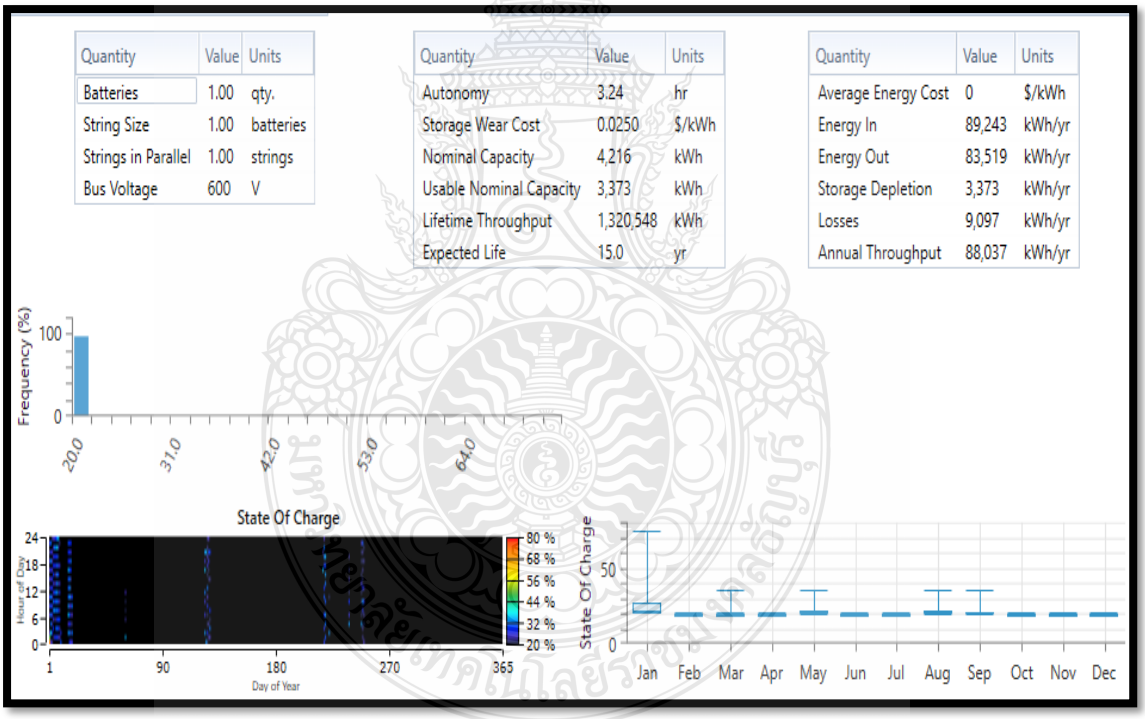

Figure 4.27 Characteristics of Lithium-ion Battery Operation with Biogas Generators /Utility Grid Network.

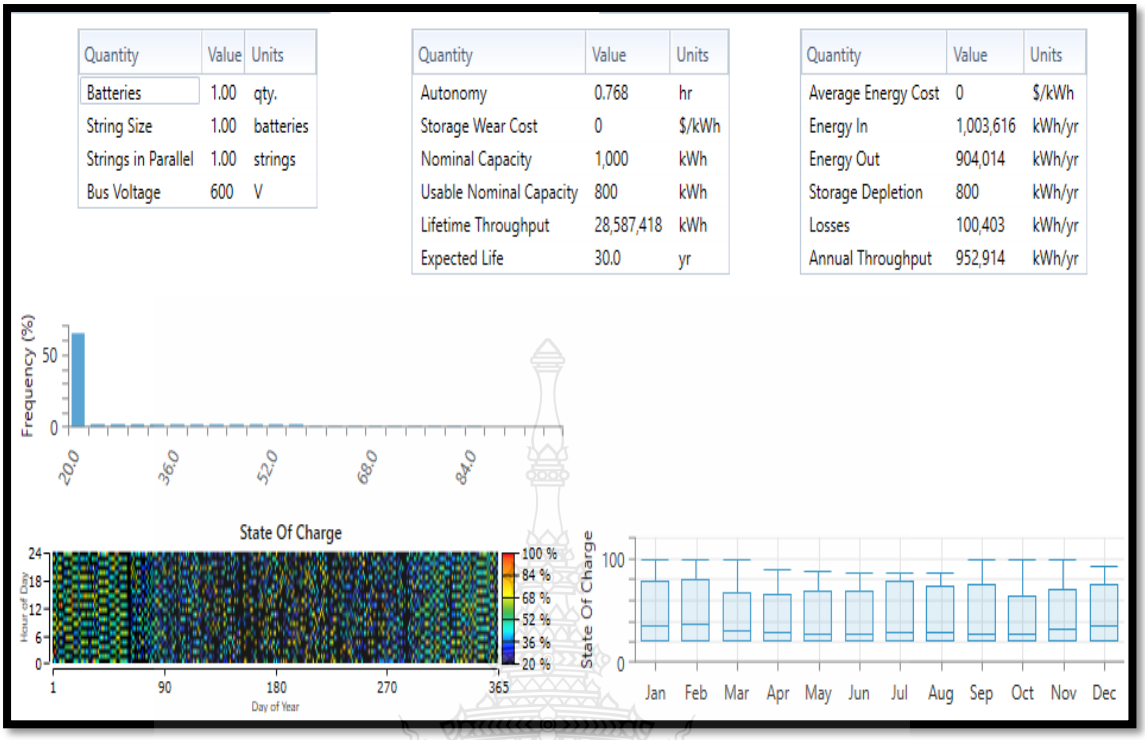

Figure 4.28 Characteristics of Zn-Brm Battery Operation with Biogas Generators/ Utility Grid Network

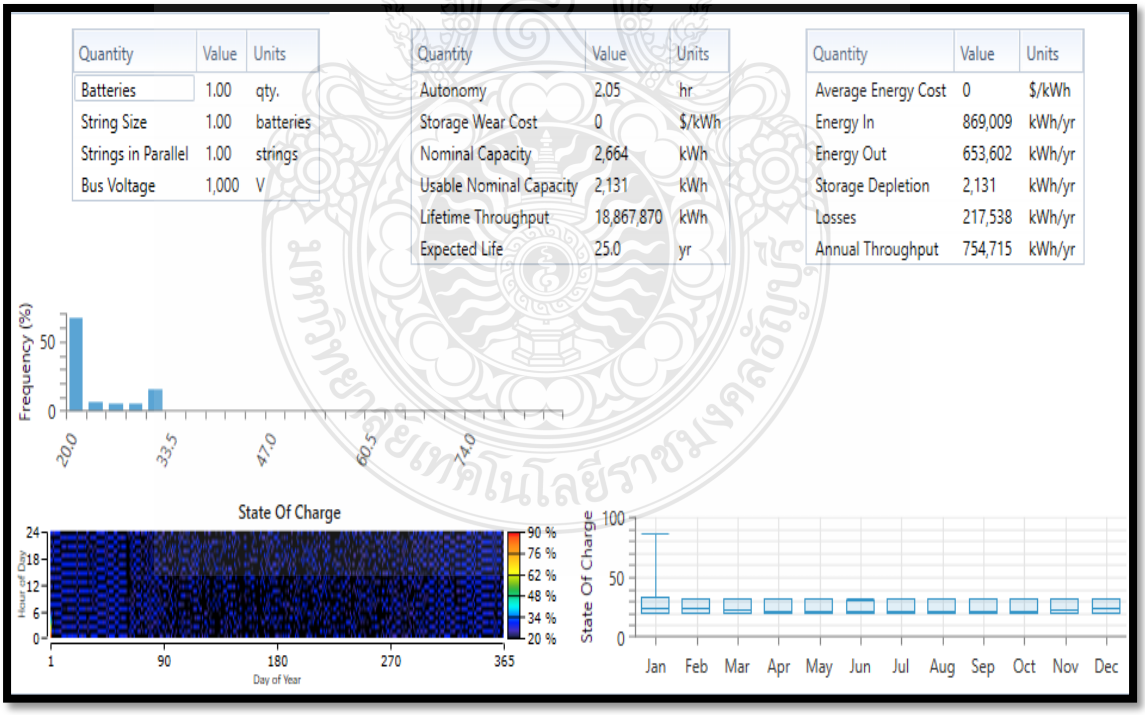

Figure 4.29 Characteristics of Flow Battery Operation with Biogas Generators/Utility Grid Network

The flow battery operated with the lowest coulombic efficiency of 75.21 % as compared against Li-ion and Zn-Brm coulombic efficiencies (93.59 % and 90.08 %). The annual frequency distribution usage of flow battery (99.94 %) was the highest in comparison with Li-ion and Zn-Brm annual frequency distribution (97.44 % and 63.95 %) application. The annual loss experienced by FB battery (217,538 kWh/yr) was greater than the annual losses experienced by Li-ion and Zn-Brm batteries (9,097 kWh/yr and 100,403 kWh/yr). FB battery had a lower annual cyclic energy flow (754,715 kWh/yr) than Zn-Brm annual cyclic flow (952,914 kWh/yr) while Li-ion battery had the lowest annual cyclic energy flow (88,037 kWh/yr). Li-ion, flow, and Zn-Brm batteries had their respective hours of operation in their descending orders (3.24 hrs, 2.05 hrs, and 0.768 hr) according to the measures of their input/output energy in ascending order and bulky power management in descending order. The charging state level of Zn-Brm battery was more efficient than the charging state level of Li-ion and flow batteries, respectively. The coulombic efficiency of each battery is the fraction of quantity of charges (during discharging period) flowing out from each battery to the quantity of charges flowing into of each battery (when charging at a particular period) across complete cycle. The nominal and usable capacities of Li-ion battery (4216 kWh/3373 kWh/600 V) tend to be greater than the nominal/usable capacities of flow battery (2664 kWh/2131 kWh/1000 V) and Zn-Brm battery (1000 kWh/800 kWh/600 V), hence, Li-ion battery has the potential tendency of supporting the biogas generators-utility grid energy service by charging the flow and Zn-Brm batteries, irrespective of the differences in their voltage capacities. While the flow battery can also charge the Zn-Brm battery too. The maximum charging level (90.0 %) of flow battery occur in January with steady distribution of charging variation ranging from 20.0 % - 34.0 % between February and December from Fig.4.27. The input energy (869,009 kWh/yr) of flow battery was more than its output energy (653,602 kWh/yr), the huge losses (217,538 kWh/yr) in flow battery was from the charging process as a result of secondary reaction (redox reaction or water electrolysis), thereby, reducing the flow battery's coulombic efficiency to 75.21 %.

The impact of the storage systems (Li-ion, Zn-Brm, and FB batteries) with the biogas generators-utility grid system configuration from Fig.4.30, Fig.4.31, and Fig.4.32 reduced the grid sales for Li-ion architecture (17.7 %; 1,959,426 kWh/yr), Zn-Brm architecture (15.8 %; 1,717,991 kWh/yr), and FB architecture (15.0 %; 1,615,938 kWh/yr). The renewable proportion for each energy storage configuration system increased to 92.9 %, 94.2 %, and 94.0 %, respectively.

Figure 4.30 Modelled Energy Flow Analysis of Proposed Biogas Generators/Grid/Li-ion Network.

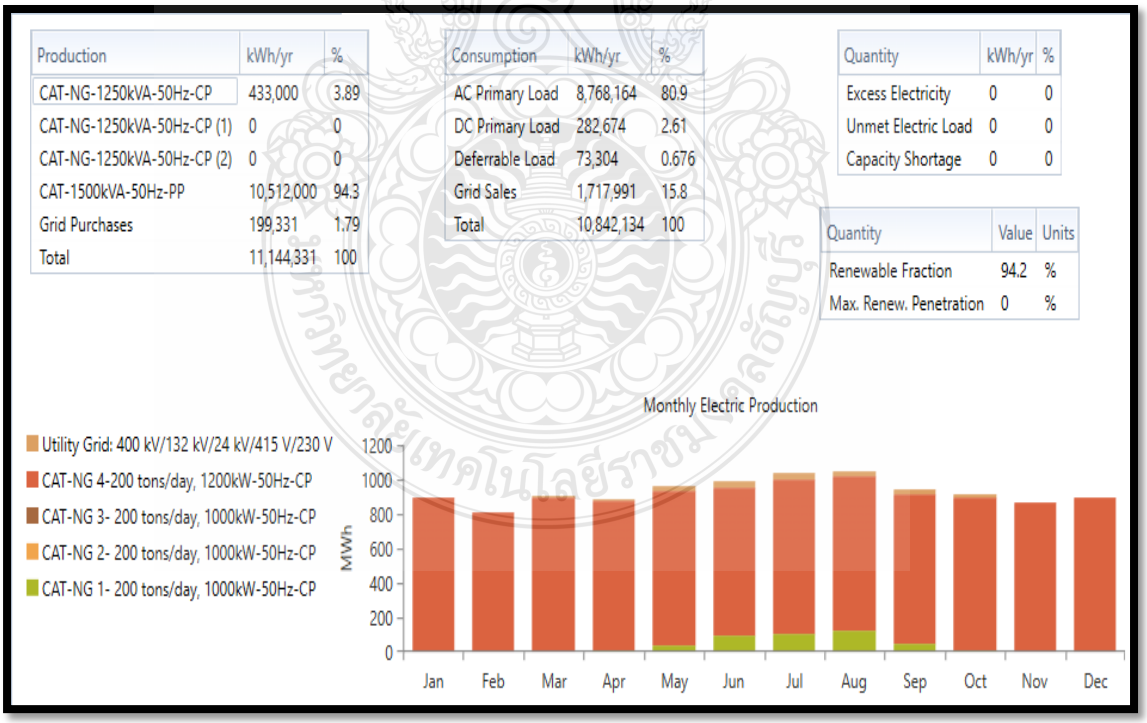

Figure 4.31 Modelled Energy Flow Analysis of Proposed Biogas Generators/Grid/Zn-Brm Network.

Figure 4.32 Modelled Energy Flow Analysis of Proposed Biogas Generators/Grid/FB Network

Their annual grid purchases were also reduced (Li-ion: 2.12 %; 239,764 kWh/yr, Zn-Brm: 1.79 %; 199,331 kWh/yr, FB: 1.83 %; 203,765 kWh/yr) as compared against the energy system's operation without storage systems from Fig.4.13 showing the contribution and effect of the storage systems in supporting the biogas generators-grid network system to sell more energy and buy lesser energy from the grid system. The controller that was adopted to operate with the biogas generators-utility grid-batteries architectural system was a load following interface control system that makes the utility grid and biogas generators to supply energy effectively to the loads at maximum capacity while the excess electricity left is stored in the batteries and sold to the grid system after overcoming capacity shortage and peak demand. The controller that was adopted to operate with the biogas generators-utility grid architectural system was a cycle charging interface control system that makes the biogas generators to operate at great potential intensity to balance the energy demanded and the excess electric energy left will be stored in the batteries.

4.8.1 Ratio of performance on proposed biogas connection to storage network

Fig.4.35 has provided the detailed summary of the total biogas fuel consumed per annum, average biogas fuel consumed per day, and average biogas fuel consumed per hour from the Zn-Brm microgrid energy, Flow battery microgrid energy, and Li-ion microgrid energy flow operation.

Considering the biogas generators/Li-ion battery configuration:

Electrical energy flow from biogas generators in kWh/yr = 11,054,000 kWh/yr

Electrical energy of biogas generators in kWh/day = 11,054,000 kWh/365 = 30,284.932 kWh/day

Electrical energy (kWh) = Mega joule (MJ) × 0.277778

Electrical energy of biogas generators in MJ/day = $\frac{30{,}284.932\ (kWh)}{0.277778}$ = 109,025.668 MJ/day

Lower heating gas value of methane in mega joules per kilogram = 20.0 MJ/m^3, 1.0 kg = 1.0 m^3

Biogas fuel consumption per day = 6910 m^3/day

Lower heating gas value of methane in MJ = 6910 m^3/day × 20.0 MJ/m^3 = 138,200 MJ/day.

Total biogas fuel consumed by the generators in MJ/day = 138,200 MJ/day

Therefore, ratio of performance (efficiency) of the biogas generators = $\frac{\text{Electrical energy generated by biogas generators (MJ/day)}}{\text{Biogas fuel consumed by biogas generators (MJ/day)}} = \frac{109{,}025.668\ (MJ/day)}{138{,}200\ (MJ/day)}$ = 0.7889 = 78.89%.

Considering the biogas generators/Zn-Brm flow battery configuration:

Electrical energy flow from biogas generators in kWh/yr = 10,945,000 kWh/yr

Electrical energy of biogas generators in kWh/day = 10,945,000 kWh/365 = 29,986.301 kWh/day

Electrical energy (kWh) = Mega joule (MJ) × 0.277778

Electrical energy of biogas generators in MJ/day = $\frac{29{,}986.301(kWh)}{0.277778}$ = 107,950.599 MJ/day

Lower heating gas value of methane in mega joules per kilogram = 20.0 MJ/m^3, 1.0 kg = 1.0 m^3

Biogas fuel consumption per day = 6701 m^3/day

Lower heating gas value of methane in MJ = 6701 m^3/day × 20.0 MJ/m^3 = 134,020 MJ/day.

Total biogas fuel consumed by the generators in MJ/day = 134,020 MJ/day

Therefore, ratio of performance (efficiency) of the biogas generators = $\frac{\text{Electrical energy generated by biogas generators (MJ/day)}}{\text{Biogas fuel consumed by biogas generators (MJ/day)}} = \frac{107{,}950.599\ (MJ/day)}{134{,}020\ (MJ/day)} = 0.8055 =$ 80.55%.

Considering the biogas generators/flow battery (FB) configuration:

Electrical energy flow from biogas generators in kWh/yr = 10,952,000 kWh/yr

Electrical energy of biogas generators in kWh/day = 10,952,000 kWh/365 = 30,005.479 kWh/day

Electrical energy (kWh) = Mega joule (MJ) × 0.277778

Electrical energy of biogas generators in MJ/day = $\frac{30{,}005.479\ (kWh)}{0.277778}$ = 108,019.640 MJ/day

Lower heating gas value of methane in mega joules per kilogram = 20.0 MJ/m^3, 1.0 kg = 1.0 m^3

Biogas fuel consumption per day = 6781 m^3/day

Lower heating gas value of methane in MJ = 6781 m^3/day × 20.0 MJ/m^3 = 135,620 MJ/day.

Total biogas fuel consumed by the generators in MJ/day = 135,620 MJ/day

Therefore, ratio of performance (efficiency) of the biogas generators = $\frac{\text{Electrical energy generated by biogas generators (MJ/day)}}{\text{Biogas fuel consumed by biogas generators (MJ/day)}} = \frac{108{,}019.640\ (MJ/day)}{135{,}620\ (MJ/day)} = 0.7965 =$ 79.65%.

4.8.2 Econometric assessment and emission from grid-biogas generators-batteries network

The Zn-Brm network configuration was discovered to be of more economic value than the Li-ion and FB network configurations. When the biogas generators-grid-Zn-Brm network operated, its present worth ($10,174,100), annual worth ($787,011) was higher in value than the biogas generators-grid-Li-ion network present worth: $9,998,843,

annual worth: $773,454 and biogas generators-grid-FB network present worth: $8,566,789 annual worth: $662,679 values. The investment return (17.0 %), internal return rating (20.3 %), and period of refund (4.83 years) for Zn-Brm configuration network was at higher economic advantage over the Li-ion configuration network econometrics (investment return: 16.5 %, internal return rating: 20.0 %, and period of refund: 4.88 years) and FB configuration network econometrics (investment return: 13.1 %, internal return rating: 16.3 %, and period of refund: 5.93 years). Hence, the biogas generators-utility grid-Zn-Brm architecture is the most economically feasible system than the biogas generators-utility grid-Li-ion and biogas generators-utility grid-FB architectural systems as tabulated from Fig.4.33 due to low emission, low period of operation, and electrical properties of the Zn-Brm battery.

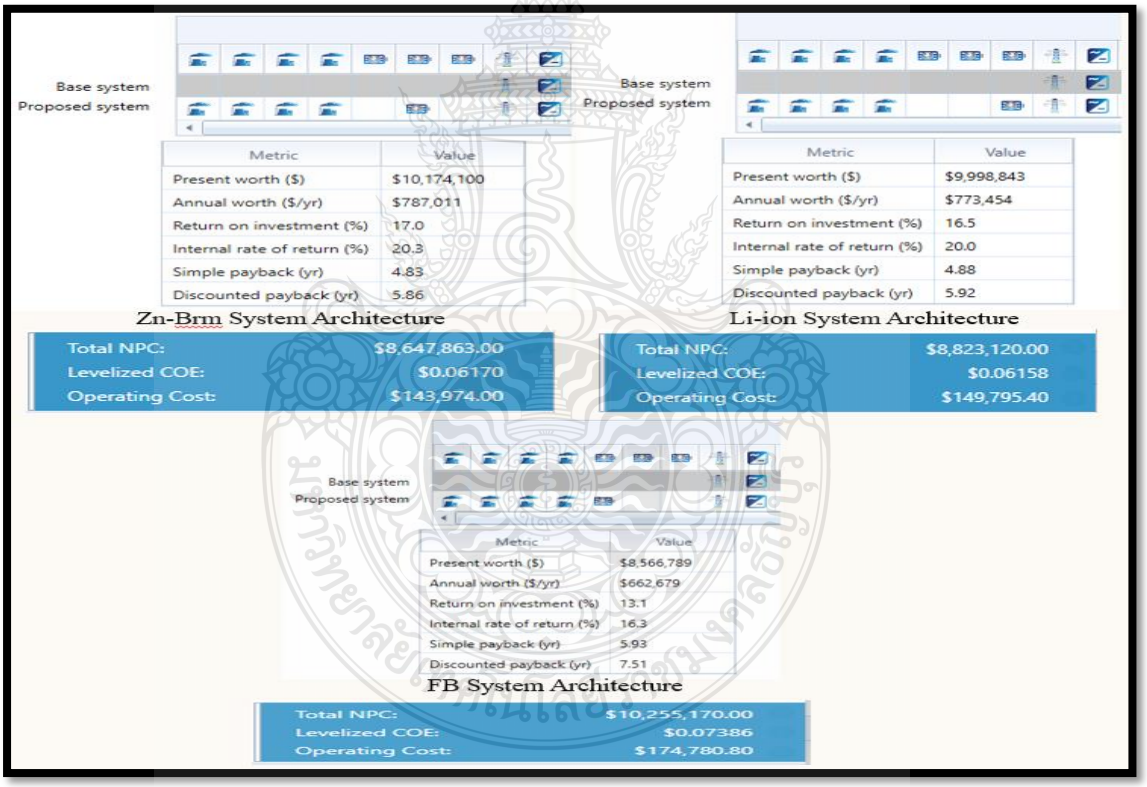

Figure 4.33 Econometric Efficiency of Grid/Biogas Generators/Batteries Network.

The results from Fig.4.23 and Fig.4.33 has analyzed the cost of operating the biogas generators-grid network without batteries (operating cost: $131,034.80, levelized electric energy: $0.05630/kWh, R.O.I$_v$: 18.7 %, I.R.R$_a$: 22.1 %, payback period: 4.47 %) to be less expensive and more economical than the cost of operating biogas generators-grid-

Zn-Brm network (operating cost: $143,974.00, levelized electric energy: $0.06170/kWh, $R.O.I_v$: 17.0 %, $I.R.R_a$: 20.3 %, payback period: 4.83 %), biogas generators-grid-Li-ion network (operating cost: $149,795.40, levelized electric energy: $0.06158/kWh, $R.O.I_v$: 16.5 %, $I.R.R_a$: 20.0 %, payback period: 4.88 %), and biogas generators-grid-FB network (operating cost: $174,780.80, levelized electric energy: $0.07386/kWh, $R.O.I_v$: 13.1 %, $I.R.R_a$: 16.3 %, payback period: 5.93 %) within On-nut community environment. Irrespective of economic differences from the four configuration energy systems, Li-ion energy system architecture was more productive in grid sales (17.7 %) than Zn-Brm (15.8 %) and FB (15.0 %) energy system architectures economically, Zn-Brm energy system architecture had the highest renewable fraction of 94.2 % because of its medium and long term potentials of enormous management in power flow, dynamic shift in energy demand and bridging power capacity over the lithium battery with short and medium term potentials of power/frequency qualities and lower concentration of bulky power management as summarized from Fig.4.25 in real time energy systems. The biogas generators/grid system architecture produced the highest annual energy (11,307,775 kWh/yr), highest grid purchase (2.16 %; 244,775 kWh/yr), and the lowest renewable fraction of 92.8 % than the other energy system architectures from the energy analysis model of Fig.4.13, Fig.4.30, Fig.4.31, and Fig.4.32, respectively. When the hybrid (Li-ion, FB, and Zn-Brm batteries) storage system was connected to the biogas generators-grid network, the emission properties of the operating network remain unchanged with the biogas generators-grid network without hybrid storage system from Fig.4.21.The specification, econometric properties of the utility grid/biogas generators/batteries architecture and average biomass feedstock (biogas fuel) supply for the renewable natural gas generators were tabulated from Table 12 and Fig.4.34 below.

Table 11 Parameters of Utility Grid/Biogas Generators/Batteries Configuration

Power Component (s)	Potential Rating (kW)	Capital Valuation ($)	Replacement Valuation ($)	Operating/Maintenance Valuation ($.op^{-1}.hr^{-1})	Fuel Price ($/m^3)
Natural gas (per unit)	1000, 400 V	1,359,675.47	355,000.00	20.5	0.360
Natural gas (per unit)	1200, 400 V	1,631,610.56	426,000.00	24.6	1.00
Converter	2250 (750 V-1250 V)	675,000	675,000	0.00	0.00
Flow battery	333, 1000 V	1,609,056.00	1,609,056.00	24,135.84	0.00
Lithium-ion	1056, 600 V	500,000	500,000	5,000.00	0.00
Zinc Bromide	3000, 600 V	400,000	400,000	5,000.00	0.00

Utility Grid	Capital Valuation ($.km^{-1})	Power Flow Price ($/kWh)	Net Surplus Flow Price ($/kWh)	Sales Capacity (kW)	Operating/Maintenance Valuation ($/yr.km)
	11,344.00	0.153	0.100	3000	160.00

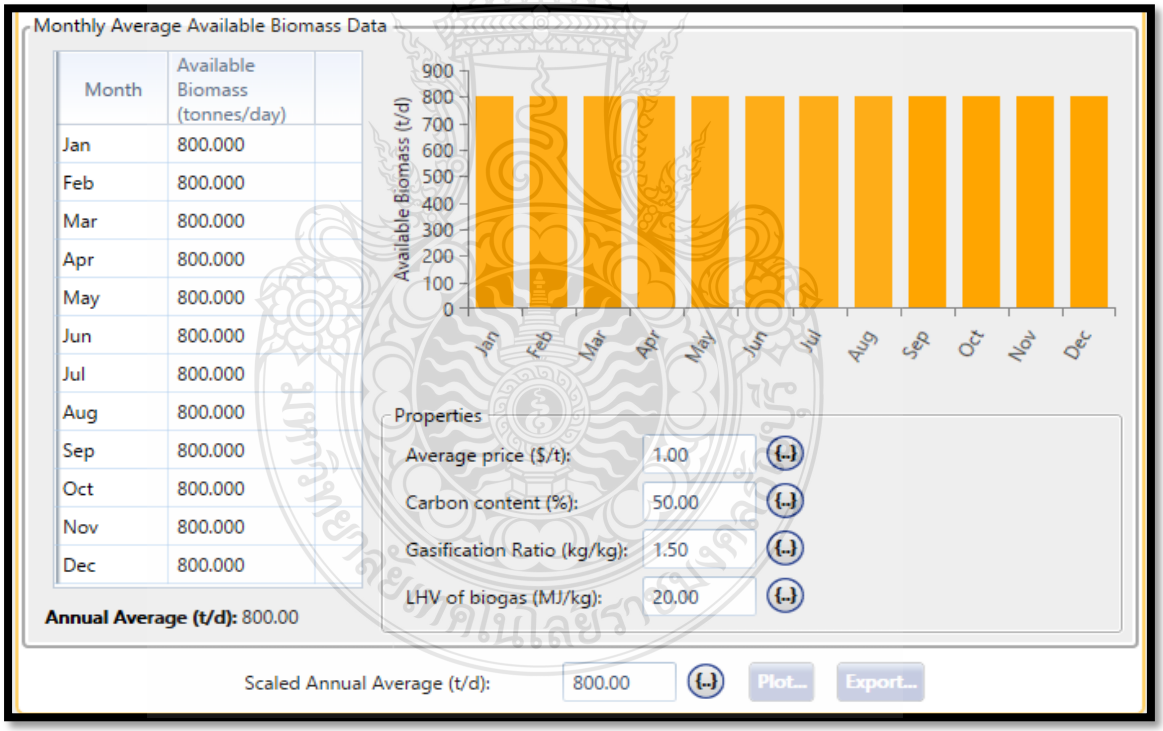

Figure 4.34 Average Fuel Supply for Biogas Generators Per Day from On-Nut Community

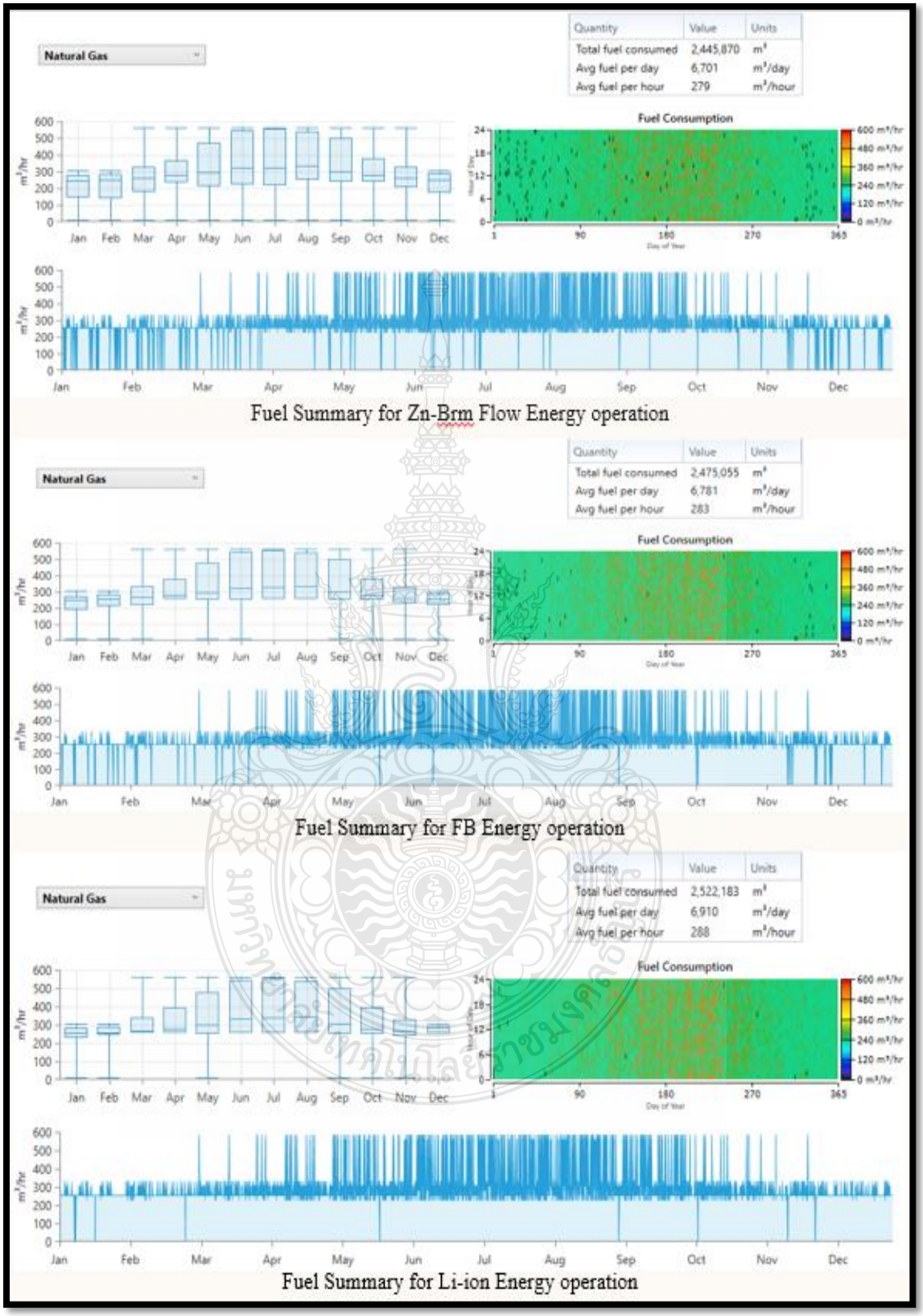

Figure 4.35 Fuel Summaries on Biogas Generators/Utility Grid/Storage Configurations

Three levels of hybrid biogas generators-utility grid- storage system configurations were analyzed with reference to their fuel usage summary. The total biogas fuel consumed, average biogas fuel usage per day, and average biogas fuel usage per hour for Zn-Brm energy system (2,445,870 m^3; 6,701 m^3/dy; 279 m^3/hour), FB energy system (2,475,055 m^3; 6,781 m^3/dy; 283 m^3/hour), and Li-ion energy system (2,522,183 m^3; 6,910 m^3/dy; 288 m^3/hour) was represented from Fig.4.35 in their order of fuel usage increment. Li-ion system configuration had the largest consumed volume of biogas fuel and average biogas fuel usage than the other storage system configurations (Zn-Brm and flow battery) as a result of high energy demand (11,083,568 kWh/yr) against the operation of Li-ion energy system when compared with the energy demand (10,842,134 kWh/yr) against the operation of Zn-Brm energy system and energy demand (10,740,080 kWh/yr) against the operation of flow battery energy system from Fig.4.30, Fig.4.31, and Fig.4.32, respectively.

4.8.3 Utility grid-batteries system operation

The grid system operation was not supported by the biogas generators and hybrid storage system; hence, no energy was sold to the grid system. The generators and batteries (Li-ion, FB, and Zn-Brm) were completely isolated from the utility grid operation. Producing annual energy of 9,056,774 kWh/yr over the energy demand (9,051,005 kWh/yr) with no renewable penetration. The net current cost ($18,821,970.00), levelized electrical energy cost ($0.1609/kWh), energy charge ($1,385,686/yr), and operating cost ($1,403,670.00) of the grid system operation was on a very high side and not economically sufficient for On-nut community as represented from Fig.4.36. The highest energy purchased (932,567 kWh) from the monthly energy production of the utility grid occur in August with cycle charging controller strategy.

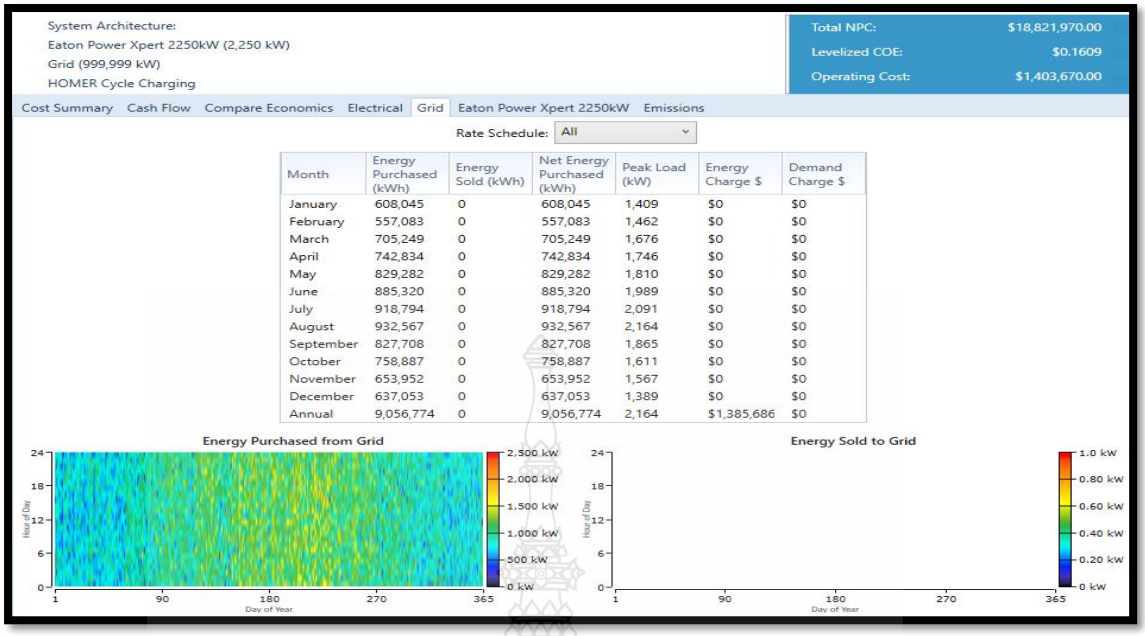

Figure 4.36 Utility Grid Energy Cycle Charging Operation.

The utility grid operation with Zn-Brm storage system generated more net current cost ($19,282,210.00), levelized electrical energy cost ($0.1648/kWh), operating cost ($1,408,330.00), and lower energy charge ($1,385,574.00/yr) than the grid operation without storage support. Furthermore, 17 kWh/yr of energy generated by the Zn-Brm battery in January was sold to the grid system, thereby, dropping the energy purchased value from the grid system to 9,056,040 kWh/yr, which was beyond the energy demand (9,051,033 kWh/yr) respectively from Fig.4.37 under load following controller strategy.

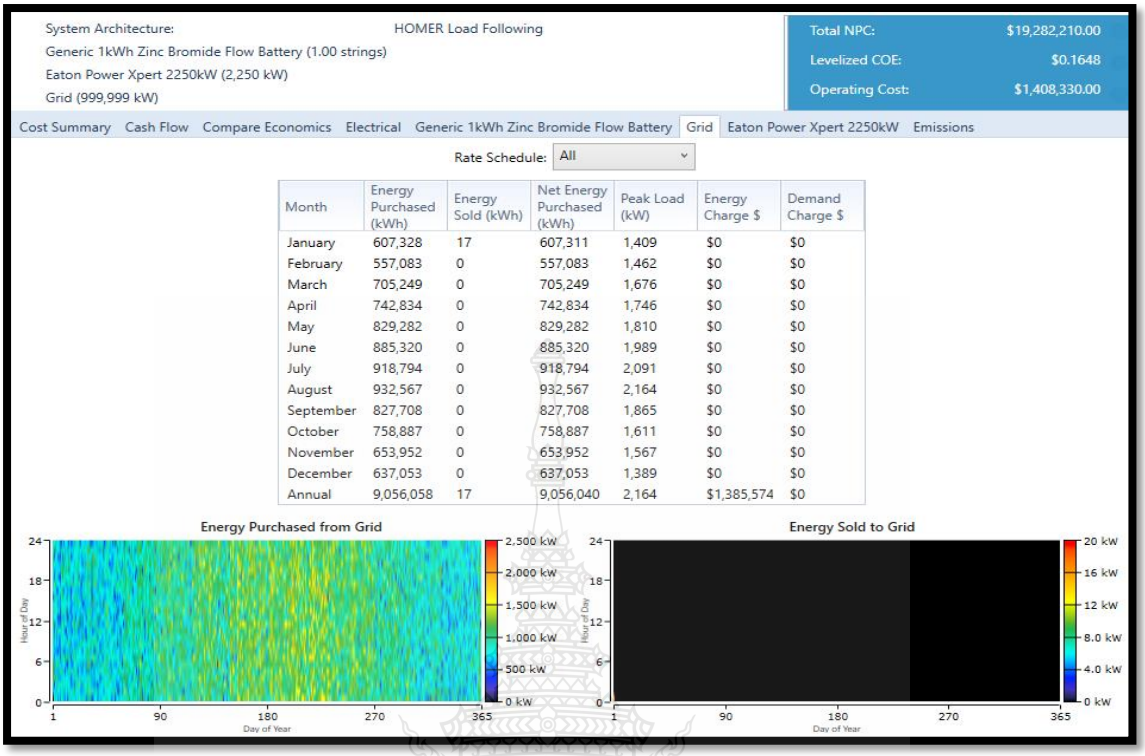

Month	Energy Purchased (kWh)	Energy Sold (kWh)	Net Energy Purchased (kWh)	Peak Load (kW)	Energy Charge $	Demand Charge $
January	607,328	17	607,311	1,409	$0	$0
February	557,083	0	557,083	1,462	$0	$0
March	705,249	0	705,249	1,676	$0	$0
April	742,834	0	742,834	1,746	$0	$0
May	829,282	0	829,282	1,810	$0	$0
June	885,320	0	885,320	1,989	$0	$0
July	918,794	0	918,794	2,091	$0	$0
August	932,567	0	932,567	2,164	$0	$0
September	827,708	0	827,708	1,865	$0	$0
October	758,887	0	758,887	1,611	$0	$0
November	653,952	0	653,952	1,567	$0	$0
December	637,053	0	637,053	1,389	$0	$0
Annual	9,056,058	17	9,056,040	2,164	$1,385,574	$0

Figure 4.37 Utility Grid/Zn-Brm Energy Load Following Operation.

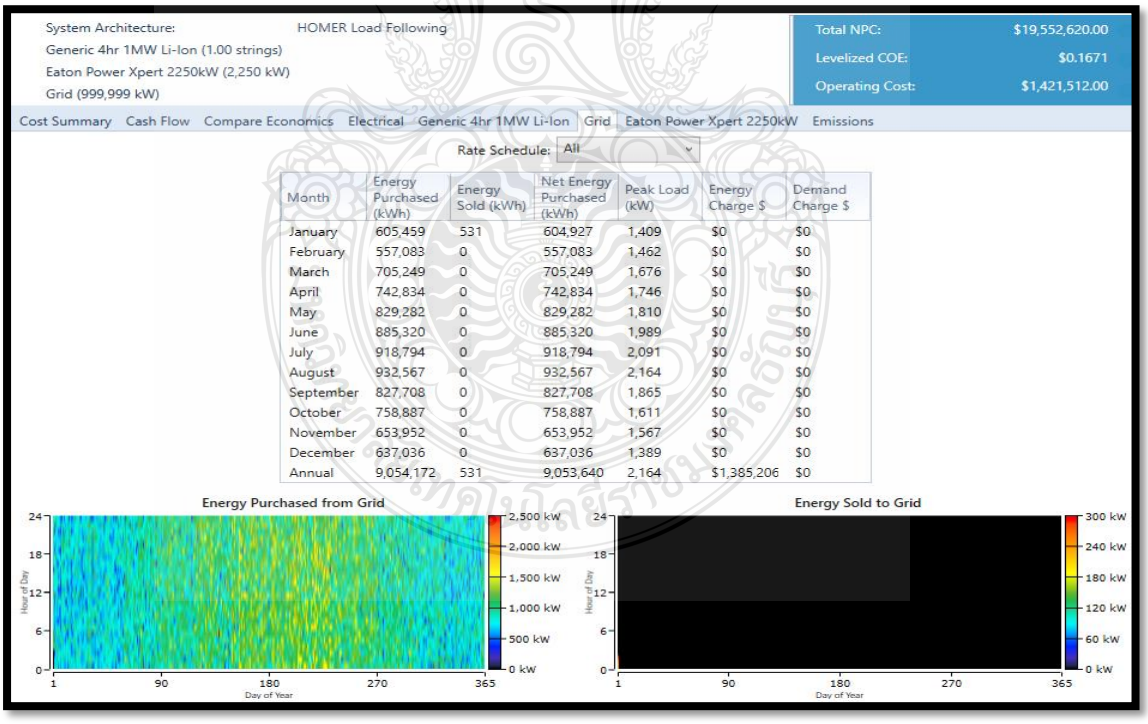

Month	Energy Purchased (kWh)	Energy Sold (kWh)	Net Energy Purchased (kWh)	Peak Load (kW)	Energy Charge $	Demand Charge $
January	605,459	531	604,927	1,409	$0	$0
February	557,083	0	557,083	1,462	$0	$0
March	705,249	0	705,249	1,676	$0	$0
April	742,834	0	742,834	1,746	$0	$0
May	829,282	0	829,282	1,810	$0	$0
June	885,320	0	885,320	1,989	$0	$0
July	918,794	0	918,794	2,091	$0	$0
August	932,567	0	932,567	2,164	$0	$0
September	827,708	0	827,708	1,865	$0	$0
October	758,887	0	758,887	1,611	$0	$0
November	653,952	0	653,952	1,567	$0	$0
December	637,036	0	637,036	1,389	$0	$0
Annual	9,054,172	531	9,053,640	2,164	$1,385,206	$0

Figure 4.38 Utility Grid/Li-ion Energy Load Following Operation.

The grid/Li ion energy operation tends to be more expensive in its net current cost ($19,552,620.00), levelized electrical energy evaluation ($0.1671/kWh), operating cost

($1,421,512.00), and lower energy charge ($1,385,206.00/yr) than the grid and grid/Zn-Brm energy systems' operation. Technically, the energy production from the grid/Li-ion system (9,054,172 kWh/yr) under load following controller strategy surpassed the annual energy demanded (9,051,541 kWh/yr) with energy sales production (531 kWh/yr) from Li-ion battery to the grid system which dropped the overall energy purchase from the grid system to 9,053,640 kWh/yr. This is not economically sufficient for the community project.

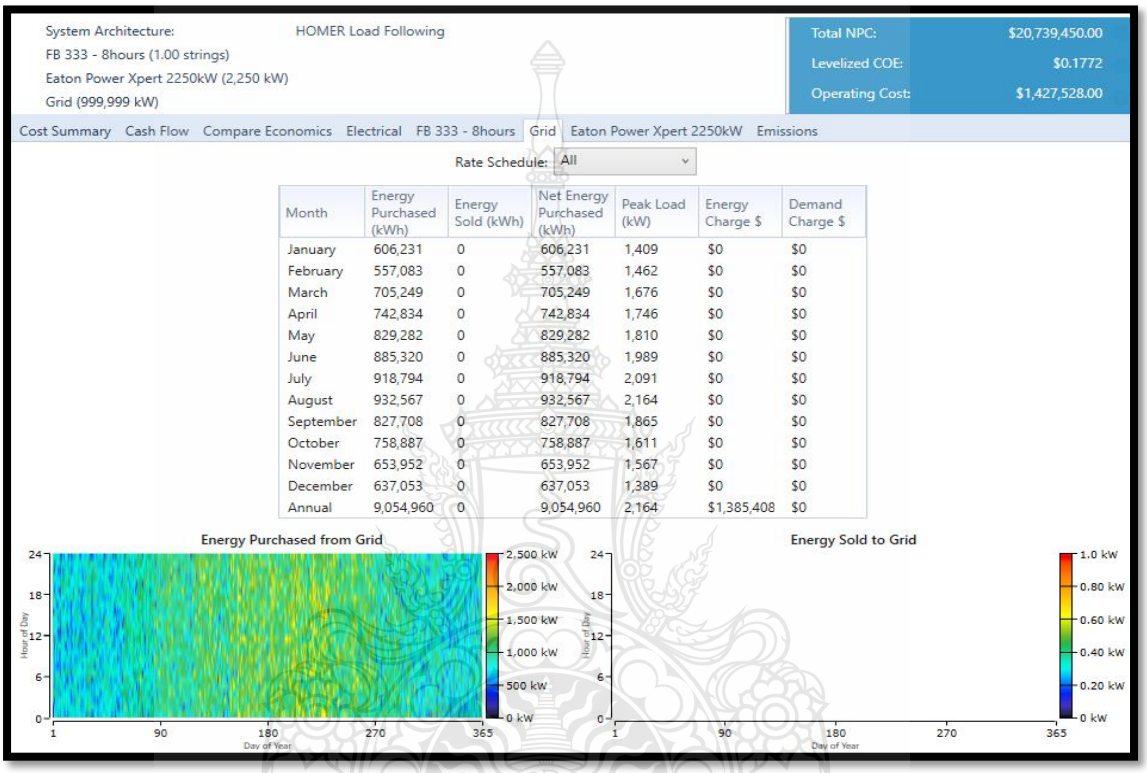

Month	Energy Purchased (kWh)	Energy Sold (kWh)	Net Energy Purchased (kWh)	Peak Load (kW)	Energy Charge $	Demand Charge $
January	606,231	0	606,231	1,409	$0	$0
February	557,083	0	557,083	1,462	$0	$0
March	705,249	0	705,249	1,676	$0	$0
April	742,834	0	742,834	1,746	$0	$0
May	829,282	0	829,282	1,810	$0	$0
June	885,320	0	885,320	1,989	$0	$0
July	918,794	0	918,794	2,091	$0	$0
August	932,567	0	932,567	2,164	$0	$0
September	827,708	0	827,708	1,865	$0	$0
October	758,887	0	758,887	1,611	$0	$0
November	653,952	0	653,952	1,567	$0	$0
December	637,053	0	637,053	1,389	$0	$0
Annual	9,054,960	0	9,054,960	2,164	$1,385,408	$0

Figure 4.39 Utility Grid/FB Energy Load Following Operation.

The most expensive energy system operation from grid/flow battery generated the highest net current cost ($20,739,450.00), levelized electrical energy cost ($0.1772/kWh), operating cost ($1,427,528.00), and lower energy charge ($1,385,408.00/yr) with no grid sales production. The grid/FB system generated energy (9,054,960 kWh/yr) above the load (9,051,005 kWh/yr) under load following controller strategy from Fig.4.39. The utility grid-storage energy system is not economically feasible but technically feasible in overcoming the annual energy demand.

4.8.4 Three Phase/Storage Dedicated/Grid Tied/Grid System Following Converter

A powerful key system that interfaces the AC utility grid and batteries, AC biogas generators and batteries, AC energy sources and DC load is the utility grid tied-grid following-storage dedicated bidirectional power converter. Switching energy conversion

between the biogas generators and batteries, grid system and batteries, AC sources and DC load for a flexible and efficient exchange of energy between the electrical buses (AC/DC and DC/AC) during operation poses a serious challenge, hitherto. A proposed utility scaled-batteries dedicated-grid tied-grid following bidirectional power converter was adopted for the biogas generators-grid system-storage energy network design with total efficiency enhancement and conversion reduction stages. The batteries (Li-ion, Zn-Brm, and flow battery) were connected in parallel to the electrical bus (DC) in order of their nominal energy and voltage capacities from Fig.4.26 for effective operation of the designed power converter, respectively.

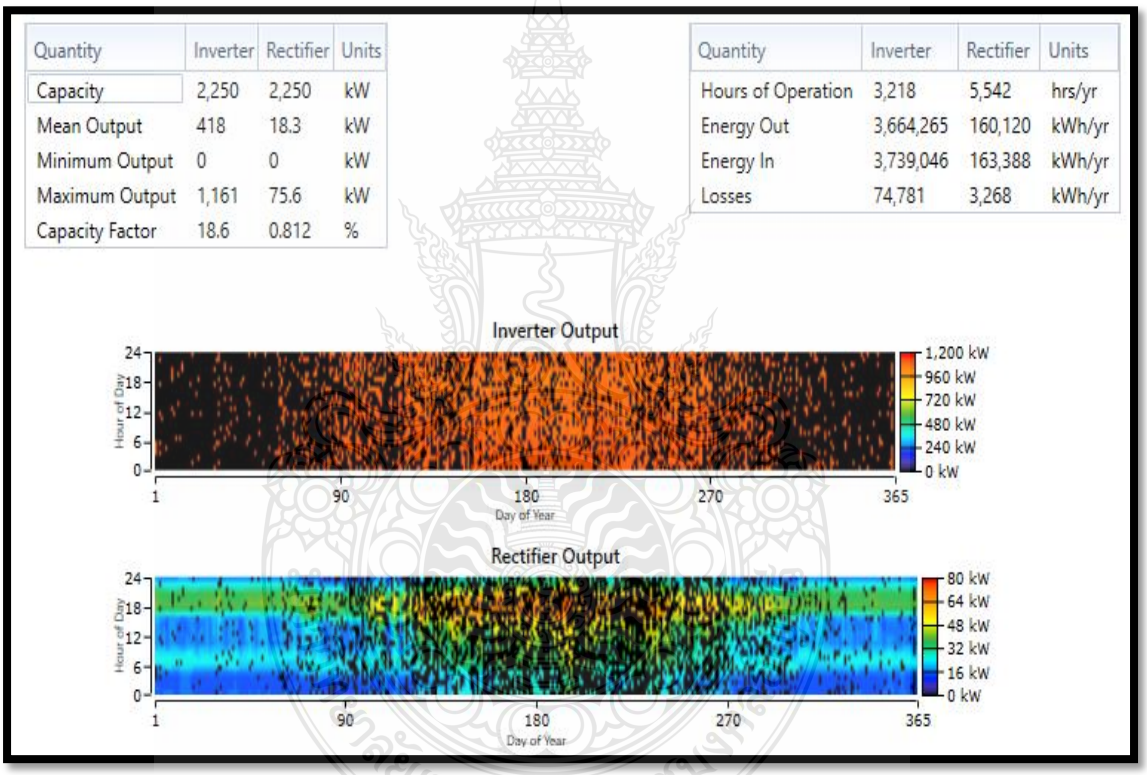

Figure 4.40 Biogas Generators/Grid/Converter/Cycle Charging Operation.

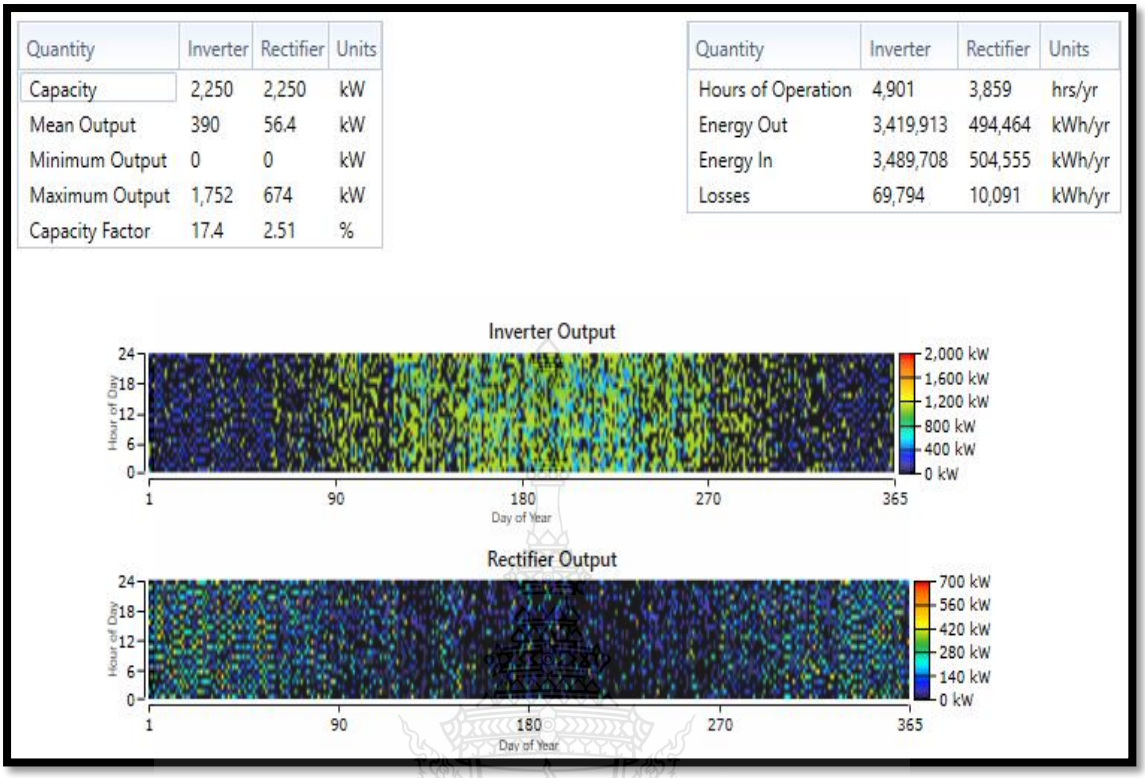

Figure 4.41 Biogas Generators/Grid/Zn-Brm/Converter/Load Following operation.

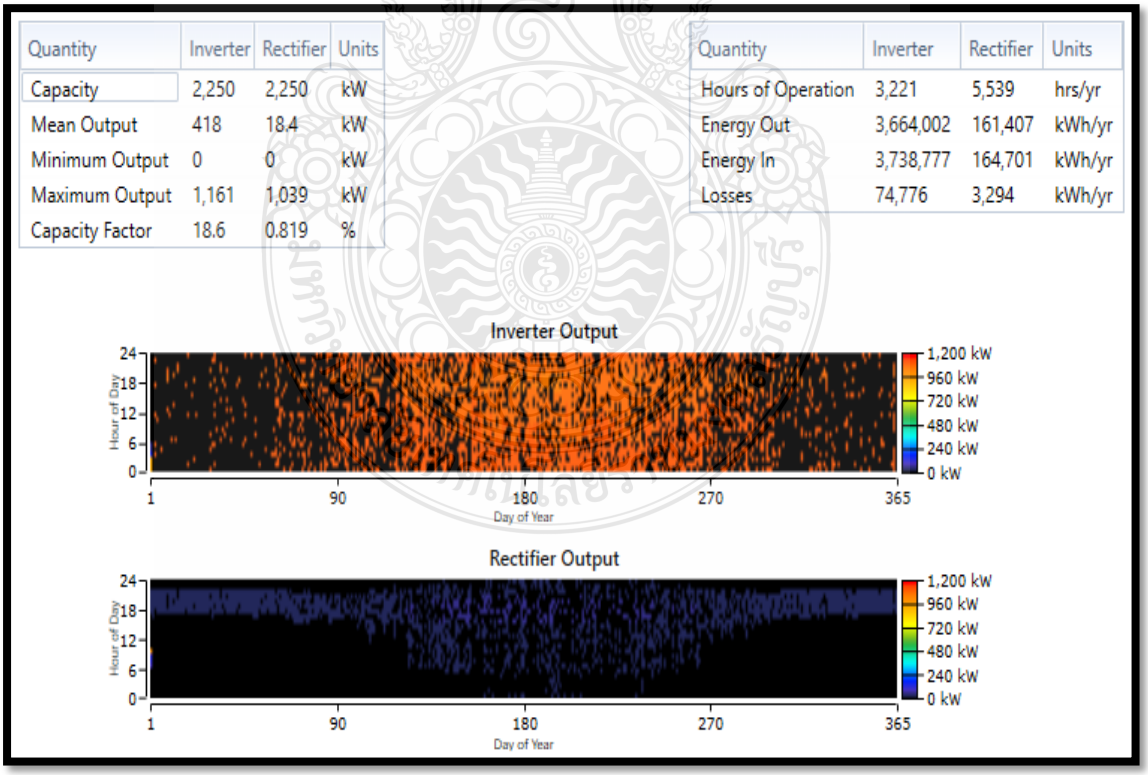

Figure 4.42 Biogas Generators/Grid/Li-ion/Converter/Cycle Charging operation.

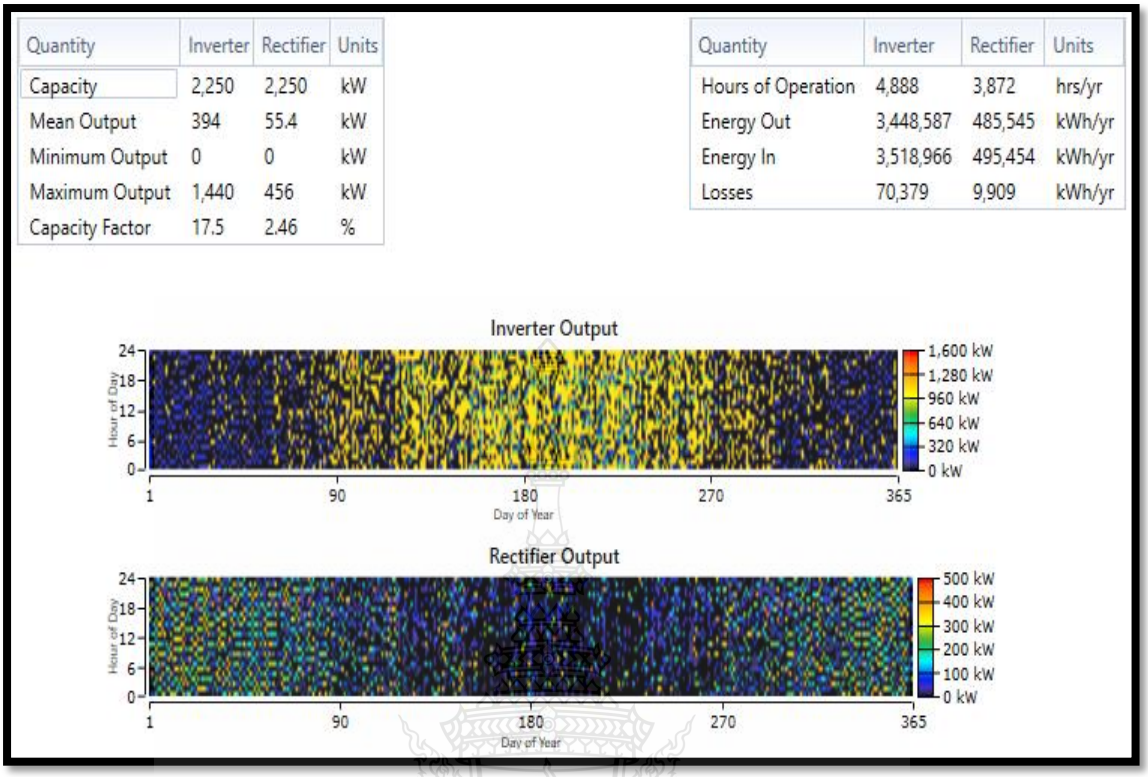

Figure 4.43 Biogas Generators/Grid/Flow Battery/Converter/Load Following operation.

The nominal voltage range capacity for the proposed power converter to operate between the AC and DC power sources is within 750 V-1250 V. Power or energy exchange between the grid system and batteries, biogas generators and batteries was achieved through a single stage of energy or power conversion from the proposed power converter, hence, there is no need for induction of extra energy stage conversion to be done by another power converter. Single stage energy converters are suitable for the batteries, but their lifetime reduces due their high discharging cycles' number. The batteries potential level from the proposed power system design from Fig.4.26 through the DC bus potential is higher than the grid phase-phase peak voltage which does not utilize the energy capacity of the single stage energy converter system fully.

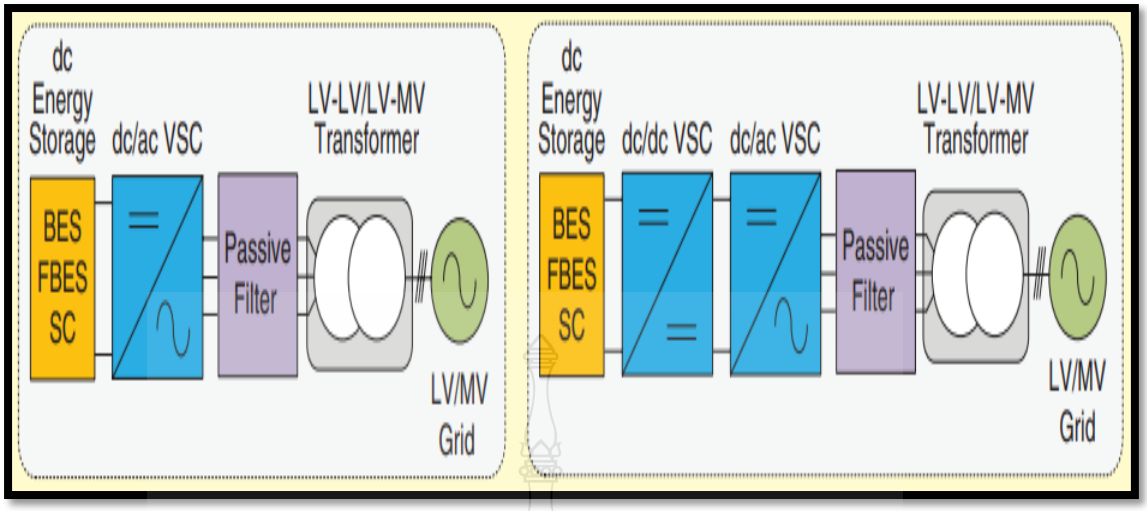

Figure 4.44 Energy Exchange Conversion Systems with (A) Single-staged potential source converter (DC-AC); (B) Two-staged DC-DC potential source converter with DC-AC potential source converter [139].

Two staged energy exchange power converter system (DC-DC/DC-AC) from Fig.4.44 exhibit more flexible operation than the single staged potential source conversion system (DC-AC) which is applicable for the batteries even when they are deeply discharged without any reduction in their life cycles. DC-DC potential source conversion enables proper management of batteries charging states within a large scale, thereby, optimizing the designed batteries capacities. The power capacity of the electronic energy conversion system that switches energy production between the AC and DC electrical buses connecting the biogas generators, utility grid, and batteries together is 2,250 kW. The efficiency of the bidirectional power converter in operation with the four-configuration energy systems maintained a constant value of 98.0 % at the inversion and rectification modes when the ratio of their output energy to input energy were determined from Fig.4.40, Fig.4.41, Fig.4.42, and Fig.4.43. The Zn-Brm configuration system produced the longest annual operating period (4,901 hours/yr) from the inverter and highest annual losses (10,091 kWh/yr) from the rectifier while the configuration of biogas generators-grid system (without batteries support) produced the longest annual operating period (5,542 hours/yr), least number of annual losses (3,268 kWh/yr) from the rectifier, the highest annual losses (74,781 kWh/yr) and lowest operating period (3,218 hours/yr) from the inverter. From the rectifying operational mode of each power system configuration, their input and output energy flow were lower than the input and output energy flow of their inverting operational mode. This illustration shows that the microgrid network utilizes more AC current than DC current from the bidirectional energy conversion process because the dominant power sources and energy demand are from AC systems. While the DC unified storage system (Li-ion, Zn-Brm, and FB) operates to support the utility grid, regulate frequency of power generation, and manage bulky energy production against potential shortage that can cause instability between the power sources and load or power fluctuation from the microgrid network.

In terms of loss minimization (69,794 kWh/yr) and longest operating hours (4,901 hours/yr) from the inversion operational mode, the Zn-Brm microgrid network is the most efficient energy system than other microgrid network configuration while the biogas generators-grid network is the most efficient energy system from the rectification operational mode with loss minimization (3,268 kWh/yr) and longest operating hours (5,542 hours/yr). The financial and technical analysis of the waste power plant (biogas) system in its different configurations of operation and control systems strategy adopted for each architecture can be tabulated from table 12, table 13, and table 14, respectively.

Table 12 Utility Grid/Biogas Generators/Energy Storage Trade Operation

Power System Configuration (s)	Electrical Energy Purchased (kWhr)	Electrical Energy Sold (kWhr)	Net Electrical Energy Purchased (kWhr)	Peak Load (kW)	Electrical Energy Charge ($)
Biogas generators-utility grid system	244,775	1,979,046	-1,734,271	294	173,427.13
Biogas generators-utility grid-Li-ion system	239,764	1,959,426	-1,719,661	294	171,966.14
Biogas generators-utility grid-Zn-Brm system	199,331	1,717,991	-1,518,661	294	151,866.06
Biogas generators-utility grid-FB	203,765	1,615,938	-1,412,173	294	141,217.29
Utility grid system	9,056,774	0	9,056,774	2,164	1,385,686.46
Utility grid-Zn-Brm system	9,056,058	17	9,056,040	2,164	1,385,574.19
Utility grid-Li-ion system	9,054,172	531	9,053,640	2,164	1,385,206.97
Utility grid-FB system	9,054,960	0	9,054,960	2,164	1,385,408.94

Table 13 Financial Summary of Utility Grid/Biogas Generators/Energy Storage Operation

Power System Configuration (s)	Overall Current Cost: NPCO ($)	Levelized Electricity Cost ($/kWhr)	Operating Cost: OPCO ($)	Investment Return: ROIV (%)	Internal Return Rate: IRRA (%)	Payback Time (years)
Biogas generators-utility grid system	8,080,592.00	0.05630	131,034.80	18.70	22.10	4.47
Biogas generators-	8,823,120.00	0.06158	149,795.40	16.50	20.00	4.88

Table 13 Financial Summary of Utility Grid/Biogas Generators/Energy Storage Operation (Continued)

utility grid-Li-ion system						
Biogas generators-utility grid-Zn-Brm system	8,647,863.00	0.06170	143,974.00	17.00	20.30	4.83
Biogas generators-utility grid-FB system	10,255,170.00	0.07386	174,780.80	13.10	16.30	5.93
Utility grid system	18,821,970.00	0.1609	1,403,670.00	0.00	Not available	Not available
Utility grid-Zn-Brm system	19,282,210.00	0.1648	1,408,330.00	-4.80	Not available	Not available
Utility grid-Li-ion system	19,552,620.00	0.1671	1,421,512.00	-7.60	Not available	Not available
Utility grid-FB system	20,739,450.00	0.1772	1,427,528.00	-5.50	Not available	Not available

Table 14 Operational Strategies of Utility Grid/Biogas Generators/Energy Storage System

Power System Configuration (s)	Control System Strategy	Average Renewable Generation to Load (%)	Renewable Penetration (%)
Biogas generators-utility grid system	Cycle charging	94.7	92.8
Biogas generators-utility grid-Zn-Brm system	Load following	97.0	94.2
Biogas generators-utility grid-Li-ion system	Load following	94.8	92.9
Biogas generators-utility grid-FB system	Load following	97.9	94.0

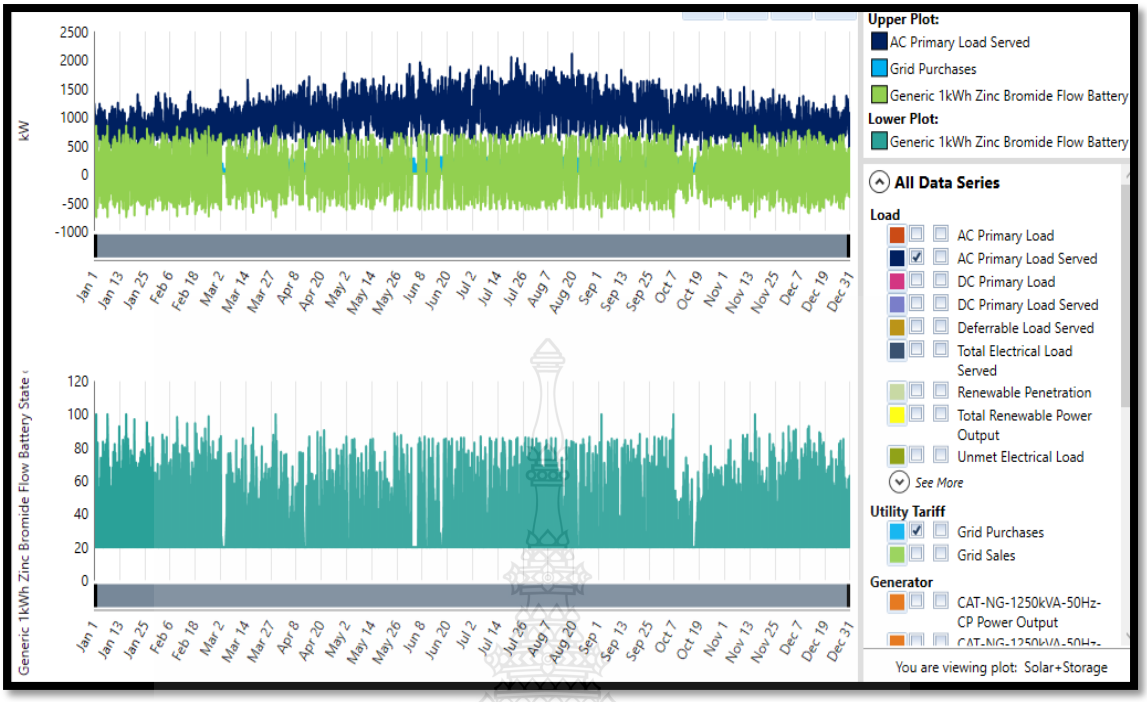

Figure 4.45 Zn-Brm/Grid Energy Purchase Waveform.

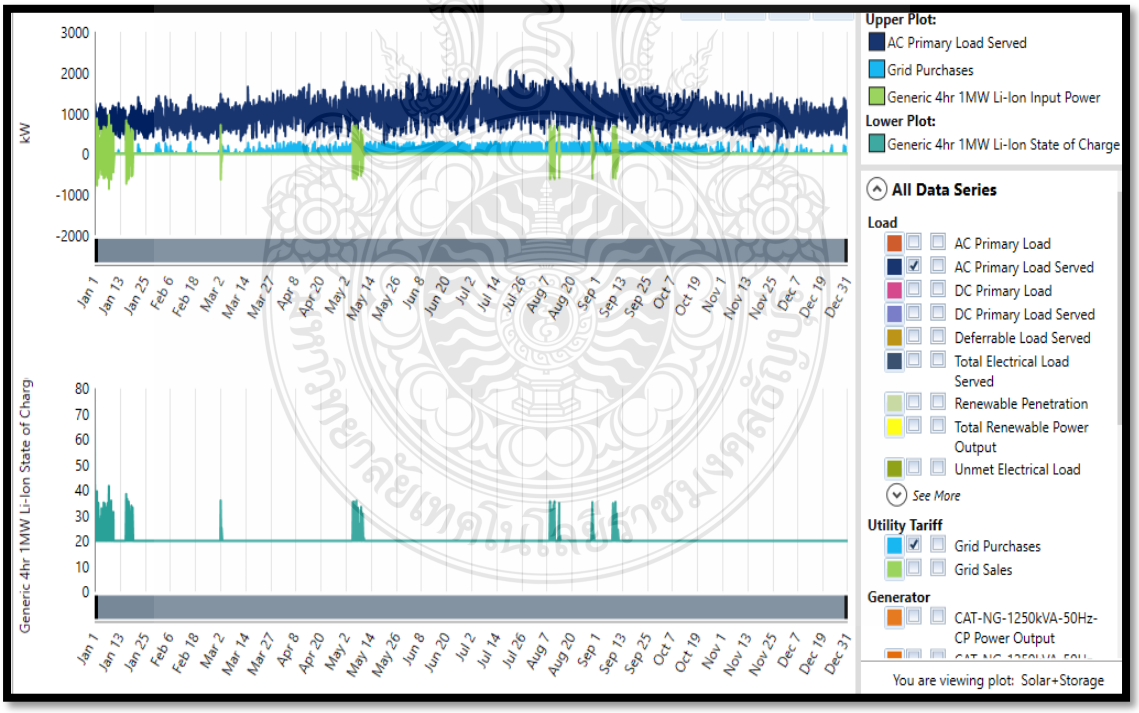

Figure 4.46 Li-ion/Grid Energy Purchase Waveform.

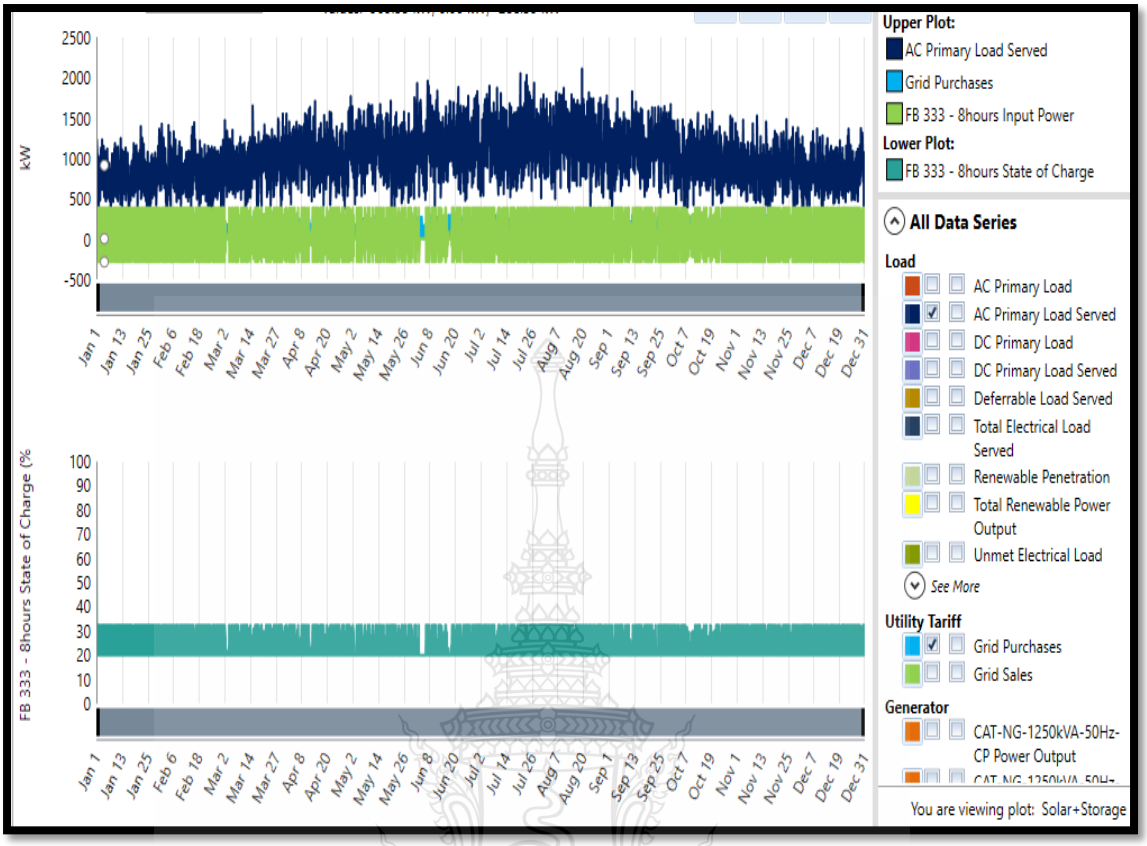

Figure 4.47 FB/Grid Energy Purchase Waveform.

CHAPTER 5
CONCLUSION AND RECOMMENDATION

5.1 Conclusions

The performance analysis and econometric assessment of On-Nut community waste power plant (biogas) system was proposed to determine the most efficient energy system configuration (biogas generators-utility grid system, biogas generators-utility grid-unified storage system, and utility grid-unified storage system) based on their financial and operational feasibilities. 800 tonnes of biomass feedstock were delivered on daily basis to On-Nut waste power plant project community for proper treatment (pre-treatment, fermentation process, anaerobic breakdown, and bio-gasification) and synthetic gas production of 48.14 tonnes of renewable methane (composition of biogas) was utilized into combined heat and electric power production of 178,632 MJ and 4,064 kW, respectively. The current energy system technology for the community adopted a generator order control system functioning as an interface closed loop feedback controller between the parallel combination of three units of biogas generators (1000 kW each) with the utility grid sharing the same AC bus connector and the fourth unit of biogas generator (1200 kW) connected to a DC bus connector. The 3 units of biogas generators sold electricity to the utility grid system as their primary function and provided support in electrifying the load as their secondary function. While the primary operation of the fourth unit of biogas generator (1200 kW) is to electrify the load and provide electric sales support (as a secondary operation) with the other units of grid connected biogas generators. The biogas generators/utility grid network configuration of the current technology achieved the highest energy sales (1,979,046 kWh) and the lowest net energy purchase (-1,734,271 kWh) from the grid system with the lowest overall current cost ($8,080,592.00), lowest levelized electricity cost ($0.05630/kWh), lowest operating cost ($131,034.80), highest investment return (18.70 %), highest internal return rate (22.10 %), and lowest payback time (4.47 years) when compared with other configurations from table 12 and table 13, respectively. The proposed microgrid system consists of the Li-ion, Zn-Brm, and FB energy system configurations by adopting load following closed loop feedback system. It was discovered that the biogas generators-utility grid-Li-ion energy system was the most efficient microgrid architecture (yearly energy production: 11,293,764 kWh/yr; yearly energy sales: 1,959,426 kWh/yr), the architecture of biogas generators-utility grid-Zn-Brm energy system was the most economical microgrid system (net present cost: $8,647,863.00, operating cost: $143,974.00, investment return: 17.00 %, internal return rate: 20.30 %, payback period: 4.83 years). The biogas generators-utility grid-FB energy system was the most expensive operating microgrid architecture (net present cost: $10,255,170.00, levelized electricity cost: $0.07386/kWh, operating cost: $174,780.00, investment return: 13.10 %, internal return rate: 16.30 %, payback period: 5.93 years).

5.2 Discussion and Contribution

In this proposed technology of the grid system-biogas generators-hybrid storage microgrid network, the fourth AC biogas generator (1200 kW) with a dedicated converter feed the DC/AC load and charge the unified batteries through a common DC connector as its primary function followed by supporting grid sales as its secondary function. Under the unified storage power system technologies, the Li-ion power system configuration recorded the highest level of efficiency in terms of energy purchase (239,764 kWh), energy sales (1,959,426 kWh), lowest net energy purchase (-1,719,661 kWh), and highest electrical energy charge ($171,966.14) above the Zn-Brm and FB power system configurations under uniform peak load (294 kW). Economically, Zn-Brm power system configuration is the most feasible energy system over Li-ion and FB power system configurations in terms of possessing the lowest overall current cost ($8,647,863.00), lowest operating cost ($143,974.00), highest investment return (17.00 %), highest internal return rate (20.30 %) and lowest payback period (4.83 years), respectively. FB energy system is the most expensive proposed energy system architecture in terms of (highest overall current cost: $10,255,170.00; highest levelized electricity cost: $0.07386/kWh; highest operating cost: $174,780.80; lowest investment return: 13.10 %; lowest internal return rate: 16.30 %; with the longest payback period: 5.93 years) than the other energy storage system technologies. Under the proposed cycle charging closed loop feedback control system, the unified power system technology was automatically resized and optimized to generate the best technical and economic performance from the hybrid configuration of 1200 kW biogas generator/grid system operation without any support from the unified storage system to back up the hybrid power sources, thereby, generating the best economic value (NPCO: $4,156,205.00, LECE: $0.02980/kWh, OPCO: $142,996.90, ROIV: 73.0 %, IRRA: 79.0 %, payback period: 1.27 years) and electromechanical efficiency (renewable fraction: 95.5 %, electric purchase: 481,760 kWh, electric sales: 1,665,031 kWh, net energy purchase: -1,183,271 kWh, peak demand: 986 kW, energy charge: $118,327.13) above the flexible power system configurations from Fig.4.24, respectively. The performance ratio analysis of the current biogas generators from Fig.4.1 without storage management (batteries) support was 18.55 % with high input of biogas fuel energy (962800 MJ/day) supply from 48.14 tonnes/day biogas fuel production to produce low output electric energy (178,632 MJ). The proposed microgrid technology of Li-ion energy, Zn-Brm flow, and FB energy flow operation generated enhanced performance ratio than the current technology from section 4.8.1. The Zn-Brm microgrid system produced the highest performance ratio (80.55 %) with the lowest biogas fuel volume and energy (6701 m^3/day; 134,020 MJ/day) consumption to serve as the highest economically efficient microgrid network. The Li-ion microgrid configuration consumed the largest biogas fuel volume and energy (6910 m^3/day; 138,200 MJ/day) with 78.89 % performance ratio and highest generated efficient electrical energy (109,025.668 MJ/day) than other architectures. The flow battery microgrid operated as the second highest performing ratio (79.65 %) network and second highest consumption

of biogas fuel (6781 m^3/day; 135,620 MJ) and electrical energy (108,019.640 MJ/day) which was not economically favorable for the community.

The significance of this proposed network development (biogas power plant technology) for On-Nut community enables the energy system to operate as an independent power generation source which in addition is flexible enough to be integrated with the utility grid network to solely reduce electric purchase from the grid system and increase electric sales back to the grid system. The current and proposed technologies were duly modelled and analyzed thoroughly. The experimental and simulation analysis has proven that the designed configurations of biogas generators/utility grid and biogas generators/utility grid/unified storage power systems were feasible economically and technically. While the configuration of utility grid/storage power system production was technically reliable but not feasible, economically, for the power system project at On-Nut community. Also, when the biogas generators were completely isolated from the grid system, by allowing the company to depend on energy supply from the grid system only without storage energy support, the company recorded a huge loss, financially from table 13. The efficiency of a microgrid energy system is determined by its capability to capacitate energy demand without capacity shortage, overcoming unmet load potential, providing ancillary assistance support for the grid system, providing flexibilities in diverse operational strategies with adequate feedback control systems and a reliable performance (technically and economically) in which the proposed microgrid technology was able to fulfill.

5.3 Recommendation and Future Work

Adopting hybrid closed loop feedback control systems such as cycle charging, predictive, and load following strategies will function as hybrid interface between the AC and DC electrical bus connectors that will forecast the future energy demand and intermittent energy source such as solar irradiation in order to improve the efficiency of the hybrid power network effectively. Solid state batteries in bulk possess solid electrolyte, longer lifespan, higher energy density, wider operation at higher temperatures without damage than the liquid electrolyte batteries which will provide bulky energy management operation for the microgrid system to operate at longer period when the generators are not operating simultaneously. The time response of the solid-state batteries will play a significant role in bridging power gap between the energy sources and load potential instantaneously, thereby, responding quickly to capacity shortage from the biogas energy plants and grid congestion if there is a delay in biogas fuel production to power the biogas generators or responding quickly to excess energy supply from the biogas generators for storage after electrifying and energizing the load potential requirement. Introduction of solar photovoltaic generator as an independent energy source with a DC-DC converter will boost the power production of the DC source and reduce the biogas fuel consumption from the biogas generator that is in connection with a

dedicated converter at the DC bus connection to reduce cost of operation and minimize losses from the bidirectional converter.

The super capacitor will help to reduce output energy flow from the solid-state batteries since they can store and discharge larger energy faster than the batteries, thus, improving the batteries life cycle operation and reducing electric demand oscillation from the batteries. In addition, the super capacitor can improve the power quality of the hybrid power technology by eliminating harmonics that are capable of damaging the batteries and causing eddy current at the energy exchange flow between the AC and DC connectors. The future recommendation of the microgrid network above will increase the entire efficiency, reduce operating cost and production cost of the biogas generators, increase grid sales tremendously, minimize losses at the energy conversion between the electrical buses (AC-DC) and reduce grid purchases better than the previously analyzed proposed technology.

Apart from high capital investment cost, quality of biomass feedstock, competition against conventional fuel, public approval (not aware about biomass energy contribution and benefit to resistance from the public), uncertainty in regulations, lack of policy supports, maturity in energy system technology, efficiency of conversion, and odor emission control as major disadvantages within the environmental area where the waste power plant microgrid system is rendering energy services. Access to broad range of biomass feedstock is inevitable on daily basis which makes biomass energy to have greater edge and advantage over other renewable energy sources which (biomass feedstock) will constantly provide biogas fuel for the waste power plant every day for electrification and thermal production. Also, this microgrid network will promote neutral carbon, preserve bio diversities, create renewable employment, stabilize electricity cost and aid economic development, locally. Moreover, energy poverty will be reduced, energy sources will be diversified, conversion technologies advancement will undergo continuous upgrading, there will be incentives, unification with solar-wind-oceanic-geothermal generators, and climate policies will align with the waste power plant microgrid system to perform a flexible and complex operational procedure, respectively.

BIBLIOGRAPHY

[1] Rajbongshi, R., Borgohain, D., & Mahapatra, S. (2017). Optimization of PV-biomass-diesel and grid base hybrid energy systems for rural electrification by using HOMER. *Energy*, *126*, 461–474. https://doi.org/10.1016/j.energy.2017.03.056.

[2] Haghighat Mamaghani, A., Avella Escandon, S. A., Najafi, B., Shirazi, A., & Rinaldi, F. (2016). Techno-economic feasibility of photovoltaic, wind, diesel and hybrid electrification systems for off-grid rural electrification in Colombia. *Renewable Energy*, *97*, 293–305. https://doi.org/10.1016/j.renene.2016.05.086.

[3] Odou, O. D. T., Bhandari, R., & Adamou, R. (2020). Hybrid off-grid renewable power system for sustainable rural electrification in Benin. *Renewable Energy*, *145*, 1266–1279. https://doi.org/10.1016/j.renene.2019.06.032.

[4] Shivarama Krishna, K., & Sathish Kumar, K. (2015). A review on hybrid renewable energy systems. *Renewable and Sustainable Energy Reviews*, *52*, 907–916. https://doi.org/10.1016/j.rser.2015.07.187.

[5] Li, J., Liu, P., & Li, Z. (2020). Optimal design and techno-economic analysis of a solar-wind-biomass off-grid hybrid power system for remote rural electrification: A case study of west China. *Energy*, *208*, 118387. https://doi.org/10.1016/j.energy.2020.118387.

[6] Shahzad, M. K., Zahid, A., ur Rashid, T., Rehan, M. A., Ali, M., & Ahmad, M. (2017). Techno-economic feasibility analysis of a solar-biomass off grid system for the electrification of remote rural areas in Pakistan using HOMER software. *Renewable Energy*, *106*, 264–273. https://doi.org/10.1016/j.renene.2017.01.033.

[7] Amutha, W. M., & Rajini, V. (2016). Cost benefit and technical analysis of rural electrification alternatives in southern India using HOMER. *Renewable and Sustainable Energy Reviews*, *62*, 236–246. https://doi.org/10.1016/j.rser.2016.04.042.

[8] Kamran, M., Asghar, R., Mudassar, M., & Abid, M. I. (2019). Designing and economic aspects of run-of-canal based micro-hydro system on Balloki-Sulaimanki Link Canal-I for remote villages in Punjab, Pakistan. *Renewable Energy*, *141*, 76–87. https://doi.org/10.1016/j.renene.2019.03.126.

[9] Kasaeian, A., Rahdan, P., Rad, M. A. V., & Yan, W.-M. (2019). Optimal design and technical analysis of a grid-connected hybrid photovoltaic/diesel/biogas under different economic conditions: A case study. *Energy Conversion and Management*, *198*, 111810. https://doi.org/10.1016/j.enconman.2019.111810.

[10] Bastholm, C., & Fiedler, F. (2018). Techno-economic study of the impact of blackouts on the viability of connecting an off-grid PV-diesel hybrid system in Tanzania to the national power grid. *Energy Conversion and Management*, *171*, 647–658. https://doi.org/10.1016/j.enconman.2018.05.107.

[11] Kaur, T., & Segal, R. (2017). Designing Rural Electrification Solutions Considering Hybrid Energy Systems for Papua New Guinea. *Energy Procedia*, *110*, 1–7. https://doi.org/10.1016/j.egypro.2017.03.092.

[12] Sen, R., & Bhattacharyya, S. C. (2014). Off-grid electricity generation with renewable energy technologies in India: An application of HOMER. *Renewable Energy*, *62*, 388–398. https://doi.org/10.1016/j.renene.2013.07.028.

[13] Gebrehiwot, K., Mondal, Md. A. H., Ringler, C., & Gebremeskel, A. G. (2019). Optimization and cost-benefit assessment of hybrid power systems for off-grid rural electrification in Ethiopia. *Energy*, *177*, 234–246. https://doi.org/10.1016/j.energy.2019.04.095.

[14] Li, C., Zhou, D., Wang, H., Cheng, H., & Li, D. (2019). Feasibility assessment of a hybrid PV/diesel/battery power system for a housing estate in the severe cold zone—A case study of Harbin, China. *Energy*, *185*, 671–681. https://doi.org/10.1016/j.energy.2019.07.079.

[15] Wilson, D. C., & Velis, C. A. (2015). Waste management – still a global challenge in the 21st century: An evidence-based call for action. *Waste Management & Research*, *33*(12), 1049–1051. https://doi.org/10.1177/0734242x15616055.

[16] Kaza, S., Yao, L., Bhada-Tata, P., & Van Woerden, F. (2018). What a Waste 2.0: A Global Snapshot of Solid Waste Management to 2050. *What a Waste 2.0 : A Global Snapshot of Solid Waste Management to 2050*. https://doi.org/10.1596/978-1-4648-1329-0.

[17] Dou, Z., & Toth, J. D. (2020). Global primary data on consumer food waste: Rate and characteristics – A review. *Resources, Conservation and Recycling*, *168*, 105332. https://doi.org/10.1016/j.resconrec.2020.105332.
[18] Dobers, G. M. (2019). Acceptance of biogas plants taking into account space and place. *Energy Policy*, *135*, 110987. https://doi.org/10.1016/j.enpol.2019.110987.
[19] Deng, L., Liu, Y., Zheng, D., Wang, L., Pu, X., Song, L., Wang, Z., Lei, Y., Chen, Z., & Long, Y. (2017). Application and development of biogas technology for the treatment of waste in China. *Renewable and Sustainable Energy Reviews*, *70*, 845–851. https://doi.org/10.1016/j.rser.2016.11.265.
[20] Martinez, J., Dabert, P., Barrington, S., & Burton, C. (2009). Livestock waste treatment systems for environmental quality, food safety, and sustainability. *Bioresource Technology*, *100*(22), 5527–5536. https://doi.org/10.1016/j.biortech.2009.02.038.
[21] Malinowski, M., & Katarzyna Wolny-Koładka. (2017). *Microbiological and Energetic Assessment of the Effects of the Biodrying of Fuel Produced from Waste*. https://doi.org/10.1515/eces-2017-0036.
[22] Alfano, B., Barretta, L., Del Giudice, A., De Vito, S., Di Francia, G., Esposito, E., Formisano, F., Massera, E., Miglietta, M. L., & Polichetti, T. (2020). A Review of Low-Cost Particulate Matter Sensors from the Developers' Perspectives. *Sensors (Basel, Switzerland)*, *20*(23), 6819. https://doi.org/10.3390/s20236819.
[23] Wolny-Koładka, K., Malinowski, M., & Zdaniewicz, M. (2021). Energy-related and microbiological evaluation of the effects of bulking agents on the brewery hot trub biodrying. *Food and Bioproducts Processing*, *127*, 398–407. https://doi.org/10.1016/j.fbp.2021.04.001.
[24] Malinowski, M., Stanisław Famielec, Katarzyna Wolny-Koładka, Sikora, J., Maciej Gliniak, Baran, D., Sobol, Z., & Salamon, J. (2021). *Impact of digestate addition on the biostabilization of undersized fraction from municipal solid waste*. *770*, 145375–145375. https://doi.org/10.1016/j.scitotenv.2021.145375.
[25] Gupta, P., Singh, R. S., Sachan, A., Vidyarthi, A. S., & Gupta, A. (2012). Study on biogas production by anaerobic digestion of garden-waste. *Fuel*, *95*, 495–498. https://doi.org/10.1016/j.fuel.2011.11.006.
[26] Helenas Perin, J. K., Biesdorf Borth, P. L., Torrecilhas, A. R., Santana da Cunha, L., Kuroda, E. K., & Fernandes, F. (2020). Optimization of methane production parameters during anaerobic co-digestion of food waste and garden waste. *Journal of Cleaner Production*, *272*, 123130. https://doi.org/10.1016/j.jclepro.2020.123130.
[27] Hamer, G. (2003). Solid waste treatment and disposal: effects on public health and environmental safety. *Biotechnology Advances*, *22*(1-2), 71–79. https://doi.org/10.1016/j.biotechadv.2003.08.007.
[28] Lup, D. T., Stroe, A. M., Chezan, P. M., & Pica, E. M. (2018). The Importance of Waste Incineration. *Studia Universitatis Babeș-Bolyai Ambientum*, *63*(1), 43–48. https://doi.org/10.24193/subbambientum.2018.1.04.
[29] Vallero, D. A. (2011). Thermal Waste Treatment. *Waste*, 219–231. https://doi.org/10.1016/b978-0-12-381475-3.10016-6.
[30] Gómez-Brandón, M., & Podmirseg, S. M. (2013). Biological waste treatment. *Waste Management & Research*, *31*(8), 773–774. https://doi.org/10.1177/0734242x13497685.
[31] Elena Cristina Rada. (2015). *Biological Treatment of Solid Waste*. https://doi.org/10.1201/b18872.
[32] Singh, A. (2019). Managing the uncertainty problems of municipal solid waste disposal. *Journal of Environmental Management*, *240*, 259–265. https://doi.org/10.1016/j.jenvman.2019.03.025.
[33] Rao, M. N., Sultana, R., & Kota, S. H. (2017). *Solid and hazardous waste management: science and engineering*. Butterworth-Heinemann.
[34] Salomone, R., Saija, G., Mondello, G., Giannetto, A., Fasulo, S., & Savastano, D. (2017). Environmental impact of food waste bioconversion by insects: Application of Life Cycle Assessment to process using Hermetia illucens. *Journal of Cleaner Production*, *140*, 890–905. https://doi.org/10.1016/j.jclepro.2016.06.154.
[35] Wolny-Koładka, K., & Zdaniewicz, M. (2021). Antibiotic Resistance of Escherichia coli Isolated from Processing of Brewery Waste with the Addition of Bulking Agents. *Sustainability*, *13*(18), 10174. https://doi.org/10.3390/su131810174.

[36] Read, Q. D., Brown, S., Cuéllar, A. D., Finn, S. M., Gephart, J. A., Marston, L. T., Meyer, E., Weitz, K. A., & Muth, M. K. (2020). Assessing the environmental impacts of halving food loss and waste along the food supply chain. *Science of the Total Environment*, *712*, 136255. https://doi.org/10.1016/j.scitotenv.2019.136255.

[37] Cattaneo, A., Federighi, G., & Vaz, S. (2020). The environmental impact of reducing food loss and waste: A critical assessment. *Food Policy*, *98*, 101890. https://doi.org/10.1016/j.foodpol.2020.101890.

[38] García-Herrero, L., De Menna, F., & Vittuari, M. (2019). Food waste at school. The environmental and cost impact of a canteen meal. *Waste Management*, *100*, 249–258. https://doi.org/10.1016/j.wasman.2019.09.027.

[39] Sterczyńska, M., Zdaniewicz, M., & Wolny-Koładka, K. (2021). Rheological and Microbiological Characteristics of Hops and Hot Trub Particles Formed during Beer Production. *Molecules*, *26*(3), 681. https://doi.org/10.3390/molecules26030681.

[40] Kopeć, M., Mierzwa-Hersztek, M., Gondek, K., Wolny-Koładka, K., Zdaniewicz, M., & Suder, A. (2021). The Application Potential of Hop Sediments from Beer Production for Composting. *Sustainability*, *13*(11), 6409. https://doi.org/10.3390/su13116409.

[41] Cudjoe, D., & Acquah, P. M. (2021). Environmental impact analysis of municipal solid waste incineration in African countries. *Chemosphere*, *265*, 129186. https://doi.org/10.1016/j.chemosphere.2020.129186.

[42] Istrate, I.-R., Galvez-Martos, J.-L., & Dufour, J. (2021). The impact of incineration phase-out on municipal solid waste landfilling and life cycle environmental performance: Case study of Madrid, Spain. *Science of the Total Environment*, *755*, 142537. https://doi.org/10.1016/j.scitotenv.2020.142537.

[43] Xiaoli, C., Ziyang, L., Shimaoka, T., Nakayama, H., Ying, Z., Xiaoyan, C., Komiya, T., Ishizaki, T., & Youcai, Z. (2010). Characteristics of environmental factors and their effects on CH4 and CO2 emissions from a closed landfill: An ecological case study of Shanghai. *Waste Management*, *30*(3), 446–451. https://doi.org/10.1016/j.wasman.2009.09.047.

[44] Adamcová, D., Radziemska, M., Ridošková, A., Bartoň, S., Pelcová, P., Elbl, J., Kynický, J., Brtnický, M., & Vaverková, M. D. (2017). Environmental assessment of the effects of a municipal landfill on the content and distribution of heavy metals in Tanacetum vulgare L. *Chemosphere*, *185*, 1011–1018. https://doi.org/10.1016/j.chemosphere.2017.07.060.

[45] Li, W., Gu, K., Yu, Q., Sun, Y., Wang, Y., Xin, M., Bian, R., Wang, H., Wang, Y., & Zhang, D. (2021). Leaching behavior and environmental risk assessment of toxic metals in municipal solid waste incineration fly ash exposed to mature landfill leachate environment. *Waste Management*, *120*, 68–75. https://doi.org/10.1016/j.wasman.2020.11.020.

[46] Hoornweg, D., Bhada-Tata, P., & Kennedy, C. (2014). Peak Waste: When Is It Likely to Occur? *Journal of Industrial Ecology*, *19*(1), 117–128. https://doi.org/10.1111/jiec.12165.

[47] Letcher, T. M., & Vallero, D. A. (2019). *Waste : a handbook for management*. Academic Press.

[48] Makisha, N., & Semenova, D. (2018). Production of biogas at wastewater treatment plants and its further application. *MATEC Web of Conferences*, *144*, 04016. https://doi.org/10.1051/matecconf/201814404016.

[49] Onen Cinar, S., Nsair, A., Wieczorek, N., & Kuchta, K. (2022). Long-Term Assessment of Temperature Management in an Industrial Scale Biogas Plant. *Sustainability*, *14*(2), 612. https://doi.org/10.3390/su14020612.

[50] Khademi, F., Samaei, M. R., Shahsavani, A., Azizi, K., Mohammadpour, A., Derakhshan, Z., Giannakis, S., Rodriguez-Chueca, J., & Bilal, M. (2022). Investigation of the Presence Volatile Organic Compounds (BTEX) in the Ambient Air and Biogases Produced by a Shiraz Landfill in Southern Iran. *Sustainability*, *14*(2), 1040. https://doi.org/10.3390/su14021040.

[51] Sauve, G., & Van Acker, K. (2020). The environmental impacts of municipal solid waste landfills in Europe: A life cycle assessment of proper reference cases to support decision making. *Journal of Environmental Management*, *261*, 110216. https://doi.org/10.1016/j.jenvman.2020.110216.

[52] Randazzo, A., Asensio-Ramos, M., Melián, G. V., Venturi, S., Padrón, E., Hernández, P. A., Pérez, N. M., & Tassi, F. (2020). Volatile organic compounds (VOCs) in solid waste landfill cover soil: Chemical and isotopic composition vs. degradation processes. *Science of the Total Environment*, *726*, 138326. https://doi.org/10.1016/j.scitotenv.2020.138326.

[53] Mattiello, A., Chiodini, P., Bianco, E., Forgione, N., Flammia, I., Gallo, C., Pizzuti, R., & Panico, S. (2013). Health effects associated with the disposal of solid waste in landfills and incinerators in populations living in surrounding areas: a systematic review. *International Journal of Public Health*, *58*(5), 725–735. https://doi.org/10.1007/s00038-013-0496-8.

[54] Wolny-Koładka, K., Malinowski, M., & Żukowski, W. (2020). Impact of Calcium Oxide on Hygienization and Self-Heating Prevention of Biologically Contaminated Polymer Materials. *Materials*, *13*(18), 4012. https://doi.org/10.3390/ma13184012.

[55] Flores, R. M., Feratero, V. J., Soneja, S. K. C., Gonzales, R. P. A. R., Burog, E., Alvarez, C. J., & Bagus, D. (2017). *A Case Study about the Improper Waste Disposal in Barangay Mojon Tampoy* [Review of *A Case Study about the Improper Waste Disposal in Barangay MojonTampoy*].https://www.researchgate.net/publication/331702185_A_Case_Study_about_the_Improper_Waste_Disposal_in_Barangay_Mojon_Tampoy.

[56] International Energy Agency. (2022). Southeast Asia Energy Outlook 2022 [Review of *Southeast Asia Energy Outlook 2022*]. In T. Gould & World Energy Outlook Team (Eds.), *International Energy Agency* (pp. 5–27). IEA Publications International Energy Agency. https://www.iea.org/reports/southeast-asia-energy-outlook-2022.

[57] Kolhe, M. L., Ranaweera, K. M. I. U., & Gunawardana, A. G. B. S. (2015). Techno-economic sizing of off-grid hybrid renewable energy system for rural electrification in Sri Lanka. *Sustainable Energy Technologies and Assessments*, *11*, 53–64. https://doi.org/10.1016/j.seta.2015.03.008.

[58] Li, C., Zhou, D., & Zheng, Y. (2018). Techno-economic comparative study of grid-connected PV power systems in five climate zones, China. *Energy*, *165*, 1352–1369. https://doi.org/10.1016/j.energy.2018.10.062.

[59] Hossain, M., Mekhilef, S., & Olatomiwa, L. (2017). Performance evaluation of a stand-alone PV-wind-diesel-battery hybrid system feasible for a large resort center in South China Sea, Malaysia. *Sustainable Cities and Society*, *28*, 358–366. https://doi.org/10.1016/j.scs.2016.10.008.

[60] Rehman, S., & Al-Hadhrami, L. M. (2010). Study of a solar PV–diesel–battery hybrid power system for a remotely located population near Rafha, Saudi Arabia. *Energy*, *35*(12), 4986–4995. https://doi.org/10.1016/j.energy.2010.08.025.

[61] Tawfik, T. M., Badr, M. A., El-Kady, E. Y., & Abdellatif, O. E. (2018). Optimization and energy management of hybrid standalone energy system: a case study. *Renewable Energy Focus*, *25*, 48–56. https://doi.org/10.1016/j.ref.2018.03.004.

[62] Haratian, M., Tabibi, P., Sadeghi, M., Vaseghi, B., & Poustdouz, A. (2018). A renewable energy solution for stand-alone power generation: A case study of KhshU Site-Iran. *Renewable Energy*, *125*, 926–935. https://doi.org/10.1016/j.renene.2018.02.078.

[63] Mehrjerdi, H. (2020). Modeling and Optimization of an Island Water-Energy Nexus Powered by a Hybrid Solar-Wind Renewable System. *Energy*, 117217. https://doi.org/10.1016/j.energy.2020.117217.

[64] Elkadeem, M. R., Wang, S., Sharshir, S. W., & Atia, E. G. (2019). Feasibility analysis and techno-economic design of grid-isolated hybrid renewable energy system for electrification of agriculture and irrigation area: A case study in Dongola, Sudan. *Energy Conversion and Management*, *196*, 1453–1478. https://doi.org/10.1016/j.enconman.2019.06.085.

[65] Gabra, S., Miles, J., & Scott, S. A. (2019). Techno-economic analysis of stand-alone wind micro-grids, compared with PV and diesel in Africa. *Renewable Energy*, *143*, 1928–1938. https://doi.org/10.1016/j.renene.2019.05.119.

[66] Rahman, Md. M., Khan, Md. M.-U.-H., Ullah, M. A., Zhang, X., & Kumar, A. (2016). A hybrid renewable energy system for a North American off-grid community. *Energy*, *97*, 151–160. https://doi.org/10.1016/j.energy.2015.12.105.

[67] Chen, T., Jin, Y., Lv, H., Yang, A., Liu, M., Chen, B., Xie, Y., & Chen, Q. (2020). Applications of Lithium-Ion Batteries in Grid-Scale Energy Storage Systems. *Transactions of Tianjin University*. https://doi.org/10.1007/s12209-020-00236-w.

[68] Xu, Y., & Shen, X. (2018). Optimal Control Based Energy Management of Multiple Energy Storage Systems in a Microgrid. *IEEE Access*, *6*, 32925–32934. https://doi.org/10.1109/access.2018.2845408.

[69] Khalid, M. (2019). A Review on the Selected Applications of Battery-Supercapacitor Hybrid Energy Storage Systems for Microgrids. *Energies*, *12*(23), 4559. https://doi.org/10.3390/en12234559.

[70] Arvind Parwal, Fregelius, M., Temiz, I., Malin Göteman, Goncalves, J., Boström, C., & Mats Leijon. (2018). Energy management for a grid-connected wave energy park through a hybrid energy storage system. *Applied Energy*, *231*, 399–411. https://doi.org/10.1016/j.apenergy.2018.09.146.
[71] Aktas, A., Erhan, K., Ozdemir, S., & Ozdemir, E. (2017). Experimental investigation of a new smart energy management algorithm for a hybrid energy storage system in smart grid applications. *Electric Power Systems Research*, *144*, 185–196. https://doi.org/10.1016/j.epsr.2016.11.022.
[72] Aznavi, S., Fajri, P., Sabzehgar, R., & Asrari, A. (2020). Optimal management of residential energy storage systems in presence of intermittencies. *Journal of Building Engineering*, *29*, 101149. https://doi.org/10.1016/j.jobe.2019.101149.
[73] Li, J., Xiong, R., Yang, Q., Liang, F., Zhang, M., & Yuan, W. (2017). Design/test of a hybrid energy storage system for primary frequency control using a dynamic droop method in an isolated microgrid power system. *Applied Energy*, *201*, 257–269. https://doi.org/10.1016/j.apenergy.2016.10.066.
[74] Wang, Y., Tan, K. T., Peng, X. Y., & So, P. L. (2016). Coordinated Control of Distributed Energy-Storage Systems for Voltage Regulation in Distribution Networks. *IEEE Transactions on Power Delivery*, *31*(3), 1132–1141. https://doi.org/10.1109/TPWRD.2015.2462723.
[75] Zhang, D., Li, J., & Hui, D. (2018). Coordinated control for voltage regulation of distribution network voltage regulation by distributed energy storage systems. *Protection and Control of Modern Power Systems*, *3*(1). https://doi.org/10.1186/s41601-018-0077-1.
[76] Jia, K., Chen, Y., Bi, T., Lin, Y., Thomas, D., & Sumner, M. (2017). Historical-Data-Based Energy Management in a Microgrid With a Hybrid Energy Storage System. *IEEE Transactions on Industrial Informatics*, *13*(5), 2597–2605. https://doi.org/10.1109/TII.2017.2700463.
[77] Chaychizadeh, F., Dehghandorost, H., Aliabadi, A., & Taklifi, A. (2018). Stochastic dynamic simulation of a novel hybrid thermal-compressed carbon dioxide energy storage system (T-CCES) integrated with a wind farm. *Energy Conversion and Management*, *166*, 500–511. https://doi.org/10.1016/j.enconman.2018.04.050.
[78] Liang, Z., Song, Z., Wang, J., Xian, W., & Zhang, G. (2019). Three-stage scheduling scheme for hybrid energy storage systems to track scheduled feed-in PV power. *Solar Energy*, *188*, 1054–1067. https://doi.org/10.1016/j.solener.2019.06.068.
[79] Ghosh, S. K., Roy, T. K., Pramanik, M. A. H., Sarkar, A. K., & Mahmud, Md. A. (2020). An Energy Management System-Based Control Strategy for DC Microgrids with Dual Energy Storage Systems. *Energies*, *13*(11), 2992. https://doi.org/10.3390/en13112992.
[80] Jiang, W., Yang, C., Liu, Z., Liang, M., Li, P., & Zhou, G. (2019). A Hierarchical Control Structure for Distributed Energy Storage System in DC Micro-Grid. *IEEE Access*, *7*, 128787–128795. https://doi.org/10.1109/access.2019.2939626.
[81] Jing, W., Lai, C. H., Wong, W. S. H., & Wong, M. L. D. (2018). A comprehensive study of battery-supercapacitor hybrid energy storage system for standalone PV power system in rural electrification. *Applied Energy*, *224*, 340–356. https://doi.org/10.1016/j.apenergy.2018.04.106.
[82] Ariyaratna, P., Muttaqi, K. M., & Sutanto, D. (2018). A novel control strategy to mitigate slow and fast fluctuations of the voltage profile at common coupling Point of rooftop solar PV unit with an integrated hybrid energy storage system. *Journal of Energy Storage*, *20*, 409–417. https://doi.org/10.1016/j.est.2018.10.016.
[83] *Slovakia - Ministry of Environment of the Slovak Republic*. (2021, September 22). One Planet Network.https://www.oneplanetnetwork.org/organisations/slovakia-ministry-environment-slovak-republic.
[84] Tabasová, A., Kropáč, J., Kermes, V., Nemet, A., & Stehlík, P. (2012). Waste-to-energy technologies: Impact on environment. *Energy*, *44*(1), 146–155. https://doi.org/10.1016/j.energy.2012.01.014.
[85] Brunner, P. H., & Rechberger, H. (2015). Waste to energy – key element for sustainable waste management. *Waste Management*, *37*, 3–12. https://doi.org/10.1016/j.wasman.2014.02.003.
[86] Garg, A. (2014). Mechanical biological treatment for municipal solid waste. *International Journal of Environmental Technology and Management*, *17*(2/3/4), 215. https://doi.org/10.1504/ijetm.2014.061795.
[87] Suparmaniam, U., Lam, M. K., Uemura, Y., Lim, J. W., Lee, K. T., & Shuit, S. H. (2019). Insights into the microalgae cultivation technology and harvesting process for biofuel production: A

review. *Renewable and Sustainable Energy Reviews*, *115*, 109361. https://doi.org/10.1016/j.rser.2019.109361.
[88] Mat Aron, N. S., Khoo, K. S., Chew, K. W., Show, P. L., Chen, W., & Nguyen, T. H. P. (2020). Sustainability of the four generations of biofuels – A review. *International Journal of Energy Research*, *44*(12), 9266–9282. https://doi.org/10.1002/er.5557.
[89] Alalwan, H. A., Alminshid, A. H., & Aljaafari, H. A. S. (2019). Promising evolution of biofuel generations. Subject review. *Renewable Energy Focus*, *28*, 127–139. https://doi.org/10.1016/j.ref.2018.12.006.
[90] Ganguly, P., Sarkhel, R., & Das, P. (2021). The second- and third-generation biofuel technologies: comparative perspectives. *Sustainable Fuel Technologies Handbook*, 29–50. https://doi.org/10.1016/b978-0-12-822989-7.00002-0.
[91] Thompson, P. (2012). The Agricultural Ethics of Biofuels: The Food vs. Fuel Debate. *Agriculture*, *2*(4), 339–358. https://doi.org/10.3390/agriculture2040339.
[92] Domen Žalec, Hanak, D. P., Matic Može, & Iztok Golobič. (2021). Process development and performance assessment of flexible calcium looping biomass gasification for production of renewable gas with adjustable composition. *International Journal of Energy Research*, *46*(5), 6197–6215. https://doi.org/10.1002/er.7558.
[93] Kumar, M., Munoz-Arriola, F., Furumai, H., & Chaminda, T. (2021). Resilience, Response, and Risk in Water Systems: Shifting Management and Natural Forcings Paradigms. In *The Open Library*. Springer Singapore Pte. Limited. https://openlibrary.org/books/OL33942537M/Resilience_Response_and_Risk_in_Water_Systems.
[94] Rhyner, C. R., Schwartz, L. J., Wenger, R. B., & Kohrell, M. G. (2017). Waste Management and Resource Recovery. In *Google Books*. CRC Press. https://books.google.com/books/about/Waste_Management_and_Resource_Recovery.html?id=PQZDDwAAQBAJ.
[95] US EPA, O. (2015, December 4). *Global Methane Initiative (GMI)*. Www.epa.gov. https://www.epa.gov/gmi.
[96] Kamperidou, V., & Terzopoulou, P. (2021). Anaerobic Digestion of Lignocellulosic Waste Materials. *Sustainability*, *13*(22), 12810. https://doi.org/10.3390/su132212810.
[97] Ahn, J.-Y., & Chang, S.-W. (2021). Effects of Sludge Concentration and Disintegration/Solubilization Pretreatment Methods on Increasing Anaerobic Biodegradation Efficiency and Biogas Production. *Sustainability*, *13*(22), 12887. https://doi.org/10.3390/su132212887.
[98] Tanigawa, S. (2017, October 3). *Fact Sheet - Biogas: Converting Waste to Energy | White Papers | EESI*. Eesi.org. https://www.eesi.org/papers/view/fact-sheet-biogasconverting-waste-to-energy.
[99] Vögeli, Y., Christian Riu Lohri, Gallardo, A., Diener, S., & Zurbrügg, C. (2014). *Anaerobic digestion of biowaste in developing countries. Practical information and case studies*.
[100] Uçkun Kiran, E., Stamatelatou, K., Antonopoulou, G., & Lyberatos, G. (2016). Production of biogas via anaerobic digestion. *Handbook of Biofuels Production*, 259–301. https://doi.org/10.1016/b978-0-08-100455-5.00010-2.
[101] Chromec, P., Seda Sevaioglu Macher, & Kedrowski, C. (2018). WTE, Hitachi Zosen Inova Moving Grate and Anaerobic Digestion Technologies. *Springer EBooks*, 1–53. https://doi.org/10.1007/978-1-4939-2493-6_398-3.
[102] US EPA. (2019, March 18). *How does anaerobic digestion work? | US EPA*. US EPA. https://www.epa.gov/agstar/how-does-anaerobic-digestion-work.
[103] S. Abanades *et al.*, "A critical review of biogas production and usage with legislations framework across the globe," *International Journal of Environmental Science and Technology*, vol. 19, May 2021, doi: https://doi.org/10.1007/s13762-021-03301-6.
[104] Kalender, S. S. (2019). Air Pollution Prevention Technologies. *Handbook of Environmental Materials Management*, 2871–2888. https://doi.org/10.1007/978-3-319-73645-7_109.
[105] Patil, J. H., Raj, M. A., Muralidhara, P. L., Desai, S. M., & Raju, G. K. M. (2012). Kinetics of Anaerobic Digestion of Water Hyacinth Using Poultry Litter as Inoculum. *International Journal of Environmental Science and Development*, 94–98. https://doi.org/10.7763/ijesd.2012.v3.195.
[106] Hu, Z.-H., & Yu, H.-Q. (2006). Anaerobic digestion of cattail by rumen cultures. *Waste Management*, *26*(11), 1222–1228. https://doi.org/10.1016/j.wasman.2005.08.003.

[107] Chusov, A., Maslikov, V. I., Vladimir Badenko, Viacheslav Zhazhkov, Dmitry Molodtsov, & Yuliya Pavlushkina. (2021). Biogas Potential Assessment of the Composite Mixture from Duckweed Biomass. *Sustainability*, *14*(1), 351–351. https://doi.org/10.3390/su14010351.
[108] Nachod, B., Keller, E., Hassanein, A., & Lansing, S. (2021). Assessment of Petroleum-Based Plastic and Bioplastics Degradation Using Anaerobic Digestion. *Sustainability*, *13*(23), 13295. https://doi.org/10.3390/su132313295.
[109] Oehmichen, K., Majer, S., & Thrän, D. (2021). Biomethane from Manure, Agricultural Residues and Biowaste—GHG Mitigation Potential from Residue-Based Biomethane in the European Transport Sector. *Sustainability*, *13*(24), 14007. https://doi.org/10.3390/su132414007.
[110] Awe, O. W., Zhao, Y., Nzihou, A., Minh, D. P., & Lyczko, N. (2017). A Review of Biogas Utilisation, Purification and Upgrading Technologies. *Waste and Biomass Valorization*, *8*(2), 267–283. https://doi.org/10.1007/s12649-016-9826-4.
[111] Maile, O. I., Muzenda, E., & Tesfagiorgis, H. (2017). Chemical Absorption of Carbon Dioxide in Biogas Purification. *Procedia Manufacturing*, *7*, 639–646. https://doi.org/10.1016/j.promfg.2016.12.095.
[112] Sheets, J. P., & Shah, A. (2018). Techno-economic comparison of biogas cleaning for grid injection, compressed natural gas, and biogas-to-methanol conversion technologies. *Biofuels, Bioproducts and Biorefining*, *12*(3), 412–425. https://doi.org/10.1002/bbb.1848.
[113] Directorate-General for Energy (European Commission), E3 Modelling, Sardi, K., De Vita, A., & Capros, P. (2020). The role of gas DSOs and distribution networks in the context of the energy transition. In *Publications Office of the European Union*. Publications Office of the European Union. https://op.europa.eu/en/publication-detail/-/publication/cad1a27a-7fbb-11eb-9ac9-01aa75ed71a1/language-en.
[114] Zheng, L., Chen, J., Zhao, M., Cheng, S., Wang, L.-P., Mang, H.-P., & Li, Z. (2020). What Could China Give to and Take from Other Countries in Terms of the Development of the Biogas Industry? *Sustainability*, *12*(4), 1490. https://doi.org/10.3390/su12041490.
[115] Jain, S., Newman , D., Nzihou, A., Dekker, H., Le Feuvre, P., Richter, H., Gobe, F., Morton, C., & Thompson, R. (2019, June). *Global Potential of Biogas* [Review of *Global Potential of Biogas*]. Worldbiogasassociation.org; WORLD BIOGAS ASSOCIATION. https://www.worldbiogasassociation.org/global-potential-of-biogas/.
[116] *Ministry of Natural Resources and Spatial Planning | GOV.SI*. (2023, August 11). Portal GOV.SI. https://www.gov.si/en/state-authorities/ministries/ministry-of-natural-resources-and-spatial-planning/.
[117] Zupančič, M., Možic, V., Može, M., Cimerman, F., & Golobič, I. (2022). Current Status and Review of Waste-to-Biogas Conversion for Selected European Countries and Worldwide. *Sustainability*, *14*(3), 1823. https://doi.org/10.3390/su14031823.
[118] *Ministry of Public Administration | GOV.SI*. (2023, July 28). Portal GOV.SI. https://www.gov.si/en/state-authorities/ministries/ministry-of-public-administration/.
[119] *Biogasanlagen - ULTRAWAVES Wasser- & Umwelttechnologien GmbH*. (2016). Ultrawaves.de. https://ultrawaves.de/biogas-plants.
[120] Savita Ahlawat, & Meenakshi Nandal. (2020). Energy Recovery from Anaerobic Digestion of Wastewater. *Springer Transactions in Civil and Environmental Engineering*. https://doi.org/10.1007/978-981-15-4668-6_20.
[121] *AN OVERVIEW OF RENEWABLE NATURAL GAS FROM BIOGAS*. (2020).https://www.epa.gov/sites/production/files/2020-07/documents/lmop_rng_document.pdf.
[122] Atelge, M. R., Krisa, D., Kumar, G., Eskicioglu, C., Nguyen, D. D., Chang, S. W., Atabani, A. E., Al-Muhtaseb, A. H., & Unalan, S. (2018). Biogas Production from Organic Waste: Recent Progress and Perspectives. *Waste and Biomass Valorization*, *11*(3), 1019–1040. https://doi.org/10.1007/s12649-018-00546-0.
[123] Ajay Singh Lodhi. (2021, May 18). *Gasification and types of gasifiers*. https://www.slideshare.net/AjaySinghLodhi/gasification-and-types-of-gasifiers.
[124] Kordi, M., & Seyyedi, S. M. (2021). Biomass Gasification Systems and Different Types of Gasifiers, Effective Parameters on Gasification Process Efficiency: An Overview. *Journal of Applied Dynamic Systems and Control*, *4*(2), 1-17.
[125] Balan, V. (2014). Current Challenges in Commercially Producing Biofuels from Lignocellulosic Biomass. *ISRN Biotechnology*, *2014*, 1–31. https://doi.org/10.1155/2014/463074.
[126] De, S., Avinash Kumar Agarwal, Goyal, A., & Bhaskar, T. (2018). *Coal and Biomass*

Gasification.https://doi.org/10.1007/978-981-10-7335-9.
[127] *Distributed Generation Using Natural Gas-Fueled Generator sets | Cat | Caterpillar*. (2018). Https://Www.cat.com/En_US/By-Industry/Electric-Power/Articles/White-Papers/Distributed-Generation-Using-Natural-Gas-Fueled-Generator-Sets.html. https://www.cat.com/en_US/by-industry/electric-power/Articles/White-papers/distributed-generation-using-natural-gas-fueled-generator-sets.html.
[128] *Cat® Natural Gas Generators | Cat | Caterpillar*. (2024). Https://Www.cat.com/En_US/Campaigns/Awareness/Electric-Power/Gas-Power-Solution.html. https://www.cat.com/en_US/campaigns/awareness/electric-power/gas-power-solution.html.
[129] Malik, P., Awasthi, M., & Sinha, S. (2022). A techno-economic investigation of grid integrated hybrid renewable energy systems. *Sustainable Energy Technologies and Assessments*, *51*, 101976. https://doi.org/10.1016/j.seta.2022.101976.
[130] Suresh, V., M., M., & Kiranmayi, R. (2020). Modelling and optimization of an off-grid hybrid renewable energy system for electrification in a rural areas. *Energy Reports*, *6*, 594–604. https://doi.org/10.1016/j.egyr.2020.01.013.
[131] Guo, M., Liu, G., & Liao, S. (2021). Normalized techno-economic index for renewable energy system assessment. *International Journal of Electrical Power & Energy Systems*, *133*, 107262–107262. https://doi.org/10.1016/j.ijepes.2021.107262.
[132] Mohammed, Y. S., Adetokun, B. B., Oghorada, O., & Oshiga, O. (2022). Techno-economic optimization of standalone hybrid power systems in context of intelligent computational multi-objective algorithms. *Energy Reports*, *8*, 11661–11674. https://doi.org/10.1016/j.egyr.2022.09.010.
[133] Popescu, F., Mahu, R., Ion, I. V., & Rusu, E. (2020). A Mathematical Model of Biomass Combustion Physical and Chemical Processes. *Energies*, *13*(23), 6232. https://doi.org/10.3390/en13236232.
[134] Naga, V., Nitin Naresh Pandhare, & Bajpai, S. (2022). *Mathematical Models for Optimization of Anaerobic Digestion and Biogas Production*. 575–591. https://doi.org/10.1007/978-981-16-8682-5_21.
[135] Hosokai, S., Matsuoka, K., Kuramoto, K., & Suzuki, Y. (2016). Modification of Dulong's formula to estimate heating value of gas, liquid and solid fuels. *Fuel Processing Technology*, *152*, 399–405. https://doi.org/10.1016/j.fuproc.2016.06.040.
[136] Mokhtara, C., Negrou, B., Settou, N., Settou, B., & Samy, M. M. (2021). Design optimization of off-grid Hybrid Renewable Energy Systems considering the effects of building energy performance and climate change: Case study of Algeria. *Energy*, *219*, 119605. https://doi.org/10.1016/j.energy.2020.119605.
[137] Sedhom, B. E., El-Saadawi, M. M., El Moursi, M. S., Hassan, Mohamed. A., & Eladl, A. A. (2021). IoT-based optimal demand side management and control scheme for smart microgrid. *International Journal of Electrical Power & Energy Systems*, *127*, 106674. https://doi.org/10.1016/j.ijepes.2020.106674.
[138] Zhang, Z., Ding, T., Zhou, Q., Sun, Y., Qu, M., Zeng, Z., Ju, Y., Li, L., Wang, K., & Chi, F. (2021). A review of technologies and applications on versatile energy storage systems. Renewable and Sustainable Energy Reviews, 148, 111263.https://doi.org/10.1016/j.rser.2021.111263.
[139] Luo, W., Stynski, S., Chub, A., Franquelo, L. G., Malinowski, M., & Vinnikov, D. (2021). Utility-Scale Energy Storage Systems: A Comprehensive Review of Their Applications, Challenges, and Future Directions. *IEEE Industrial Electronics Magazine*, *15*(4), 17–27. https://doi.org/10.1109/mie.2020.3026169.

APPENDICES

APPENDIX A

Cost Summary of Current and Proposed Microgrid System

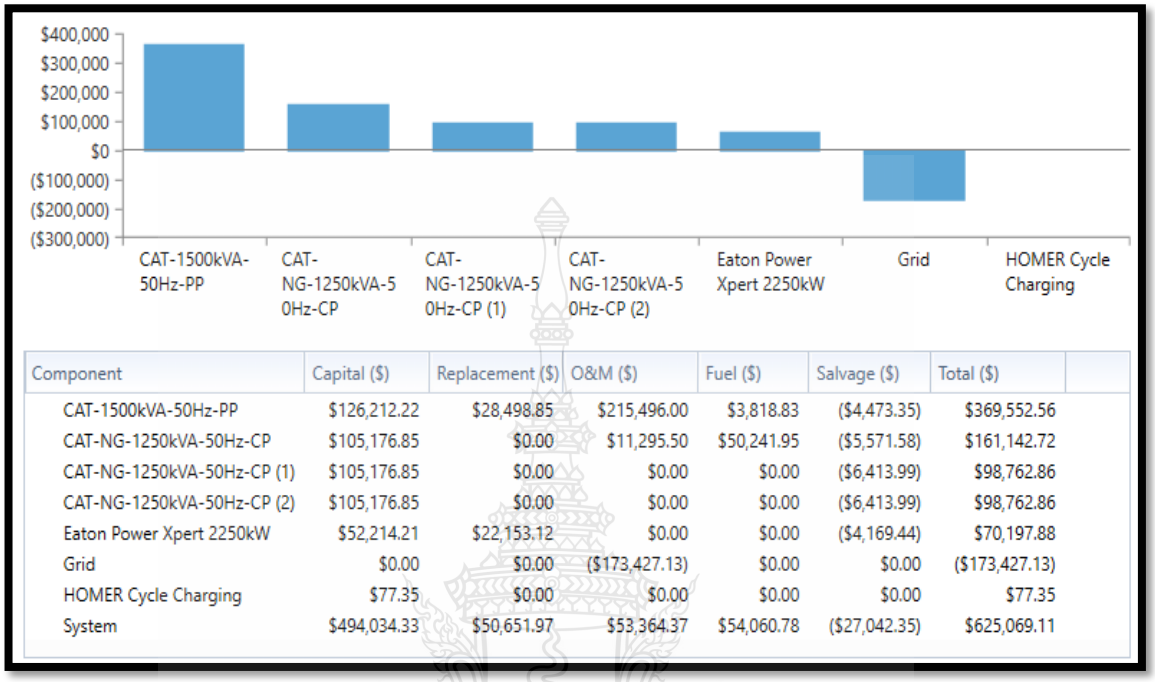

Component	Capital ($)	Replacement ($)	O&M ($)	Fuel ($)	Salvage ($)	Total ($)
CAT-1500kVA-50Hz-PP	$126,212.22	$28,498.85	$215,496.00	$3,818.83	($4,473.35)	$369,552.56
CAT-NG-1250kVA-50Hz-CP	$105,176.85	$0.00	$11,295.50	$50,241.95	($5,571.58)	$161,142.72
CAT-NG-1250kVA-50Hz-CP (1)	$105,176.85	$0.00	$0.00	$0.00	($6,413.99)	$98,762.86
CAT-NG-1250kVA-50Hz-CP (2)	$105,176.85	$0.00	$0.00	$0.00	($6,413.99)	$98,762.86
Eaton Power Xpert 2250kW	$52,214.21	$22,153.12	$0.00	$0.00	($4,169.44)	$70,197.88
Grid	$0.00	$0.00	($173,427.13)	$0.00	$0.00	($173,427.13)
HOMER Cycle Charging	$77.35	$0.00	$0.00	$0.00	$0.00	$77.35
System	$494,034.33	$50,651.97	$53,364.37	$54,060.78	($27,042.35)	$625,069.11

Figure 5.1 Annual Cost Summary of Biogas/Grid Network System.

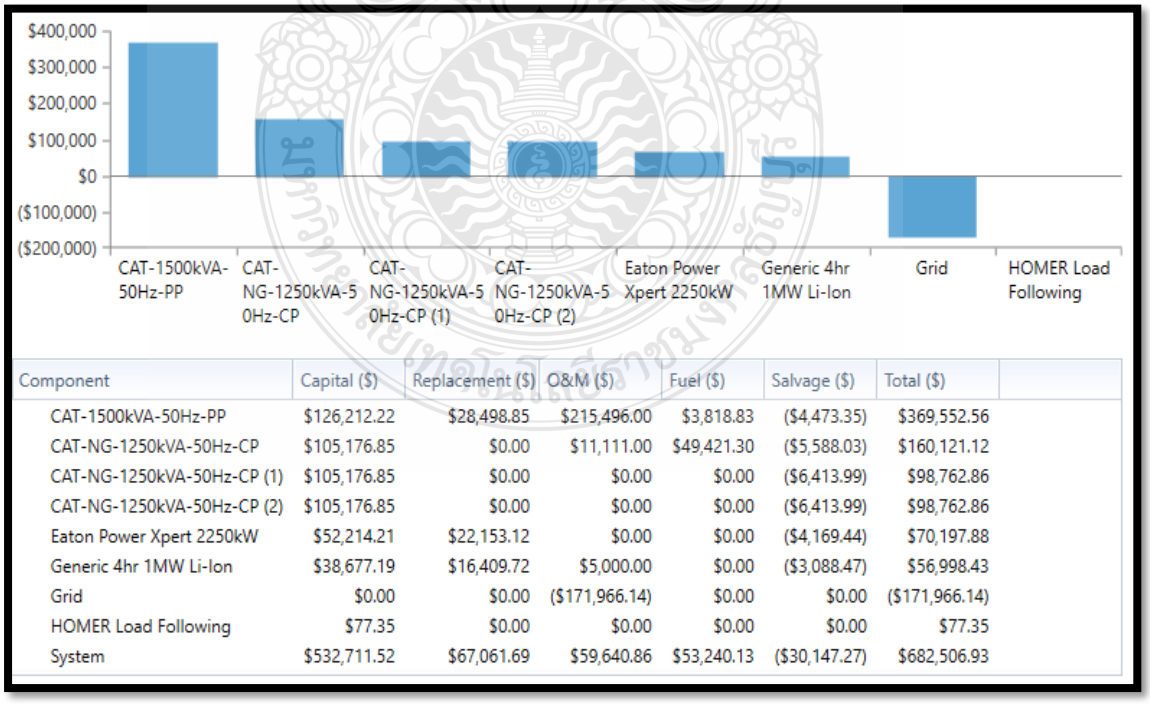

Component	Capital ($)	Replacement ($)	O&M ($)	Fuel ($)	Salvage ($)	Total ($)
CAT-1500kVA-50Hz-PP	$126,212.22	$28,498.85	$215,496.00	$3,818.83	($4,473.35)	$369,552.56
CAT-NG-1250kVA-50Hz-CP	$105,176.85	$0.00	$11,111.00	$49,421.30	($5,588.03)	$160,121.12
CAT-NG-1250kVA-50Hz-CP (1)	$105,176.85	$0.00	$0.00	$0.00	($6,413.99)	$98,762.86
CAT-NG-1250kVA-50Hz-CP (2)	$105,176.85	$0.00	$0.00	$0.00	($6,413.99)	$98,762.86
Eaton Power Xpert 2250kW	$52,214.21	$22,153.12	$0.00	$0.00	($4,169.44)	$70,197.88
Generic 4hr 1MW Li-Ion	$38,677.19	$16,409.72	$5,000.00	$0.00	($3,088.47)	$56,998.43
Grid	$0.00	$0.00	($171,966.14)	$0.00	$0.00	($171,966.14)
HOMER Load Following	$77.35	$0.00	$0.00	$0.00	$0.00	$77.35
System	$532,711.52	$67,061.69	$59,640.86	$53,240.13	($30,147.27)	$682,506.93

Figure 5.11 Annual Cost Summary of Biogas-Grid-Lithium-ion Network System.

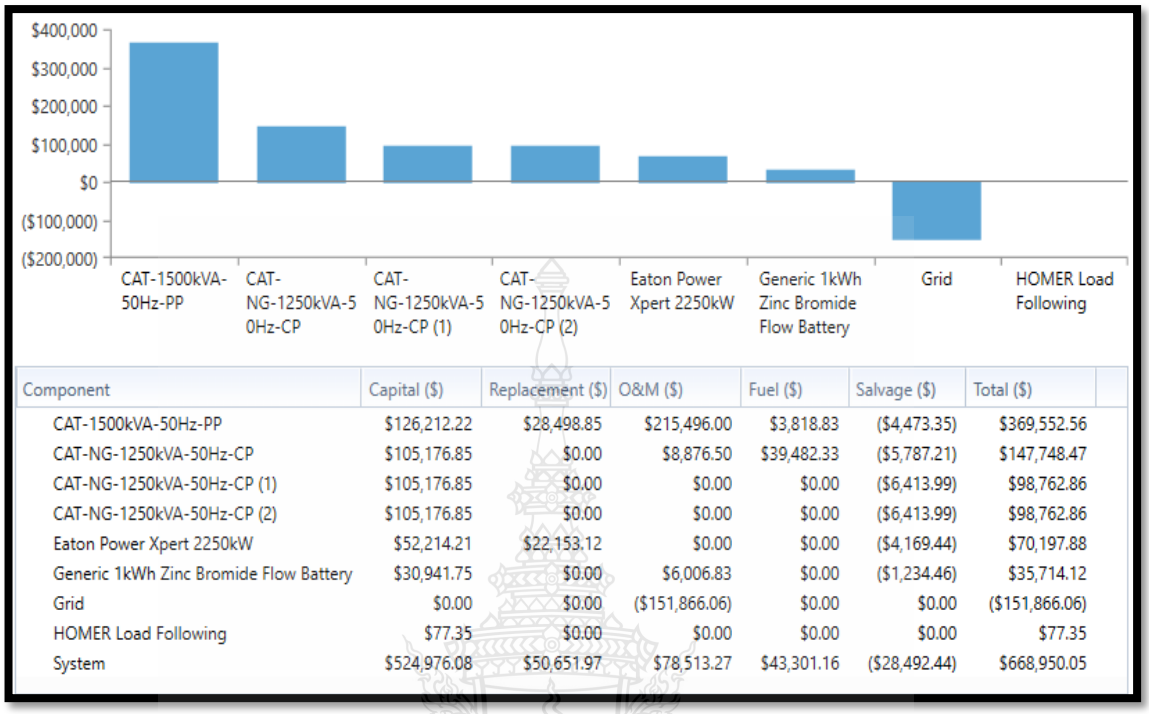

Component	Capital ($)	Replacement ($)	O&M ($)	Fuel ($)	Salvage ($)	Total ($)
CAT-1500kVA-50Hz-PP	$126,212.22	$28,498.85	$215,496.00	$3,818.83	($4,473.35)	$369,552.56
CAT-NG-1250kVA-50Hz-CP	$105,176.85	$0.00	$8,876.50	$39,482.33	($5,787.21)	$147,748.47
CAT-NG-1250kVA-50Hz-CP (1)	$105,176.85	$0.00	$0.00	$0.00	($6,413.99)	$98,762.86
CAT-NG-1250kVA-50Hz-CP (2)	$105,176.85	$0.00	$0.00	$0.00	($6,413.99)	$98,762.86
Eaton Power Xpert 2250kW	$52,214.21	$22,153.12	$0.00	$0.00	($4,169.44)	$70,197.88
Generic 1kWh Zinc Bromide Flow Battery	$30,941.75	$0.00	$6,006.83	$0.00	($1,234.46)	$35,714.12
Grid	$0.00	$0.00	($151,866.06)	$0.00	$0.00	($151,866.06)
HOMER Load Following	$77.35	$0.00	$0.00	$0.00	$0.00	$77.35
System	$524,976.08	$50,651.97	$78,513.27	$43,301.16	($28,492.44)	$668,950.05

Figure 5.12 Annual Cost Summary of Biogas-Grid-Zinc Bromide Flow Network System

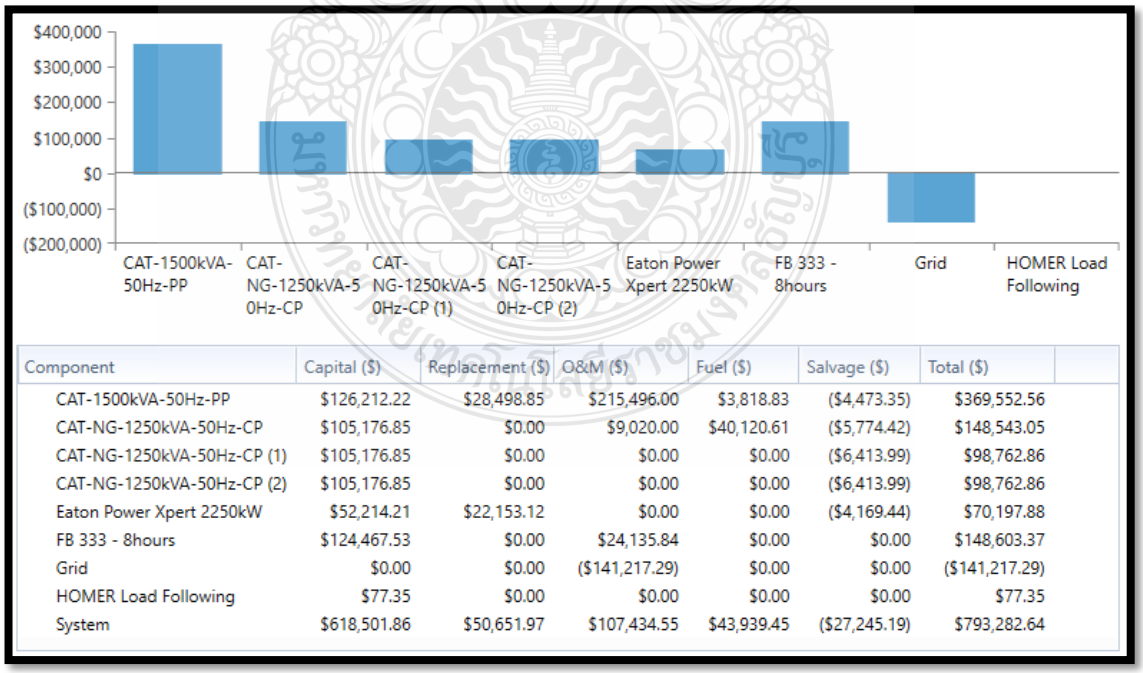

Component	Capital ($)	Replacement ($)	O&M ($)	Fuel ($)	Salvage ($)	Total ($)
CAT-1500kVA-50Hz-PP	$126,212.22	$28,498.85	$215,496.00	$3,818.83	($4,473.35)	$369,552.56
CAT-NG-1250kVA-50Hz-CP	$105,176.85	$0.00	$9,020.00	$40,120.61	($5,774.42)	$148,543.05
CAT-NG-1250kVA-50Hz-CP (1)	$105,176.85	$0.00	$0.00	$0.00	($6,413.99)	$98,762.86
CAT-NG-1250kVA-50Hz-CP (2)	$105,176.85	$0.00	$0.00	$0.00	($6,413.99)	$98,762.86
Eaton Power Xpert 2250kW	$52,214.21	$22,153.12	$0.00	$0.00	($4,169.44)	$70,197.88
FB 333 - 8hours	$124,467.53	$0.00	$24,135.84	$0.00	$0.00	$148,603.37
Grid	$0.00	$0.00	($141,217.29)	$0.00	$0.00	($141,217.29)
HOMER Load Following	$77.35	$0.00	$0.00	$0.00	$0.00	$77.35
System	$618,501.86	$50,651.97	$107,434.55	$43,939.45	($27,245.19)	$793,282.64

Figure 5.13 Annual Cost Summary of Biogas-Grid-Flow Battery Network System.

Relating the current energy system design from Fig.5.11 with the proposed energy system design (from Fig.5.12, Fig.5.13, and Fig.5.14), the levelized electricity cost from each microgrid system can be obtained by dividing their respective total annual cost by the total energy demanded (energy consumption) from each network as illustrated pictorially from Fig.4.13, Fig.4.30, Fig.4.31, and Fig.4.32, respectively.

APPENDIX B

Excess Energy of Current and Proposed Microgrid Configurations

Excess energy on current energy system:

Excess energy on current microgrid system = Annual energy production – Annual energy consumption

Annual energy production = 11,307, 775 kWh/year

Annual energy consumption = 11,103, 188 kWh/yr

Excess energy loss= 11,307,775 – 11,103,188 = 204,587 kWh/yr.

Excess energy on proposed Li-ion energy system:

Excess energy on Li-ion microgrid system = Annual energy production – Annual energy consumption

Annual energy production = 11,293, 764 kWh/year

Annual energy consumption = 11,083,568 kWh/yr

Excess energy loss= 11,293,764 – 11,083,568 = 210,196 kWh/yr.

Excess energy on proposed Zn-Brm energy system:

Excess energy on Zn-Brm microgrid system = Annual energy production – Annual energy consumption

Annual energy production = 11,144,331 kWh/year

Annual energy consumption = 10,842,134 kWh/yr

Excess energy loss = 11,144,331 – 10,842,134 = 302,197 kWh/yr.

Excess energy on proposed FB energy system:

Excess energy on FB microgrid system = Annual energy production – Annual energy consumption

Annual energy production = 11,155,765 kWh/year

Annual energy consumption = 10,740,080 kWh/yr

Excess energy loss = 11,155,765 – 10,740,080 = 415,685 kWh/yr.

APPENDIX C

Emission, Renewable Penetration, and Energy Trade of Current and Proposed Microgrid Configurations

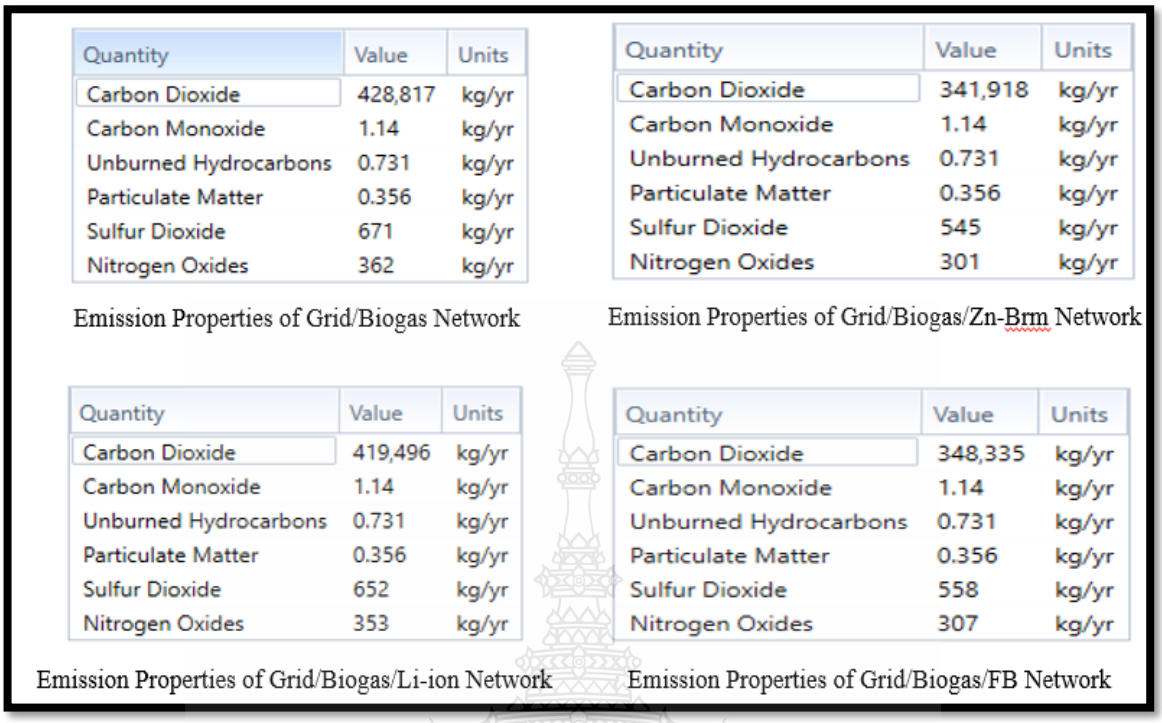

Quantity	Value	Units
Carbon Dioxide	428,817	kg/yr
Carbon Monoxide	1.14	kg/yr
Unburned Hydrocarbons	0.731	kg/yr
Particulate Matter	0.356	kg/yr
Sulfur Dioxide	671	kg/yr
Nitrogen Oxides	362	kg/yr

Emission Properties of Grid/Biogas Network

Quantity	Value	Units
Carbon Dioxide	341,918	kg/yr
Carbon Monoxide	1.14	kg/yr
Unburned Hydrocarbons	0.731	kg/yr
Particulate Matter	0.356	kg/yr
Sulfur Dioxide	545	kg/yr
Nitrogen Oxides	301	kg/yr

Emission Properties of Grid/Biogas/Zn-Brm Network

Quantity	Value	Units
Carbon Dioxide	419,496	kg/yr
Carbon Monoxide	1.14	kg/yr
Unburned Hydrocarbons	0.731	kg/yr
Particulate Matter	0.356	kg/yr
Sulfur Dioxide	652	kg/yr
Nitrogen Oxides	353	kg/yr

Emission Properties of Grid/Biogas/Li-ion Network

Quantity	Value	Units
Carbon Dioxide	348,335	kg/yr
Carbon Monoxide	1.14	kg/yr
Unburned Hydrocarbons	0.731	kg/yr
Particulate Matter	0.356	kg/yr
Sulfur Dioxide	558	kg/yr
Nitrogen Oxides	307	kg/yr

Emission Properties of Grid/Biogas/FB Network

Figure 5.14 Emission Properties of Current and Proposed Microgrid Network.

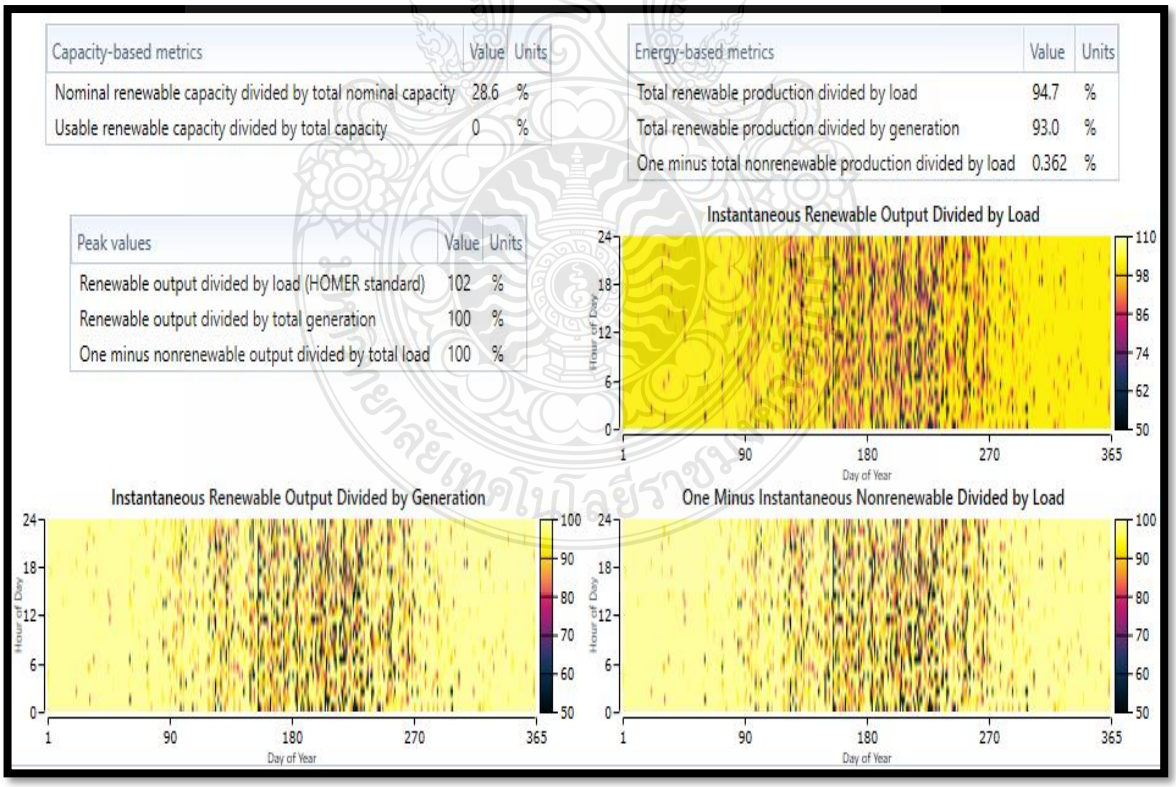

Capacity-based metrics	Value	Units
Nominal renewable capacity divided by total nominal capacity	28.6	%
Usable renewable capacity divided by total capacity	0	%

Energy-based metrics	Value	Units
Total renewable production divided by load	94.7	%
Total renewable production divided by generation	93.0	%
One minus total nonrenewable production divided by load	0.362	%

Peak values	Value	Units
Renewable output divided by load (HOMER standard)	102	%
Renewable output divided by total generation	100	%
One minus nonrenewable output divided by total load	100	%

Figure 5.15 Renewable Penetration of Utility Grid/Biogas Generators Network.

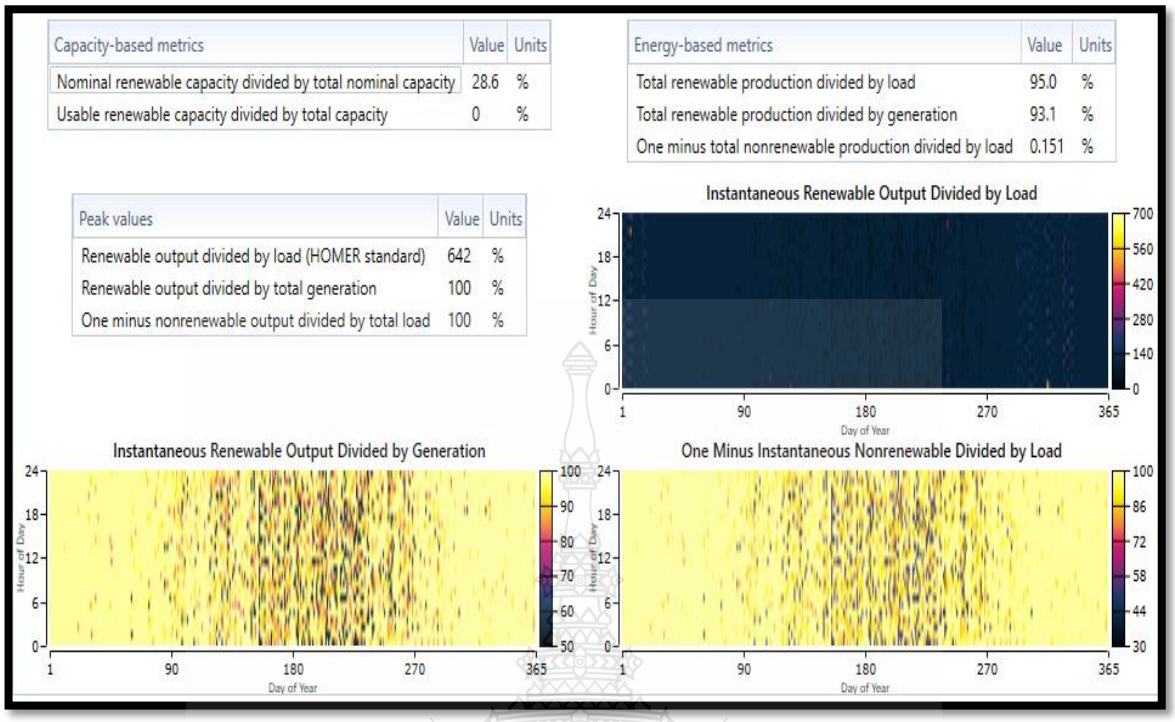

Figure 5.16 Renewable Penetration of Biogas/Grid/Lithium-ion Network System.

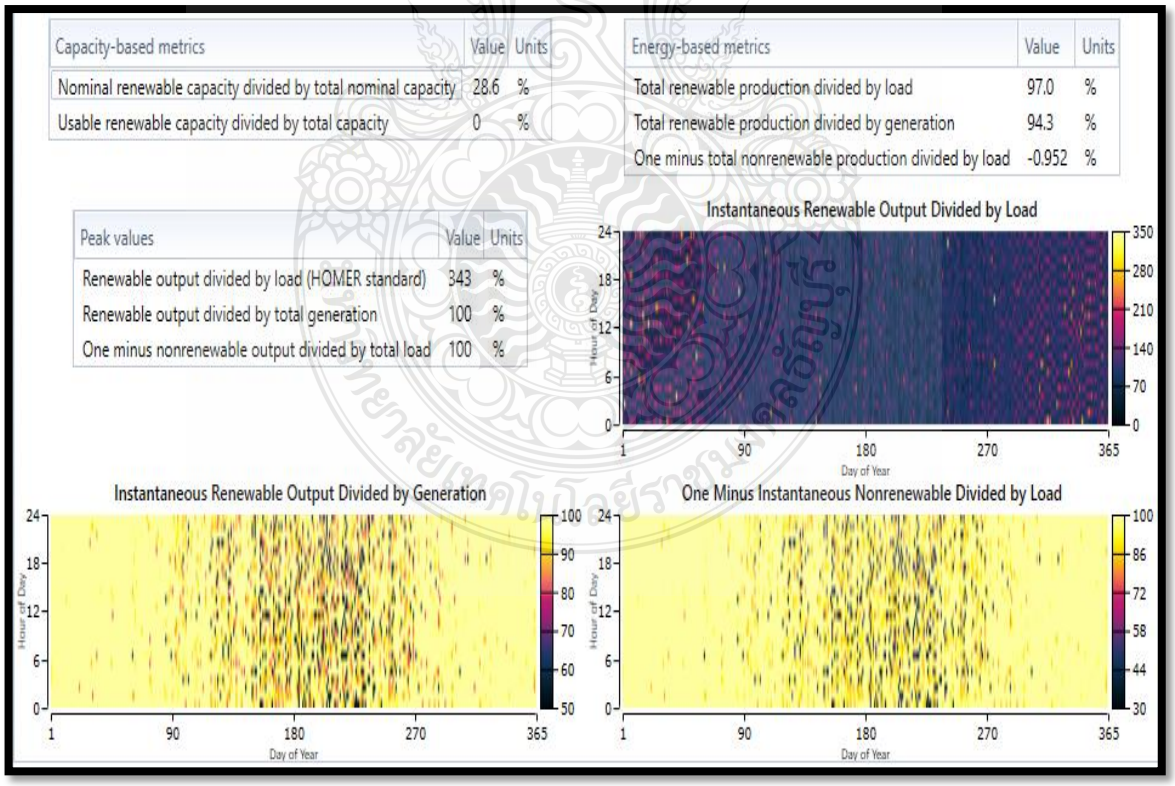

Figure 5.17 Renewable Penetration of Biogas/Grid/Zinc Bromide Flow Network System.

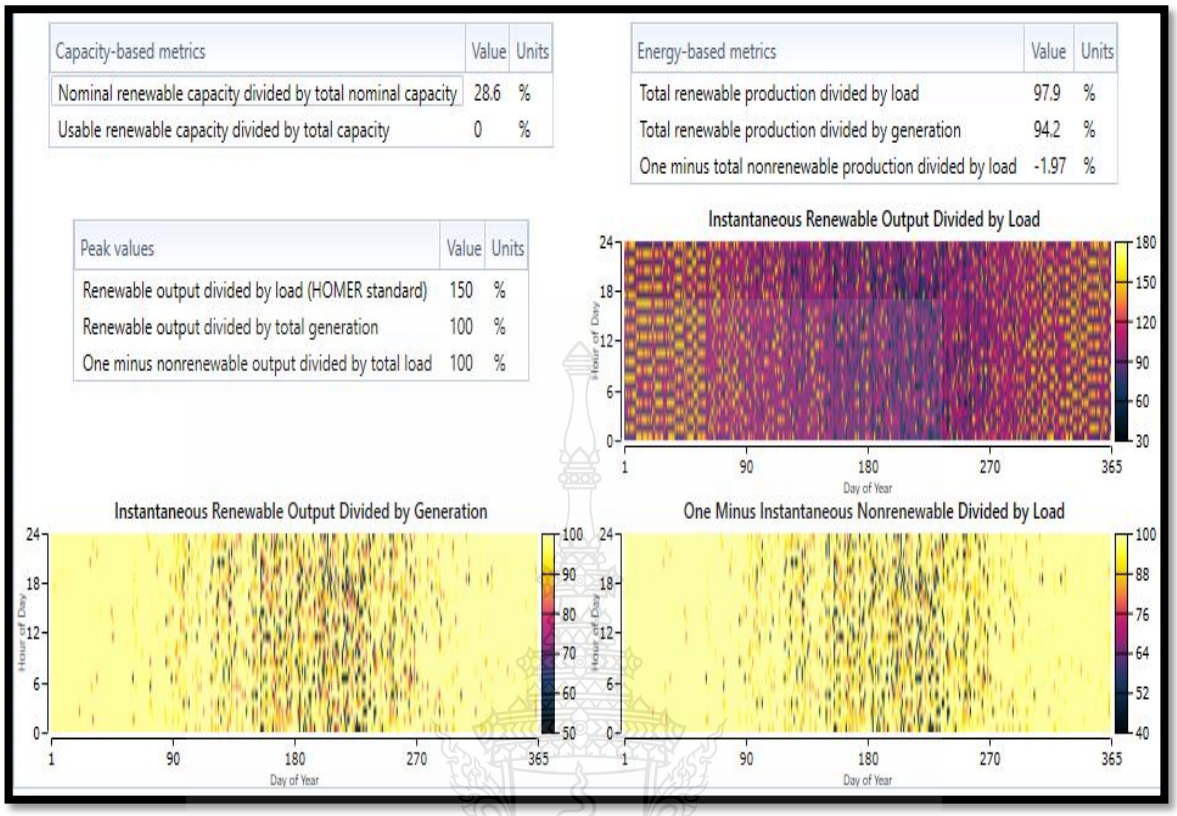

Figure 5.18 Renewable Penetration of Biogas/Grid/Flow Battery Network System.

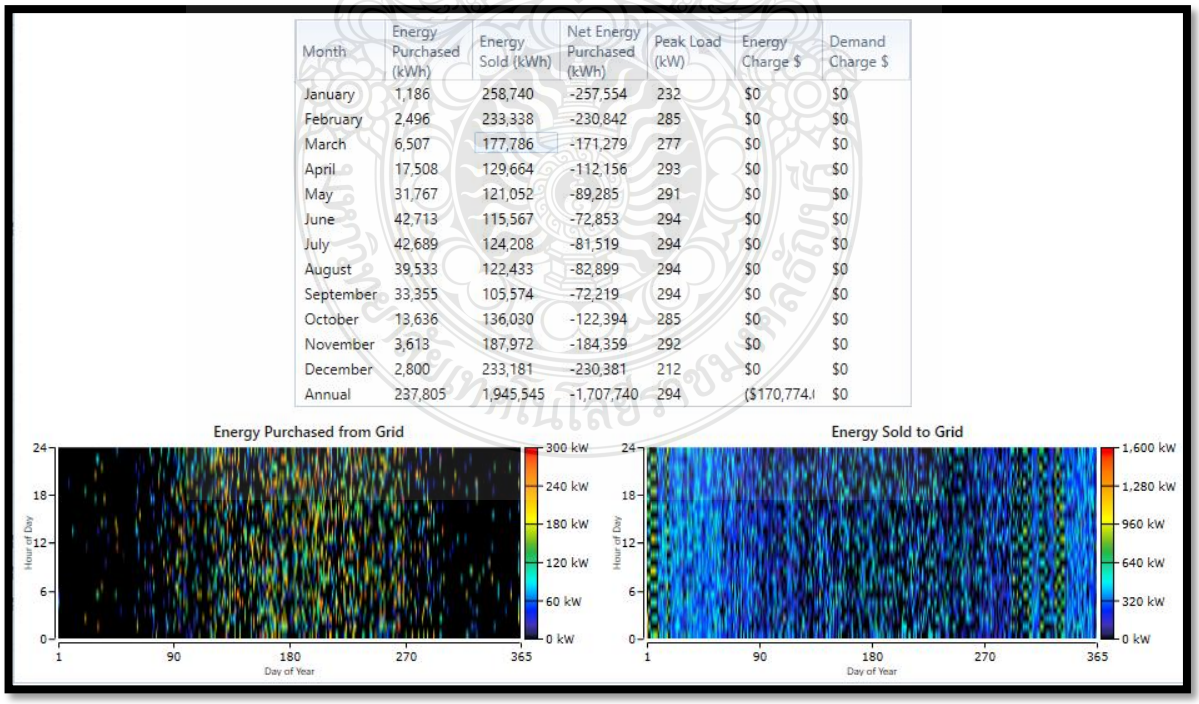

Figure 5.19 Energy Trade of Biogas Generators/Utility Grid/Li-ion Network.

Month	Energy Purchased (kWh)	Energy Sold (kWh)	Net Energy Purchased (kWh)	Peak Load (kW)	Energy Charge $	Demand Charge $
January	1,024	248,409	-247,385	232	$0	$0
February	1,444	220,867	-219,423	285	$0	$0
March	4,663	164,483	-159,821	282	$0	$0
April	14,149	114,394	-100,246	293	$0	$0
May	24,939	100,873	-75,934	291	$0	$0
June	37,545	78,635	-41,091	294	$0	$0
July	35,136	85,186	-50,049	294	$0	$0
August	34,483	86,903	-52,420	293	$0	$0
September	28,929	85,315	-56,386	294	$0	$0
October	11,374	125,200	-113,826	285	$0	$0
November	3,423	184,810	-181,387	292	$0	$0
December	1,948	222,574	-220,626	212	$0	$0
Annual	199,057	1,717,649	-1,518,592	294	($151,859..	$0

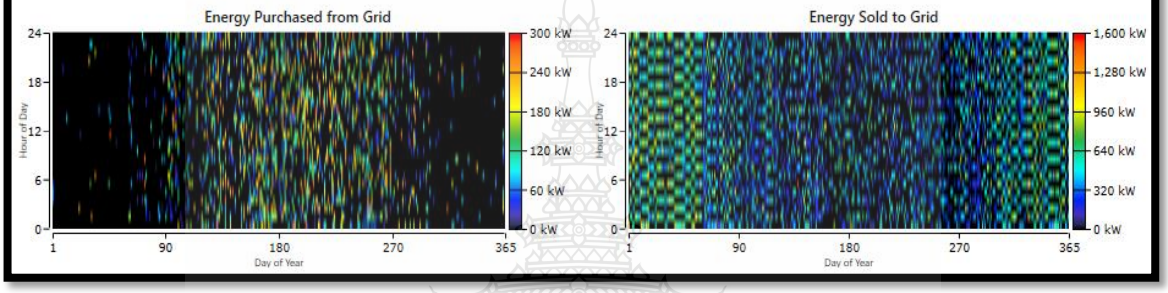

Figure 5.20 Energy Trade of Biogas Generators/Utility Grid/Zn-Brm Network.

Month	Energy Purchased (kWh)	Energy Sold (kWh)	Net Energy Purchased (kWh)	Peak Load (kW)	Energy Charge $	Demand Charge $
January	795	235,451	-234,655	232	$0	$0
February	1,520	207,972	-206,452	285	$0	$0
March	4,511	154,349	-149,838	277	$0	$0
April	14,693	107,630	-92,937	293	$0	$0
May	25,204	95,438	-70,234	294	$0	$0
June	38,673	76,696	-38,023	294	$0	$0
July	36,109	79,766	-43,657	294	$0	$0
August	35,321	82,338	-47,017	294	$0	$0
September	30,207	77,027	-46,821	294	$0	$0
October	11,323	116,882	-105,558	285	$0	$0
November	3,521	173,262	-169,741	292	$0	$0
December	1,888	209,128	-207,241	212	$0	$0
Annual	203,765	1,615,938	-1,412,173	294	($141,217..	$0

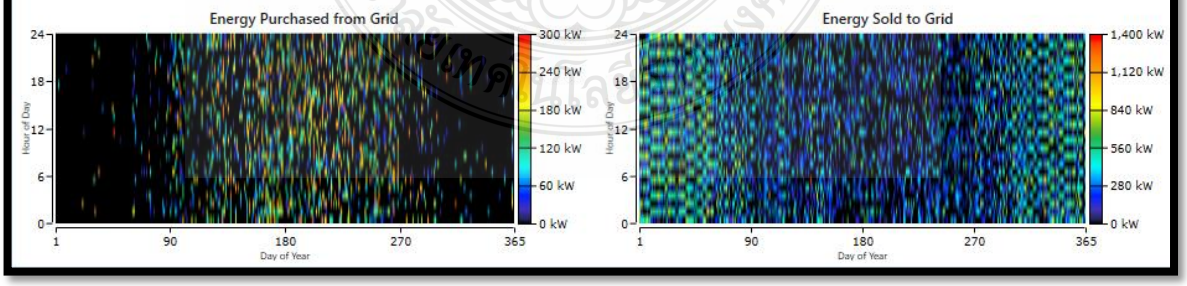

Figure 5.21 Energy Trade of Biogas Generators/Utility Grid/Flow Battery Network.

Biography

Name-Surname	Oluwaseun Olanrewaju AKINTE
Date of Birth	6th of January 1981
Address	39 Village No.1, Rangsit, Nakhon-Nayok Road, Klong 6, Thanyaburi, Pathum Thani 12110.
Education	Olabisi Onabanjo University, Ago-Iwoye, Nigeria (2005-2010). Bachelor of Science in Electrical and Electronic Engineering Coventry University, United Kingdom (2015-2016). Master of Science in Electrical and Electronic Engineering Rajamangala University of Technology Thanyaburi (2020-2024). Doctor of Engineering in Energy and Materials Engineering
Work Experience	Rajamangala University of Technology Thanyaburi (2023-2025) The Research and Service Energy Center, Rajamangala University of Technology Thanyaburi (RSEC-RMUTT) **Energy System Design Analyst for RSEC-RMUTT** **Research Assistant:** IEET paper publication, Brain Power Congress Success Arena Academy (Jan 2020- Oct 2020) **Academic Tutor:** Mathematics, Physics, Further mathematics Electromechanical Integrators Incorporation; H.E.C.L (2017-2019) **Site Engineer:** Electromechanical/renewable energy workshop construction Babington Macaulay Junior Seminary (2013-2015) **Academic Tutor:** Applied Electricity, Further mathematics, Mathematics,and Electronics. National Youth Service Corp (NYSC), Nigeria (2011-2012) **Academic Tutor:** Physics and Mathematics. Jubaili Brothers Engineering Limited (Jan 2009 - June 2009) **Internship:** Installation, corrective maintenance and preventive maintenance of marapco synchronous generators: 13 kV-2000 kV.

Biography (Continued)

Telephone 06-3968-0542

Email Address oluwaseun_o@mail.rmutt.ac.th